Synthesis of thermoresponsive copolymers by RAFT polymerization : characterization and study of their interaction with proteins

The Hien Ho

IMMM-UMR CNRS n°6283   Université du Maine

Equipe Méthodologie et Synthèse des Polymères   Faculté des Sciences et Techniques

THESE

Présentée en vue de l'obtention du grade de

DOCTEUR

Spécialité : Chimie et Physicochimie des polymères

Par

Hien The HO

Synthèse de copolymères thermosensibles par polymérisation radicalaire contrôlée RAFT. Caractérisation et étude de leur interaction avec des protéines

Soutenue le 19 septembre 2012, devant le jury composé de :

Mme Bernadette CHARLEUX	Professeur, Université Claude Bernard, Lyon1	**Rapporteur**
Mme Sophie MONGE	Maître de Conférence-HDR, Université Montpellier 2	**Rapporteur**
M. Jean-François LUTZ	Directeur de Recherche CNRS, Institut Charles Sadron	**Examinateur**
Mme Nathalie CASSE	Maître de Conférence-HDR, Université du Maine	**Examinatrice**
M. Frédéric LEISING	Docteur, Chercheur Associé, Société CHRYSO	**Examinateur**
M. Laurent FONTAINE	Professeur, Université du Maine	**Directeur de thèse**
Mme Sagrario PASCUAL	Maître de Conférence-HDR, Université du Maine	**Co-encadrante**
Mme Véronique MONTEMBAULT	Maître de Conférence-HDR, Université du Maine	**Co-encadrante**

Abbreviations

ACVA	4,4'-azobis(4-cyanovaleric acid)
ADMP	2-(dodecylthiocarbonothioylthio)-2-methylpropionic acid-3-azido-1-propanol ester
ADVN	2,2'-azobis(2,4-dimethylvaleronitrile)
AIBN	2,2'-azobisisobutyronitrile
AMA	allyl methacrylate
AN	acrylonitrile
AOI	2-(acryloyloxy)ethylisocyanate
ATR	attenuated total reflection
ATRP	atom transfer radical polymerization
n-BA	*n*-butyl acrylate
t-BA	*tert*-butyl acrylate
t-BDB	*tert*-butyl dithiobenzoate
n-BMA	*n*-butyl methacrylate
t-BMA	*tert*-butyl methacrylate
BPO	dibenzoyl peroxide
bpy	2,2'-bipyridine
BSA	bovin serum albumin
BSPA	3-(benzylsulfanylthiocarbonylsulfanyl)propionic acid
BuAc	butyl acetate
CCMA	cyclic carbonate methacrylate
CDB	cumyl dithiobenzoate
CMP	2-(1-carboxy-1-methylethylsulfanylthiocarbonylsulfanyl)-2-methylpropionic acid
CPAD	4-(4-cyanopentanoic acid) dithiobenzoate
CPC	1-cyanoethyl 2-pyrrolidone-1-carbodithioate
CPDA	cumyl phenyldithioacetate
CPDB	2-cyanoprop-2-yl dithiobenzoate
CPDN	2-cyanoprop-2-yl-1-dithionaphthalate
CPFDB	2-cyanoprop-2-yl-4-fluoro dithiobenzoate
CRP	controlled radical polymerization
CTA	chain transfer agent
DCM	dichloromethane
DCTB	trans-2-[3-(4-tert-butylphenyl)-2-methyl-2-propenylidene]malononitrile
DEAM	*N,N*-diethyl acrylamide
DEAEMA	2-(diethylamino)ethyl methacrylate
DEGMEMA	diethylene glycol methyl ether methacrylate
DEPMA	diethoxypropyl methacrylate
DIPEA	diisopropylethylamine
DLS	dynamic light scattering
DMA	*N,N*-dimethyl acrylamide
DMAc	*N,N*-dimethyl acetamide

DMAEMA	2-(dimethylamino)ethyl methacrylate
DMF	*N,N*-dimethylformamide
DMP	2-dodecylsulfanylthiocarbonylsulfanyl-2-methylpropionic acid
DMPP	dimethylphenyl phosphine
DMSO	dimethylsulfoxide
dNbpy	4,4'-bis(5-nonyl)-2,2'-bipyridine
DP_n	number-average polymerization degree
DTT	dithiothreitol
EA	ethyl acrylate
EAc	ethyl acetate
EBB	ethyl-2-bromobutyrate
EBiB	ethyl 2-bromoisobutyrate
EDC	1-ethyl-3-(3-dimethylamino)-propyl) carbodiimine
2-EHA	2-ethylhexyl acrylate
EMA	ethyl methacrylate
EPDTB	1-(ethoxy carbonyl) prop-1-yl dithiobenzoate
ES	epoxystyrene
FPLC	cation-exchange fast protein liquid chromatography
FT-IR	Fourier transform infra-red
GA	glycidyl acrylate
GMA	glycidyl methacrylate
HEA	2-hydroxyethyl acrylate
HEMA	2-hydroxyethyl methacrylate
HIPE	high internal phase emulsion
HMA	hostasol methacrylate
HMTETA	1,1,4,7,10,10-hexamethyltriethylenetetramine
HPLC	high performance liquid chromatography
HPMA	*N*-(2-hydroxypropyl) methacrylamide
HRMS	high resolution mass spectrometry
H-TETA	(1,1,4,7,10,10-hexakis) hexyl-1,4,7,10-tetraazadecane
I	isoprene
IBA	isobornyl acrylate
ICEMA	isocyanatoethyl methacrylate
IFN	interferon-2αa
IPDI	3-isocyanatomethyl-3,5,5-trimethylcyclohexyl isocyanate
IPDM	2-isopropenyl-4,4-dimethylazlactone
LA	lauryl acrylate
LCST	lower critical solution temperature
LMA	lauryl methacrylate
MA	methyl acrylate
macroCTA	macromolecular chain transfer agent
MAh	maleic anhydride
MALDI-TOF	matrix-assisted laser desorption and ionization time of flight

MAMA-SG1	*N*-(2-methylpropyl)-*N*-(1-diethylphosphono-2,2-dimethylpropyl)-*O*-(2-carboxylprop-2-yl)hydroxylamine
MBTTCP	methyl-2-(*n*-butyltrithiocarbonyl) propanoate
MCPDB	*S*-methoxycarbonylphenylmethyl dithiobenzoate
MEK	methylethyl ketone
MEO$_2$MA	2-(2-methoxyethoxy)ethyl methacrylate
Me$_6$TREN	tris[2-(dimethylamino)ethyl] amine
MIP	molecular imprinted polymers
MMA	methyl methacrylate
M$_n$	number-average molecular weight
M$_{n,NMR}$	number-average molecular weight determined by ^{1}H NMR spectroscopy
M$_{n,SEC}$	number-average molecular weight determined by SEC
M$_{n,th}$	theoretical number-average molecular weight
MPC	2-methacryloyloxyethylphosphorylcholine
M$_w$	weight-average molecular weight
MWNT	multi-walled carbon nanotube
NAM	*N*-acryloylmorpholine
NAS	*N*-acryloyloxysuccinimide
NHS	*N*-hydroxysuccinimidyl
NHSVB	*N*-oxysuccinimidyl-4-vinylbenzoate
NIPAM	*N*-isopropyl acrylamide
NMAS	*N*-methacryloyloxysuccinimide
NMP	nitroxide-mediated polymerization
NMR	nuclear magnetic resonance
NRC	nitroxide radical coupling
NVP	*N*-vinylpyrrolidone
OEGMA	oligo(ethylene glycol)methyl ether acrylate
ODN	oligonucleotide
PABTC	2-(*n*-butyltrithiocarbonylthio)propionic acid
P(*n*-BA)	poly(*n*-butyl acrylate)
P(*t*-BA)	poly(*tert*-butyl acrylate)
P(*n*-BMA)	poly(*n*-butyl methacrylate)
P(*t*-BMA)	poly(*tert*-butyl methacrylate)
PBS	phosphate buffered saline
PCCMA	poly(cyclic carbonate methacrylate)
PCEMA	2-(phenoxycarbonyloxy)ethyl methacrylate
PDEGMEMA	poly(diethylene glycol monomethyl ether methacrylate)
PDEPMA	poly(diethoxypropyl methacrylate)
PDI	polydispersity index
PDMA	poly(*N,N*-dimethyl acrylamide)

PDMAEMA	poly((2-dimethylamino)ethyl methacrylate)
PDMDETA	*N,N',N',N'',N''*-pentamethyldiethylenetriamine
PEA	poly(ethyl acrylate)
PEBr	1-phenylethyl bromide
PEG	poly(ethylene glycol)
PEGA	poly(ethylene glycol) monomethyl ether acrylate
PEGMA	poly(ethylene glycol) monomethyl ether methacrylate
P(2-EHA)	poly(2-ethylhexyl acrylate)
PEO	poly(ethylene oxide)
PFP	pentafluorophenyl
PFPA	pentafluorophenyl acrylate
PFPMA	pentafluorophenyl methacrylate
PFPMI	pentafluorophenyl-4-maleimidobenzoate
PFS	pentafluorostyrene
PGMA	poly(glycidyl methacrylate)
PHEA	poly(2-hydroxyethyl acrylate)
PHEMA	poly(2-hydroxyethyl methacrylate)
PHPMA	poly(*N*-2-(hydroxypropyl) methacrylamide)
PI	polyisoprene
PIBA	poly(isobornyl acrylate)
PICEMA	poly(2-isocyanatoethyl methacrylate)
PIPDM	poly(2-isopropenyl-4,4-dimethylazlactone)
PLA	poly(*D,L*-lactide)
PLMA	poly(lauryl methacrylate)
PMA	poly(methyl acrylate)
PMMA	poly(methyl methacrylate)
PMPC	poly(2-methacryloyloxyethylphosphorylcholine)
PNAM	poly(*N*-acryloylmorpholine)
PNAS	poly(*N*-acryloyloxysuccinimide)
PNHSVB	poly(*N*-oxysuccinimidyl-4-vinylbenzoate)
PNIPAM	poly(*N*-isopropyl acrylamide)
PNMAS	poly(*N*-methacryloyloxysuccinimide)
PNP	*p*-nitrophenyl
PNPA	*p*-nitrophenyl acrylate
PNPMA	*p*-nitrophenyl methacrylate
PNVP	poly(*N*-vinylpyrrolidone)
POEGA	poly(oligo(ethylene glycol)methyl ether acrylate)
POEGMA	poly(oligo(ethylene glycol)methyl ether methacrylate)
PPCEMA	poly(2-(phenoxycarbonyloxy)ethylmethacrylate)
PPEGA	poly(poly(ethylene glycol) monomethyl ether acrylate)
PPEGMA	poly(poly(ethylene glycol) monomethyl ether methacrylate)
PPFPA	poly(pentafluorophenyl acrylate)
PPFPMA	poly(pentafluorophenyl methacrylate)

PPFPVS	poly(pentafluorophenyl-4-vinylbenzene sulfonate)
PPFS	polypentafluorostyrene
PPMI	*N*-(*n*-propyl)-2-pyridylmethanimine
PPNPA	poly(*p*-nitrophenyl acrylate)
PPNPMA	poly(*p*-nitrophenyl methacrylate)
PS	polystyrene
PVBC	poly(4-vinylbenzyl chloride)
PVDM	poly(2-vinyl-4,4-dimethylazlactone)
PVPDM	poly(2-(4'-vinyl)phenyl-4,4-dimethylazlactone)
RAFT	reversible addition-fragmentation chain transfer
RDRP	reversible deactivation radical polymerization
RI	differential refractometer
S	styrene
SCK	shell-crosslinked knedel-like
SDS-PAGE	sodium dodecyl sulfate polyacrylamide gel electrophoresis
SEC	size exclusion chromatography
SET	single electron transfer
SG1	*N*-*tert*-butyl-*N*-1-diethylphosphono-(2,2-dimethylpropyl) nitroxide
TBP	*N,N*-dimethyl-*S*-thiobenzoylthiopropionamide
TEA	triethylamine
TEDETA	*N,N,N',N'*-tetraethyldiethylenetriamine
TEMPO	2,2,6,6-tetramethyl-1-piperidinyloxyl radical
terpy	terpyridine
TIPS-MI	triisopropylsilyl-protected *N*-propargyl maleimide
THF	tetrahydrofuran
TMI	*m*-isopropenyl-α,α-dimethylbenzylisocyanate
TPA	vinyl triphenylamine
TPO	(2,4,6-trimethylbenzoyl)diphenylphosphine oxide
VDM	2-vinyl-4,4-dimethylazlactone
TT	thiazolidine-2-thione
VPDM	2-(4'-vinyl)phenyl-4,4-dimethylazlactone
UV	ultraviolet
UV-Vis	ultraviolet-visible

Chapter II: Synthesis of α-azlactone-functionalized polymers by RAFT polymerization

Chapter III: Synthesis of ω-azlactone-functionalized polymers by RAFT polymerization

Chapter IV: Synthesis of stable azlactone-functionalized nanoparticles prepared from thermoresponsive copolymers synthesized by RAFT polymerization

Chapter V: Synthesis of azlactone-functionalized thermoresponsive copolymers based on poly(ethylene oxide) and poly(*N*-isopropyl acrylamide) by RAFT polymerization

INTRODUCTION GENERALE

Les polymères sensibles à des *stimuli* extérieurs (température, pH…) et réactifs vis-à-vis des amines suscitent un intérêt croissant dans le domaine des biotechnologies en raison de l'étendue de leurs applications potentielles telles que l'immobilisation de biomolécules (ADN, peptides, protéines) en vue de l'obtention de conjugués polymères/biomolécules. Ces systèmes permettent d'améliorer certaines propriétés telles que l'immunogénicité, la stabilité ou la solubilité des biomolécules comme les protéines. Les premiers travaux[1] dans le domaine des bioconjugués ont porté sur l'ancrage covalent de protéines sur le poly(ethylène glycol) (PEG) conduisant à une diminution de l'immunogénicité des protéines considérées. La présence de la fonction amine sur la lysine présente dans les protéines, permet d'envisager de les coupler avec des polymères à fonctionnalité spécifique, réactive vis-à-vis des amines. A ce jour, les esters activés (*N*-hydroxysuccinimidyl et pentafluorophényl) sont largement étudiés pour de telles applications. L'inconvénient de ces fonctions réside dans la formation de produits secondaires lors de l'ancrage de l'amine. C'est pourquoi, au cours de ce travail, nous nous sommes plus particulièrement tournés vers la fonctionnalité oxazolin-5-one (aussi appelée azlactone) qui possède l'avantage de réagir avec des amines dans des conditions douces sans former de sous-produit de réaction (*Schéma 1*).
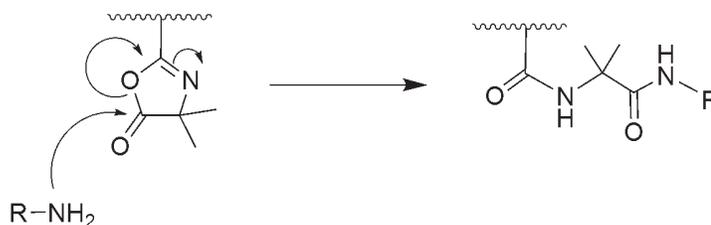
Schéma 1 : Réaction du cycle azlactone avec une amine primaire.

---

[1] (a) Langer, R.; Folkman, J. *Nature,* **1976** *263*, 797-800. (b) Abuchowski, A.; Vanes, T. ; Palczuk, N. C.; Davis, F. F. *J. Biol. Chem*. **1977**, *252*, 3578-3581.

L'objectif de ce travail est de synthétiser des (co)polymères thermosensibles présentant une fonctionnalité azlactone pour l'ancrage de biomolécules (protéines/ADN). Pour ce faire, la polymérisation radicalaire contrôlée par addition-fragmentation réversible[2] (RAFT : Reversible Addition-Fragmentation chain Transfer) a été choisie, en raison de son caractère contrôlé, de sa tolérance vis-à-vis des groupements hétérofonctionnels et de la cytotoxicité limitée des polymères issus d'une polymérisation RAFT. Dans ces travaux de thèse, le poly(acrylamide de *N*-isopropyle) (PNIPAM) est choisi pour accéder aux (co)polymères thermosensibles. L'intérêt du PNIPAM est qu'il possède une température critique de démixtion[3] (LCST~ 32°C) en solution aqueuse qui peut être modulée pour atteindre une température proche du corps humain.

La fonctionnalité azlactone est incorporée en position α, en position ω ou le long des chaînes macromoléculaires afin d'étudier l'impact de telles structures sur leur réactivité vis-à-vis d'amines diverses et d'une protéine modèle (le lysozyme). Ainsi, trois stratégies de synthèse seront plus particulièrement étudiées (*Schéma 2*).

---

[2] Chiefai, J.; Chong, Y. K.; Ercole, F.; Krstina, J.; Jeffery, J.; Le, T. P. T.; Mayadunne, R. T. A.; Meijs, G. G.; Moad, C. L.; Moad, G.; Rizzaddo, E.; Thang, S. H. *Macromolecules* **1998**, *31*, 5559-5562.
[3] Schild, H. G. *Prog. Polym. Sci*. **1992**, *17*, 163-249.
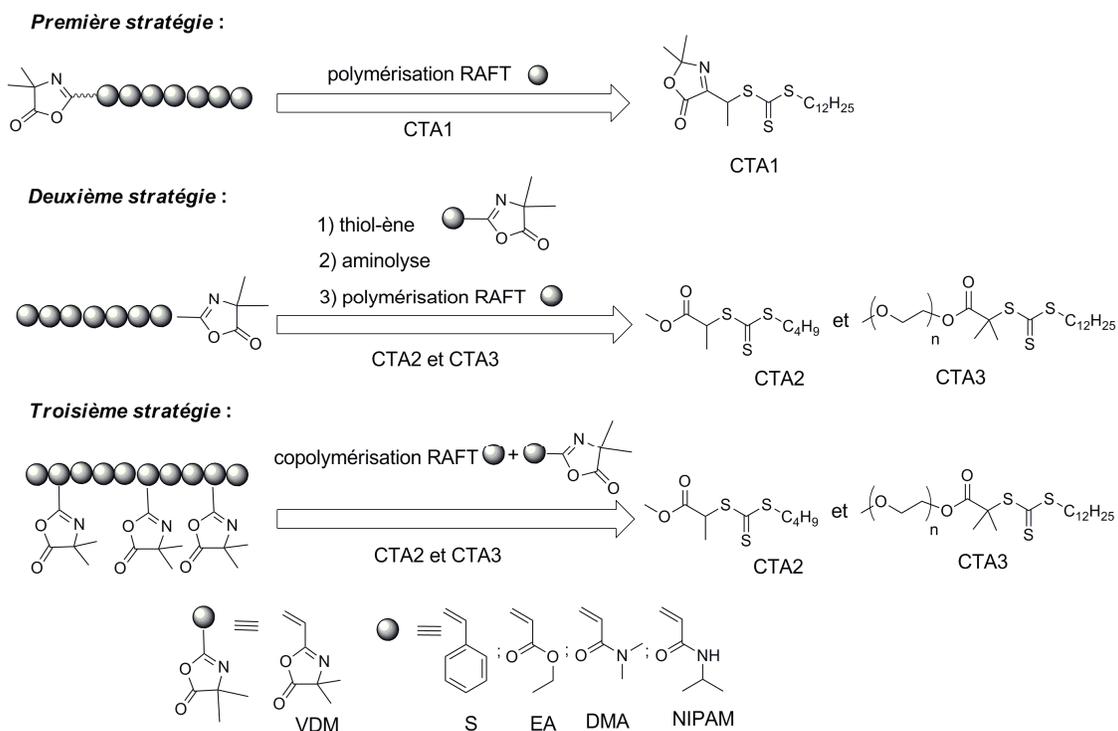
Schéma 2 : Stratégies de synthèse des (co)polymères à fonctionnalité azlactone.

La ***première stratégie*** consiste en la synthèse d'un nouvel agent de transfert possédant la fonctionnalité azlactone et son utilisation lors de la polymérisation RAFT de divers monomères. Cette stratégie permettra d'accéder à des polymères fonctionnalisés en position α.

La ***seconde stratégie*** repose sur la modification chimique des extrémités de chaînes macromoléculaires issues d'une polymérisation RAFT afin d'y incorporer la fonctionnalité azlactone en position ω.

La ***troisième stratégie*** porte sur la copolymérisation RAFT de divers monomères avec la 2-vinyl-4,4-diméthylazlactone (VDM) afin d'obtenir des copolymères possédant des fonctionnalités azlactone pendantes.

La première partie de ce manuscrit est consacrée à une étude bibliographique portant sur les différentes stratégies de synthèse par polymérisation radicalaire contrôlée des (co)polymères réactifs vis-à-vis des amines.

Le chapitre deux porte sur la synthèse et la caractérisation d'un nouvel agent de transfert à fonctionnalité azlactone. Un dérivé trithiocarbonate a été choisi car les polymères à extrémité trithiocarbonate présentent une cytotoxicité moins importante que les polymères possédant un groupement dithioester.[4] Ce nouvel agent de tranfert est ensuite utilisé pour accéder à des polymères bien définis renfermant la fonctionnalité azlactone en position α.

L'introduction de la fonctionnalité azlactone en position ω des chaînes macromoléculaires fait l'objet du troisième chapitre.

Le quatrième chapitre porte sur la copolymérisation RAFT entre la 2-vinyl-4,4-diméthylazlactone (VDM) et divers acrylamides (acrylamide de *N,N*-diméthyle (DMA) et NIPAM). La capacité de ces copolymères à former des nanoparticules stables à fonctionnalité azlactone est étudiée.

Enfin, le dernier chapitre est consacré à la synthèse de copolymères à base de PNIPAM et de poly(oxyde d'éthylène) possédant la fonctionnalité azlactone en position ω et le long des chaînes macromoléculaires ainsi qu'à la bioconjugaison de ces copolymères avec le lysozyme.

---

[4] (a) Chang, C.-W.; Bays, E.; Tao, L.; Alconcel, N. S.; Maynard, H. D. *Chem. Commun.* **2009**, 3580-3582. (b) Pissuwan, D.; Boyer, C.; Gunasekaran, K.; Davis, T. P.; Bulmus, V. *Biomacromolecules* **2010**, *11*, 412-420. (c) Stenzel, M. H.; Barner-Kowollik, C.; Davis, T. P.; Dalton, H. M. *Macromol. Biosci.* **2004**, *4*, 445-453.

Chapter I

Bibliography Study

Well-defined amine-reactive polymers through Controlled Radical Polymerization

Chapter I: Well-defined amine-reactive polymers through Controlled Radical Polymerization

1. Introduction

Reactive polymers containing functional groups that can react easily with amines are of particular interest and have emerged with potential applications such as drug delivery, bioconjugation, and surface modification.[1] The amino functionality is widely found in natural and synthetic (macro)molecules and several functional groups are reactive towards amines. Aside from basicity, one of the dominant reactivity of amines is their nucleophilicity. Amino groups can thus react with electrophilic centers of acylating and alkylating reagents through nucleophilic substitution, leading to amide and alkylamine groups, respectively (*Scheme 1*). The presence of acylating or alkylating moieties into functional polymers make them reactive towards amines and a wide range of such reactions have been used in the literature.[2]
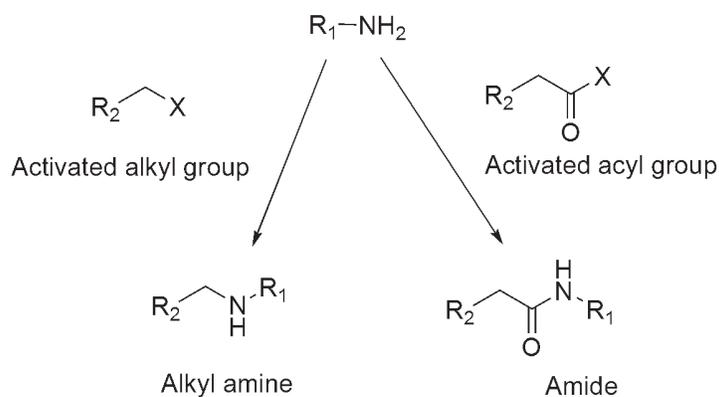
Scheme 1: Reactions of a primary amine with alkylating and acylating reagents.

The specific features of functional synthetic polymers are provided by the presence of chemical functional groups as chain-ends or in-chain (pendant) structures. Functional polymers are obtained through post-functionalization of pre-existing (natural or

synthetic) polymers or by direct (co)polymerization of the functionalized monomer(s). Controlled radical polymerization (CRP, also named reversible deactivation radical polymerization[3] RDRP) is arguably one of the most versatile methods for the synthesis of well-defined polymers bearing functional groups. CRP is tolerant with a wide range of functions and allows the synthesis of well-defined polymers with precise control over molecular weights, molecular weight distribution, functionality and architecture. Among the existing CRP techniques, nitroxide-mediated polymerization[4] (NMP), atom transfer radical polymerization[5] (ATRP) and reversible addition-fragmentation chain transfer[6] (RAFT) polymerization are the three most well-known methods. These CRP techniques provide to the chemist a useful toolbox for the direct synthesis of well-defined polymers reactive towards amines. Monomers bearing an amine reactive functionality may be directly (co)polymerized through CRP provided that the functionality is chemoselective and orthogonal with respect to the polymerization process. The amine reactive functionality is thus introduced in the side chain of the final polymer. Incorporation of the reactive functionality at the polymer chain-ends can also be achieved using CRP: it can be incorporated into the initiating moiety of NMP, ATRP, or RAFT initiator/chain transfer agent, affording α-functional polymer, or be affixed to the terminating portion of initiator/chain transfer agent, providing ω-functional polymer (*Scheme 2*).
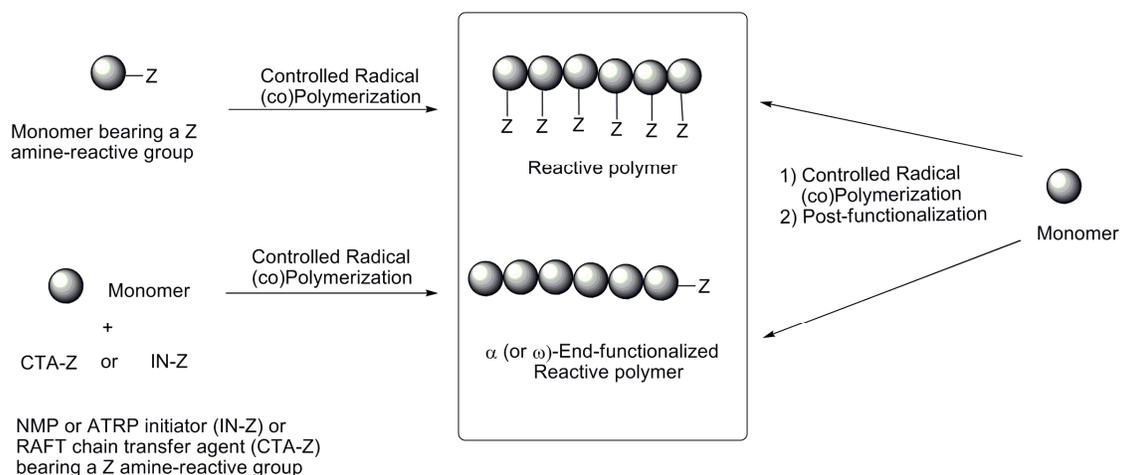
Scheme 2: Routes to prepare amine-reactive polymers.

The reaction of amines with alkylating or acylating functionalities may require the presence of a catalyst to achieve high yields and it can be accompanied by the formation of a side-product, making purification of the resulting polymer tedious. In the context of biological applications, such reactions should be avoided whenever possible, since the catalyst and/or by-product can be toxic. In this chapter, we provide a survey of the synthetic methods useful to prepare well-defined reactive polymers containing functional groups that do not necessitate a catalyst to react with amines.

2. Overview of reactive groups towards amines without any catalyst

Amino-based compounds can react with alkylating and acylating agents to give secondary amines or tertiary amines and amide bonds, respectively. Some of those alkylation and acylation are of particular interest as they proceed without any catalyst. For instance, functionalities such as epoxide, azlactone (or oxazolone), isocyanate, carbonate, anhydride, thiazolidine-2-thione and activated esters rapidly react with primary amines in mild conditions, without any catalyst and give high yields. These reactions are based on the ring-opening of heterocyclic electrophiles or based on the carbonyl chemistry of the "non-aldol" type such as formation of urea and amide. Some of them possess "click" characteristics as described by Kolb *et al.*[7] When functionalities including epoxide, azlactone, isocyanate, cyclic carbonate and cyclic anhydride are attached to a polymer, the reaction with an amine proceeds without the formation of molecular side-products.

The epoxide is an electrophilic ring that can easily undergo ring-opening reaction with a large variety of nucleophiles including primary amines (*Scheme 3*). The reaction of epoxide with primary amines can be performed in various experimental conditions to target amino-alcohols in high yields.
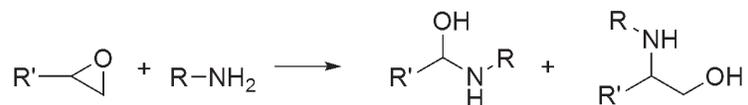
Scheme 3: Reaction of the epoxide with a primary amine.

Other heterofunctionalities including azlactone (or oxazolone), activated ester, thiazolidine-2-thione, cyclic anhydride and isocyanate are now emerging as powerful functionalities due to their high reactivity towards primary amines. These functionalities

can rapidly and quantitatively react with primary amines at room temperature and in the absence of a catalyst to produce the corresponding amide and urea (*Schemes* 4-7).[8-10] Accordingly, the reaction of azlactone, activated ester and isocyanate with amines present advantages of conventional "click" type reaction.[11-13]
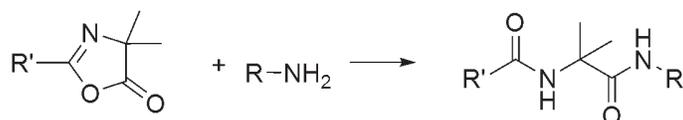
Scheme 4: Reaction of the azlactone with a primary amine.
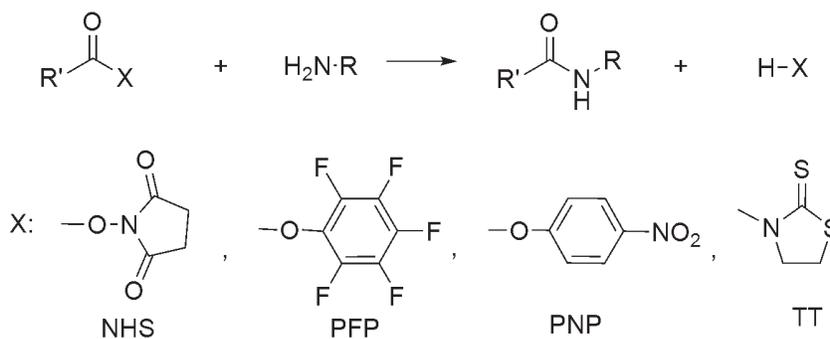
Scheme 5: Reaction of a primary amine with an activated ester (NHS = N-hydroxysuccinimidyl, PFP = pentafluorophenyl, PNP = p-nitrophenyl) and thiazolidine-2-thione (TT).
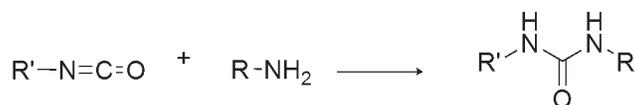
Scheme 6: Reaction of isocyanate with a primary amine.
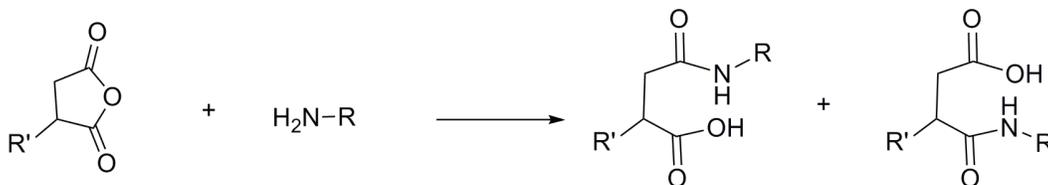
Scheme 7: Reaction of a primary amine with cyclic anhydride.

9

Another useful functionality for anchoring primary amines is the carbonate group. In the carbonate functional class, the five-membered cyclic carbonate is most like azlactone or epoxide because it has a high reactivity towards primary amines and when carried out by a polymer, the reaction proceeds without the formation of molecular by-products. This reaction can proceed relatively rapidly at ambient or slightly elevated temperatures and does not release by-products, yielding the corresponding hydroxyl urethane (*Scheme 8a*). Moreover, aliphatic functional carbonate with pendant phenyl groups allows quantitative reaction with amines due to the highly selective cleavage of the asymmetric carbonate group (*Scheme 8b*). However, this reaction proceeds with the formation of phenol.
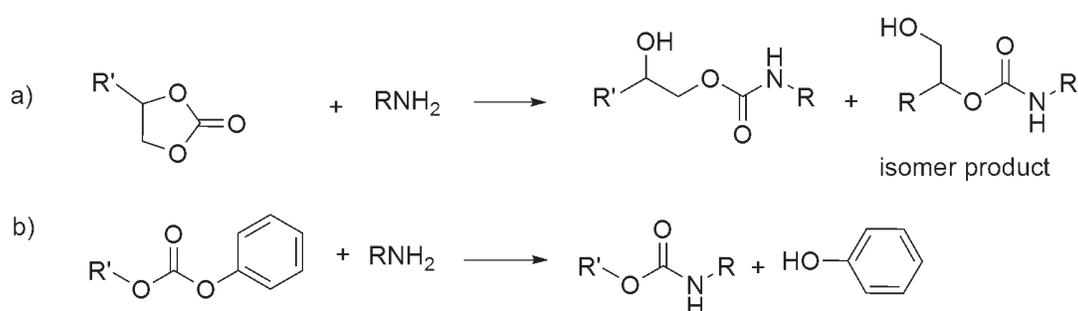
Scheme 8: Reaction of carbonates: a) a cyclic carbonate and b) an aliphatic carbonate with a primary amine.

3. Strategies to target synthetic well-defined (co)polymers containing a reactive group towards amines using CRP

Reactive polymers towards amines can be obtained either by the direct incorporation of functional groups during the polymerization or either by post-modification of a well-defined polymer.

3.1. Introduction of functional groups during the polymerization

Functional groups reactive towards amines can be introduced either at the chain-end (α- or ω- positions) of the polymer or within the macromolecular chain using CRP techniques and appropriate monomer, initiator, or chain transfer agent (*Scheme 2*). Monomers, initiators, or chain transfer agents carrying common acylating groups such as acyl chlorides cannot be used due to their high reactivity, making them difficult to polymerize and to handle.[14] Activation of the carboxylic acid moiety of the monomer, initiator, or chain transfer agent is thus required, wich consists in the replacement of the hydroxyl group of the carboxylic acid with a leaving group as the acid would otherwise simply form salts with the amine. Beside such thiazolidine-2-thione, activated esters (NHS and PFP esters), amine reactive functionalities (epoxide, azlactone, carbonate, isocyanate, anhydride) that are orthogonal with the CRP processes have been widely used to prepare well-defined amino-reactive polymers.

3.1.1. At the chain-end

Different strategies are reported in the literature to target polymers containing a reactive group towards amines at the chain-end *via* CRP including ATRP, RAFT and

NMP processes. The functional group could be fixed at the beginning of macromolecular chains (α-position) or at the end of macromolecular chains (ω-position) by using an alkoxyamine, a nitroxide, an ATRP initiator and a RAFT agent (*Table 1*).

Table 1: Summary of functional compounds used in CRP to target amino-reactive polymers.

Functionality	CRP method	Structure	Ref.
Epoxide	NMP	 R_1, R_2, R_3, R_4: alkyl	15
	ATRP		25
			26
	RAFT		46
Azlactone	NMP		16
	ATRP		27
	RAFT	 R= H, -CH$_3$	47

Carbonate	ATRP		28
		n = 1 and 4	44, 45
			43
NHS ester	NMP	R = H, -CH$_3$	17-24
	ATRP	R = H, -CH$_3$	29-42
	RAFT		48
			49
		n = 3 n = 11	50, 52
			51
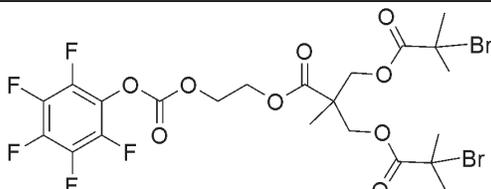
PFP ester	ATRP		43
	RAFT		53-59
			60
TT-ester	RAFT		61, 66
			62, 63
			64
			65
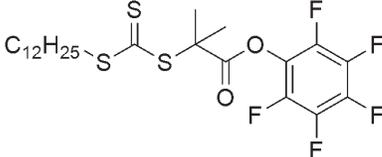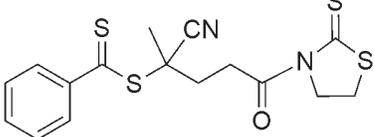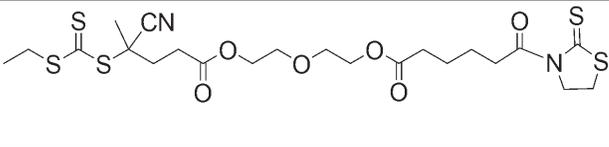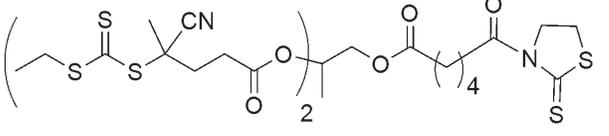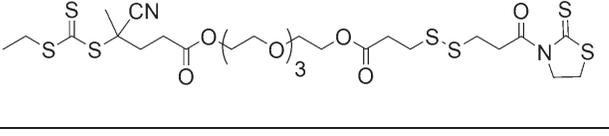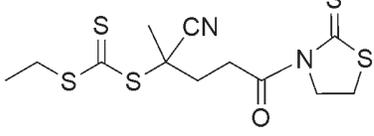
3.1.1.1. Using an alkoxyamine or a free nitroxide

NMP is an useful method for the synthesis of well-defined telechelic polymers which are synthesized either using an alkoxylamine in which the functional group was incorporated in the initiating segment or in the terminating segment (*Figure 1*) or, either using an appropriate nitroxide.
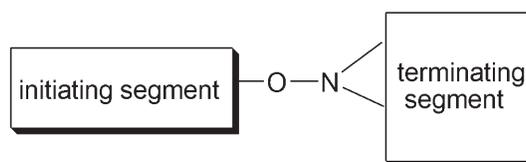
Figure 1: General structure of an alkoxyamine.

In this part, epoxide, azlactone, and NHS ester-functionalized alkoxyamines or nitroxides are described, as they do not involve catalyst to react with amines. Moreover, reactive groups which do not lead to molecular side-product are first studied.

3.1.1.1.a. Reactive groups not leading to molecular side-products

Epoxide

Fuso *et al.*[15] reported the synthesis of a library of glycidyl functionalized nitroxides and their use to mediate the polymerization of styrene (S) and *n*-butyl acrylate (*n*-BA). Size exclusion chromatography (SEC) analysis of resulting polymers shows that polydispersities indices (PDIs) are below 1.30.

Azlactone

Fansler *et al.*[16] described the synthesis of an azlactone-functionalized alkoxylamine (Azl-NMP, *Scheme 9*) to target azlactone functionalized polystyrene (PS) with number-average molecular weight (M_n) ranging from 2790 g.mol^{-1} to 23900 g.mol^{-1}

with PDI from 1.76 to 2.05. Furthermore, star polymers were obtained by reacting the azlactone-terminated PS with the tris(2-aminoethyl)amine. In a second approach, the Azl-NMP (*Scheme 9*) reacts with the tris(2-aminoethyl)amine for the synthesis of a trifunctional alkoxylamine. This compound was then used to mediate the polymerization of S to yield the tri-arms star PS (M_n = 16300 g.mol^{-1}, PDI= 1.18).
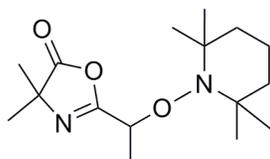
Azl-NMP

Scheme 9: Structure of azlactone-functionalized alkoxylamine.

3.1.1.1.b. Reactive groups leading to molecular side-products

NHS-ester

Vinas *et al.*[17] reported the synthesis of NHS-ester functionalized alkoxyamine (NHS-NMP1, *Scheme 10a*) used as an alkoxylamine to target NHS-terminated PS and poly(*n*-butyl acrylate) P(*n*-BA). Well-defined PS (PDI = 1.19) with M_n equal to 6800 g.mol^{-1} and well-defined P(*n*-BA) were obtained in bulk in the presence of NHS-NMP1 (*Scheme 10a*) at 120°C (for S) or 115°C (for *n*-BA). The NHS-functionalized PS subsequently reacts with ethanolamine to target hydroxyl-functionalized PS. The hydroxyl-terminated PS was then used as macroinitiator for the ring-opening polymerization of *D,L*-lactide leading to PS-*b*-P(*D,L*-lactide) copolymers. The same strategy was employed by other groups to synthesize a series of well-defined NHS-terminated PS and P(*n*-BA) which were then coated onto amino-functionalized

silica particles using the grafting onto strategy.[18] Chenal *et al.*[19] reported the quantitative coupling of a neuroprotective peptide and the partial conjugation with lysozyme to a NHS-functionalized copolymer based on poly(ethylene glycol) monomethyl ether methacrylate (PEGMA) and fluorescent acrylate. The NHS-NMP1 (*Scheme 10a*) was used to mediate the copolymerization.

Other groups have employed NHS-NMP1 (*Scheme 10a*) to target well-defined NHS-terminated copolymers by performing the copolymerization of glycidyl methacrylate (GMA) and S, the copolymerization of 2-(dimethylamino)ethyl methacrylate (DMAEMA) and S, the copolymerization of acrylonitrile (AN) and *tert*-butyl methacrylate (*t*-BMA), the copolymerization of S and AN, and finally the copolymerization of S and methyl methacrylate (MMA).[20-23] Harrison *et al.*[24] recently used NHS-NMP1 and NHS-NMP2 (*Scheme 10*) as alkoxyamines to mediate the polymerization of isoprene (I) in bulk at 115°C. Well-defined NHS-functionalized polyisoproprenes (PIs) were obtained with controlled molecular weights (M_n up to 2410 g.mol^{-1}) and polydispersity indices below 1.10. NHS-functionalized PIs then react with ethylene diamine in tetrahydrofuran (THF) at room temperature providing amino-functionalized PIs.

NHS-NMP1   NHS-NMP2
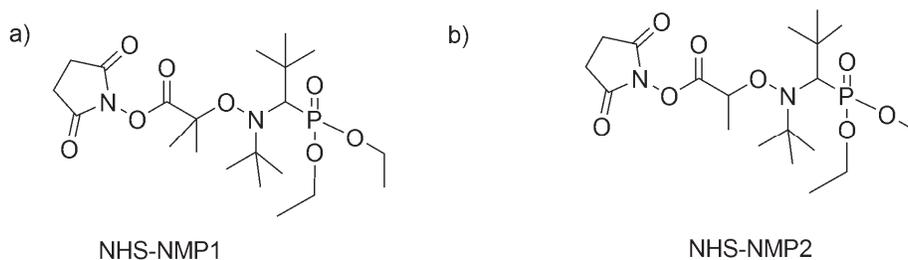
Scheme 10: NHS-ester terminated alkoxylamines.

3.1.1.2. Using an ATRP initiator

An ATRP initiator is often an alkyl halide (RX) based on an alkyl group (R) and an halogen (X: -Br, -Cl). The ATRP initiator will form an alkyl radical (R$^\bullet$) by atom transfer in the presence of a transition metal complexed with ligands. This radical R$^\bullet$ initiates the polymerization. Using an ATRP initiator containing a functional group such as epoxide, carbonate, NHS-ester, azlactone is an easy way to target reactive polymers towards amines.

3.1.1.2.a. Reactive groups not leading to molecular side-products

Epoxide

Matyjaszewski and coworkers reported the synthesis of an epoxide terminated poly(*tert*-butyl acrylate) P(*t*-BA) using the Epoxide-ATRP1 initiator (*Scheme 11*).[25] The P(*t*-BA) was obtained with a low polydispersity index (PDI = 1.22) and a molecular weight of 5600 g.mol^{-1}.
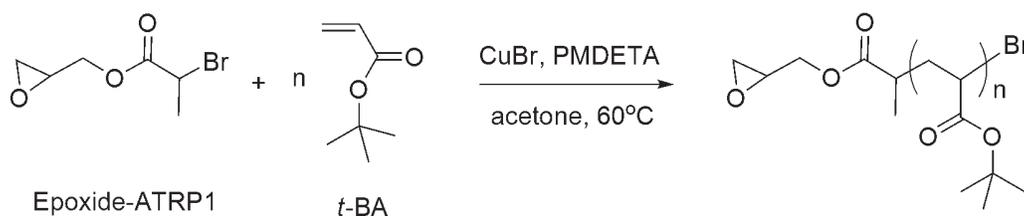
Epoxide-ATRP1   *t*-BA

Scheme 11: Polymerization of tert-butyl acrylate (t-BA) using CuBr/ N,N',N',N'',N''-pentamethyldiethylenetriamine (PMDETA) as the catalytic system and Epoxide-ATRP1 as ATRP the initiator in acetone at 60°C.

An epoxide-functionalized PS (M$_n$ = 1590 g.mol^{-1}, PDI = 1.27) was synthesized by using the Epoxide-ATRP2 initiator with CuBr/2,2'-bipyridine (bpy) as the catalytic system in bulk at 110°C (*Scheme 12*). The resulting polymer was then used as a

macromonomer for the photoinduced cationic polymerization to yield a graft copolymer.[26]
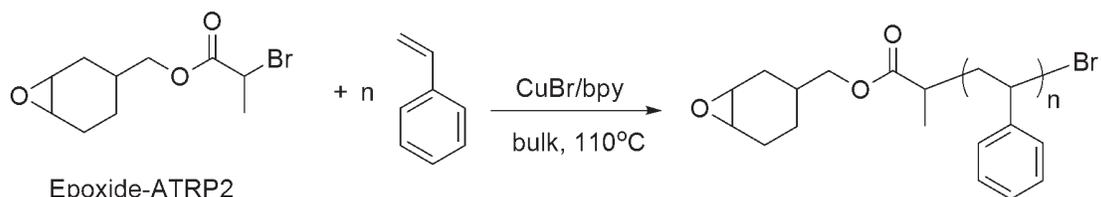
Scheme 12: Polymerization of S in bulk using CuBr/bpy as the catalytic system and Epoxide-ATRP2 as initiator at $110^{o}C$.

Azlactone

Lewandowski *et al.*[27] described the synthesis of an azlactone-functionalized ATRP initiator (Azl-ATRP, *Scheme 13*) for the polymerization of MMA using CuCl/bpy as catalytic system at $70^{o}C$ in bulk (*Scheme 13*). Poly(methyl methacrylate)s (PMMAs) were obtained with controlled molecular weights and polydispersity indices below 1.31. Linear azlactone-terminated PMMA (M_n = 10300 g.mol^{-1}, PDI = 1.18) was able to react with tris(2-aminoethyl)amine in toluene without any catalyst at $60^{o}C$ to yield a star polymer (M_n = 34900 g.mol^{-1}, PDI = 1.10).
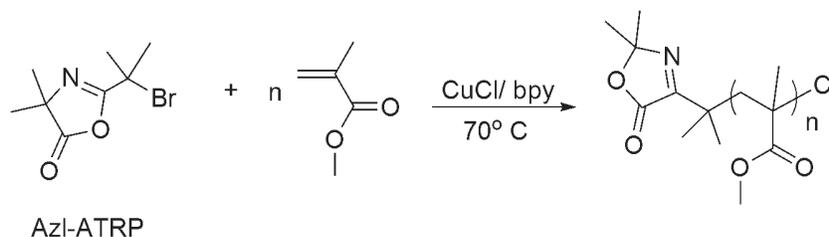
Scheme 13: Polymerization of MMA using an azlactone-functionalized ATRP initiator and CuCl/bpy as the catalytic system in bulk at $70^{o}C$.

 The authors also described the synthesis of an ATRP multifunctional initiator by reacting the Azl-ATRP initiator (*Scheme 13*) with the trimethylolpropane. This initiator was subsequently used to carry out the polymerization of MMA leading to star polymer ($M_n = 16400$ g.mol^{-1}, PDI = 1.24).

Cyclic carbonate

Wadgaonkar *et al.*[28] reported the synthesis of cyclic carbonate terminated PMMA by using a carbonate-functionalized ATRP initiator (Carbonate-ATRP1, *Scheme 14*).
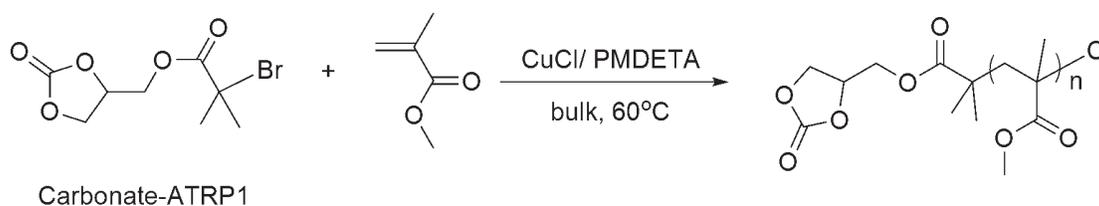
Carbonate-ATRP1

Scheme 14: Polymerization of MMA using CuCl/PMDETA as the catalytic system and a cyclic carbonate ATRP initiator in bulk at 60° C.

Well-defined carbonate-terminated PMMAs (M_n = 3570 - 44130 g.mol^{-1}, PDI = 1.17-1.30) were obtained in bulk at 60°C with [Carbonate-ATRP1]$_0$:[CuCl]$_0$:[PMDETA]$_0$ = 1:1:1. The reactivity of resulting PMMAs has been measured with *n*-propylamine in dimethylsulfoxide (DMSO) at 50°C for 48h. The conversion of the cyclic carbonate group into urethane group has been observed by Fourier transform infra-red (FT-IR) spectroscopy.

3.1.1.2.b. Reactive groups leading to molecular side-products

NHS-ester

Han and Pan synthesized the *N*-(2-bromo-2-methylpropionyloxy)succinimide (NHS-ATRP1, *Scheme 15*) as a functional ATRP initiator for the polymerization of S using CuBr/bpy as the catalytic system (M_n = 3400-11360 g.mol^{-1}, PDI = 1.04-1.09).[29] Ladmiral *et al.*[30] reported the ATRP synthesis of NHS-terminated glycopolymers (M_n = 4500-10200 g.mol^{-1}, PDI = 1.10-1.31) based on glucofuranoside and galactopyronoside monomers by using NHS-ATRP2 (*Scheme 15*). These functional sugar polymers subsequently reacted with α,ω-diamino-terminated poly(ethylene glycol) for the preparation of ABA triblock copolymers.
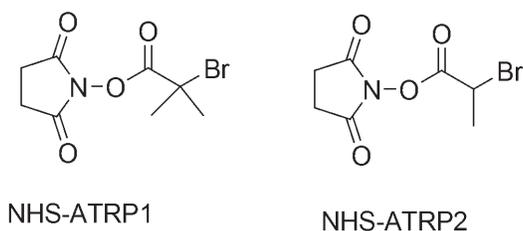
NHS-ATRP1

NHS-ATRP2

Scheme 15: Structures of NHS-functionalized ATRP initiators.

The NHS-ATRP2 (*Scheme 15*) was successfully used to initiate the ATRP copolymerization of 2-naphthoxytriethyleneglycol methacrylate with a fluorescent rhodamine B methacrylate monomer by using CuBr/bpy as the catalytic system.[31] These copolymers (M_n = 6.9 and 12 kDa, PDI = 1.05-1.06) were used to target supramolecular glycopolymers in water.

Haddleton and coworkers described the well-controlled (co)polymerization of PEGMA with hostasol methacrylate (HMA) using NHS-ATRP2 initiator (*Scheme 15*) and using CuBr/*N*-ethyl-2-pyridylmethanimine as the catalytic system in toluene at 50°C to yield NHS-functionalized copolymers which were then coupled onto hair fibers.[32] The

same group coupled α-keratine to NHS-functionalized poly(poly(ethylene glycol) monomethyl ether methacrylate) (PPEGMA) (M_n= 10300–13400 g.mol^{-1}, PDI = 1.09-1.11) and poly(diethylene glycol methyl ether methacrylate) (PDEGMEMA, M_n = 2000-46500 g.mol^{-1}, PDI = 1.22-1.81).[33] Moreover, well-defined NHS-functionalized PPEGMA polymers (M_n = 2.8 and 6.4 kDa, PDI < 1.15) (*Scheme 16(a)*) react with lysozyme in order to target new bioconjugates.[34]

In a similar approach, the quantitative conjugation of NHS-terminated poly(2-methacryloyloxyethylphosphorylcholine)s (PMPC, M_n = 2.3-8.2 kg.mol^{-1}, PDI = 1.2-1.5) with lysozyme was reported by Emrick and coworkers (*Scheme 16(b)*).[35] The polymerization of 2-methacryloyloxyethylphosphorylcholine (MPC) was performed in the presence of CuBr/bpy used as the catalytic system and NHS-terminated initiators (NHS-ATRP1 and NHS-ATRP2, *Scheme 15*) in DMSO/methanol at room temperature. The NHS-terminated PMPC was then attached with a lysozyme in different aqueous buffers (pH = 6-9.4) to target lysozyme-PMPC conjugates. However, the NHS-terminated PMPC was not efficient to react with an amine moiety of interferon-2αa (IFN).[36]
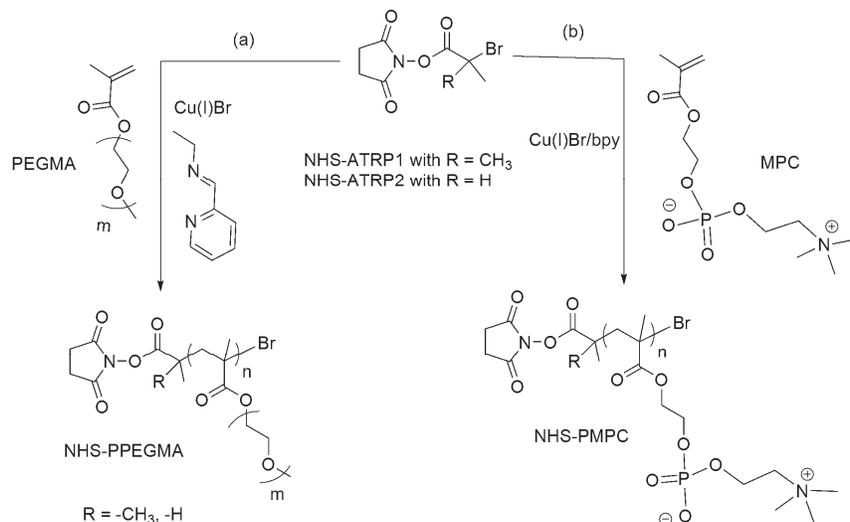
Scheme 16: Synthesis of NHS-terminated polymers by ATRP: (a) NHS-PPEGMA and (b) NHS-PMPC.

Zarafshani *et al.*[37] have recently reported the synthesis of thermoresponsive oligo(ethylene glycol)methyl ether methacrylate (OEGMA) based copolymers for bioconjugation of trypsin using ATRP. The synthesis of NHS-functionalized copolymers of 2-(2-methoxyethoxy)ethyl methacrylate (MEO$_2$MA) and OEGMA was carried out using NHS-ATRP1 and NHS-ATRP2 as initiators in the presence of CuCl/bpy at 60°C (*Scheme 17*). These copolymers (M$_n$ = 7400-13400 g.mol^{-1}, PDI = 1.15-1.24) were then conjugated to trypsin in borax-HCl buffer at 4°C and room temperature in 2 h (*Scheme 17*).
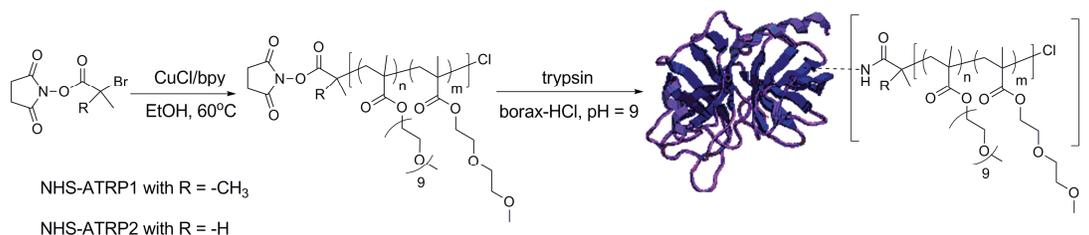
Scheme 17: General strategy to target P(MEO$_2$MA-co-OEGMA)-trypsin conjugates.

P(MEO$_2$MA-*co*-OEGMA)-trypsin conjugates were found to be thermoresponsive and showed enhanced enzymatic activity in comparison with unmodified trypsin. Other bioconjugates were obtained using the same strategy with NHS-functionalized poly(oligo(ethylene glycol)methyl ether methacrylate)[38] (POEGMA), PPEGMA[39] and NHS-functionalized poly((2-dimethylamino)ethyl methacrylate)[40] (PDMAEMA) previously synthesized by ATRP.

In another study, Tan *et al.*[41] showed that the NHS-terminated P(MEO$_2$MA-*co*-OEGMA) copolymer (M_n = 6220-18120 g.mol^{-1}, PDI = 1.28-1.66) obtained *via* ATRP could be used as composite chromatography materials by grafting the copolymer onto amino-functionalized silica monoliths.

Delaittre *et al.*[42] reported the ATRP synthesis of NHS-functionalized PEOGMA-*b*-PS (M_n = 7400-13400 g.mol^{-1}, PDI = 1.15-1.24) block copolymers. The NHS-functionalized nanoparticles obtained from the self-assembly of such amphiphilic block copolymers could react with primary amine for potential bioconjugation.

PFP-ester

McRae *et al.*[43] reported the synthesis of well-defined PFP-functionalized PMPC (M_n = 5000-27000 g.mol^{-1}, PDI = 1.2-1.5) using PFP-ATRP1 (*Scheme 18*) as the ATRP initiator to mediate the polymerization of MPC in the presence of CuBr/bpy as the catalytic system in DMSO/methanol at room temperature. A PFP-functionalized PMPC (M_n = 11700 g.mol^{-1}, PDI = 1.3) subsequently reacts with lysozyme in borate buffer (pH = 9) to target the PMPC-lysozyme bioconjugate. After 12 hours, the conjugation yield was determined to be more than 80% by high performance liquid chromatography

(HPLC) and fast protein liquid chromatography (FPLC). In this work, well-defined two-arm PFP-functionalized PMPCs (M_n = 9400-213000 g.mol^{-1}, PDI = 1.2-1.3) were also synthesized by using the PFP-functionalized two-arm initiator (PFP-ATRP2, *Scheme 18*) and subjected to bioconjugation with lysozyme.
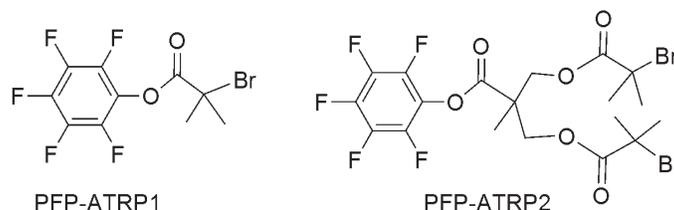
Scheme 18: Structures of PFP-functionalized ATRP initiators.

Linear carbonate

Chen *et al.*[44] described the synthesis of NHS-carbonate-terminated PMPC (M_n = 6000-53000 g.mol^{-1}, PDI = 1.30–2.9) using carbonate-ATRP2 (*Scheme 19*) as the ATRP initiator and CuBr/bpy as the catalytic system in ionic liquid at room temperature. The NHS-carbonate-terminated PMPC (M_n = 8000 g.mol^{-1}, PDI = 1.30) was then used for protein conjugation using a lysozyme in sodium borate buffer at pH = 9.0 (*Scheme 19*). The quantitative conjugation was characterized by cation-exchange FPLC.
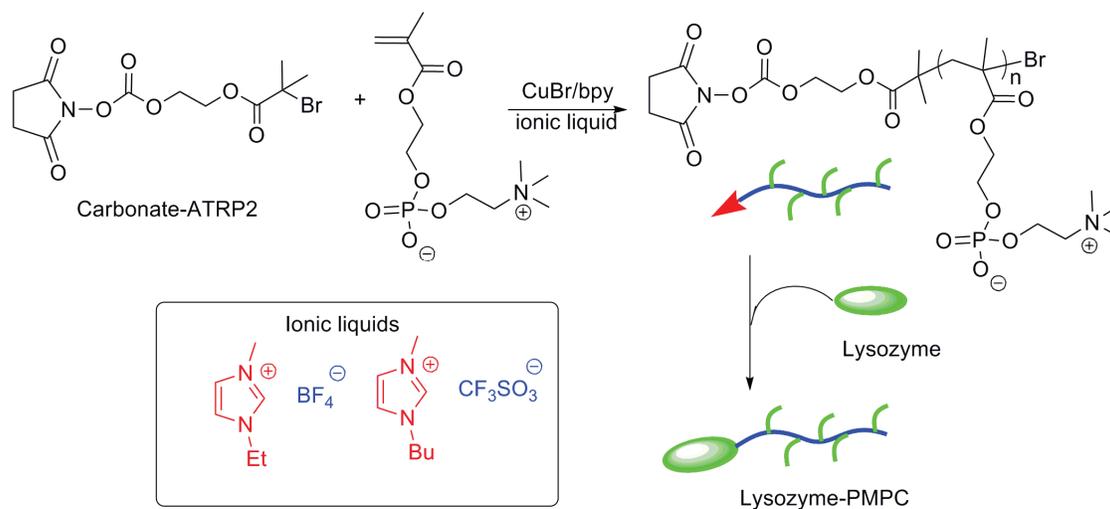
Scheme 19: Polymerization of MPC using CuBr/bpy as the catalytic system, NHS-carbonate-functionalized ATRP initiator in ionic liquid at room temperature. Protein conjugation of the resulting PMPC.

In a similar work, ferritin-polymer conjugates were reported by Emrick and coworkers.[45] In this study, NHS-carbonate-terminated PPEGMAs (M_n = 54000-19000 g.mol^{-1}, PDI = 1.09–1.15) were synthesized by ATRP using carbonate-ATRP3 (*Scheme 20*) as the initiator and CuBr/PDMETA as the catalytic system in toluene at room temperature. The conjugation of NHS-carbonate PPEGMAs to ferritin was then performed in phosphate buffered saline (PBS) (pH = 9.0) with a 50 fold excess of polymer. The quantitative conjugation was characterized by FPLC. However, authors showed that using a NHS-carbonate-terminated PMPC synthesized in a similar way that the NHS-carbonate-terminated PPEGMA, there was no conjugation to ferritin due to the hydrolysis of NHS-carbonate-terminated PMPC during the reaction. Well-defined PFP-carbonate-terminated PMPCs (M_n = 6450-16000 g.mol^{-1}, PDI = 1.30-1.40) were synthesized by using carbonate-ATRP4 (*Scheme 20*) and successfully conjugated with lysozyme.[43]
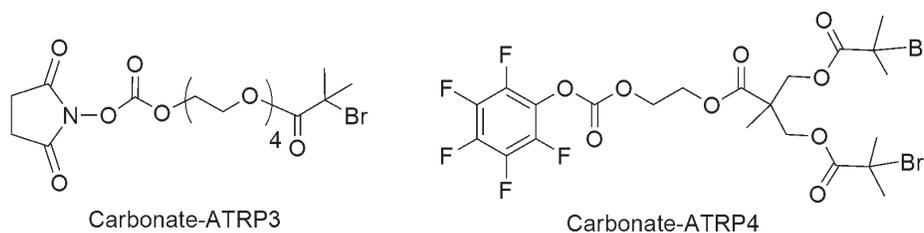
Scheme 20: Structures of carbonate-functionalized ATRP initiators.

3.1.1.3. Using a Reversible Addition/Fragmentation chain Transfer (RAFT) agent

Telechelic polymers can be easily obtained by RAFT polymerization *via* the judicious selection of the RAFT agent (*Scheme 21*). The α-functional polymer can be synthesized by fixing the functionality onto the R group of the RAFT agent while the ω-end-group functionalized polymer can be targeted *via* the Z group of the RAFT agent.
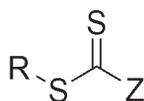
Scheme 21: Structure of a RAFT agent.

3.1.1.3.a. Reactive groups not leading to molecular side-products

Epoxide

Vora *et al.*[46] have synthesized epoxide and oxetane functionalized RAFT agents (*Scheme 22*). These RAFT agents were used to control the polymerization of several (metha)acrylates (*n*-BA, 2-ethylhexyl acrylate 2-EHA, lauryl acrylate LA and *n*-butyl methacrylate *n*-BMA) and S with polydispersity indices below 1.10. Epoxide-terminated polymers were modified with different functional molecules such as amines, alcohols and carboxylic acids.
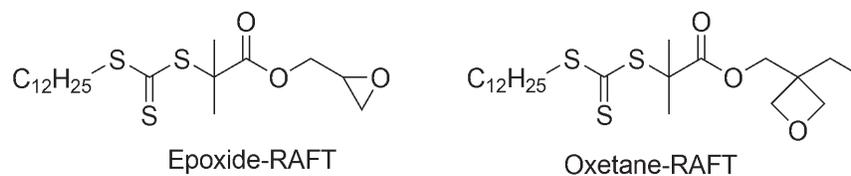
Scheme 22: Structures of epoxide and oxetane-functionalized RAFT agents.

Azlactone

Lewandowski *et al.*[47] reported the synthesis of two azlactone-functionalized xanthates (Azl-RAFT1 and Azl-RAFT2) used as RAFT agents for the polymerization of acrylates and S (*Scheme 23*).
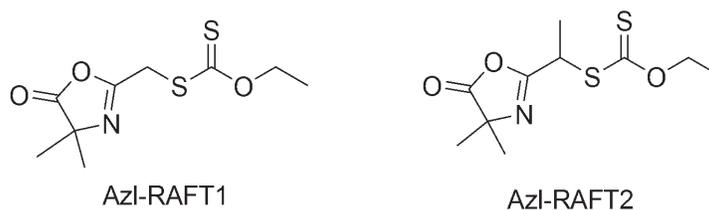
Scheme 23: Azlactone-functionalized RAFT agents.

The RAFT polymerization of 2-EHA was carried out using Azl-RAFT1 (*Scheme 24*) as RAFT agent and using 2,2'-azobisiosbutyronitrile (AIBN) as the thermal initiator in ethyl acetate (EAc) at 70°C. Typically, an azlactone-terminated poly(2-ethylhexyl acrylate) (P(2-EHA)) with a M_n of 5720 g.mol^{-1} and a high polydispersity index (PDI = 1.88) has been obtained. Using similar conditions, the RAFT polymerization of styrene and isobornyl acrylate (IBA) was performed using Azl-RAFT2 (*Scheme 24*). However, high polydispersity indices were obtained either for PS (M_n = 2820 g.mol^{-1}, PDI = 1.84) or for poly(isobornyl acrylate) (PIBA, M_n = 3630 g.mol^{-1}, PDI = 1.82).
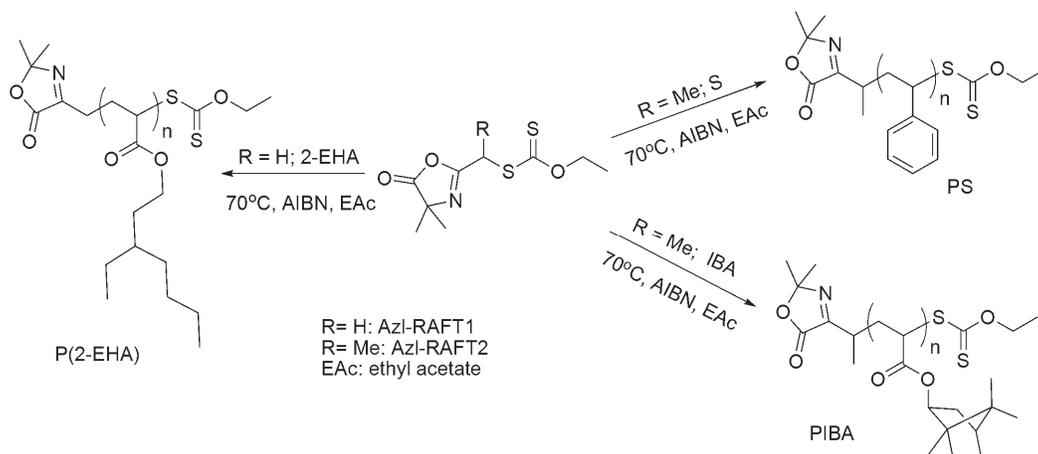
Scheme 24: Polymerization of 2-EHA, IBA and S in the presence of azlactone-functionalized RAFT agents.

3.1.1.3.b. Reactive groups leading to molecular side-products

NHS-ester

Bathfield *et al.*[48] reported the synthesis of a NHS-functionalized RAFT agent (NHS-RAFT1, *Scheme 25*) and its use to mediate the RAFT polymerization of *N*-acryloylmorpholine (NAM) in dioxane at 90°C. Well-defined NHS-terminated poly(*N*-acryloylmorpholine)s (PNAM, M_n = 212000 and 410000 g.mol^{-1}, PDI ≤ 1.11) were obtained.
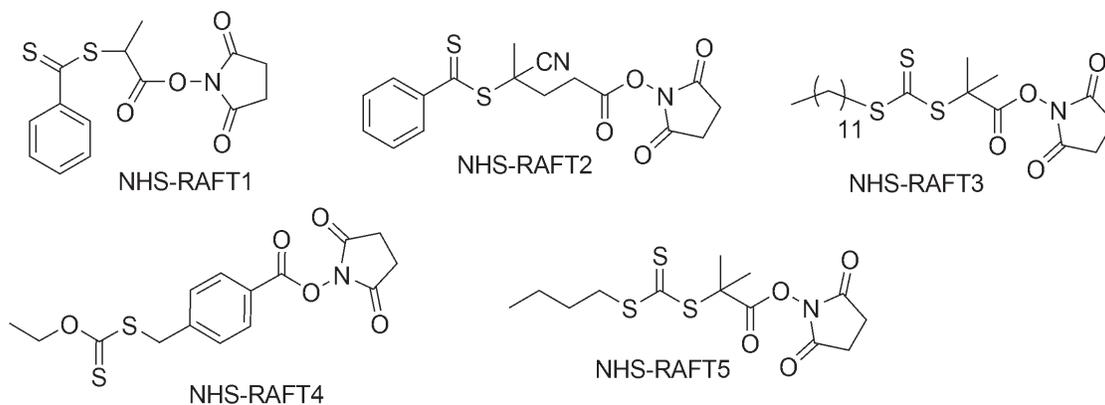
Scheme 25: Structures of NHS-functionalized RAFT agents.

The NHS–RAFT2 (*Scheme 25*) was used for the synthesis of NHS-terminated poly(*N*-oxysuccinimidyl-4-vinylbenzoate) (PNHSVB) (M_n = 4400-61000 g.mol^{-1}, PDI = 1.03-1.07) and subsequent coupling with amine-functionalized terpyridine (terpy), creating a new polymer bearing terpy ligands.[49] Han *et al*.[50] reported the polymerization of S using NHS-RAFT3 (*Scheme 25*) as the RAFT agent and AIBN as the initiator in THF at 110°C producing NHS-functionalized PS (M_n = 44000-13280 g.mol^{-1}, PDI = 1.03-1.06).

McDowall *et al*.[51] reported the synthesis of NHS-terminated poly(*N*-vinylpyrrolidone) (PNVP, M_n = 16900-334000 g.mol^{-1}, PDI = 1.38-1.41) obtained from the bulk polymerization of *N*-vinylpyrrolidone (NVP) in the presence of NHS-RAFT4 used as the RAFT agent (*Scheme 25*) and AIBN used as the initiator at 60°C. PNVPs were then used for conjugation to lysozyme. The coupling of NHS-terminated PNVP with lysozyme was performed in anhydrous DMSO and triethylamine (TEA) at 25°C under nitrogen. In a similar work, thermoreponsive NHS-terminated poly(*N*-isopropyl acrylamide) (PNIPAM, M_n = 5100-15700 g.mol^{-1}, PDI $\leq$ 1.10) were synthesized by polymerization of *N*-isopropyl acrylamide (NIPAM) using NHS-RAFT5 (*Scheme 25*) as the RAFT agent and using AIBN in dioxane at 60°C. The resulting polymer was then conjugated to lysozyme in phosphate buffer (pH = 7.5).[52]

PFP- ester

Roth *et al*.[53] described the synthesis of a new PFP-ester-functionalized RAFT agent (PFP-RAFT1, *Scheme 26*) which has been used to mediate the polymerization of several monomers (e.g. MMA, DEGMEMA, PEGMA and lauryl methacrylate (LMA)).

Resulting PFP-functionalized polymers were then employed for several purposes. For instance, Theato and coworkers reported the versatile synthesis of collagen-polymer conjugates *via* the attachment of PFP-terminated PDEGMEMA (M_n = 5600 g.mol^{-1}, PDI=1.26) to amine-functionalized collagen in the presence of TEA in *N,N*-dimethylformamide (DMF) at 35°C.[54] Well-defined PFP-functionalized PDEGMEMAs (PDI ≤ 1.14) were also employed as reactive polymers towards fluorescent amines and thyroxin.[55-56]

PFP-RAFT1

PFP-RAFT2
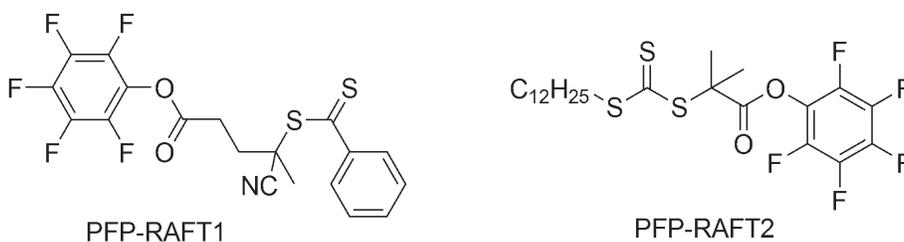
Scheme 26: Structures of PFP-functionalized RAFT agents.

A simple route towards α,ω-heterotelechelic thermoresponsive POEGMA was investigated by Theato and coworkers. The "one-pot" coupling of different amines and functional methylmethane thiosulfonates was carried out on PFP-terminated POEGMA (M_n = 3550 g.mol^{-1}, PDI = 1.14) previously synthesized by RAFT polymerization using PFP-RAFT1 as RAFT agent (*Scheme 26*).[57] In the same approach, a PFP-functionalized PMMA (M_n = 9800 g.mol^{-1}, PDI = 1.14) was coupled with a fluorescent dye Texas Red leading to well-defined α-Texas Red-functionalized PMMA (M_n = 12200 g.mol^{-1}, PDI = 1.13) with a yield of dye labeling equal to 74%.[58]

Wiss *et al.*[59] employed two different strategies to target alkyne- and azide-terminated polymers which were then used as precursors for "click" reaction (*Scheme 27*). Functionalizations using alkyne-based amine and azido-based amine of

either the RAFT agent (Route A, *Scheme 27*) prior to polymerization of methacrylates (MMA, DEGMEMA, *t*-BMA) or either the resulting polymers PDEGMEMA and poly(*tert*-butyl methacrylate) (P(*t*-BMA)) after polymerization (Route B, *Scheme 27*) were studied.
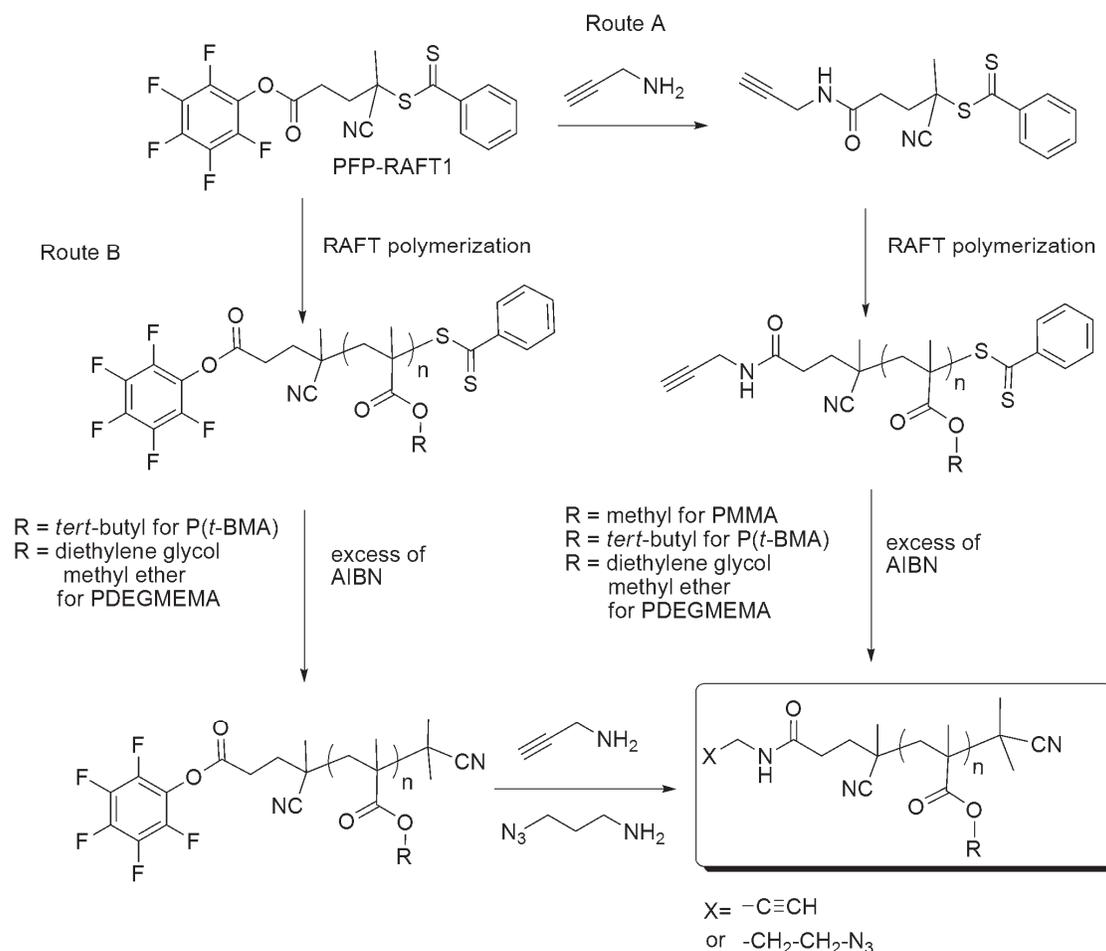
Scheme 27: Overview of the different synthetic routes towards alkyne and azido-based polymers obtained by RAFT polymerization of methacrylates mediated by a PFP-functionalized RAFT agent.

Godula *et al.*[60] synthesized a new PFP-terminated RAFT agent (PFP-RAFT2, *Scheme 28*) which was employed to mediate the polymerization of (2-oxopropyl)acrylate in the presence of 4,4'-azobis(4-cyanovaleric acid) (ACVA) as the initiator in DMF at

65°C. The resulting well-defined PFP-terminated poly((2-oxopropyl)acrylate) (M_n = 114100 g.mol^{-1}, PDI = 1.15) then reacts with *N*-propargylamine in the presence of diisopropylethylamine (DIPEA) in DMF at room temperature to yield an alkyne-functionalized polymer.
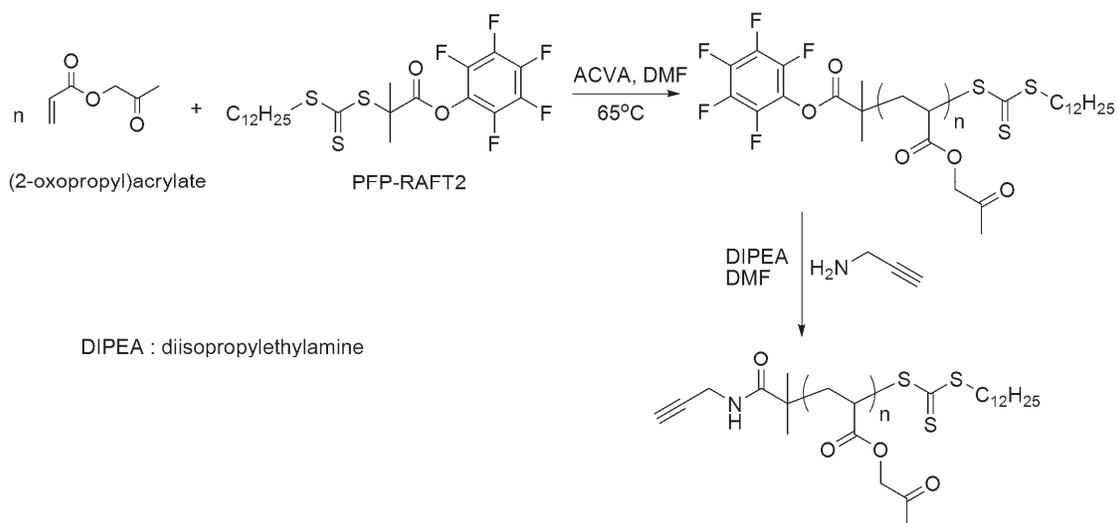
Scheme 28: Synthesis of PFP-terminated poly((2-oxopropyl)acrylate) by RAFT polymerization and its subsequent reaction with N-propargylamine.

Thiazolidine-2-thione

Davis and coworkers reported the bioconjugation of lysozyme with TT-functionalized poly(*N*-(2-hydroxypropyl) methacrylamide) (PHPMA) and PPEGMA polymers obtained *via* RAFT polymerization (*Entries 1-4, Table 2*).[61-64] Well-defined TT-functionalized PHPMAs were synthesized using either a TT-terminated dithioester or trithiocarbonate as chain transfer agents to mediate the RAFT polymerization of *N*-(2-hydroxypropyl) methacrylamide (HPMA).[61,62] The resulting PHMPAs obtained were then attached with lysozyme in PBS solution to target protein-polymer conjugates. Moreover, a TT-terminated PHPMAs (M_n = 7600 g.mol^{-1}, PDI = 1.16) were also coupled

with dendritic mannose to target the polymer-dendritic carbohydrate bioconjugate.[66] In similar conditions, TT-functionalized PPEGMAs were also synthesized and subsequently conjugated with lysozyme.[63] The same group reported the synthesis of well-defined thiazolidine-2-thione-functionalized PPEGMA (M_n = 4800 g.mol^{-1}, PDI = 1.09) and its conjugation with lysozyme (*Entry 4, Table 2*).[64] The disulfide bond within the lysozyme-polymer conjugate could be cleaved in the presence of tris(2-carboxyethyl) phosphine hydrochloride to released the lysozyme. Luo *et al.*[65] reported the RAFT polymerization of poly(ethylene glycol) monomethyl ether acrylate (PEGA) using a novel TT-functionalized trithiocarbonate as the RAFT agent and AIBN as the initiator in dioxane at 75°C (*Entry 5, Table 2*). The resulting TT-terminated poly(poly(ethylene glycol) monomethyl ether acrylate) (PPEGA) was then reacted with glucose oxidase.

Table 2: Experimental conditions used for the synthesis of well-defined thiazolidine-2-thione-functionalized polymers by RAFT polymerization.

Entry	TT-functinonalized RAFT agent	Monomer	Experimental conditions	Targeting molecule	Ref.
1	[chemical structure]	HPMA	AIBN/dioxane-methanol/65°C	lysozyme	61
			AIBN/ N,N-dimethylacetamide (DMAc)/70°C	dendritic mannose	66
2	[chemical structure]	HPMA	AIBN/ DMAc-methanol/65°C	lysozyme	62
		PEGMA	AIBN/dioxane/65°C		63
3	[chemical structure]	HPMA	AIBN/ DMAc-methanol/65°C	lysozyme	62
		PEGMA	AIBN/dioxane/65°C		63
4	[chemical structure]	PEGMA	AIBN/dioxane/80°C	lysozyme	64
5	[chemical structure]	PEGA	AIBN/dioxane/75°C	glucose oxidase	65
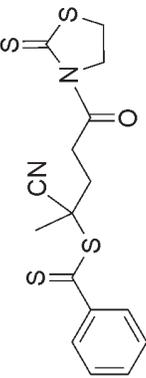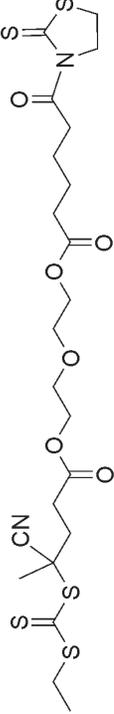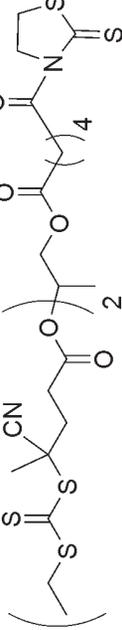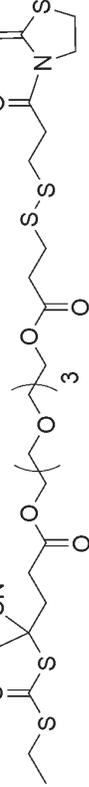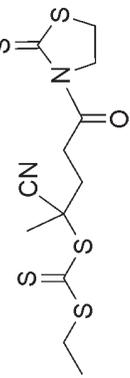
3.1.2. Using a functional monomer

A serie of amine-reactive monomers has been polymerized using CRP techniques

Table 3: Summary of functional monomers used in CRP to target amino-reactive polymers.

Functionality	Monomer	CRP method	Ref.
Epoxide		NMP	67
		ATRP	87
		NMP	68-72
		ATRP	88-122
		RAFT	150-161
		NMP	73
		ATRP	73
Azlactone		NMP	74
		ATRP	123-127
		RAFT	162-166
Isocyanate		NMP	75-77
		ATRP	128, 129
		RAFT	167-170, 172
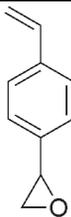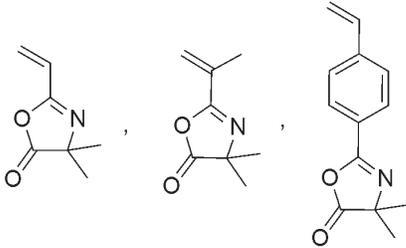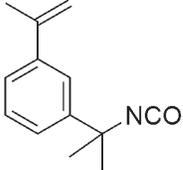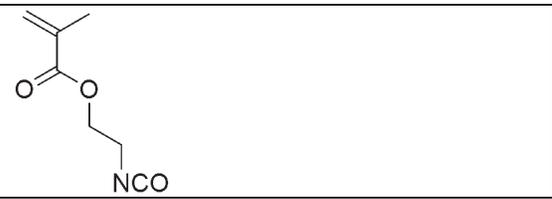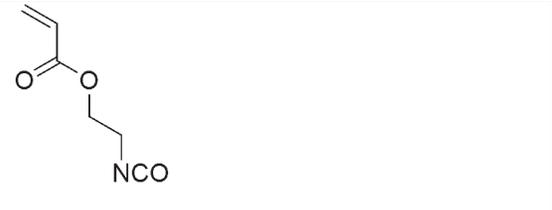
		RAFT	171-173
		RAFT	13
NHS-ester		NMP	78, 79
		ATRP	131-134
		RAFT	190-194, 197-211
		ATRP	135-141
		RAFT	195, 196
		NMP	78
		ATRP	142-144
		RAFT	78
PFP-ester		NMP	80, 81
		NMP	82
		RAFT	
		ATRP	145
		RAFT	212-222
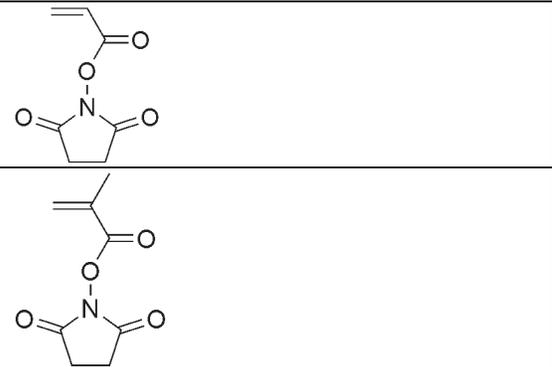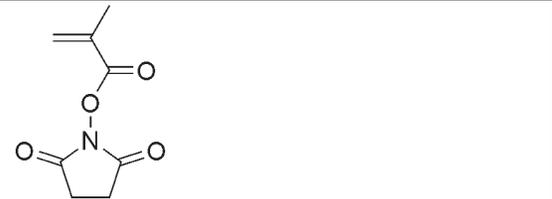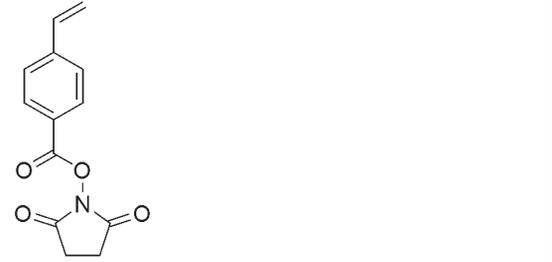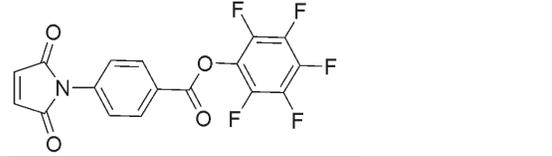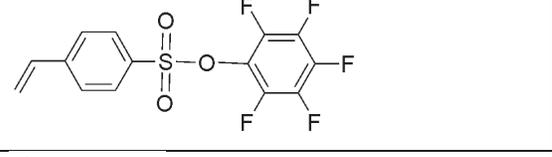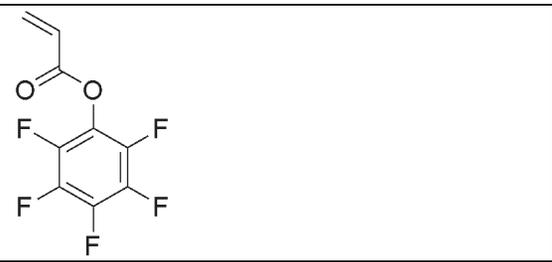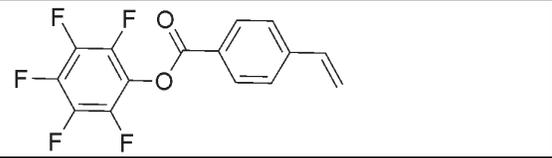
		RAFT	223-231
		RAFT	232, 233
PNP-ester		RAFT	234, 235
		ATRP	146
		RAFP	236, 237
Carbonate		NMP	83
		ATRP	147-149
		ATRP	130
Anhydride		NMP	84-86
		RAFT	174-189
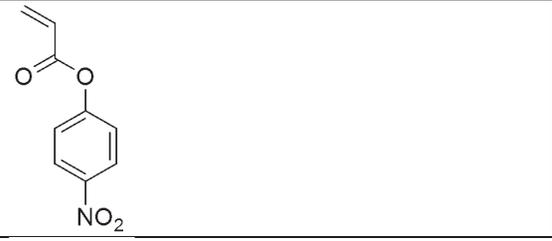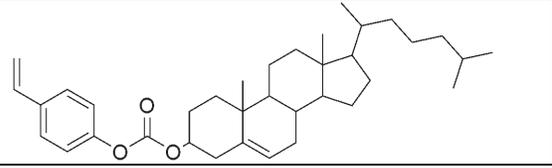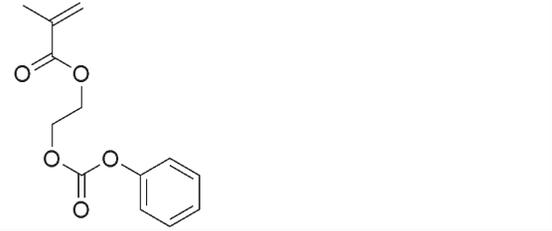
3.1.2.1. By Nitroxide-Mediated Polymerization (NMP)

NMP could be applied to monomers containing reactive polymers with reactive groups towards amines if structures of alkoxyamines and of nitroxides used to mediate the polymerizations are appropriately chosen.

3.1.2.1.a. Reactive groups not leading to molecular side-products

Epoxide

Hawker and coworkers developed an universal alkoxyamine: *N-tert*-butyl-*N*-(2-methyl-1-phenylpropyl)-*O*-(1-phenylethyl)hydroxylamine[67] (A1, *Scheme 29*) which has been used to mediate the copolymerization of different functional monomers such as glycidyl acrylate (GA). The copolymerization of GA and *t*-BA has been carried out in bulk at 120^oC. Low polydispersity indices (PDIs ≤ 1.28) and controlled M_n ($M_n = 20000$-23000 g.mol^{-1}) were obtained at low levels of incorporation of GA (below 25%). When the amount of GA increases, polydispersities indices rise to 1.55.
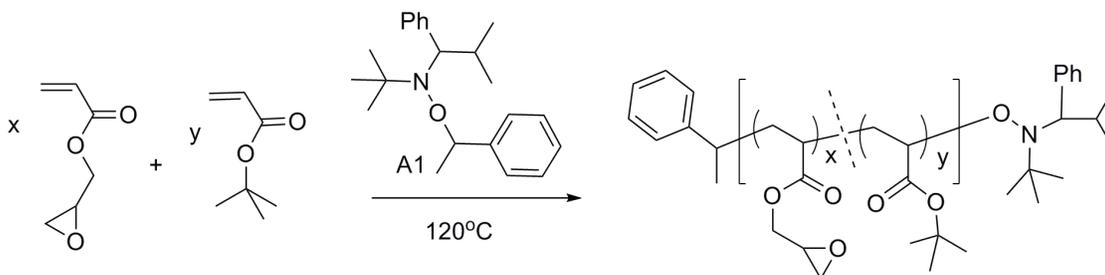
Scheme 29: Copolymerization of GA and t-BA by NMP.

Moreover, this universal alkoxyamine (A1, *Scheme 29*) was also used as initiator for the copolymerization of GMA, S and trimethylsilylethinylstyrene in bulk at 120^oC. The resulting copolymer was deprotected with tetrabutylammonium fluoride, led to the corresponding alkyl-functionalized copolymer ($M_n = 30500$ g.mol^{-1}, PDI = 1.30).[68]

Grubbs *et al.*[69] have reported the random copolymerization of methyl acrylate (MA) and GMA using NMP (*Scheme 30*). The resulting copolymer (M_n = 6340 g.mol^{-1}, PDI = 1.25) was used as a macromolecular alkoxylamine to mediate the polymerization of I at 125°C. A well-defined P(MA-*co*-GMA)-*b*-PI block copolymer of M_n equal to 42000 g.mol^{-1} and PDI equal to 1.22 was synthesized (*Scheme 30*).
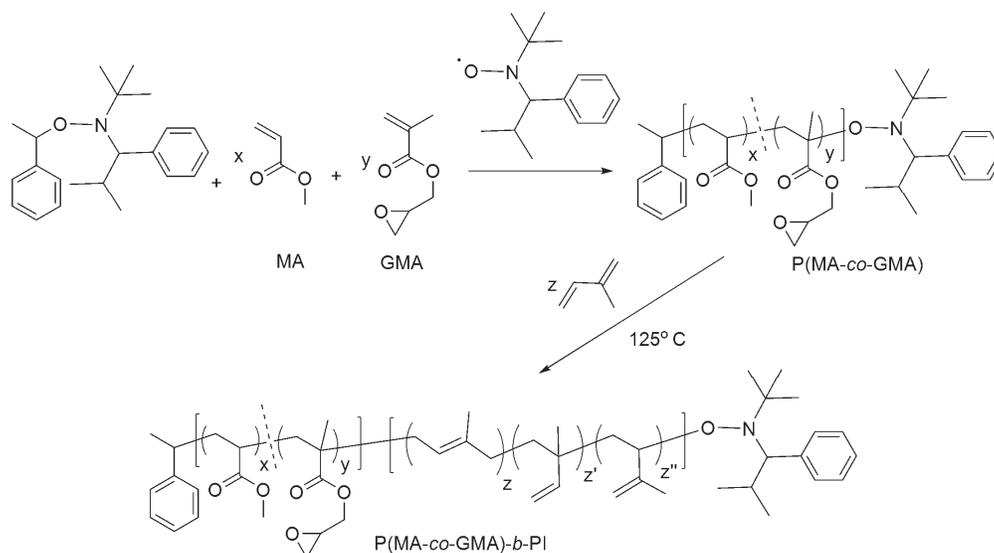
Scheme 30: Synthesis of block copolymer based on MA, GMA and I via NMP.

Maric and coworkers reported the synthesis of well-defined copolymers bearing epoxide side groups by NMP of S and GMA in dioxane at 90°C with variable amounts of GMA ($f_{GMA,0}$ = 0.12-0.94).[70] Some of these copolymers (M_n = 8600-11400 g.mol^{-1}, PDI = 1.25-1.38) were employed as macroinitiators for the polymerization of S at 110°C leading to P(S-*co*-GMA)-*b*-PS block copolymers. The *N*-(2-methylpropyl)-*N*-(1-diethylphosphono-2,2-dimethylpropyl)-*O*-(2-carboxylprop-2-yl)hydroxylamine (MAMA-SG1, *Scheme 31*) was used as an alkoxylamine to mediate the NMP copolymerization of S with different methacrylate monomers (e.g MMA, ethyl methacrylate EMA, *n*-BMA) in *p*-xylene at 90°C. Resulting copolymers with M_n up to

33500 g.mol^{-1} and polydispersity indices below 1.46 were then employed as macroalkoxyamines to mediate the copolymerization of S/GMA and of MMA/EMA/n-BMA in p-xylene at 90°C. Final block copolymers present high polydispersity indices (PDI = 1.36-2.77).[71]
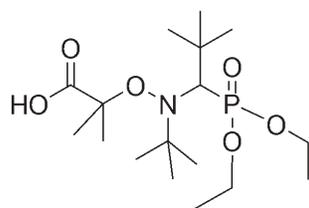
MAMA-SG1

Scheme 31: Structure of MAMA-SG1 akoxylamine.

In a similar approach, Lessard *et al.*[72] reported the synthesis of P(t-BMA-*co*-S)-*b*-P(GMA-*co*-MMA-*co*-S) block copolymers using NMP (*Scheme 32*). P(t-BMA-*co*-S) copolymers were synthesized by copolymerization of t-BMA and S in the presence of MAMA-SG1 and free radical N-*tert*-butyl-N-1-diethylphosphono-(2,2-dimethylpropyl) nitroxide (SG1) ([SG1]$_0$/[MAMA-SG1]$_0$ ~ 0.1) in bulk at 90°C. The P(t-BMA-*co*-S) copolymer of M$_n$ = 14200 g.mol^{-1} and PDI = 1.30 was then used as macroinitiator to initiate a ternary batch polymerization of GMA, MMA, and S in dioxane at 85°C to yield the P(t-BMA-*co*-S)-*b*-P(GMA-*co*-MMA-*co*-S) block copolymers (M$_n$ = 32900 g.mol^{-1}, PDI = 1.30) bearing epoxide functional groups.

P(*t*-BMA-*co*-S)   SG1

P(*t*-BMA-*co*-S)-*b*-P(GMA-*co*-MMA-*co*-S)
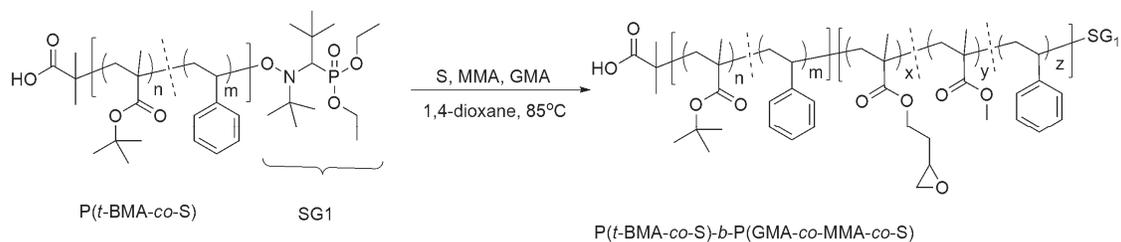
Scheme 32: Copolymerization of S, MMA, GMA using P(t-BMA-co-S) as the macromolecular alkoxyamine in dioxane at 85°C.

Jones *et al.*[73] reported the synthesis of epoxystyrene (ES) and its copolymerization with S by NMP and ATRP. The copolymerization of ES and S was carried out using dibenzoyl peroxide (BPO) and 2,2,6,6-tetramethyl-1-piperidinyloxyl (TEMPO) radical in bulk at 120°C (*Scheme 33*). Although high polydispersity indices of P(ES-*co*-S) were obtained (PDI > 1.50), the epoxide group was found to be stable under the conditions of polymerization.
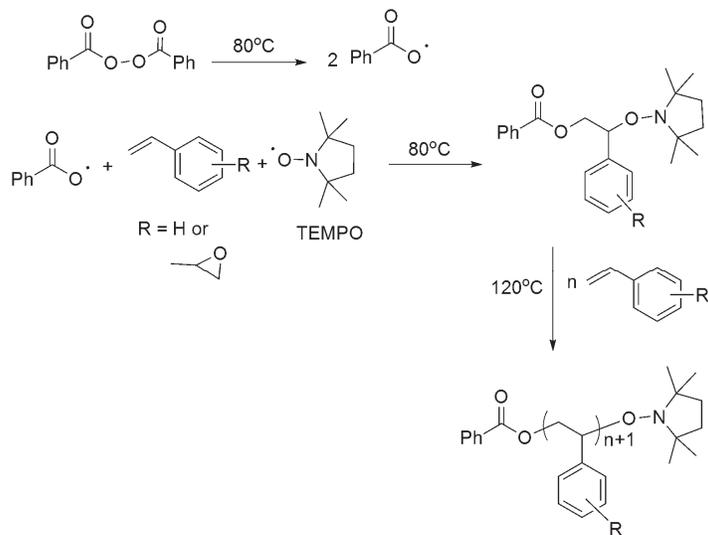
Scheme 33: Copolymerization of ES and S by NMP in the presence of TEMPO and BPO in bulk at 120°.

Azlactone

Tully *et al.*[74] showed that the polymerization of 2-vinyl-4,4-dimethylazlactone (VDM) carried out in bulk in the presence of A1 (*Scheme 34*) used as an alkoxyamine and in the presence of the corresponding nitroxide (N1, *Scheme 34*) leads to well-defined polymers poly(2-vinyl-4,4-dimethylazlactone)s (PVDMs) with PDIs below 1.10. When bulk polymerizations of 2-(4'-vinyl)phenyl-4,4-dimethylazlactone (VPDM, *Scheme 34*) and 2-isopropenyl-4,4-dimethylazlactone (IPDM, *Scheme 34*) were performed in similar experimental conditions, a poly(2-(4'-vinyl)phenyl-4,4-dimethylazlactone) (PVPDM) was obtained with a controlled M_n up to 35600 g.mol^{-1} and PDI below 1.30. High polydispersity indices (PDIs > 1.50) were obtained for poly(2-isopropenyl-4,4-dimethylazlactone)s (PIPDMs). Introducing styrene as a comonomer during the NMP of IPDM leads to statistical copolymers (M_n = 31500- 46100 g.mol^{-1}) with PDIs below 1.40. Additionally, copolymerizations of VDM and a series of monomers such as *N,N*-dimethyl acrylamide (DMA), NVP, AN and S were also performed by NMP using A1 and N1 (*Scheme 34*) at 123°C to yield well-defined statistical copolymers (PDI < 1.30). Furthermore, well-defined block copolymers bearing azlactone functional groups such as PVDM-*b*-PS (M_n = 34300-90800 g.mol^{-1}; PDI = 1.15-1.26) and P(*n*-BA)-*b*-PVDM (M_n = 26600-41600 g.mol^{-1}; PDI = 1.09-1.19) were synthesized using NMP at 123°C. However, attempts for the synthesis of a PVDM-*b*-P(*n*-BA) and PS-*b*-PVDM block copolymers using PVDM and PS macroinitiators, respectively were not successful. The azlactone-functionalized PVDM and PVDM-*b*-PS were reacted with amines such as benzylamine, to show the reactivity of azlactone groups.
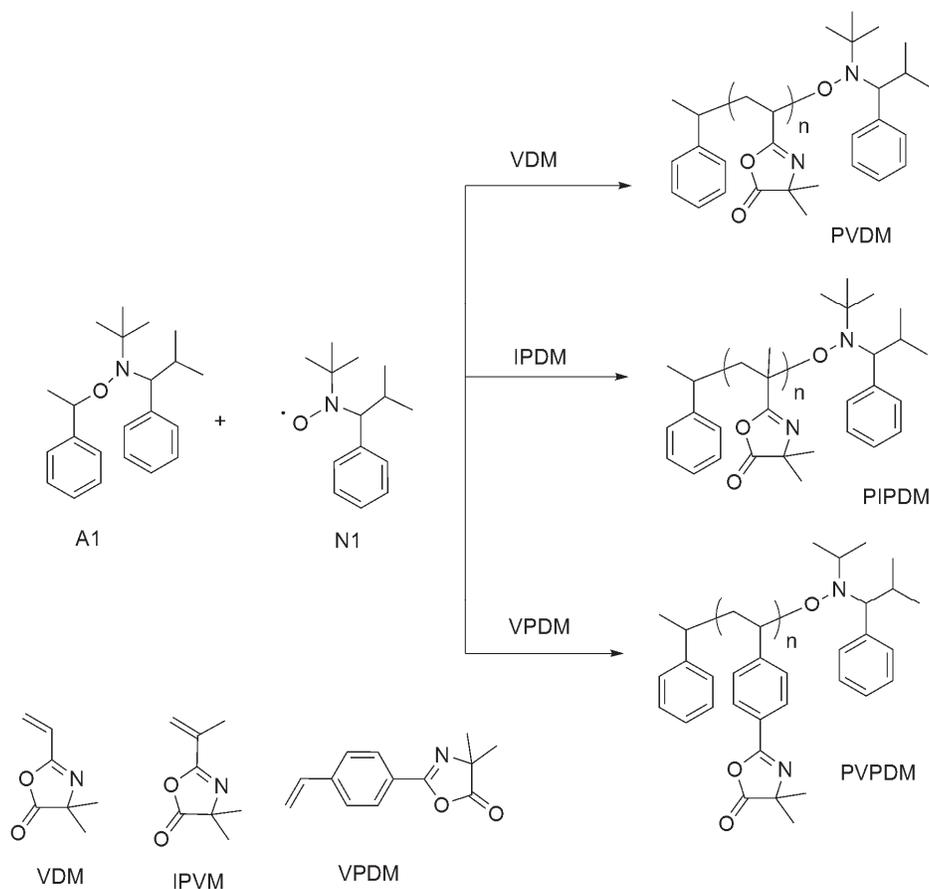
Scheme 34: NMP of VDM, IPDM, VPDM using an alkoxylamine and a free nitroxide in bulk at 123°C.

Isocyanate

Hodges *et al.*[75] reported the synthesis of the TEMPO-functionalized Rasta resin (TEMPO-resin) and its use to mediate the copolymerization of *m*-isopropenyl-α,α-dimethylbenzylisocyanate (TMI) with *n*-BA, S and pentafluorostyrene (PFS) *(Scheme 35).* As one example, the copolymerization of TMI and S was performed in the presence of TEMPO-functionalized Rasta resin at 130°C to yield isocyanate-functionalized resin. This functional resin was then successfully used to scavenge a wide variety of primary and secondary amines.
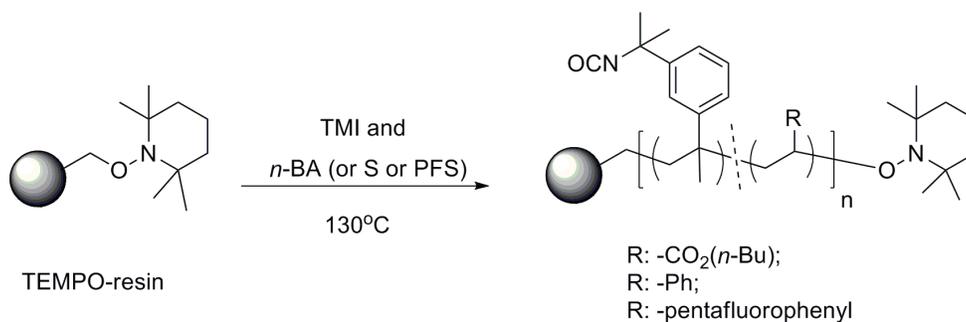
Scheme 35: Synthesis of isocyanate-functionalized Rasta resin by NMP.

Wisnoski *et al.*[76] reported the NMP copolymerization of 4-vinyl pyridine and TMI using TEMPO-resin in bulk at 170°C to afford the isocyanate-functionalized resin and subsequently used it to scavenge the 4-bromophenethylamine. A High Internal Phase Emulsion (HIPE) support was grafted. P(S-*co*-TMI) was synthezied using TEMPO-functionalized HIPE as the alkoxylamine to mediate the nitroxide mediated copolymerization of S and TMI in bulk at 120°C.[77]

3.1.2.1.b. Reactive groups leading to molecular side-products

NHS-ester

Hawker and coworkers reported the nitroxide-mediated copolymerization of *N*-oxysuccinimidyl-4-vinylbenzoate (NHSVB) and S using an alkoxylamine (A2, *Scheme 36*) at 125°C.[78] The well-defined P(NHSVB-*co*-S) copolymer (M_n = 43000 g.mol^{-1}, PDI = 1.13) obtained was then reacted to an amine-functionalized dendrimer leading to dendritic copolymers. Moreover, the copolymerization of *N*-acryloyloxysuccinimide (NAS) and S was performed in bulk in the presence of the alkoxylamine (A2, *Scheme 36*) leading to well-defined random copolymers.
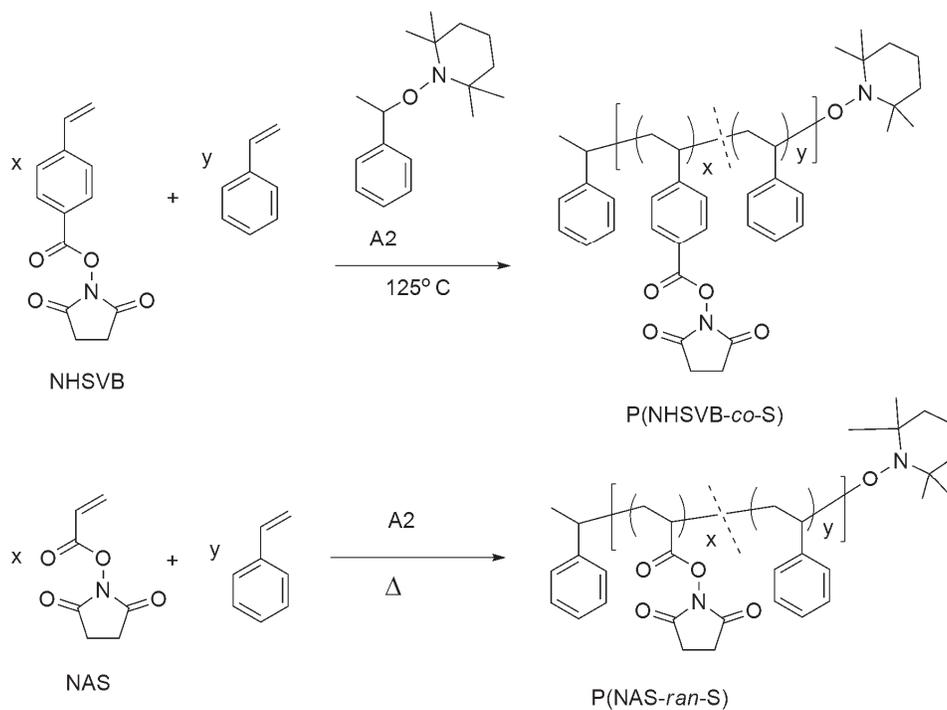
Scheme 36: Synthesis of NHS-functionalized copolymers P(NHSVB-co-S) and P(NAS-ran-S) using NMP.

Gigmes and coworkers recently reported the synthesis of poly(*N*-acryloyloxysuccinimide) (PNAS), P(NAS-*co*-NVP) and poly(*D,L*-lactide)-*b*-poly(NAS-*co*-NVP) by NMP.[79] The polymerizations of NAS were carried out in the presence of MAMA-SG1 (*Scheme 31*) and free radical SG1 (0-7.5% mol to MAMA-SG1) in DMF at 110°C. The amount of free radical SG1 equal to 2.5% mol to MAMA-SG1 was suggested to give the best polymerization control. Low polydispersity indices of polymers support the controlled character of the polymerization. Furthermore, the copolymerization of NAS and NVP was performed using MAMA-SG1 and free radical SG1 (5% mol to MAMA-SG1) in DMF at 100°C. The P(NAS-*co*-NVP)s copolymers have polydispersity indices below 1.4. In a similar procedure, the copolymerization of NAS and NVP was performed from a poly(*D,L*-lactide)-SG1

(PLA-SG1) used as the macromolecular alkoxyamine in DMF at 120°C to lead to PLA-*b*-P(NAS-*co*-NVP) block copolymers (M_n = 11000-17000 g.mol^{-1}, PDI = 1.34-1.64) which were then used for the synthesis of nanoparticles.

PFP-ester

Kakuchi *et al.*[80] reported the synthesis of poly(pentafluorophenyl-4-maleimidobenzoate-*co*-styrene) P(PFPMI-*co*-S) in the presence of MAMA-SG1 used as the alkoxyamine at 120°C in bulk (*Scheme 37*). Well-defined P(PFPMI-*co*-S)s were obtained with M_n ranging from 2800 g.mol^{-1} to 12000 g.mol^{-1} and polydispersity indices between 1.15 and 1.17. Resulting P(PFPMI-*co*-S)s then react with 2,4-dimethoxybenzylamine in THF at room temperature for post-polymerization.
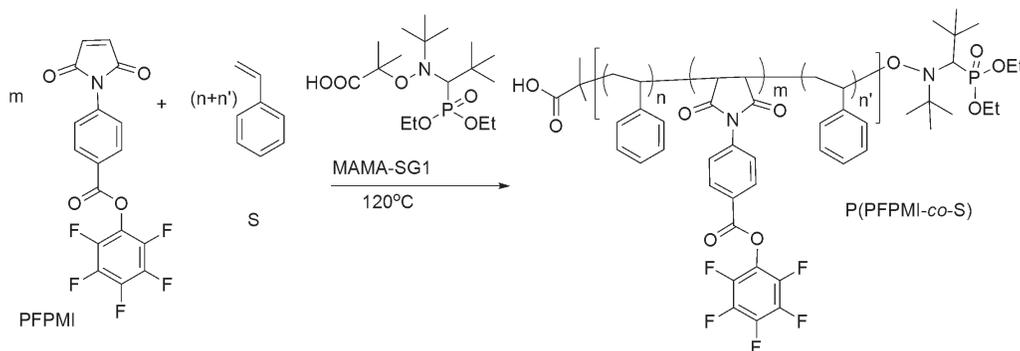
Scheme 37: Copolymerization of PFPMI and S
in the presence of MAMA-SG1 at 120°C in bulk.

In a similar work, the copolymerization of S, PFPMI and triisopropylsilyl-protected *N*-propargyl maleimide (TIPS-MI) was carried out using MAMA-SG1 as the alkoxyamine at 120°C leading to well-defined copolymers (M_n = 3520 - 12190 g.mol^{-1}; PDI = 1.14-1.18).[81] Resulting P(S-*co*-PFPMI-*co*-TIPS-MI)s copolymers then react with

an excess of 11-azido-3,6,9-trioxaundecan-1-amine in THF to target azido-functionalized copolymers.

Nilles and Theato[82] reported the synthesis of poly(pentafluorophenyl-4-vinylbenzene sulfonate) (PPFPVS) (M_n = 25700 g.mol^{-1}; PDI = 1.31) using MAMA-SG1 (Scheme 31) as the alkoxylamine in THF at 120°C. PFP-functionalized poly(octyl styrene)-*b*-PPFPVS (M_n = 69200 g.mol^{-1}; PDI = 1.47) block copolymers were also synthesized by NMP.

Linear carbonate

Boonpangrak *et al.*[83] have synthesized molecular imprinted polymers (MIP) by performing the copolymerization of cholesteryl-(4-vinyl)phenyl carbonate and divinylbenzene in the presence of an alkoxylamine, 3-(*tert*-butylphenyl)-1,1-dimethyl-3-(2,2,6,6-tetramethylpiperidinooxy)propylcyanide (A3, *Scheme 38*) in *m*-xylene used as the solvent at 125°C for 48h (*Scheme 38*).
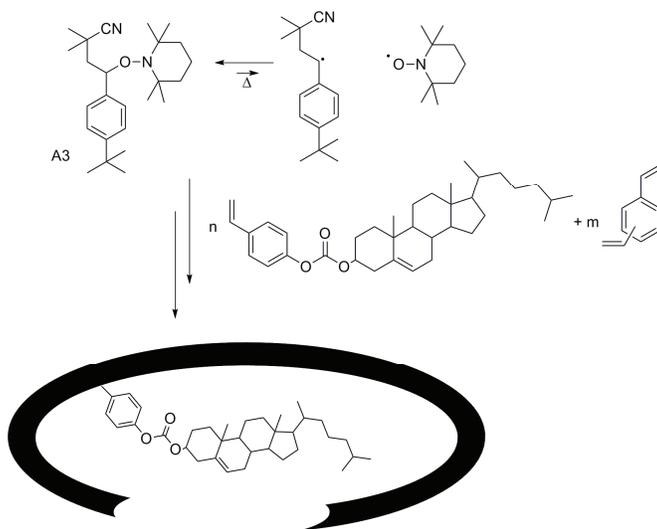
Scheme 38: Preparation of cholesterol-based molecular-imprinted polymer using NMP.

Cyclic anhydride

Benoit *et al.*[84] reported the copolymerization of maleic anhydride (MAh) and S carried out in the presence of A1 (*Scheme 39*) used as an alkoxyamine and in the presence of the corresponding nitroxide N1 (*Scheme 39*) at 120^oC which leads to well-defined P(S-*alt*-MAh) copolymer with PDIs below 1.20. Moreover, well-defined P(S-*alt*-MAh)-*b*-PS block copolymers were synthesized using the P(S-*alt*-MAh) (M_n = 5000 g.mol^{-1}, PDI = 1.19) as the macromolecular alkoxyamine to mediate the polymerization of S. Lessard and Maric reported the synthesis of well-defined P(S-*alt*-MAh)-*b*-PS block polymers by NMP using the free radical SG1 and MAMA-SG1.[85] The TEMPO was also used as the alkoxylamine to mediate the copolymerization of MAh and S in the presence of BPO in bulk at 120^oC. However, the resulting copolymers have high polydispersity indices (PDIs =1.21-1.35).[86]
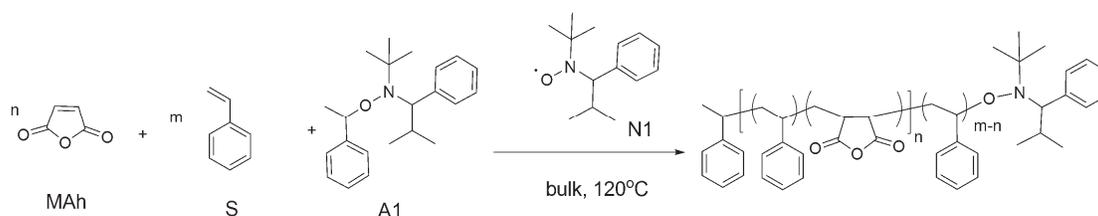
Scheme 39: NMP of S and MAh at 120^oC.

3.1.2.2. By Atom Transfer Radical Polymerization (ATRP)

ATRP process could be adapted to a wide range of functional monomers to target well-defined reactive polymers towards amines. Therefore, ATRP of monomers bearing a functional group such as epoxide, azlactone, isocyanate, cyclic and linear carbonates, and

activated esters (NHS, PFP) has been mostly employed to synthesize amino-reactive polymers.

3.1.2.2.a. Reactive groups not leading to molecular side-products

Epoxide

In 1997, Matyjaszewski *et al.*[87] published their work on the homopolymerization of GA by ATRP using methyl-2-bromopropionate as the initiator, CuBr/4,4'-bis(5-nonyl)-2,2'-bipyridine (dNbpy) as the catalytic system in bulk at 90°C (*Scheme 40*). High molecular weights were obtained ($4320 \leq M_n \leq 52800$ g.mol^{-1}) while keeping the polydispersity indices below 1.25.

Scheme 40: Polymerization of GA by ATRP using methyl-2-bromopropionate as the initiator and CuBr/dNbpy as the catalytic system in bulk at 90°C.

Other groups employed the ATRP to target well-defined epoxide-functionalized (co)polymers using the GMA as the monomer. Table 4 reports the ATRP experimental conditions used to target such well-defined PGMA-based copolymers.

Table 4. ATRP experimental conditions used to target well-defined PGMA-based copolymers

Entry	Monomer	Initiator	Catalytic system	Solvent	Temperature	targeting molecule	Ref.
1	GMA	2-bromopropionitrile	CuBr/N-(n-propyl)-2-pyridylmethanimine (PPMI)	Diphenylether, anisole, ethyl methyl ketone, methanol, water, and bulk	Room temperature	-	88, 89
2	GMA	2-bromopropionitrile	CuBr/PPMI	Diphenylether	30°C	S-(-)-α-ethylbenzylamine	90
3	GMA	2-bromopropionitrile	CuBr/dNbpy	Anisole	60°C	-	91
4	GMA	chloro-functionalized silicon	CuCl/CuCl$_2$/bpy	DMF/water	Room temperature	glucose oxidase (amine)	92
5	GMA	bromo-functionalized silica	CuBr/bpy	Methanol/water	Room temperature	iminodiacetic acid	93
6	GMA	bromo-functionalized silica particles	CuBr/bpy	DMF	Room temperature	carboxylic acid-functionalized-quantum dots	94
7	GMA	bromo-functionalized superparamagnetic iron oxide nanoparticles	CuBr/bpy	THF	35°C	ethylenediamine	95
8	GMA/PEGMA	bromo-functionalized superparamagnetic iron oxide nanoparticles	CuBr/bpy	THF	45°C	NaN$_3$	96

9	GMA/2-(diethylamino)ethyl methacrylate (DEAEMA)	bromo-functionalized tantalum pentoxide (Ta$_2$O$_5$)	CuCl/CuBr$_2$/bpy	Water/methanol	Room temperature	proteins (bovine serum albumin, ovalbumin)	97
10	GMA	Bromo-functionalized gold surface	CuCl/CuBr$_2$/bpy	Water/methanol	Room temperature	methanol/NaOH	98-100
11	GMA/MMA	bromo-functionalized silicon wafer	CuCl/CuBr$_2$/bpy	Water/methanol	Room temperature	octylamine	101
12	GMA/ DEAEMA	bromo-functionalized silicon wafer	CuBr/CuCl$_2$/bpy	Water/Methanol	Room temprature	propylamine, amino-2-propanol, taurin, (2-aminoethyl) trimethylammonium chloride hydrochloride	102
13	GMA	bromo-functionalized filter paper	CuCl/CuBr$_2$/PMDETA	Toluene	30ºC	bis(3-aminopropyl)-terminated poly(dimethylsiloxane)	103
14	GMA	bromo-functionalized PS film	CuBr/bpy	Methanol/water	25ºC	5-(Biotinamido)pentylamine	104
15	GMA	bromo-HIPE	CuCl/bpy	Methanol/water	Room temperature	hydrolysis	105
16	GMA	bromo-functionalized poly(ethylene oxide) (PEO$_{113}$-Br)	CuBr/PMDETA	Anisole	30ºC	NaN$_3$	106
17	GMA	PEO$_{45}$-Br	CuCl/bpy	Toluene	60ºC	ethyldiamine, di triethylene triamine, triethylene tetramine, poly(ethyleneimine)	107

18	GMA	bromo-functionalized polycaprolactone	CuCl/bpy	DMF	50°C	-	108
19	GMA	chloro-functionalized polycaprolactone	CuCl/bpy	DMF	60°C	-	109
20	GMA	ethyl 2-bromoisobutyrate (EBiB)	CuBr/bpy	DMF	60°C	ammonia, N-tert-butoxycarbonyl-ethylenediamine	110
21	GMA	EBiB	CuBr/PMDETA	Bulk	50°C	ethanolamine	111
22	GMA	EBiB	CuBr/PMDETA	Diphenyl ether	Room temperature	NaN$_3$	112
23	GMA/t-BA	EBiB	CuCl /PMDETA	Bulk	50°C	ethylenediamine	113
24	GMA/t-BA	EBiB	CuBr/PMDETA	Diphenylether	30°C	NaN$_3$	114
25	GMA/ n-BA	EBiB	CuBr/PMDETA or CuCl/ PMDETA	Toluene/ diphenylether	50°C	-	115
26	GMA/n-BMA	ethyl-2-bromopropionate	CuCl/CuCl$_2$/ Phenanthroline	4-methyl-2-pentanone	90°C	-	116
27	GMA/S	EBiB	CuBr /PMDETA	DMF, toluene and bulk	40°C, 60°C, 80°C.	-	117
28	GMA/S	bromo-functionalized poly(styrene-co-divinylbenzne)	CuBr/ (1, 1, 4, 7, 10,10-hexakis)hexyl-1, 4, 7, 10-tetraazadecane (H-TETA)	Toluene	60, 70°C	morpholine	118-120
29	GMA/MMA	EBiB	CuBr and CuBr$_2$/1,1,4,7,10,10-hexamethyltriethylenetetramine (HMTETA)	Acetone	50°C	NaN$_3$	121

Leroux *et al.*[122] reported the synthesis of an epoxide-functionalized star PGMA using a multi-functional ATRP initiator (I1, *Scheme 41*) in the presence of CuBr/bpy as the catalytic system in THF at 90°C (*Scheme 41*).
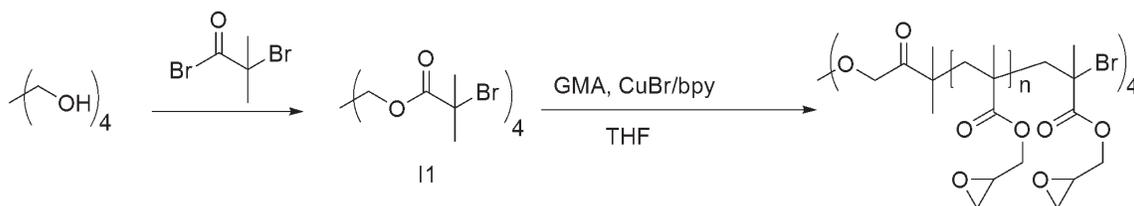
Scheme 41: Synthesis of star-shaped PGMA by ATRP using CuBr/bpy as the catalytic system in THF at 90°C.

Jones *et al.*[73] reported the synthesis of P(ES-*stat*-S) using ATRP polymerization. The copolymerization of ES and S was performed in the presence of I2 (*Scheme 42*) used as the initiator and CuBr/bpy used as the catalytic system in bulk at different temperatures. At temperatures below 100°C, well-defined P(ES-*stat*-S) could be obtained with low polydispersity indices (PDI ≤ 1.28).
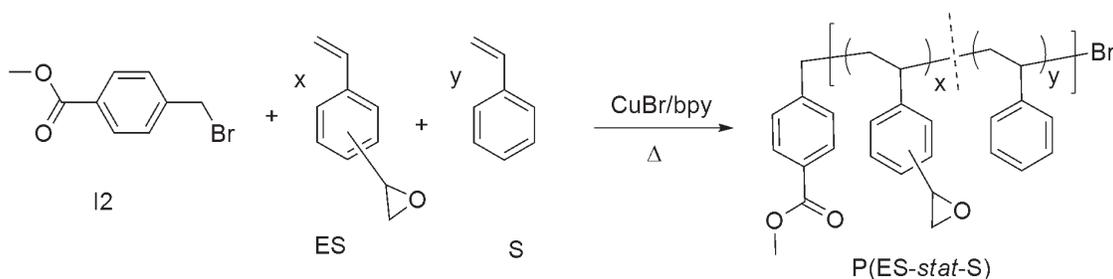
Scheme 42: Synthesis of P(ES-stat-S) by ATRP in the presence of CuBr/bpy in bulk at different temperatures.

Azlactone

Fournier *et al.*[123] reported for the first time the ATRP of VDM using EBiB as the initiator and CuBr/tris[2-(dimethylamino)ethyl] amine (Me$_6$TREN) as the catalytic system in toluene at 25°C. The conversion of VDM reached 59% after 4h while maintaining a relatively low polydispersity index (PDI = 1.36). Furthermore, the synthesis of well-defined statistical copolymers and block copolymers based on VDM, S and MA was reported. Moreover, the synthesis of PVDM-based Rasta resins successfully used to scavenge the benzylamine was performed by ATRP.[124] In this work, a Wang resin was treated with 2-bromoisobutyryl bromide in order to target bromo-functionalized Wang resins able to initiate the (co)polymerization of VDM and S using CuBr/Me$_6$TREN as the catalytic system in toluene. The low polydispersity indices (PDI = 1.11-1.14) of PVDM, P(VDM-*co*-S) and PS-*b*-P(VDM-*co*-S) cleaved (co)polymers showed that the ATRP of VDM and S onto Wang resins was controlled. Moreover, the PVDM grafted Wang resins also react with *N,N,N',N'*-tetraethyldiethylenetriamine (TEDETA) to create supported ligands for copper bromide.[125] These complexes were then employed as solid support catalyst to mediate the ATRP of MMA leading to PMMAs with controlled M$_n$ and relatively low polydispersity indices. Additionally, after the polymerization, 96% of the initial copper was anchored onto the Wang resins.

Cullen *et al.*[126] reported the preparation of silicon surface-anchored with PVDMs brushes synthesized by ATRP of VDM using CuBr/PMDETA as the catalytic system in toluene at 80°C. The PVDM-functionalized surface was then coupled with RNase A in Na$_2$SO$_4$ solution (pH = 7) for enzyme and protein immobilizations. PVDM brushes offer a versatile route to immobilize enzyme/proteins *via* the ring-opening of the azlactone

cycle without the need of activation or pretreatment while retaining high relative activities of the bounded enzymes. Furthermore, Sun et al.[127] synthesized a well-defined PVDM (M_n = 5800 g.mol^{-1}, PDI = 1.11) using EBiB as the initiator and CuBr/PMDETA as the catalytic system in toluene at 50°C. Resulting PVDM reacts successfully with different primary amines to target a library of functional polymers.

Isocyanates

Jérôme and coworkers reported the first copolymerization of S and TMI by ATRP using the 1-phenylethyl bromide (PEBr) as the initiator and CuBr/HTMETA as the catalytic system in toluene at 110°C.[128,129] Subsequently, the P(S-*co*-TMI) reacts with hydroxyl-terminated PMMA in the presence of dibutyl tin dilaurate in toluene at 50°C leading to P(S-*co*-TMI)-*g*-PMMA graft copolymers. Moreover, the isocyanate-functionalized P(S-*co*-TMI) reacts with a secondary amine: the 9-methyl(aminoethyl)anthracene (*Scheme 43*).
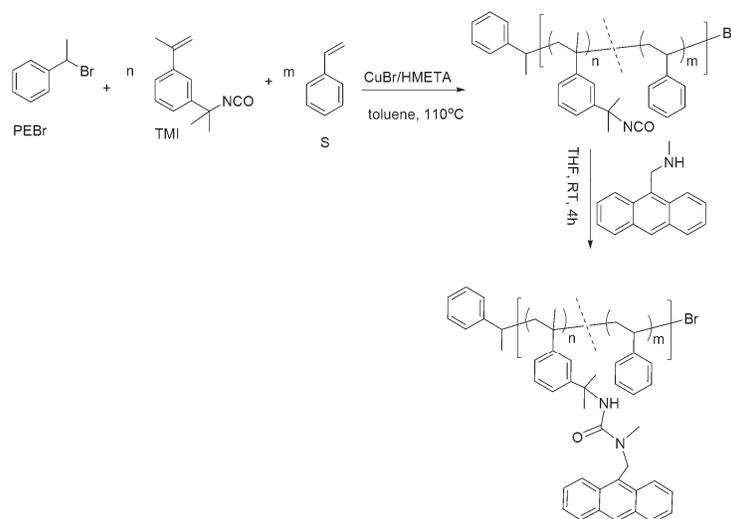
Scheme 43: Synthesis of P(S-co-TMI) by ATRP and its reactivity towards an amino-functionalized anthracene.

Cyclic carbonate

Jana *et al.*[130] reported the synthesis of a novel cyclic carbonate methacrylate (CCMA) which was employed in ATRP to target carbonate-functionalized copolymers (*Scheme 44*). A well-defined poly(cyclic carbonate methacrylate) (PCCMA, M_n = 25840 g.mol^{-1}, PDI = 1.11) was synthesized by the ATRP of CCMA using EBiB as the initiator and CuBr/bpy as the catalytic system in DMF at 80°C. Similar conditions were used to target triblock copolymers based on PCCMA, PMMA and poly(ethylene glycol) (PEG) using PEG as ATRP macroinitiator. The pendant cyclic carbonate groups then react with 2-phenylethylamine in DMF for the enhancement of polymer solubility and film-forming characteristics.
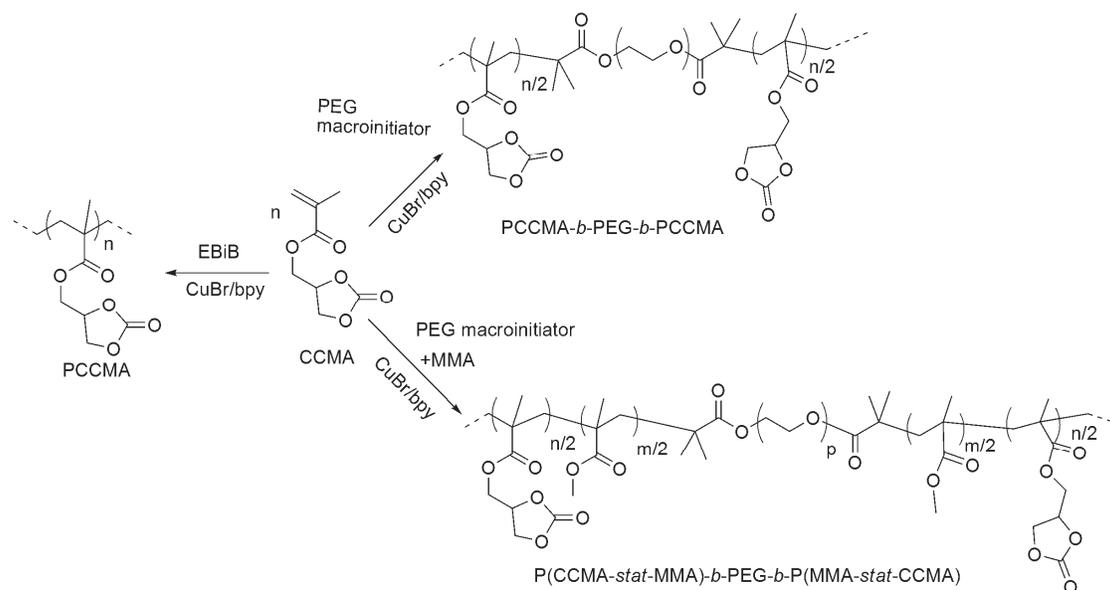
Scheme 44: Synthesis of carbonate-functionalized (co)polymers by ATRP using CuBr/bpy as the catalytic system.

3.1.2.2.b. Reactive groups leading to molecular side-products

NHS-ester

Hu *et al.*[131] reported the preparation of well-defined glycoconjugate polyacrylamides by ATRP of NAS using 2-bromo-2-methyl(2-hydroxyethyl)propanoate as the initiator and CuBr/bpy as the catalytic system in bulk at 80°C and subsequent modification of the resulting PNAS (P1, *Scheme 45*) (M$_n$ = 51700 g.mol^{-1}, PDI = 1.30) with galactosamine in DMF at 60°C. Other groups reported the synthesis of PNAS-based copolymers (P2 and P3, *Scheme 45*) using functionalized PEOs as ATRP macroinitiators to mediate the polymerization of NAS in the presence of CuBr/bpy as the catalytic system in bulk.[132,133] The resulting NHS-functionalized copolymers then react with different primary amines such as cystamine, *n*-butylamine, ethylenediamine for the synthesis of functional copolymers and nanoparticles. Pan and coworkers synthesized a NHS-functionalized hexa-armed star copolymer by performing the ATRP copolymerization of NAS with S using a hexa-armed poly(*L*-lactide) star macroinitiator.[134] The star copolymer was then coupled with ethylenediamine used as cross-linking agent and the subsequent hydrolysis of poly(*L*-lactide) led to the synthesis of hollow nanoparticles.
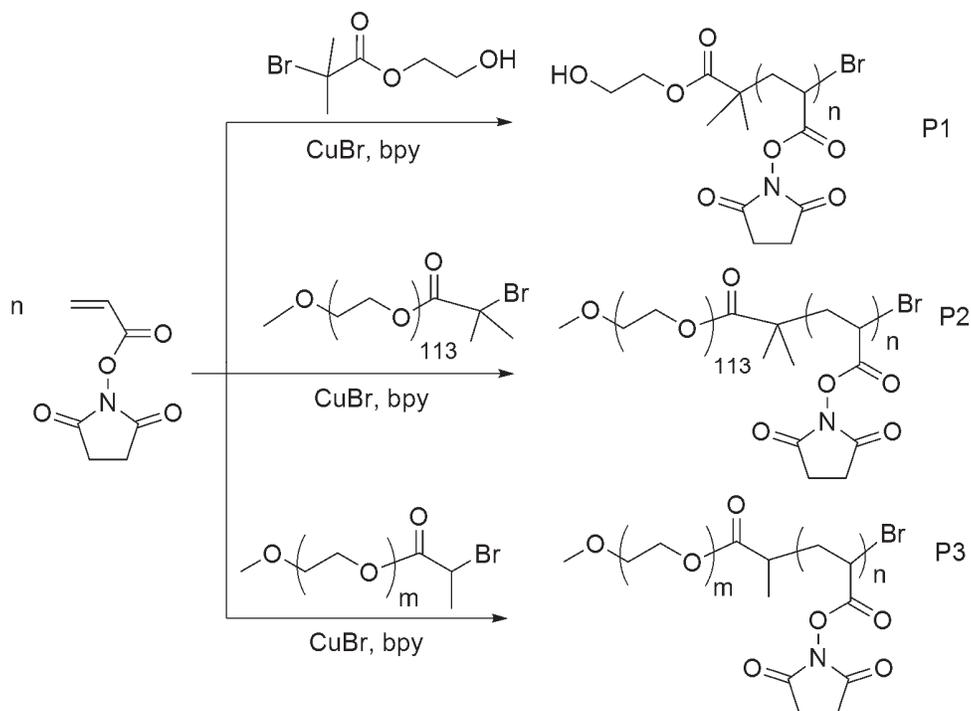
Scheme 45: Polymerization of NAS by ATRP using CuBr/bpy as the catalytic system.

Godwin *et al.*[135] reported the polymerization of *N*-methacryloyloxysuccinimide (NMAS) using 2-bromo-2-methyl(2-hydroxyethyl)propanoate as the ATRP initiator and CuBr/bpy as the catalytic system in DMSO at 80°C and 100°C leading to well-defined poly(*N*-methacryloyloxysuccinimide)s (PNMASs, M_n = 12300-40700 g.mol^{-1}, PDI = 1.15-1.20). PNMASs were then coupled with amino-terminated glycine-glycine-β-naphthylamide hydrobromide as drug-linker and subsequently with 1-amino-2-propanol in DMSO in the presence of TEA at 50°C to target drug-polymer conjugates. In similar conditions, Pedone *et al.*[136] reported the polymerization of NMAS using 2-bromo-2-methyl(2-hydroxyethyl)propanoate as the initiator and PEO macroinitiators yielding to PNMAS and PEO-*b*-PNMAS block copolymers. The NHS-functionalized PEO-*b*-PNMAS then reacts with tertiary amines, quaternary ammonium, imidazole and

hydroxypropyl moieties in order to target copolymers which could be used to complex plasmid DNA. In a similar work, several PNMASs were used as precursors for polymer-based DNA vectors by Putnam and coworkers.[137] Rickert *et al.*[138] reported the conjugation of PNMAS with tomoxifen to target anticancer drug-polymer conjugates.

Monge *et al.*[139] described the synthesis of PNMAS-*b*-PMMA block copolymers (M_n = 26200 g.mol^{-1}, PDI = 1.26) using well-defined PNMASs (PDI ≤ 1.19) as macroinitiators and CuBr/PPMI as the catalytic system in DMSO at 50°C.

Shunmugam and Tew reported the synthesis of well-defined NHS-functionalized copolymers based on PS, PMMA and PNMAS by ATRP using CuBr/PMDETA as the catalytic system in 50% (w/w) anisole at 90°C.[140] These NHS-functionalized polymers were then attached with terpyridine to target copolymers bearing ligands for lanthanide ions (Dy^{3+}, Tb^{3+}, Eu^{3+}, or Sm^{3+}).

Ghosh *et al.*[141] recently described the synthesis of a new reactive copolymer (P4, *Scheme 46*) which could simultaneously react with amine- and thiol-based compounds. The copolymerization of NMAS and a disulfide-based methacrylate (M1, *Scheme 46*) was carried out in the presence of EBiB used as the initiator and CuBr/PMDETA used as the catalytic system in anisole at 65°C leading to copolymers (P4, *Scheme 46*) with M_n ranging from 8100 g.mol^{-1} to 19000 g.mol^{-1} and PDIs ranging from 1.30 to 1.60. The reactive copolymer (P4, *Scheme 46*) of M_n = 9700 g.mol^{-1} and PDI = 1.60 then reacts with propylamine and subsequently with 1-undodecanethiol.
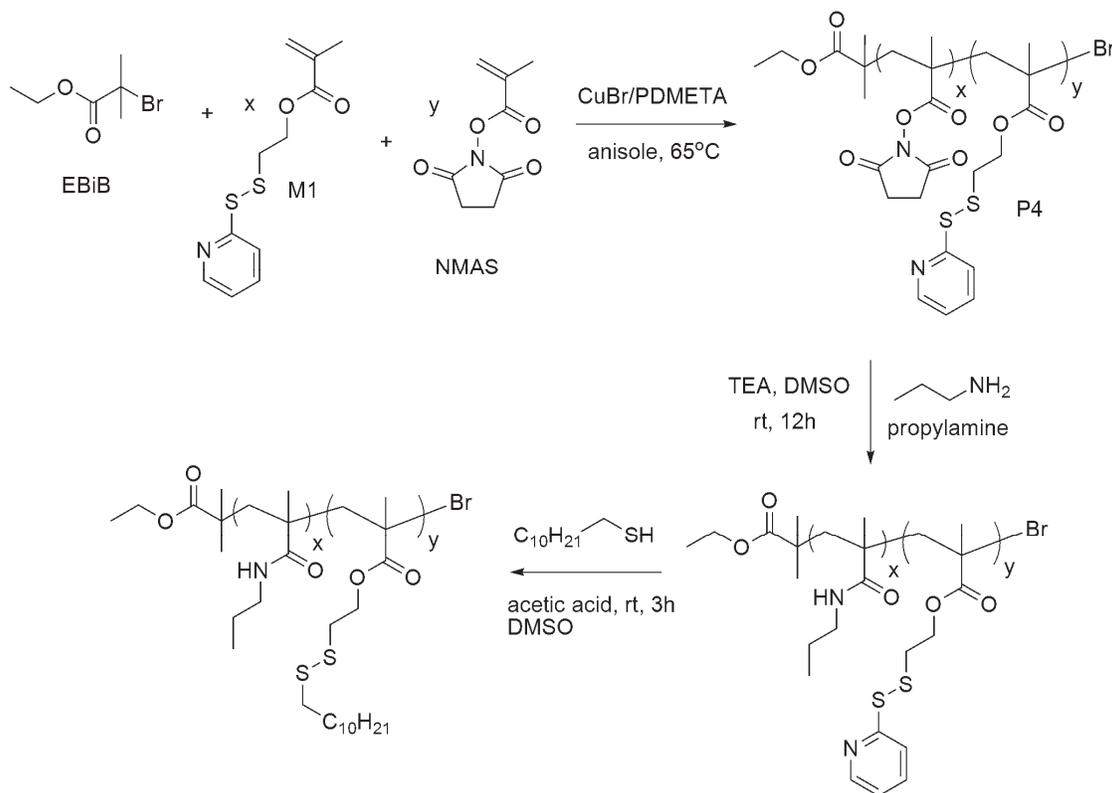
Scheme 46: Synthesis of block copolymers based on NMAS and disulfide-based methacrylate by ATRPusing CuBr/PMDETA as the catalytic system and their functionalization with amine- and thiol-based molecules.

Locklin and coworkers reported the synthesis of NHS-functionalized block copolymers brushes based on PNHSVB, poly (2-hydroxyethyl acrylate) (PHEA), P(*t*-BA) and PS by surface-initiated ATRP.[142] The polymerization of NHSVB was firstly carried out using a bromo-functionalized silicon surface as the ATRP initiator and CuBr/CuCl$_2$/PMDETA as the catalytic system in DMSO at 50°C. The resulitng PNHSVB brushes were then used as the surface ATRP macroinitiator to polymerize of 2-hydroxyethyl acrylate (HEA), *t*-BA and S. Resulting block copolymers brushes subsequently react with 1-amino-methylpyrene and octadecylamine in TEA/DMF at 40°C. The efficient incorporation of pyrene chromophore into (co)polymer brushes was

measured by UV-Vis spectrophotometry. PNHSVB brushes were also used to immobilize the amine-based cyclopropenone as a masked dibenzocyclooctyne[143] and and a photoreactive amine-functionalized (3-hydroxymethyl)naphthalene-2-ol as a naphtoquinone methide precursor[144] to prepare photoreactive polymer brushes for copper-free and Diels-Alder photo-click reactions, respectively.

PFP- ester

Singha *et al.*[145] reported the synthesis of biofunctionalized polymethacrylamides *via* the post-polymerization modification of poly(pentafluorophenyl methacrylate)s PPFPMAs obtained by ATRP. The PPFPMA (M_n = 13000 g.mol^{-1}, PDI = 1.30) was synthesized using EBiB as the initiator and CuBr/PMDETA as the catalytic system at 70°C. The PPFPMA was then modified with allylamine to give well-defined polymers with pendant alkene groups and were subsequently reacted with thiol-terminated peptide by radical addition (*Scheme 47*).
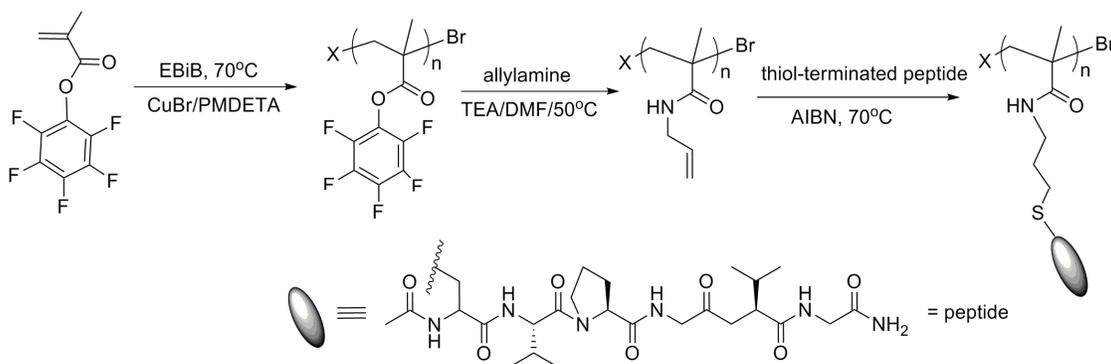
Scheme 47: Biofunctionalized polymethacrylamide via the post-polymerization modification of PPFPMA obtained by ATRP.

PNP-ester

Liu *et al.*[146] reported the ATRP synthesis of well-defined PS-*b*-(*p*-nitrophenyl methacrylate) (PS-*b*-PPNPMA) block polymers (PDI = 1.29-1.38) (*Scheme 48*). The first block polymer was synthesized by the bulk polymerization of S in the presence of ethyl-2-bromobutyrate (EBB) used as the initiator and CuBr/bpy used as the catalytic system at 110°C. The resulting PS (M_n = 14730 g.mol^{-1}, PDI = 1.18) was then used as the macroinitiator to control the polymerization of *p*-nitrophenyl methacrylate (PNPMA) to target the PNP-functionalized block copolymers. The PS-*b*-PPNPMA obtained subsequently react with *n*-butylamine in THF to target PS-*b*-poly(*n*-butyl methacrylamide) block copolymers.
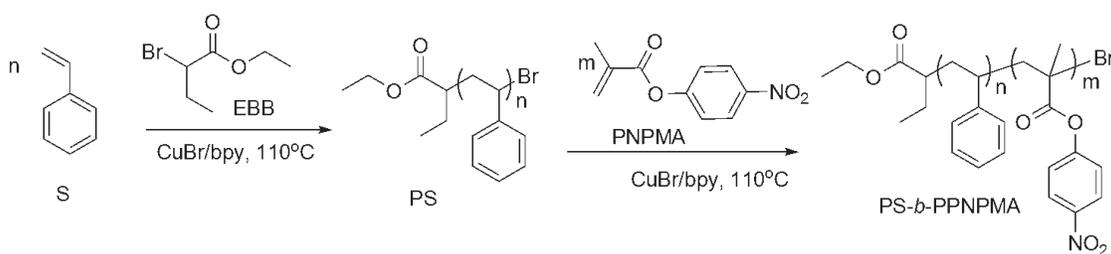
Scheme 48: Synthesis of PS-b-PPNPMA by ATRP.

Linear carbonates

Popescu *et al.*[147] reported the synthesis of linear carbonate-functionalized (co)polymers based on 2-(phenoxycarbonyloxy)ethyl methacrylate (PCEMA) using ATRP (*Scheme 49*). In a typical procedure, the ATRP of PCEMA was performed in the presence of EBiB used as the ATRP initiator and CuBr/bpy as the catalytic system in butyl acetate (BuAc) at 90°C. However, the high polydispersity index of poly(2-(phenoxycarbonyloxy)ethyl methacrylate) (PPCEMA, PDI = 2.5) showed that the

polymerization is uncontrolled. However copolymerizations of PCEMA with methacrylates (*e.g.* MMA, allyl methacrylate (AMA), *n*-BMA) led to polymers with lower polydispersity indices (PDI = 1.4-1.5). These copolymers were subjected to react with different amines leading to multifunctional polymethacrylates.
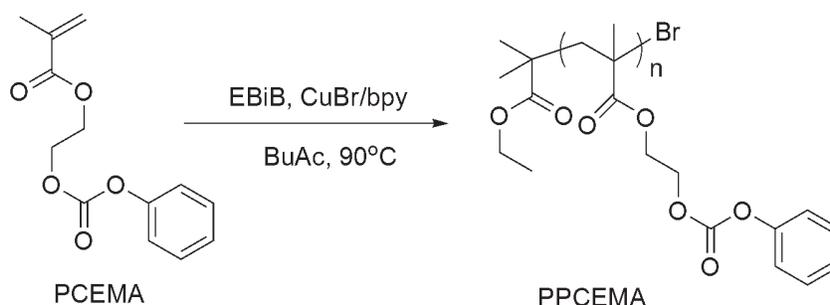
Scheme 49: ATRP of PCEMA using CuBr/bpy as the catalytic system in BuAc at 90°C.

4-Fluorobenzenesulfonyl chloride was also used as the initiator together with CuCl/bpy as the catalytic system in BuAc at 110°C to target a P(PCEMA-*co*-MMA) copolymer (M$_n$ = 8100 g.mol^{-1}, PDI = 1.30) and P(*t*-BMA)-*b*-PPCEMA block copolymer (M$_n$ = 134000 g.mol^{-1}, PDI = 1.44).[148] These carbonate-functionalized copolymers then react with different amines and subsequently with methyl iodide to obtain amphiphatic copolymers with bacteriostatic properties. Such carbonate-functionalized copolymers have been employed to target new bioconjugates with lysozyme and peptide.[149]

3.1.2.3. By Reversible Addition-Fragmentation chain Transfer (RAFT) polymerization

RAFT polymerization has been applied to a wide range of functional monomers under different experimental conditions. Therefore, RAFT polymerization is a powerful process to synthesize well-defined amino-reactive polymers based on functional monomer such as epoxide, activated esters (NHS-ester and PFP-ester), azlactone and isocyanate monomers.

3.1.2.3.a. Reactive groups not leading to side-products

Epoxides

Zhu *et al.*[150] reported the RAFT polymerization of GMA using 2-cyanoprop-2-yl-1-dithionaphtalate (CPDN, *Scheme 50*) as the RAFT agent and AIBN as the initiator in benzene at 60^oC and in bulk or benzene at 60^oC and 80^oC. The controlled polymerization of GMA was shown by an increase of M_ns with monomer conversion while the polydispersity indices were kept below 1.30.
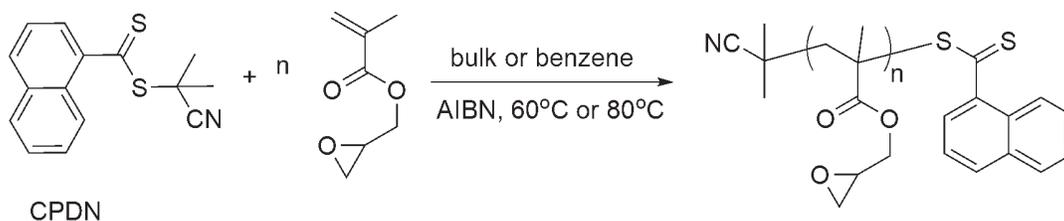
Scheme 50: Synthesis of PGMA by RAFT polymerization.

Additionally, Fu *et al.*[151] reported the synthesis of a poly(4-vinylbenzyl chloride)-*b*-PGMA (PVBC-*b*-PGMA) block copolymer (M_n = 15900 g.mol^{-1}, PDI = 1.18) prepared using CPDN as the RAFT agent.

Davis and coworkers prepared PGMA-*b*-polypentafluorostyrene (PGMA-*b*-PPFS) block copolymers by RAFT polymerization (*Scheme 51*).[152] The first block PGMA was synthesized by the polymerization of GMA in the presence of 2-cyanoprop-2-yl dithiobenzoate (CPDB) chain transfer agent using different $[GMA]_0/[CPDB]_0$ molar ratios. The polymerization leads to polymers with controlled M_n and low polydisperisty indices (PDI $\leq$ 1.1). PGMAs were then used as macromolecular RAFT agents for the polymerization of PFS at 60°C and 80°C. Well-defined PGMA-*b*-PPFS block copolymers (M_n = 10100-19500 g.mol^{-1}, PDI = 1.04-1.13) were obtained.
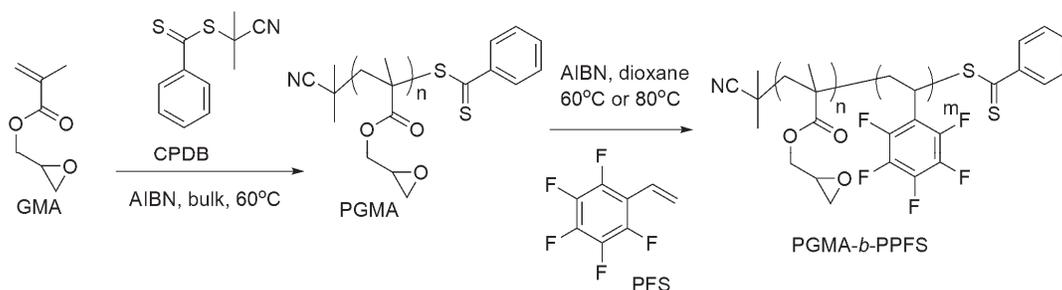
Scheme 51: Synthesis of PGMA and PGMA-b-PPFS by RAFT polymerization.

Chambon *et al.*[153] reported the synthesis of poly(glycerol monomethacrylate)-*b*-P(2-hydroxypropyl methacrylate-*stat*-GMA) block copolymers using CPDB as the RAFT agent. The resulting block copolymers subsequently react with Jeffamine in aqueous solution affording cross-linked diblock copolymer vesicles.

Other groups employed the RAFT polymerization to target well-defined epoxide functionalized copolymers such as PGMA-*b*-PMMA-*b*-PGMA, PMMA-*b*-PGMA-*b*-PMMA and POEGMA-*b*-PGMA.[154,155]

Yin *et al.*[156] studied the RAFT polymerization of GMA at ambient temperature under ultraviolet (UV) light radiation in the presence of 2-cyanoprop-2-yl-4-fluoro dithiobenzoate (CPFDB) and (2,4,6-trimethylbenzoyl)diphenylphosphine oxide (TPO) used as RAFT agent and photoinitiator, respectively (*Scheme 52*). A well-defined PGMA of M_n equal to 6800 g.mol^{-1} and PDI equal to 1.20 was obtained. Moreover, a P(*n*-BMA)-*b*-PGMA block copolymer (M_n = 27800 g.mol^{-1}, PDI = 1.17) was synthesized by polymerization of GMA at 30°C using P(*n*-BMA) as macromolecular RAFT agent in the presence of TPO used as the initiator. Using the same conditions, the RAFT copolymerization of 2-((3-phenylallylidene)amino)ethyl methacrylate with GMA was also investigated by Luo *et al.*[157]
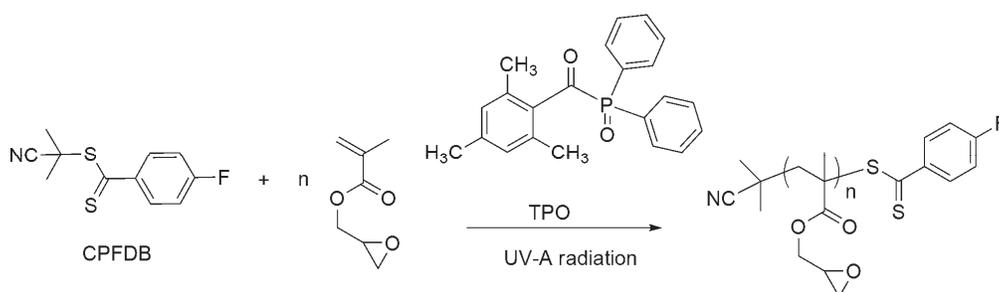
Scheme 52: Polymerization of GMA using RAFT polymerization in the presence of CPFDB used as the RAFT agent and TPO used as the photoinitiator.

Ostaci *et al.*[158] synthesized epoxide-based P(GMA-*co*-MMA-*co*-propargyl methacrylate) copolymers (M_n = 14300-24700 g.mol^{-1}, PDI = 1.59-1.99) using RAFT copolymerization of GMA, MMA and propargyl methacrylate in the presence of *S*-methoxycarbonylphenylmethyl dithiobenzoate used as the RAFT agent and AIBN used as the initiator at 70°C in benzene (*Scheme 53*). The resulting copolymer was then attached onto hydroxyl-functionalized silicon surface to target brush copolymers.

A similar strategy was used to prepare PGMA brush grafted onto silicon surface. PGMA brushs then react with amine-functionalized polyethylene.[159]
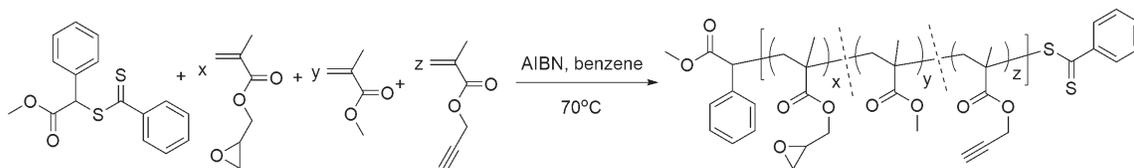
Scheme 53: RAFT copolymerization of GMA, MMA and propargyl methacrylate using S-methoxycarbonylphenylmethyl dithiobenzoate as the RAFT agent.

Farquet *et al.*[160] synthesized PGMA grafted onto poly(ethylene-*alt*-tetrafluorethylene) film *via* GMA polymerization in the presence of CPDB used as the RAFT agent, AIBN used as the initiator and under UV irradiation. Furthermore, Li *et al.*[161] reported the synthesis of PGMA brushes onto silicon surface *via* surface RAFT mediated process. The resulting PGMA brushes were then used as macromolecular RAFT agents to mediate the polymerization of PEGMA leading to PGMA-*b*-PPEGMA block copolymer brushes.

Azlactone

Schilli *et al.*[162] reported for the first time the synthesis of PVDM based block copolymers by RAFT polymerization. In this study, 1-cyanoethyl 2-pyrrolidone-1-carbodithioate (CPC) and CPDB (*Scheme 54*) were used as the RAFT agents for the polymerization of VDM in the presence of AIBN in benzene at 65°C. Low polydispersity indices of PVDM (PDIs ≤ 1.10) were only obtained by using CPDB as the RAFT agent. Thermoresponsive PVDM-*b*-P(NIPAM-*co*-VDM) block copolymers (M_n = 10400-13200

g.mol^{-1}, PDI = 1.14-1.22) were subsequently synthesized by the copolymerization of NIPAM and VDM using PVDM as the macromolecular RAFT agent and using AIBN as the initiator in benzene at 65°C.
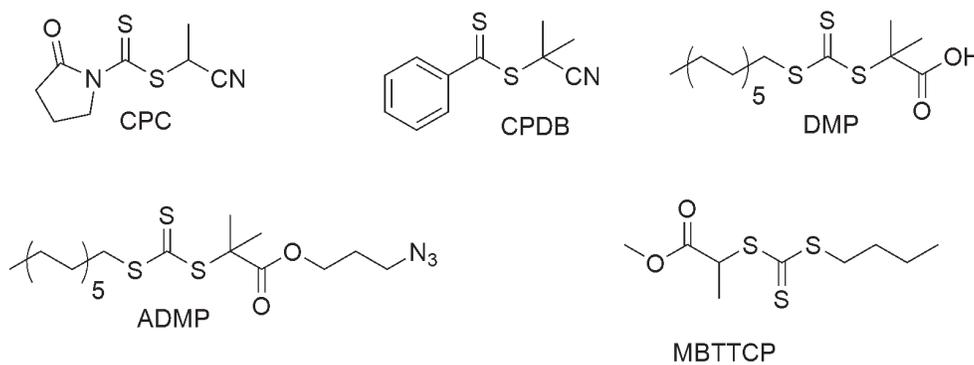
Scheme 54: Chemical structure of RAFT agents used for the polymerization of VDM.

Lokitz *et al.*[163] synthesized well-defined PVDM by RAFT polymerization using CPDB and 2-dodecylsulfanylthiocarbonylsulfanyl-2-methylpropionic acid (DMP, *Scheme 54*) as RAFT agents. Moreover, carboxylic acid-terminated PVDM obtained by RAFT polymerization using DMP as the RAFT agent were then grafted onto epoxide-functionalized silicon surface. The resulting PVDM brushes subsequently reacted with N_α,N_α-bis-(carboxymethyl)-*L*-lysine hydrate in aqueous solution (pH = 5) for bio-inspired application. In the same group, an azide-functionalized PVDM was also synthesized by RAFT polymerization using an azide-functionalized DMP (ADMP, *Scheme 54*) as the RAFT agent in benzene at 65°C.[164]

Pascual *et al.*[165] have investigated the use of RAFT polymerization for the preparation of PVDM-based block copolymers with controlled molecular weights and low polydispersity indices (PDI ≤ 1.30) (*Scheme 55*). Cumyl dithiobenzoate (CDB) and CPDB were employed as RAFT agents to synthesize well-defined PVDM first blocks.

Well-defined block copolymers based on PVDM, PS and poly(methacrylate) (PMA) blocks were obtained (PDI ≤ 1.30).
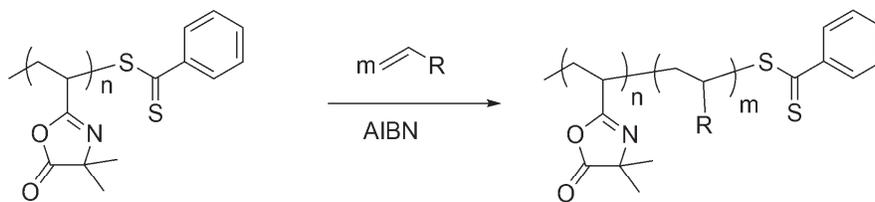
R: -phenyl for PVDM-*b*-PS

R : -C(O)OCH$_3$ for PVDM-*b*-PMA

Scheme 55: Synthesis of block copolymers based on PVDM, PMA and PS using RAFT polymerization.

Levere *et al.*[166] recently synthesized new stable azlactone-functionalized thermoresponsive nanoparticles based on PNIPAM, PDMA and PVDM by RAFT polymerization using methyl-2-(*n*-butyltrithiocarbonyl) propanoate (MBTTCP, *Scheme 54*) as the RAFT agent. Well-defined PNIPAM-*b*-P(VDM-*co*-DMA) (M$_n$ = 33400-64600 g.mol^{-1}, PDI = 1.10-1.20) and PDMA-*b*-P(VDM-*co*-NIPAM) (M$_n$ = 19500 g.mol^{-1}, PDI = 1.04) block copolymers were obtained using PNIPAM and PDMA as macromolecular RAFT agents for the copolymerization of DMA/VDM and of NIPAM/VDM, respectively. Above their LCST, these thermoresponsive VDM-functionalized copolymers form nanoparticles which were cross-linked by the addition of 2,2'-(ethylenedioxy)bis(ethylamine). Moreover, the remaining azlactone groups in the core-cross-linked nanoparticles were suitable to react with dansylhydrazine as shown by SEC analysis using UV detection.

Isocyanates

Barner *et al.*[167] reported the grafting of P(S-*co*-TMI) onto polypropylene supports. The P(S-*co*-TMI) was synthesized *via* γ-initiated RAFT copolymerization of S and TMI in the presence of cumyl phenyldithioacetate (CPDA) as the RAFT agent in bulk at ambient temperature. The scavenging ability of resulting isocyanate-functionalized polypropylene supports was tested using benzylamine.

Duong *et al.*[168,169] reported the RAFT polymerization of OEGMA using AIBN as the initiator and CDB as the RAFT agent (*Scheme 56*, a)) or an acetal-based RAFT agent (*Scheme 56*, b)) in toluene at 70°C. The resulting POEGMAs were then used as macromolecular RAFT agents for the copolymerization of S and TMI in the presence of AIBN used as the initiator in bulk at 100°C. Well-defined POEGMA-*b*-P(S-*co*-TMI)s were obtained with controlled M_n and low polydispersity indices (PDI ≤ 1.23). Moreover, isocyanate-functionalized block copolymers react with amine-functionalized platinum(IV) drug complex or hexamethylenediamine for the formation of core-cross-linked nanoparticules. Using a similar strategy, nanoparticles based on PPEGMA-*b*-P(MMA-*co*-TMI) were synthesized using RAFT polymerization by Stenzel and coworkers.[170]
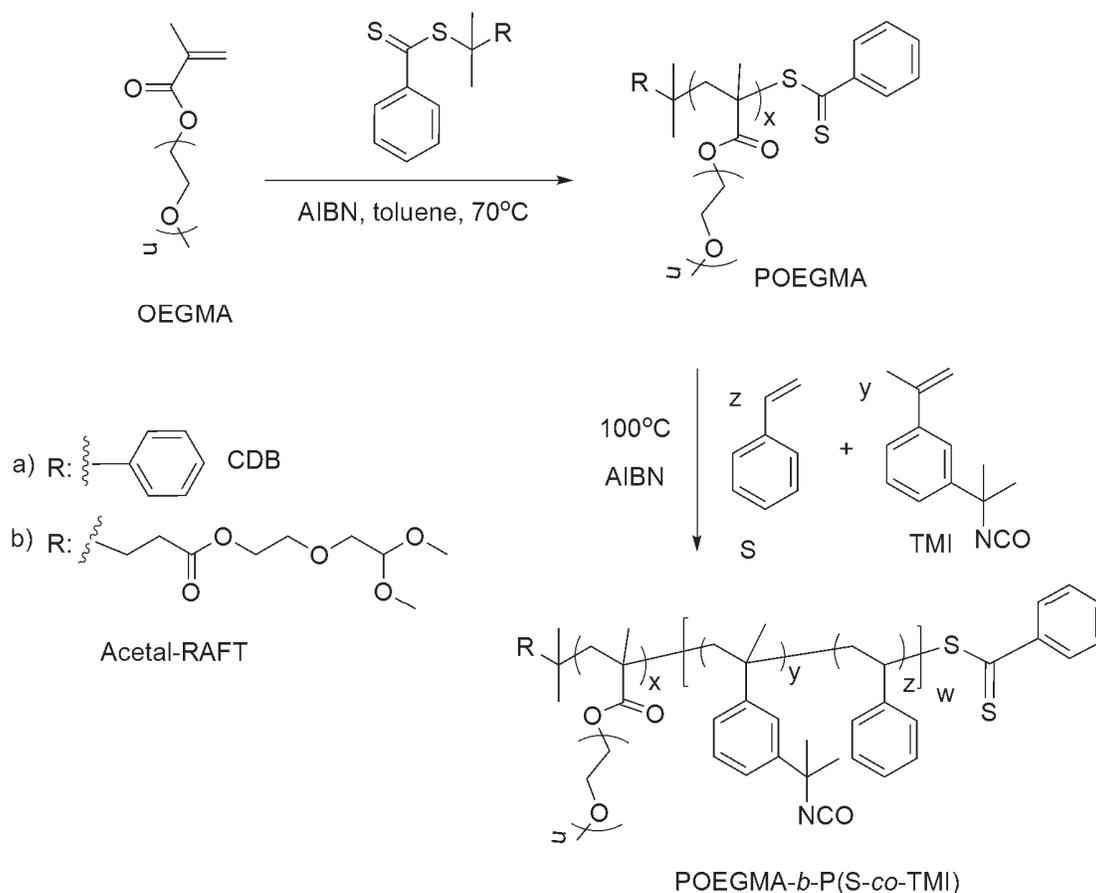
Scheme 56: Synthesis of POEMA-b-P(S-co-TMI) by RAFT polymerization.

Hawker and coworkers reported the preparation of stable nanoparticles by cross-linking isocyanate-functionalized copolymers using 2,2'-(ethylenedioxy)bis(ethylamine).[171] Syntheses of poly(2-isocyanatoethyl methacrylate-*co*-methyl methacrylate) (P(ICEMA-*co*-MMA)s) (M_w = 149000 g.mol^{-1}, PDI = 1.23) and P(ICEMA-*co*-S) (M_w = 36-114 kg.mol^{-1}, PDI = 1.07-1.19) were prepared by the copolymerization of 2-isocyanatoethyl methacrylate (ICEMA) with MMA and with S in the presence of *S*-methoxycarbonylphenylmethyl dithiobenzoate (MCPDB) used as the RAFT agent either in benzene or in toluene at 75°C (*Scheme 57*).
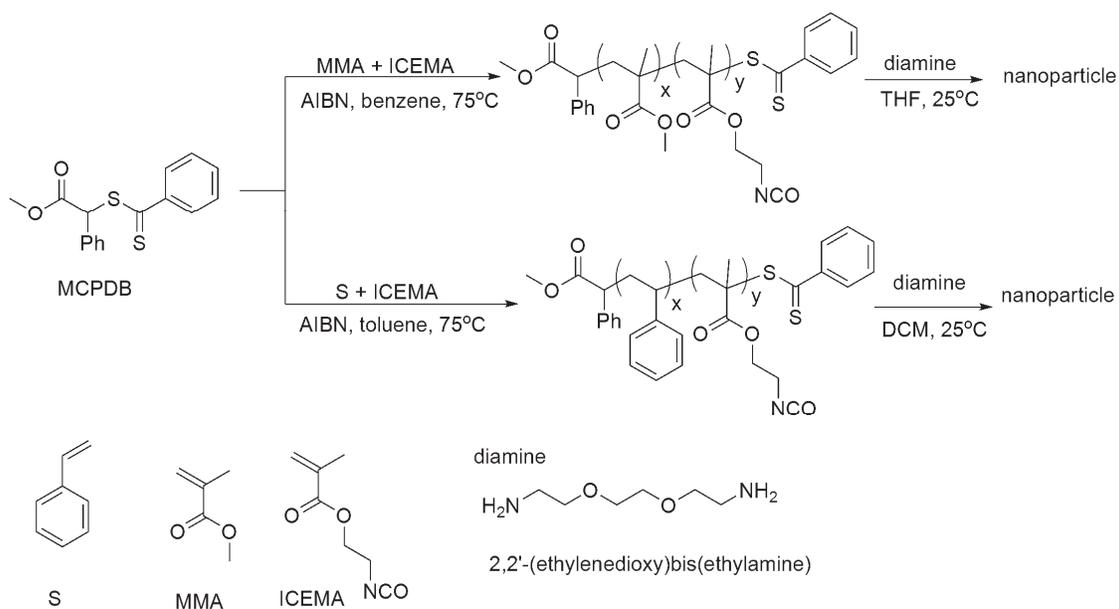
Scheme 57: Synthesis of isocyanate-based copolymers
P(ICEMA-co-MMA) and P(ICEMA-co-S) by RAFT polymerization and the formation of
the corresponding stable nanoparticles.

Moraes *et al.*[172] described an original one-pot (in two-steps) RAFT polymerization to synthesize block copolymers bearing reactive isocyanate groups. Copolymerizations of TMI and ICEMA with S and MMA were performed in the presence of CPDB and 2-(*n*-butyltrithiocarbonylthio)propionic acid (PABTC) used as RAFT agents and AIBN used as the initiator (*Scheme 58*).
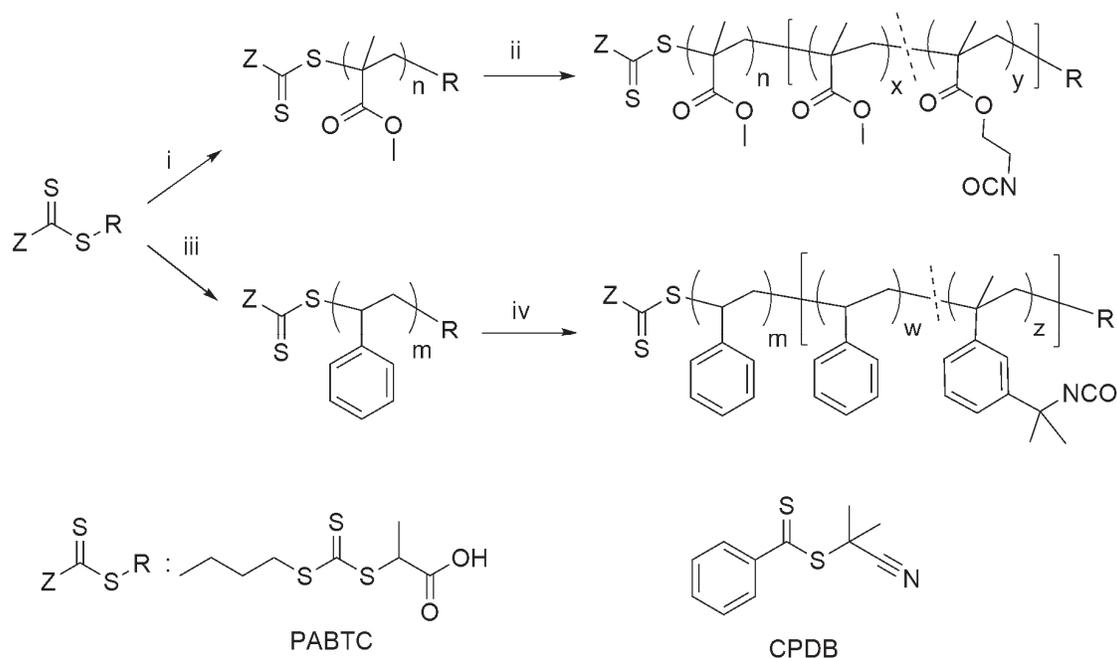
Scheme 58: One-pot reaction to target isocyanate-functionalized copolymers by RAFT polymerization:(i) CPDB, nMMA, p-xylene, 125°C; (ii) xMMA, yICEMA, p-xylene, AIBN, 125°C; (iii) mS, PABTC or CPDB, dioxane, AIBN, 60°C; (iv) wS, zTMI, AIBN, dioxane, 60°C.

In a similar study, a well-defined isocyanate-functionalized P(*n*-BA)-*b*-P(*n*-BA-*co*-TMI) (M_n = 68000 g.mol^{-1}, PDI = 1.28) block copolymer was synthesized using CPDB as RAFT agent by Perrier and coworkers.[173] The resulting block copolymer was subsequently attached with hydroxyl-terminated poly(ethylene glycol) monomethyl ether for the synthesis of a pseudo-star polymer.

Flores *et al.*[13] optimized the RAFT polymerization of 2-(acryloyloxy)ethylisocyanate (AOI) using *N,N*-dimethyl-*S*-thiobenzoylthiopropionamide (TBP) as the RAFT agent and 2,2'-azobis(2,4-dimethylvaleronitrile) (ADVN) as the initiator at 50°C and subsequent reactions using thiol-, alcohol- and amine- derivatives (*Scheme 59*).
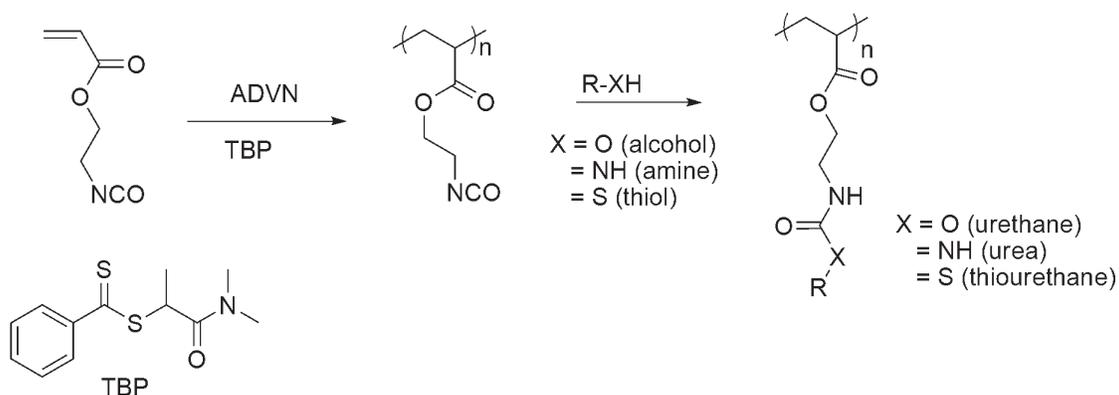
Scheme 59: Direct RAFT polymerization of AOI and subsequent functionalization through reaction with alcohols, amines, and thiols.

Cyclic anhydride

Brouwer *et al.*[174] reported the successful synthesis of P(S-*alt*-MAh) copolymer (M_n = 4100 g.mol^{-1}, PDI = 1.06) and polyolefin-*b*-P(S-*alt*-MAh) (M_n = 11000 g.mol^{-1}, PDI = 1.12) block copolymers using RAFT copolymerization of S and MAh using CPDB and dithioester-terminated polyolefin as transfer agents respectively, in the presence of AIBN as the initiator and in BuAc at 60°C. In similar work, Hao *et al.*[175] reported the synthesis of poly(6-[4-(4'-methoxyphenyl)-phenoxy]hexylmethacrylate) by RAFT polymerization using CPDB as the chain transfer agent and AIBN as the initiator in dioxane at 60°C. The resulting polymer was used as macromolecular chain transfer agent to mediate the copolymerization of S with MAh.

Hong *et al.*[176] reported the grafting of P(S-*alt*-MAh) onto multi-walled carbon nanotubes (MWNTs). The P(S-*alt*-MAh) was synthesized *via* RAFT copolymerization of S and MAh using a dithioester-functionalized MWNTs as the RAFT agent in THF at 80°C. The resulting grafting copolymers further react with an amino-terminated sugar to lead to the glycoconjugate P(S-*alt*-MAh) enwrapped MWNTs.

Boyer *et al.*[177] reported the RAFT polymerization of a PPEGA-*b*-P(S-*alt*-MAh) (M_n = 24200 g.mol^{-1}, PDI= 1.35) and a PHPMA-*b*-P(S-*alt*-MAh) (M_n = 46500 g.mol^{-1}, PDI = 1.15) block copolymers. These copolymers were then self-assembled onto gold nanoparticles using the high affinity of the trithiocarbonate and dithioester-terminated block copolymers with gold surface in aqueous solution and then subsequently react with ethylenediamine in the presence of 1-ethyl-3-(3-dimethylamino)-propyl) carbodiimine (EDC) to cross-linking the polymer layer of the nanoparticles.

Other groups employed the RAFT polymerization to target well-defined (co)polymers using the MAh as the comonomer. Table 5 reports the experimental conditions of RAFT polymerization used to prepare such well-defined copolymers.

Table 5: Experimental conditions of RAFT polymerization used for the synthesis of well-defined PMAh-based copolymers

Entry	Monomer	RAFT agent	Initiator	Temperature	Solvent	Ref.
1	S/MAh		No	22°C	THF	178
2	S/MAh		No	Room temperature (UV irradiation)	THF	179
3	S/MAh		AIBN	60°C	bulk	180
				75°C	butanone	181
4	4-vinylbenzyl chloride/MAh		AIBN	60°C	methylethyl ketone (MEK)	182
5	S/MAh		AIBN	60°C	dioxane	183
6	S/MAh		AIBN	60°C	dioxane	183
7	S/MAh		AIBN	80°C	dioxane	184
			AIBN	60°C	dioxane, THF	185
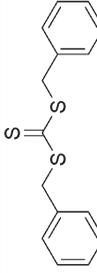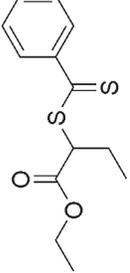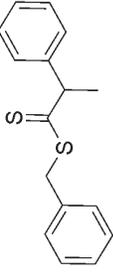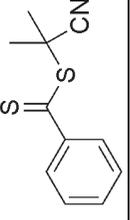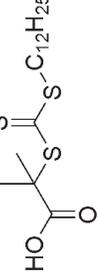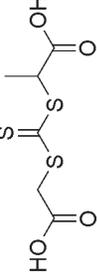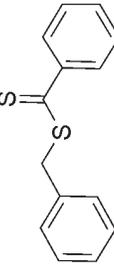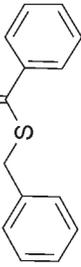
8	NVP/S/MAh		AIBN	80°C	dioxane	186
9	S/MAh; para-methylstyrene/MAh; para-chlorostyrene/MAh; para-methoxystyrene/MAh		AIBN	60°C	dioxane	187
10	stearyl methacrylate/MAh		AIBN	60°C	dioxane	188
11	S/MAh		2,2'-azobis(isobutyrate)	0°C (UV-light)	benzene	189
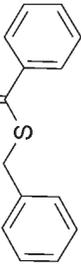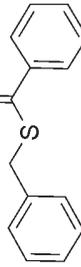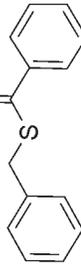
3.1.2.3.b. Reactive groups leading to molecular side-products

NH-ester

The successful statistical copolymerization of NAS with DMA was performed using the RAFT process in the presence of *tert*-butyl dithiobenzoate (*t*-BDB) and AIBN.[190] A good control of M_n (M_n = 5000-13000 g.mol^{-1}) and low polydispersity indices (PDI < 1.10) were obtained. Additionally, PDMA-*b*-PNAS block copolymers were also synthesized by RAFT polymerization of NAS using a PDMA as the macromolecular RAFT agent and AIBN as the initiator in dioxane at 90°C. The same group reported the copolymerization of NAS and NAM in the presence of *t*-BDB and AIBN in dioxane at 60°C leading to the well-defined P(NAS-*co*-NAM) (M_n ~ 13000 g.mol^{-1}, PDI < 1.10).[191] Moreover, well-defined poly(*t*-butyl methacrylamide)-*b*-P(NAS-*co*-NAM) block copolymers were synthesized using RAFT polymerization and subsequently attached to oligonucleotide (ODN) for bioconjugation.[192,193] Well-defined poly(*n*-BMA-*co*-NAS) was synthesized by Vosloo and coworkers.[194]

Yanjarappa *et al.*[195] reported the RAFT copolymerization of NMAS with HPMA using CPDB as the RAFT agent and AIBN as the initiator in DMF at 80°C to target well-defined P(HPMA-*co*-NMAS)s (M_n = 3000-50000 g.mol^{-1}, PDI = 1.1-1.3). The P(HPMA-*co*-NMAS) (M_n = 33100 g.mol^{-1}, PDI = 1.15) was reacted with a peptide in the presence of an excess of TEA in DMSO at 50°C yielding 80% bioconjugation.

Savariar and Thayumanavan reported the copolymerization of NMAS and NIPAM using NMP, ATRP and RAFT polymerization.[196] However, the control of the copolymerization of NMAS and NIPAM could only be obtained by RAFT polymerization.

Quan *et al.*[197] reported the synthesis of PNAS-*b*-PNIPAM block copolymers using 2-(phenylcarbonothioylthio) acetic acid (RAFT5, *Scheme 60*) as the chain transfert agent and AIBN as initiator at 70°C in THF. The carboxylic acid-terminated PNAS-*b*-PNIPAM was then used as macroinitiator for the ring-opening polymerization of *ε*-caprolactone, leading to PNAS-*b*-PNIPAM-poly(*ε*-caprolactone) triblock copolymers. The resulting triblock copolymer subsequently reacts with amino-functionalized biotin to afford the biotinylated block copolymer for tumor targeting application.

Other groups finally took advantage of well-defined NHS-based copolymers synthesized by RAFT polymerization to prepare stable nanoparticles (*Scheme 60*) (*Table 6*).
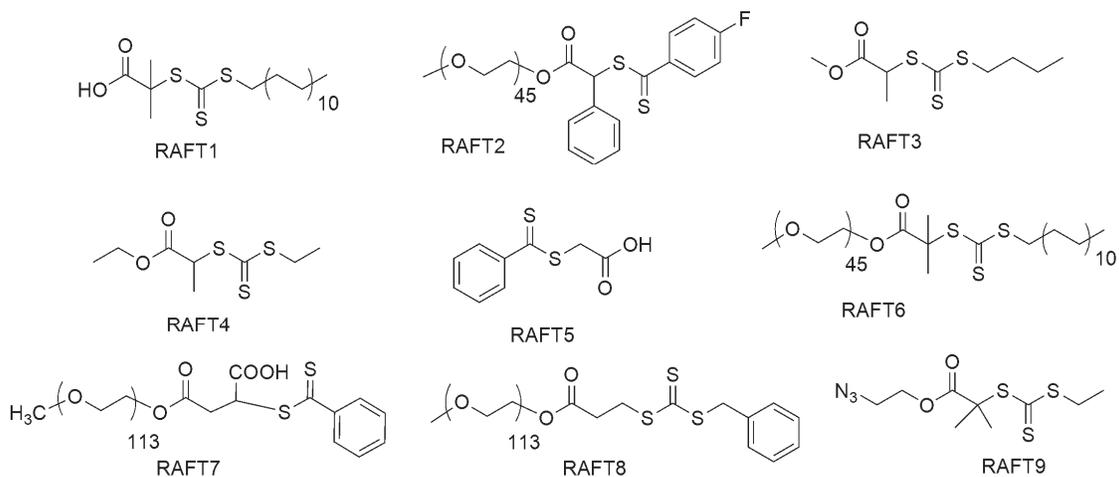
Scheme 60: Structure of RAFT agents employed for the synthesis of stable nanoparticles (Table 6).

Wooley and coworkers described the preparation of shell-cross-linked knedel-like (SCK) nanoparticles (*Entries 1 & 6, Table 6*) by using NHS-functionalized amphiphilic block copolymers synthesized by RAFT polymerization.[198,208-211] Li *et al.*[198] reported the

RAFT polymerization of a NHS-functionalized poly(methyl acrylate)-*b*-P(NAS-*co*-NAM) (PMA-*b*-P(NAS-*co*-NAM)) block copolymer with a M_n of 21800 g.mol^{-1} and a PDI of 1.18. This copolymer was then self-assembled into micelles in aqueous solution and subsequently reacted with 2,2'-(ethylenedioxy)bis(ethylamine) to afford shell cross-linked nanoparticles (*Entry 1, Table 6*). A similar strategy was employed by Perrier *et al.*[199] to target shell-cross-linked nanoparticles from poly(ethyl acrylate)-*b*-P(NAS-*co*-HEA) (PEA-*b*-P(NAS-*co*-HEA)) (*Entry 4, Table 6*).

Li *et al.*, Pascual *et al.*, and Quan *et al.* described the elaboration of cross-linked nanoparticles from thermoresponsive PEO-*b*-P(DMA-*co*-NAS)-*b*-PNIPAM[200,201] (*Entry 2, Table 6*), PNIPAM-*b*-P(NAS-*co*-DMA)[202] (*Entry 3, Table* 6), PNIPAM-*b*-PNAS-*b*-P(ε-caprolactone)[203] (*Entry 5, Table 6*) block copolymers synthesized by RAFT polymerization.

In another approach, Zhang *et al.*[204] developed reversible core-cross-linked micelles *via* the reaction of NAS moieties of PEO-*b*-P(NIPAM-*co*-NAS) with cystamine (*Entry 7, Table 6*). A well-defined thermoresponsive PEO-*b*-P(NIPAM-*co*-NAS) block copolymer of M_n = 23500 g.mol^{-1} and PDI of 1.12 was synthesized *via* RAFT polymerization. Nanoparticles were obtained in water at temperature above the lower critical solution temperature (LCST) of the block copolymer. Cross-linking of the nanoparticle core was achieved *via* the facile reaction of NAS residues with cystamine. The disulfide bonds within the cross-linked nanoparticle can be conveniently cleaved in the presence of dithiothreitol (DTT) and re-formed again upon addition of cystamine as a thiol/disulfide exchange promoter, leading to reversible core-cross-linked micelles. In addition, another core crosslinked micellar system synthesized from a block copolymer

based on a first PEO block and a second block obtained by the statistical copolymerization of NIPAM, NAS and methacrylate containing 1,8-naphthalimide groups, was used for Hg^{2+} detection (*Entry 8, Table 6*).[205]

Li *et al.*[206] reported the synthesis of thermoresponsive stable nanoparticles grafted onto the single-walled carbon nanotubes in water *via* nitrene addition reaction with azido-terminated PDMA-*b*-P(NIPAM-*co*-NAS) block copolymers and core-cross-linking reaction with ethylenediamine (*Entry 9, Table 6*).

Liu *et al.*[207] reported the synthesis of a reversible cross-linked PNAS-based polymers grafted onto mesoporous silica to trap and release Rhodamine B. PNAS grafted onto mesoporous silica was obtained by the RAFT polymerization of NAS in the presence of dithioester-functionalized silica used as the RAFT agent and AIBN used as the initiator in dioxane at 70°C. The NHS-functionalized silica was then suspended with Rhodamine B in buffer (pH = 7.4) and subsequently reacts with cystamine at 45°C to trap fluorescent molecule. The disulfide bond of cystamine could be cleaved using DTT as the reducing agent for the release of Rhodamine B from the porous silica.

Table 6: Synthesis of stable nanoparticules from NHS-based copolymers obtained by RAFT polymerization.

Entry	Block copolymer	RAFT agent[a]	Cross-linker agent	Ref.
1	PMA-*b*-P(NAS-*co*-NAM)	RAFT1	2,2'-(ethylenedioxy)bis(ethylamine)	198
2	PEO-*b*-(DMA-*co*-NAS)-*b*-NIPAM	RAFT2	ethylenediamine cystamine	200-201
3	PNIPAM-*b*-P(NAS-*co*-DMA)	RAFT3	ethylenediamine	202
4	PEA-*b*-P(NAS-*co*-HEA)	RAFT4	hexamethylenediamine	199
5	PNIPAM-*b*-PNAS-*b*-P(ε-caprolactone)	RAFT5	cystamine	203
6	PEO-*b*-PNAS-*b*-PS	RAFT6	cypate-diamine, HL-800-amine, 2,2'-(ethylenedioxy)bis(ethylamine) pyrazine-based diamine	208-211
7	PEO-*b*-P(NIPAM-*co*-NAS)	RAFT7	cystamine	204
8	PEO-*b*-P(NIPAM-*co*-NAS-*co*-NUMA)	RAFT8	cystamine	205
9	PDMA-*b*-P(NIPAM-*co*-NAS)	RAFT9	ethylenediamine	206

[a] For structures of RAFT agents, see Scheme 60

PFP-ester

Eberhardt *et al.*[212] reported the RAFT polymerization of pentafluorophenyl methacrylate (PFPMA) using CDB or 4-(4-cyanopentanoic acid) dithiobenzoate (CPAD) as RAFT agents in dioxane at 80°C. PPFPMAs were obtained with controlled M_n up to 17000 g.mol^{-1} and low polydispersity indices (PDI < 1.3) (*Scheme 61*).
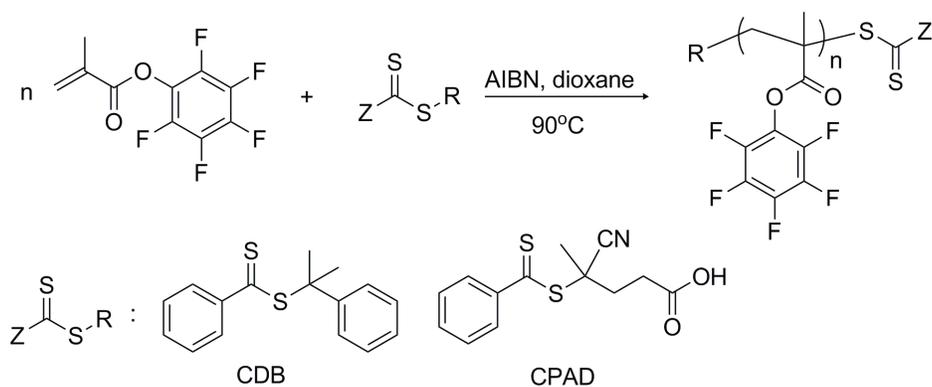
Scheme 61: Synthesis of PPFPMA via RAFT polymerization.

PPFPMAs were then used as macromolecular RAFT agents for the polymerization of MMA, NAM and *N,N*-diethyl acrylamide (DEAM). Moreover, PPFPMA-*b*-PNAM block copolymer and the PPFPMA-*b*-PDEAM block copolymers were reacted with *N*-isopropylamine to target thermoresponsive block copolymers.

Gibson *et al.*[213,214] synthesized well-defined PPFPMA using RAFT polymerization as a platform for the preparation of a library of functional polymers *via* post-polymerization modification of PPFPMA with primary amines. Libraries of functional polymer brushes *via* post-modification of PFPMA brushes obtained by surface-initiated RAFT polymerization were reported by Günay *et al.*[213].

Zentel and coworkers reported the synthesis of functional amphiphilic PHPMA-*b*-poly(lauryl methacrylate) PHPMA-*b*-PLMA block copolymers *via* the post-polymerization of PPFPMA-based block copolymers.[216-219] In such studies, the RAFT polymerization of PFPMA was carried out using CPAD as the RAFT agent and AIBN as the initiator in dioxane at 70°C. Resulting PPFPMAs were then employed as macromolecular RAFT agents for the polymerization of LMA using AIBN as the initiator at 70°C leading to well-defined PPFPMA-*b*-PLMA block copolymers (PDI $\leq$ 1.30).

These PFP-ester-functionalized block copolymers were then subjected to reaction with hydroxypropylamine to lead to PHPMA-*b*-PLMA (*Scheme 62*).
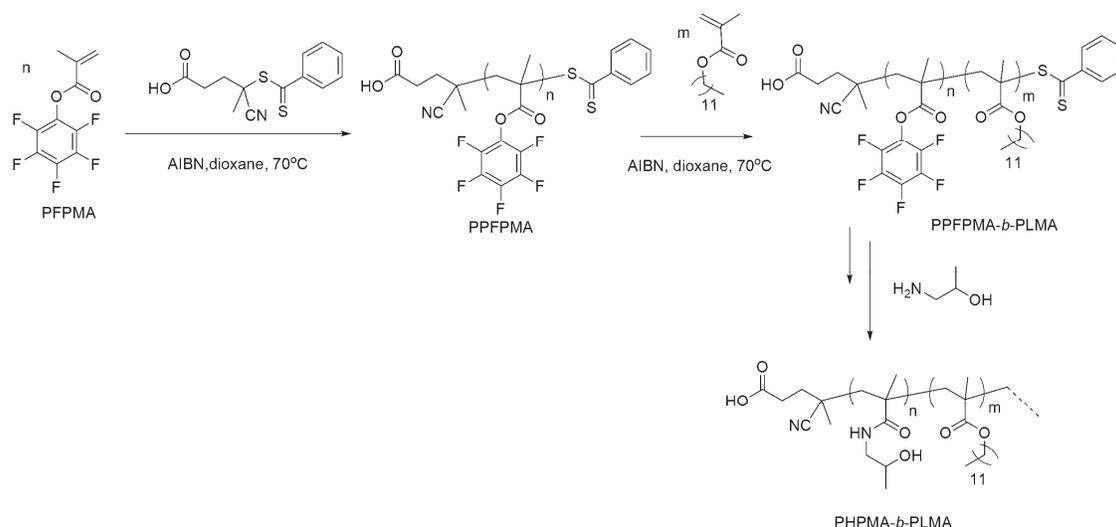
Scheme 62: RAFT polymerization of PPFPMA-based block copolymers and their post-modification.

POEGMA-*b*-PPFPMA block copolymer (M_n = 18800 g.mol^{-1}, PDI = 1.24) synthesized by successive RAFT polymerizations of OEGMA and PFPMA was reacted with *N*-isopropylamine in the presence of *N*-biotinylaminoethyl methanethiosulfonatein in DMF to prepare the ω-biotin-functionalized double thermoresponsive POEGMA-*b*-P(*N*-isopropyl methacrylamide) block copolymer.[220] In similar strategy, the different amino-terminated OEGMAs were reacted with poly(pentafluorophenyl acrylate) (PPFPA) and PFPMA in the presence of methyl methanethiosulfonate to target thermoresensible POEGMA (co)polymers.[221]

Nuhn *et al*. reported the RAFT polymerization of PPFPMA-*b*-POEGMA (M_n = 21600-25800 g.mol^{-1}, PDI = 1.14-1.20) and POEGMA-*b*-PPFPMA (M_n = 9600-39900 g.mol^{-1}, PDI = 1.13-1.23) block copolymers using CPAD as the RAFT agent. These

copolymers were then treated with an excess of AIBN in dioxane at 78^oC to remove the dithioester group. These resulting copolymers were self-assembled in DMSO and subsequently react with spermine as cross-linker and oregon green cadaverine as fluorescent dye in the presence of TEA at 50^oC to afford the core cross-linked nanoparticles that could be used as siRNA carrier for cellular delivery application.[222]

Boyer and Davis described the synthesis of PPFPA by RAFT polymerization and their use in a one-pot synthesis of glycopolymers (*Scheme 63*).[223] The polymerization of PFPA was performed using 3-(benzylsulfanylthiocarbonylsulfanyl)propionic acid (BSPA) as the RAFT agent with $[BSPA]_0/[AIBN]_0 = 5$ in benzene at 70^oC. PPFPAs have well-defined structure with M_n up to 16000 $g.mol^{-1}$ and narrow molecular weight distributions (PDI ≤ 1.20). These PPFPAs reacted with amine-functionalized amines and biotin maleimide in a one-pot process to yield biotin-functionalized glycopolymers. Furthermore, well-defined PPFPAs were also copolymerized with difunctionnal monomers used as cross-linkers (e.g. *N,N'*-bis(acryloyl)cystamine, *N,N*-methylene bisacrylamide, 1,6-hexanediol diacrylate) in the presence of AIBN used as the initiator in toluene at 70^oC to afford star-like polymers with M_n ranging from 42000 $g.mol^{-1}$ to 118000 $g.mol^{-1}$ with polydispersity indices from 1.14 to 2.65. Well-defined star polymers (PDI ≤ 1.18) then react with different amines for post-modification.[224] In the same group, acid degradable nanoparticles based on POEGMA-*b*-P(PFPA-*co*-vinylbenzyl chloride) precursors were synthesized using BSPA as the RAFT agent and AIBN as the initiator in acetonitrile at 65^oC.[225]
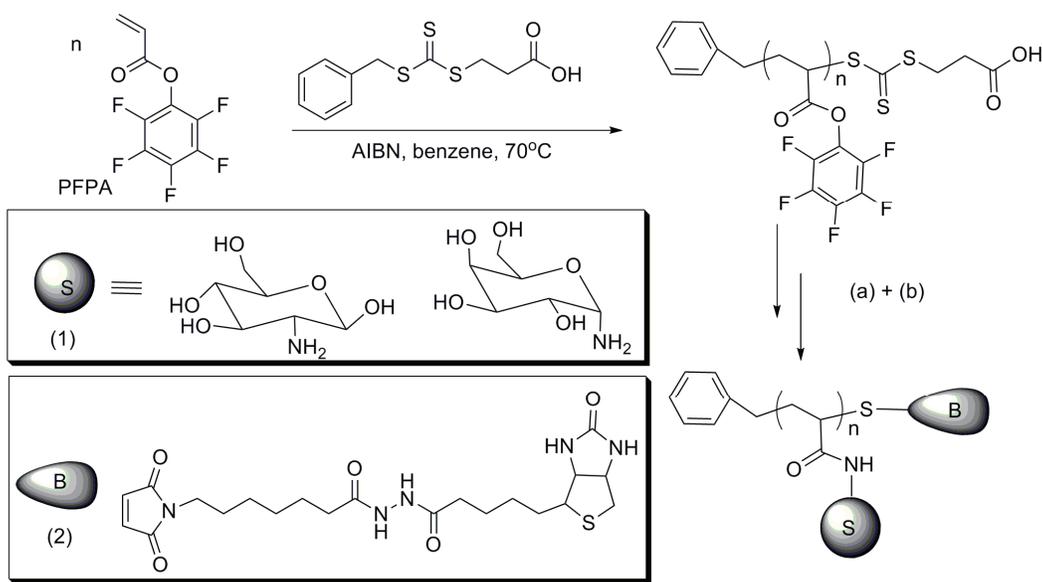
Scheme 63: Synthesis of PPFPA by RAFT polymerization and the subsequent one-pot synthesis of glycopolymers . Conditions: (a) nucleophilic substitution of sugar amine (1) in DMF–water (50/50 vol%) at room temperature, (b) in-situ aminolysis of the RAFT end-group and the thiol-ene reaction using biotin modified maleimide (2).

Zentel and coworkers described the successive RAFT polymerization of MMA, S, DEGMEMA and PFPA of vinyl triphenylamine (TPA) and PFPA to target PMMA-*b*-PPFPA block copolymer[226], PS-*b*-PPFPA[227], PDEGMEMA-*b*-PPFPA[227] and PTPA-*b*-PPFPA[228] block copolymer respectively. These block copolymers reacted with dopamine in order to prepare new dispersants for TiO_2, SnO_2 and ZnO. Poly(vinyl paramethyltriphenylamine)-*b*-PFPA synthesized by RAFT polymerization have been used to anchorthe surface of CdSe@ZnS quantum dots yielding quantum dot/polymer hydrids.[229] Moreover, block copolymers based on TPA and PPFA were employed to attach with amine-functionalized perylene and dopamine. Resulting copolymers were dispersed with ZnO for solar cell application.[230] Poly(methylsilsesquioxane)-*b*-PPFPA

block copolymers prepared by RAFT polymerization are considered to be promising coating materials that offer an easy access to adherent reactive surface coating on a broad range of substrates.[231]

Besides PFP-ester (meth)acrylates-based polymers, Nilles and Theato synthesized well-defined poly(pentafluorophenyl-4-vinylbenzoate)s and poly(pentachlorophenyl-4-vinylbenzoate)s-based block copolymers by RAFT polymerization using different dithiobenzoates as RAFT agents and AIBN as the initiator at 90°C (*Scheme 64*).[232,233]

Scheme 64: RAFT polymerization of various activated 4-vinylbenzoates using different dithiobenzoates as the RAFT agents and AIBN as the initiator at 90°C.

PNP-ester

Hu *et al.*[234] reported the synthesis of well-defined PNP-functionalized polymers based on poly(*p*-nitrophenyl acrylate) (PPNPA) by RAFT polymerization. well-defined PPNPAs (M_n = 2500-11080 g.mol^{-1}, PDI = 1.02-1.18) were obtained from the bulk polymerization of *p*-nitrophenyl acrylate (PNPA) in the presence of 1-(ethoxy carbonyl) prop-1-yl dithiobenzoate (EPDTB) as the chain transfer agent and AIBN as the initiator

at 80°C (*Scheme 65*). PPNPAs (M$_n$ = 5350 g.mol^{-1}, PDI = 1.02) were used as macromolecular chain transfer agents to mediate the polymerization of S using AIBN as the initiator in DMSO at 70°C to afford well-defined PPNPA-*b*-PS (PDI < 1.20) block copolymers.
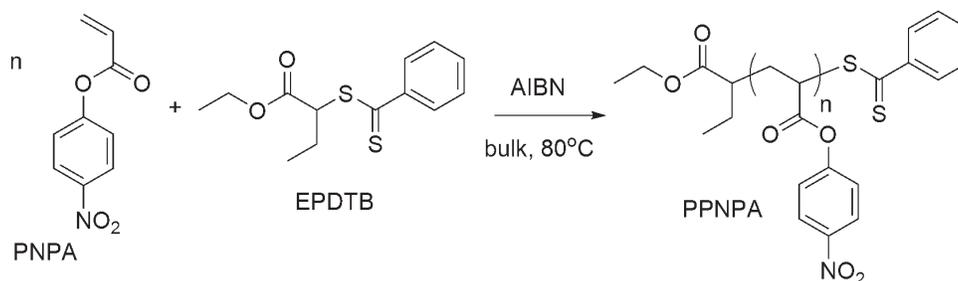
Scheme 65: RAFT polymerization of PNPA using EPDTB as the RAFT agent.

In similar conditions, the block copolymer PPNPA-*b*-PS (PDI =1.13) was assembled in nitromethane and subsequently reacts with the ethylenediamine at room temperature to afford stable nanoparticles. The PNP-ester-functionalized shell-cross-linked micelles obtained were used to react with glucosamine hydrochloride in DMSO to afford the stable glucosamine-carrying micelles.[235]

Maynard and coworkers reported the RAFT polymerization of PNPMA using CDB as the RAFT agent and AIBN as the initiator in DMSO at 70°C leading to well-defined PPNPMAs (M$_n$= 7700-19400 g.mol^{-1}, PDI = 1.15-1.29). The PPNPMA (M$_n$ = 9600 g.mol^{-1}, PDI = 1.15) then reacts with glycine methyl ester in the presence of TEA in DMSO at 50°C to target the glycinate-polymer conjugates. Using ten-fold excess of gylcine methyl ester, the glycinate-functionalized yield could be up to 86%.[236] A well-defined PPNPMA-*b*-poly(diethoxypropyl methacrylate) (PPNPMA-*b*-PDEPMA) block copolymer (M$_n$ = 12000 g.mol^{-1}, PDI = 1.24) was also synthesized using the

PPNPMA (M_n = 7000 g.mol^{-1}, PDI = 1.22) as the macromolecular chain transfer agent to mediate the polymerization of diethoxypropyl methacrylate (DEPMA) in the presence of AIBN as the initiator in DMF at 70°C (*Scheme 66*). The PPNPAM-*b*-PDEPMA block copolymer was then reacted with allylamine in TEA/DMSO at 50°C leading to the corresponding allylamine-functionalized block polymer.[237]
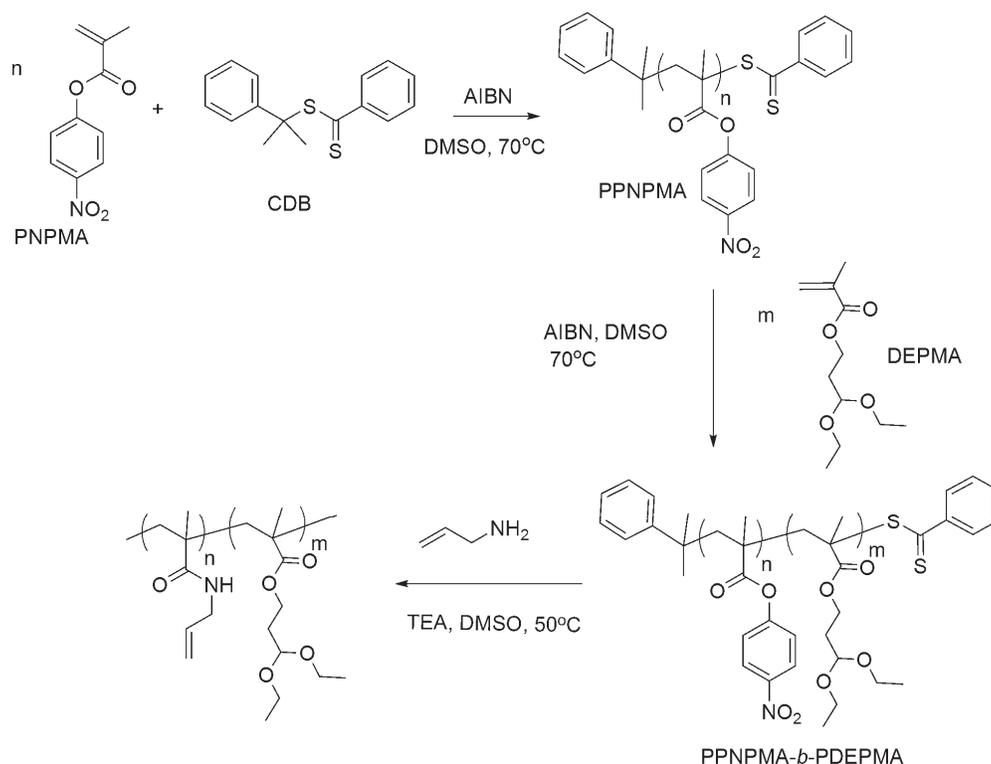
Scheme 66: Synthesis of block copolymers based on PNPMA and DEPMA using RAFT polymerization and subsequent functionalization with allylamine.

3.2. Post-functionalization of well-defined (co)polymers obtained by CRP

CRPs are useful methods to target directly well-defined reactive (co)polymers towards amines. Moreover, reactive groups towards amines can be introduced on the polymer using the post-functionalization of the backbone or of the chain-ends.

3.2.1. At the chain-end

3.2.1.a. Reactive groups not leading to molecular side-products

Epoxide

Coessens *et al.*[238] reported the ATRP of MA followed by the incorporation of an epoxide at the chain-end by using 1,2-epoxy-5-hexene *via* radical addition reaction.

Jia *et al.*[239] synthesized an epoxide-terminated PS and an epoxide-terminated P(*t*-BA) by a combination of single electron transfer (SET) and nitroxide radical coupling (NRC) using Cu(I)Br/Me$_6$TREN as the catalytic system in toluene/DMSO mixture (1/1, v/v) at 25°C for 10 min (*Scheme 67*).
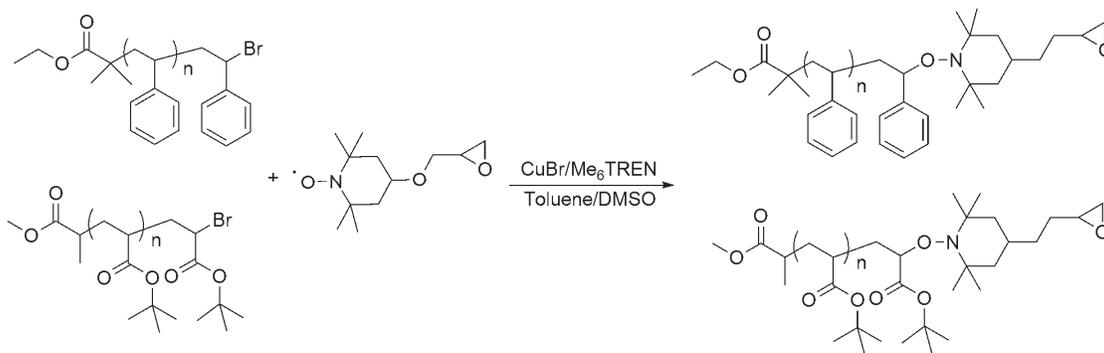
Scheme 67: End-group modification of PS and P(t-BA) with an epoxide- functionalized nitroxide radical by NRC.

The chain-end modification yields were determined by ^{1}H NMR spectroscopy and are equal to 94.8% and 96% for PS (M_n = 2190 g.mol^{-1}, PDI = 1.07) and P(*t*-BA) (M_n = 2190 g.mol^{-1}, PDI = 1.09), respectively.

Azlactone

Ho *et al.*[240] recently described the synthesis of well-defined azlactone-functionalized PNIPAM by RAFT polymerization followed by aminolysis and thiol-ene reactions. A well-defined PNIPAM (M_n = 7850 g.mol^{-1}, PDI = 1.05) was prepared by polymerization of NIPAM in the presence of MBTTCP as the RAFT agent and AIBN as the initiator at 70°C. The ω-trithiocarbonate-terminated PNIPAM was subjected to aminolysis and the resulting ω-thiol PNIPAM was reacted with VDM by Michael's addition reaction. The reactivity of the ω-azlactone ring has been assessed with 4-fluorobenzylamine.

Isocyanate

Yin *et al.*[241] reported the synthesis of ω-isocyanate-functionalized PMMA (M_n = 10000 g.mol^{-1}; PDI = 1.15 and 30000 g.mol^{-1}; PDI = 1.20) by ATRP (*Scheme 68*). In the first step, the ATRP of MMA was performed using EBiB as the initiator and CuBr/HMTETA as the catalytic system in toluene 85°C (*Scheme 68*). In the second step, an excess of TMI was added into the polymerization medium when the conversion of MMA reached 85%. The isocyanate end-group of PMMA was confirmed by FT-IR spectroscopy.
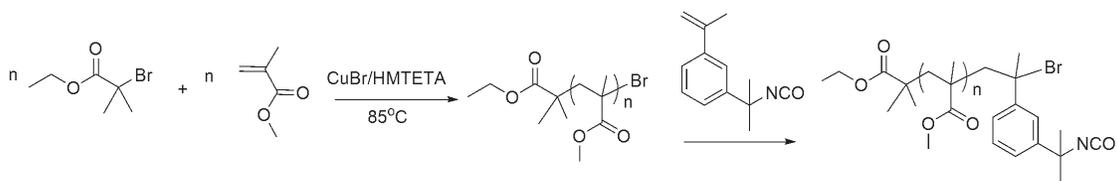
Scheme 68: Synthesis of ω-isocyanate PMMA by chain-end modification of ω-bromo-

functionalized PMMA obtained by ATRP.

3.2.1.b. Reactive groups leading to molecular side-products

NHS-ester

Xu *et al.*[242] synthesized well-defined NHS-terminated PNIPAM *via* RAFT polymerization followed by esterification of the chain-end. Typically, the polymerization of NIPAM was performed in the presence of 2-(1-carboxy-1-methylethylsulfanylthiocarbonylsulfanyl)-2-methylpropionic acid (CMP) used as the RAFT agent and of ACVA used as the initiator in dioxane at 70°C. Chain-ends of PNIPAM (M_n = 4100 g.mol^{-1}, PDI = 1.12) were then converted from carboxylic acids to NHS ester through dicyclohexylcarbodiimide coupling. The NHS-functionalized PNIPAM then reacts with poly(ethylene oxide)-*b*-poly[*N*-(3-aminopropyl)methacrylamide]-*b*-poly(2-diisopropylamino)ethyl methacrylate) to afford thermoresponsive shell cross-linked nanoparticles.

PFP-ester

Roth *et al.*[53] described the synthesis of PFP-ester-functionalized PMMAs using two strategies. In the first strategy, the RAFT polymerization of MMA was carried out using CDB as the RAFT agent and AIBN as the initiator in dioxane at 80°C. A large amount of PFP-ester-functionalized diazo initiator was subsequently used to convert the

ω-dithioester end-group to ω-PFP-ester terminated PMMA. In the second strategy, the PMMA was functionalized at the α- and ω- positions. The α-PFP ester functionality was introduced using pentafluorophenyl-(4-phenylthiocarbonylthio-4-cyanovalerate) (PFP-RAFT1, *Scheme 69*) as the RAFT agent during the polymerization of MMA. And the ω-PFP-ester was introduced by chain-end modification as described for the first strategy. These α,ω-PFP-ester PMMAs were subjected to react with different amines.
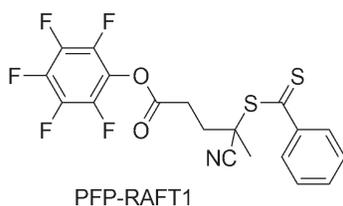
PFP-RAFT1

Scheme 69: Structure of PFP-functionalized RAFT agent: PFP-RAFT1.

3.2.2. On the polymer backbone

Isocyanate

Cao *et al.*[244] prepared a well-defined block copolymer containing isocyanate pendant groups *via* the post-polymerization modification of PS-*b*-PHEA block copolymer with 3-isocyanatomethyl-3,5,5-trimethylcyclohexyl isocyanate (IPDI) at 50°C for 24h in toluene (*Scheme 70*). The PS-*b*-PHEA block copolymers were previously synthesized by NMP.
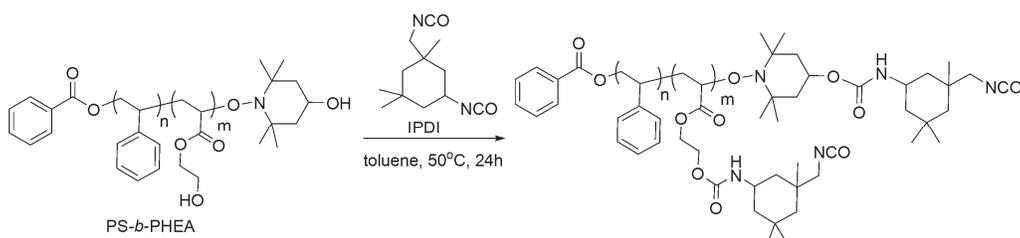
Scheme 70: Post-polymerization modification of PS-b-PHEA block copolymers previously synthesized by NMP.

Zheng *et al.*[244] reported the synthesis of P(MA-*co*-4-(azidocarbonyl) phenyl methacrylate) (M_n = 4500-19900 g.mol^{-1}, PDI = 1.20-1.07) using ^{60}C γ-initiated RAFT copolymerization of MA and 4-(azidocarbonyl)phenyl methacrylate in the presence of benzyl-1*H*-imidazole-1-carbodithioate as RAFT agent in bulk at room temperature. The azido groups were then transformed into isocyanate groups.

NHS-carbonate

Lane *et al.*[245] reported the synthesis of PHEMA brushes *via* surface ATRP mediated process of HEMA using CuCl/CuCl$_2$/bpy as the catalytic system in water/methanol. The PHEMA brushes then react with *N,N'*-disuccinimidylcarbonate in the presence of 4-dimethylaminopyridine in DMF at room temperature leading to NHS-carbonate-functionalized PHEMA brushes reactive towards horseradish peroxidase C in phosphate buffer (pH = 7.5^{o}C) at 4°C.

4. Conclusion

The main different CRP processes (NMP, ATRP and RAFT) provide convenient routes to amine-reactive polymers with predictable molecular weights and narrow molecular weight distribution. Positioning of the amino-reactive functionality either at the chain-ends or in the side chain can easily be achieved through the use of an appropriate functional initiator/chain transfer agent or monomer, respectively. A wide range of well-defined macromolecular architectures and functional polymeric materials (homo- and copolymers, surfaces, nanoparticles, etc…) can thus be prepared, providing versatile avenues to a variety of bioconjugates through reaction with the amino functionality of various biological entities.

In this work, we were interested in developing highly efficient chemical approaches to functional polymers having a high reactivity towards amino groups in view of bioconjugation applications. The azlactone ring was selected as the amine reactive functionality since this chemical group reacts easily under mild conditions without the need of a catalyst and with no by-product elimination. Amongst the CRP methodologies, RAFT polymerization was chosen due to its facile and robust control and to the nearly quantitative chain-end functionalization.[246]

References

[1] (a) Pasut, G.; Veronese, F. M. *Prog. Polym. Sci.* **2007**, *32*, 933-961. (b) Lutz, J.-F.; Börner, H. G. *Prog. Polym. Sci.* **2008**, *33*, 1-39. (c) Goddard, J. M.; Hotchkiss, J. H. *Prog. Polym. Sci.* **2007**, *32*, 698-725. (d) Galvin, C. J.; Genzer, J. *Prog. Polym. Sci.* **2012**, *37*, 871-906.

[2] Gauthier, M. A.; Gibson, M. I.; Klok, H.-A. *Angew. Chem. Int. Ed.* **2009**, *48*, 48-58.

[3] Jenkins, A. D.; Jones, R. G. ; Moad, G. *Pure Appl. Chem.* **2010**, *82*, 483-491.

[4] (a) Georges, M. K.; Veregin, R. P. N.; Kazmaier, P. M.; Hamer, G. K. *Macromolecules* **1993**, *26*, 2987-2988. (b) Hawer, C. J.; Bosman, A. W.; Harth, E. *Chem. Rev.* **2001**, *101*, 3661-3688.

[5] (a) Matyjaszewski, J.; Wang, J. *J. Am. Chem. Soc.* **1995**, *117*, 5614-5615. (b) Matyjaszewski, K.; Gaynor, S.; Wang, J. S. *Macromolecules* **1995**, *28*, 2093-2095. (c) Kato, M.; Kamigaito, M.; Sawamoto, M.; Higashimura, T. *Macromolecules* **1995**, *28*, 1721-1726. (d) Matyjaszewski, K.; Xia, J. *Chem. Rev.* **2001**, *101*, 2921-2990. (e) Kamigaito, M.; Ando, T.; Sawamoto, M. *Chem. Rev.* **2001**, *101*, 3689-3745.

[6] Chiefai, J.; Chong, Y. K.; Ercole, F.; Krstina, J.; Jeffery, J.; Le, T. P. T.; Mayadunne, R. T. A.; Meijs, G. G.; Moad, C. L.; Moad, G. Rizzaddo, E.; Thang, S. H. *Macromolecules* **1998**, *31*, 5559-5562.

[7] Kolb, H. C.; Finn, M. G.; Sharpless, K. B. *Angew. Chem. Int. Ed.* **2001**, *40*, 2004-2021.

[8] Heilmann, S. M.; Ramussen, J. K.; Krepski, L. R. *J. Polym. Sci. Part A: Polym. Chem.* **2001**, *39*, 3655-3677.

[9] Bodanszky, M. *Principles of Peptide Synthesis*, 2nd Edition, Spinger-Verlag, Berlin, **1993**.

[10] Bruckner, R. *Advanced Organic Chemistry: Reaction Mechanisms*, Harcourt/Academic Press, San Diego, **2002**.

[11] Buck, M. E.; Lynn, D. M. *Polym. Chem.* **2012**, *3*, 66-90.

[12] Theato, P. *J. Polym. Sci. Part A: Polym. Chem.* **2008**, *46*, 6677-6687.

[13] Flores, J. D.; Shin, J.; Hoyle, C. E.; McCormick, C. L. *Polym. Chem.* **2010**, *1*, 213-220.

[14] Serenson, W.R.; Campbell, T.W., *Preparative Methods of Polymer Chemistry*, New York: Interscience, **1961**

[15] Fuso, F.; Wunderlich, W.; Kramer, A.; Fink, J. *US Patent* **2004,** No 0049043 A1

16   Fansler, D. D.; Lewandowski, K. M.; Wendland, S. M. Gaddam, B. N. *US Patent* **2004**, No 6680362 B1.

17   Vinas, J.; Chagneux, N.; Gigmes, D.; Trimaille, T.; Favier, A.; Bertin, D. *Polymer* **2008**, *49*, 3639-3647.

18   Parvole, J.; Ahrens, L.; Blas, H.; Vinas, J.; Boissière, C.; Sanchez, C.; Save, M.; Charleux, B. *J. Polym. Sci. Part A: Polym. Chem*. **2010**, *48*, 173-185.

19   Chenal, M.; Boursier, C.; Guillaneuf, Y.; Taverna, M.; Couvreur, P.; Nicolas, J. *Polym. Chem*. **2011**, *2*, 1523-1530.

20   Moayeri, A.; Lessard, B.; Maric, M. *Polym. Chem*. **2011**, *2*, 2084-2092.

21   Zhang, C.; Maric, M. *Polymers* **2011**, *3*, 1398-1422.

22   Maric, M.; Consolante, V. *J. Appl. Polym. Sci*. **2012**, DOI: 10.1002/APP.37949

23   Maric, M.; Lessar, B. H. Consolante, V.; Ling, E. J. Y. *React. Funct. Polym*. **2011**, *71*, 1137-1147.

24   Harrisson, S.; Couvreur, P.; Nicolas, J. *Macromolecules* **2011**, *49*, 9230-9238.

25   Zhang, X.; Xia, J.; Matyjaszewski, K. *Macromolecules* **2000**, *33*, 2340-2345.

26   Degirmenci, M.; Izgin, O.; Acikses, A.; Genli, N. *React. Funct. Polym.* **2010**, *70*, 28-34.

27   Lewandowski, K. M.; Fansler, D. D. Gaddam, B. N.; Heilmman, S. M.; Krepski, L. R.; Roscoe, S. B.; Wendland, M. S. *US Patent* **2005**, No: US 6894133B2.

28   Palaskar, D. V.; Sane, P. S.; Wadgaonkar, P. P. *React. Funct. Polym.* **2010**, *70*, 931-937.

29   Han, D.-H.; Pan, C.-Y. *Polymer* **2006**, *47*, 6956-6962.

30   Ladmiral, V.; Monaghan, L.; Mantovani, G.; Haddleton, D. M. *Polymer* **2005**, *46*, 8536-8545.

31   Geng, J.; Biedermann, F.; Zayed, M. J.; Tian, F.; Scherman, O. A. *Macromolecules* **2011**, *44*, 4276-4281.

32   Nicolas, J.; Khoshdel, E.; Haddleton, D. M. *Chem. Commun.* **2007**, 1722-1724.

33   Slavin, S.; Khoshdel, E.; Haddleton, D. M. *RSC Advances* **2011**, *1*, 58-66.

34   Lecolley, F.; Tao, L.; Mantovani, G.; Durkin, I.; Lautru, S.; Haddleton, D. M. *Chem. Commun*. **2004**, 2026-2027.

35   Samata, D.; McRae, S.; Cooper, B.; Hu, Y.; Emrick, T.; Pratt, J.; Chales, S. A. *Biomacromolecules* **2008**, *9*, 2891-2897.

36   Lewis, A.; Tang, Y.; Brocchini, S.; Choi, J. W.; Godwin, A. *Bioconjugate Chem*. **2008**, *19*, 2144-2155.

37   Zarafshani, Z.; Obata, T.; Lutz, J.-F. *Biomacromolecules* **2010**, *11*, 2130-2135.

38   Munro, N. H.; Hanton, L. R.; Moratti, S. C.; Robinson, B. H. *Carbohydrate Polym.* **2009**, *77*, 496-505.

39   Lele, B. S.; Murata, H.; Matyjaszewski, K.; Russell, A. J. *Biomacromolecules* **2005**, *6*, 3380-3387.

40   Bao, H.; Hu, J.; Gan, L. H.; Li, L. *J. Polym. Sci. Part A: Polym. Chem.* **2009**, *47*, 6682-6692.

41   Tan, I.; Zarafshani, Z.; Lutz, J.-F.; Titirici, M.-M. *ACS Appl. Mater. Interf.* **2009**, *1*, 1869-1872.

42   Delaittre, G.; Justribó-Hernández, G.; Notlte, R. J. M.; Cornelissen, J. J. L. M. *Macromol. Rapid Commun.* **2011**, *32*, 19-24.

43   McRae, S.; Chen, X.; Kratz, K.; Samanta, D.; Henchey, E.; Schneider, S.; Emrick, T. *Biomacromolecules* **2012**, dx.doi.org/10.1021/bm3004836.

44   Chen, X.; McRae, S.; Samanta, D.; Emrick, T. *Macromolecules* **2010**, *43*, 6261-6263.

45   Hu, Y.; Samata, D.; Parelkar, S. S.; Hong, S. W.; Wang, Q.; Russell, T. P.; Emrick, T. *Adv. Funct. Mat.* **2010**, *20*, 3603-3612.

46   Vora, A.; Nasrullah, M. J.; Webster, D. C. *Macromolecules* **2007**, *40*, 8586-8592.

47   Lewandowski, K. M.; Fansler, D. D.; Wendland, M. S.; Heilmann, S. M.; Gaddam, B. N. *US Patent* **2004** Patent No.: US 6762257 B1.

48   Bathfield, M.; D'Agosto, F.; Spitz, R.; Charreyre, M.-T.; Delair, T. *J. Am. Chem. Soc.* **2006**, *128*, 2546-2547.

49   Aamer, K. A.; Tew, G. N. *J. Polym. Sci. Part A: Polym. Chem.* **2007**, *45*, 5618-5625.

50   Han, D.-H.; Yang, L.-P.; Zhang, X.-F.; Pan, C.-Y. *Eur. Polym. J.* **2007**, *43*, 3873-3881.

51   McDowall, L.; Chen, G.; Stenzel, M. H. *Macromol. Rapid Commun.* **2008**, *29*, 1666-1671.

52   Li, H.; Bapat, A. P.; Li, M.; Sumerlin, B. S. *Polym. Chem.* **2011**, *2*, 323-327.

53   Roth, P. J.; Wiss, K. T.; Zentel, R.; Theato, P. *Macromolecules* **2008**, *41*, 8513-8519.

54   Wiss, K. T.; Krishna, O. D.; Roth, P. J.; Kiick, K. L.; Theato, P. *Macromolecules* **2009**, *42*, 3860-3863.

55   Roth, P. J.; Haase, M.; Baché, T.; Theato, P.; Zentel, R. *Macromolecules* **2010**, *43*, 895-902.

56   Roth, P. J.; Jochum, F. D.; Zentel, R.; Theato, P. *Biomacromolecules* **2010**, *11*, 234-238.

57   Roth, P. J.; Jochum, F. D.; Forst, R. F.; Zentel, R.; Theato, P. *Macromolecules* **2010**, *43*, 4638-4645.

58   Roth, P. J.; Kim, K. S.; Bae, S. H.; Sohn, B. H.; Theato, P.; Zentel, R. *Macromol. Rapid Commun.* **2009**, *30*, 1274-1278.

59   Wiss, K. T.; Theato, P. *J. Polym. Sci. Part A: Polym. Chem.* **2010**, *48*, 4758-4767.

60   Godula, K.; Rabuka, D.; Nam, K. T.; Bertozzi, C. R. *Angew. Chem. Int. Ed.* **2009**, *48*, 4973-4976.

61   Tao, L.; Liu, J.; Xu, J.; Davis, T. P. *Org. Biomol. Chem.* **2009**, *7*, 3481-3485.

62   Tao, L.; Xu, J.; Gell, D.; Davis, T. P. *Macromolecules* **2010**, *43*, 3721-3727.

63   Liu, Y.; Li, M.; Wang, D.; Yao, J.; Shen, J.; Liu, W.; Feng, S.; Tao, L.; Davis, T. P. *Aust. J. Chem.* **2011**, *64*, 1602-1610.

64   Tao, L.; Liu, J.; Xu, J.; Davis, T. P. *Chem. Commun.* **2009**, 6560-6562.

65   Luo, X.; Liu, J.; Liu, G.; Wang, R.; Liu, Z.; Li, A. *J. Polym. Sci. Part A: Polym. Chem.* **2012**, *50*, 2786-2793.

66   Xu, J.; Boyer, C.; Bulmus, V.; Davis, T. P. *J. Polym. Sci. Part A: Polym. Chem.* **2009**, *47*, 4302-4313.

67   Benoit, D.; Chaplinski, V.; Braslau, R.; Hawker, C. J. *J. Am. Chem. Soc.* **1999**, *121*, 3904-3920.

68   Fleischmann, S.; Hinrichs, K.; Oertel, U.; Reichelt, S.; Eichhorn, K. -J.; Voit, B. *Macromol. Rapid Commun.* **2008**, *29*, 1177-1185.

69   Grubbs, R. B.; Dean, J. M.; Broz, M. E.; Bates, F. S. *Macromolecules* **2000**, *33*, 9522-9534.

70   Moayeri, A.; Lessard, B.; Maric, M. *Polym. Chem.* **2011**, *2*, 2084-2092.

71   Lessard, B.; Maric, M. *J. Polym. Sci. Part A: Polym. Sci.* **2009**, *47*, 2547-2588.

72   Lessard, B.; Tervo, C.; Wahl, S. D.; Clerveaux, F. J.; Tang, K. K. Yasmine, S.; Andjelic, S.; Alessandro, A. D.; Maric, M. *Macromolecules* **2010**, *43*, 868-878.

73   Jones, R. G.; Yoon, S.; Nagasaki, Y. *Polymer* **1999**, *40*, 2411-2418.

74   Tully, D. C.; Roberts, M. J.; Geierstanger, B. H.; Grubbs, R. B. *Macromolecules* **2003**, *36*, 4302-4308.

75   Hodges, J. C.; Harikrishnan, L. S.; Ault-Justus, S. *J. Comb. Chem.* **2002**, *2*, 80-88.

76   Wisnoski, D. D.; Leister, W. H.; Strauss, K. A.; Zhao, Z.; Lindsley, C. W. *Tetrahedron Lett.* **2003**, *44*, 4321-4325.

77   Desforges, A.; Arpontet, M.; Deleuze, H.; Mondain-Monval, O. *React. Funct. Polym.* **2002**, *53*, 183-192.

78   Desai, A.; Atkinson, N.; Rivera, F.; Devonport, W.; Rees, I.; Branz, S. E.; Hawker, C. J. *J. Polym. Sci. Part A: Polym. Chem.* **2000**, *38*, 1033-1044.

79   Handke, N.; Trimaille, T.; Luciani, E.; Rollet, M.; Delair, T.; Verrier, B.; Bertin, D.; Gigmes, D. *J. Polym. Sci. Part A: Polym. Chem.* **2011**, *49*, 1341-1350.

80   Kakuchi, R.; Zamfir, M.; Lutz, J.-F.; Theato, P. *Macromol. Rapid Commun.* **2012**, *33*, 54-60.

81   Zamfir, M.; Theato, P.; Lutz, J.-F. *Polym. Chem*. DOI: 10.1039/c1py00514f.

82   Nilles, K.; Theato, P. *Polym. Chem*. **2011**, *2*, 376-384.

83   Boonpangrak, S.; Whitcombe, M. J.; Parchaysittkul, V.; Mosbach, K.; Ye, L. *Biosens. Bioelectron.* **2006**, *22*, 349-354.

84   Benoit, D.; Hawker, C. J.; Huang, E. E.; Lin, Z.; Russell, T. P. *Macromolecules* **2000**, *33*, 1505-1507.

85   Lessard, B.; Maric, M. *Macromolecules* **2010**, *43*, 879-885.

86   Park, E.-S.; Kim, M.-N.; Lee, I.-M.; Lee, H. S.; Yoon, J.-S. *J. Polym. Sci. Part A: Polym. Chem*. **2000**, *38*, 2239-2244.

87   Matyjaszewski, K.; Coca, S.; Jasieczek, C. B. *Macromol. Chem. Phys.* **1997**, *198*, 4011-4017.

88   Krishnan, R.; Srinivasan, K. S. V. *Macromolecules* **2003**, 36, 1769-1771.

89   Krishnan, R.; Srinivasan, K. S. V. *Macromolecules* **2004**, *37*, 3614-3622.

90   Chen, X. J.; Zhao, M.; Gu, S. S. *Polym. Bull*. **2012**, *68,* 1525-1535.

91   Hayek, A.; Xu, Y.; Okada, T.; Barlow, S.; Zhu, X.; Moon, J. H.; Marder, S. R.; Yang, S. *J. Mater. Chem*. **2008**, *18*, 3316-3318.

92   Xu, F. J.; Cai, Q. J.; Li, Y. L.; Tang, E. T.; Neoh, K. G. *Biomacromolecules* **2005**, *6*, 1012-1020.

93   El Idrissi, K.; Eddarir, S.; Tokarski, C.; Rolando, C. *J. Chromatography B* **2011**, *879*, 2852-2859.

94   Yuan, L.; Hua, X.; Wu, Y.; Pan, X.; Liu. S. *Anal. Chem*. **2011**, *83*, 6800-6809.

95   Huang, C.; Neoh, K. G.; Tang, E.-T.; Shuter, B. *J. Mater. Chem.* **2011**, *21*, 16094-16102.

96   Huang, C.; Neoh, K. G.; Kang, E.-T. *Langmuir* **2012**, *28*, 563-571.

97   Barbey, R.; Kauffmann, E.; Ehrat, M.; Klok, H.-A. *Biomacromolecules* **2010**, *11*, 3467-3479.

98   Edmondson, S.; Huck, W. T. S. *Adv. Mater.* **2004**, *16*, 1327-1331.

99 Edmondson, S.; Frieda, K.; Comrie, J. E.; Onck, P. R.; Huck, W. T. S. *Adv. Mater.* **2006**, *18*, 724-728.

100 Wang, M.; Comrie, J. E.; Bai, Y.; He, X.; Guo, Sha, Huck, W. T. S. *Adv. Funct. Mater.* **2009**, *19*, 2236-2243.

101 Edmondson, S.; Huck, W. T. S. *J. Mater. Chem.* **2004**, *14*, 730-734.

102 Barbey, R.; Klok, H.-A. *Langmuir* **2010**, *26*, 18219-18230.

103 Nyström, D.; Lindqvist, J.; Östmark, E.; Antoni, P.; Carlmark, A.; Hult, A.; Malmström, E. *ACS Appl. Mater. Interfaces* **2009**, *1*, 816-823.

104 Nyström, D.; Malmström, E.; Hult, A.; Blakey, I.; Boyer, C.; Davis, T. P.; Whittaker, M. R. *Langmuir* **2010**, *26*, 12748-12754.

105 Cummins, D.; Wyaman, P.; Duxbury, C. J.; Thies, J.; Koning, C. E.; Heise, A. *Chem. Mater.* **2007**, *19*, 5285-5292.

106 Li, C.; Ge, Z.; Fang, J.; Liu, S. *Macromolecules* **2009**, *42*, 2916-2924.

107 Ma, M.; Li, F.; Chen, F.-J; Cheng, S.-X; Zhuo, R.-X. *Macromol. Biosci.* **2010**, *10*, 183-191.

108 Sha, K.; Li, D.; Li, Y.; Liu, X.; Wang, S.; Guan, J.; Wang, J. *J. Polym. Sci. Part A: Polym. Chem.* **2007**, *45*, 5037-5049.

109 Zhang, B.; Li, Y.; Ai, P.; Sa, Z.; Zhao, Y.; Li, M.; Wang, D.; Sha, K. *J. Polym. Sci. Part A: Polym. Chem.* **2009**, *47*, 5509-5526.

110 Ma, M.; Li, F.; Yuan, Z.-F.; Zhuo, R.-X. *Acta Biomater.* **2010**, *6*, 2658-2665.

111 Xu, F. J.; Chai, M. Y.; Li, W. B.; Ping, Y.; Tang, G. P.; Yang, W. T.; Ma, J. Liu, F. S. *Biomacromolecules* **2010**, *11*, 1437-1442.

112 Zhang, Y.; He, H.; Gao, C. *Macromolecules* **2008**, *41*, 9581-9594.

113 Qin, J.; Jiang, X.; Gao, L.; Chen, Y.; Xi, F. *Macromolecules* **2010**, *43*, 8094-8100.

114 Yuan, Y.-Y.; Du, Q.; Wang, Y.-C.; Wang, J. *Macromolecules* **2010**, *43*, 1739-1746.

115 Canamero, P. F.; Fuente, J. L. D. L.; Madruga, L. E.; Fernandez-Gracia, M. *Macromol. Chem. Phys.* **2004**, *205*, 2221-2228.

116 Chen, Z.; Bao, H.; Liu, J. *J. Polym. Sci. Part A: Polym. Chem.* **2001**, *39*, 3726-3732.

117 Brar, A. S.; Goyal, A. K. *Eur. Polym. J.* **2008**, *44*, 4082-4091.

118 Bicak, N.; Gazi, M.; Galli, G.; Chiellini, E. *J. Polym. Sci. Part A: Polym. Chem.* **2006**, *44*, 6708-6716.

119 Karagoz, B.; Bayramoglu, G.; Altintas, B.; Bicak, N.; Arica, M. Y. *Ind. Eng. Chem. Res.* **2010,** *49*, 9655-9665.

120   Bayramoglu, G.; Karagoz, B.; Altintas, B.; Arica, M. Y.; Bicak, N. *Bioprocess. Biosyst. Eng.* **2011**, *34*, 735-746.

121   Tsarevsky, N. V.; Bencherif, S. A.; Matyjaszewski, K. *Macromolecules* **2007**, *40*, 4439-444.

122   Jones, M.-C.; Tewari, P.; Blei, C.; Hales, K.; Pochan, D. J.; Leroux, J.-C. *J. Am. Chem. Soc.* **2006**, *128*, 14599-14605.

123   Fournier, D.; Pascual, S.; Fontaine, L. *Macromolecules* **2004**, *37*, 330-335.

124   Fournier, D.; Pascual, S.; Montembault, V.; Haddleton, D. M.; Fontaine, L. *J. Comb. Chem.* **2006**, *8,* 522-530.

125   Fournier, D.; Pascual, S.; Montembault, V.; Fontaine, L. *J. Polym. Sci. Part A: Polym. Chem.* **2006**, *44*, 5316-5328.

126   Cullen, S. P.; Mandel, I. C.; Gopalan, P. *Langmuir* **2008**, *24*, 13701-13709.

127   Sun, B.; Liu, X.; Buck, M. E.; Lynn, D. M. *Chem. Commun.* **2010**, *46,* 2016-2018.

128   Koulic, C.; Yin, Z.; Pagnoulle, C.; Gilbert, B.; Jérôme, R. *Polymer* **2001**, *42*, 2947-2957.

129   Yin, Z.; Koulic, C.; Pagnoulle, C.; Jérôme, R. *Macromol. Chem. Phys.* **2002**, *203*, 2021-2028.

130   Jana, S.; Yu, H.; Parthiban, A.; Chai, C. L. L. *J. Polym. Sci. Part A: Polym. Chem.* **2010**, *48*, 1622-1632.

131   Hu, Z.; Liu, Y.; Hong, C.; Pan, C. *J. Appl. Polym. Sci.* **2005**, *98*, 189-194.

132   Huang, C.-Q.; Hong, C.-Y.; Pan, C.-Y. *Chin. J. Polym. Sci.* **2008**, *26*, 341-352.

133   Hasneen, A.; Cho, I.-S.; Kim, K.-W.; Paik, H.-J. *Polym. Bull.* **2012**, *68*, 681-691.

134   Yu, X.; Tang, X.; Pan, C. *Polymer* **2005**, *46*, 11149-11156.

135   Godwin, A.; Hartenstein, M.; Müller, A. H. E.; Brocchini, S. *Angew. Chem. Int. Ed.* **2001**, *40,* 594-597.

136   Pedone, E.; Li, X.; Koseva, N.; Alpar, O.; Brocchini, S. *J. Mater. Chem.* **2003**, *13*, 2825-2837.

137   Wang, S. Y.; Sood, N.; Putnam, D. *Mol. Ther.* **2009**, *17*, 480-490.

138   Rickert, E.; Trebley, J. P.; Peterson, A. C.; Morrell, M. M.; Weatherman, R. V. *Biomacromolecules* **2007**, *8*, 3608-3612.

139   Monge, S.; Haddleton, D. M. *Eur. Polym. J.* **2004**, *40*, 37-45.

140   Shunmugam, R.; Tew, G. N. *J. Polym. Sci. Part A: Polym. Chem.* **2005**, *43*, 5831-5843.

141   Ghosh, S.; Basu, S.; Thayumanavan, S. *Macromolecules* **2006**, *39*, 5595-5597.

142   Orski, S. V.; Fries, K. H.; Sheppard, G. R.; Locklin, J. *Langmuir* **2010**, *26*, 2136-2143.

143   Orski, S. V.; Poloukhtine, A. A.; Arumugam, S.; Mao, L.; Popik, V. V.; Locklin, J. *J. Am. Chem. Soc*. **2010**, *132*, 11024-11026.

144   Arumugam, S.; Orki, S. V.; Locklin, J.; Popik, V. V. *J. Am. Chem. Soc*. **2012**, *134*, 179-182.

145   Singha, N.; Gibson, M. I.; Koiry, B. P.; Danial, M.; Klok, H.-A. *Biomacromolecules* **2011**, *12*, 2908-2913.

146   Liu, Y.; Wang, L.; Pan, C.-Y. *Macromolecules* **1999**, *32*, 8301-8305.

147   Popescu, D.; Keul, H.; Moeller, M. *Macromol. Chem. Phys*. **2008**, *209*, 2012-2025.

148   Adelmann, R.; Mennicken, M.; Popescu, D.; Heine, E.; Keul, H.; Moeller, M. *Eur. Polym. J.* **2009**, *45*, 3093-3107.

149   Popescu, D.; Keul, H.; Moeller, M. *React. Funct. Polym*. **2010**, *70*, 767-774.

150   Zhu, J. Zhou, D.; Zhu, X.; Chen, G. *J. Polym. Sci. Part A: Polym. Chem*. **2004**, *42*, 2558-2565.

151   Fu, G. D.; Xu, L. Q.; Yao, F.; Zhang, K.; Wang, X. F.; Zhu, M. F.; Nie, S. Z. *ACS Appl. Mater. Interfaces* **2009**, *2*, 239-243.

152   Gudipati, C. S.; Tan, M. B. H.; Hussain, H.; Liu, Y.; He, C.; Davis, T. P. *Macromol. Rapid Commun.* **2008,** *29*, 1902-1907.

153   Chambon, P.; Blanazs, A.; Battaglia, G.; Armes, S. P. *Langmuir* **2012**, *28*, 1196-1205.

154   Strube, O. I.; Nothdurft, L.; Drache, M.; Naake, G. S. *Macromol. Chem. Phys*. **2011**, *212*, 574-582.

155   Siegwart, D. J.; Whitehead, K. A.; Nuhn, L.; Shay, G.; Cheng, H.; Jiang, S.; Ma, M.; Lytton-Jean, A.; Vegas, A.; Fenton, P.; Levins, C. G.; Love, K. T.; Lee, H.; Cortez, C.; Collins, S. P.; Li, Y. F.; Jang, J.; Querbes, W.; Zurenko, C.; Novabrantseva, T.; Langer, R.; Anderson, D. G. *PNAS* **2011**, *108*, 12996-13001.

156   Yin, H.; Zheng, H.; Lu, Y.; Liu, P.; Cai, Y. *J. Polym. Sci. Part A: Polym. Chem*. **2007**, *45*, 5091-5102.

157   Luo, Q.; Zheng, H.; Peng, Y.; Gao, H.; Lu, L.; Cai, Y. *J. Polym. Sci. Part A: Polym. Chem.* **2009**, *47*, 6668-6681.

158   Ostaci, R. V.; Damiron, D.; Grohens, Y.; Léger, L.; Drockenmuller, E. *Langmuir* **2010**, *26*, 1304-1310.

159   Damiron, D.; Mazzolini, J.; Cousin, F.; Boisson, C.; D'agosto, F.; Drockenmuller, E. *Polym. Chem*. **2012**, *3*, 1838-1845.

160   Farquet, P.; Padeste, C.; Solak, H. H.; Gürsel, A.; Scherer, G. G.; Wokaun, A. *Macromolecules* **2008**, *41*, 6309-6316.

161   Li, L.; Kang, E.; Neoh, K. *Appl. Surf. Sci.* **2008**, *254*, 2600-2604.

162   Schilli, C. M.; Müller, A. H. E.; Rizzardo, E.; Thang, H. S.; Chong, Y. K. B. *Advance in Controlled/Living Radical Polymerization* **2003**, *Chapter 41*, pp 603-618, Edited by Krzystof Matyjaszewski.

163   Lokitz, B. S.; Messman, J. M.; Hinestrosa, J. P.; Alonzo, J.; Verduzco, R.; Brown, R. H.; Osa, M.; Ankner, J. F.; II, K. S. M. *Macromolecules* **2009**, *42*, 9018-9026.

164   Cantu, E. S.; Lotiz, B. S.; Hinestrosa, J. P.; Deodhar, C.; Messman, J. M.; Ankner, J. F.; II, K. S. M. *Langmuir* **2011**, *27*, 5986-5996.

165   Pascual, S.; Blin, T.; Saikia, P. J.; Thomas, M.; Gosselin, P.; Fontaine, L. *J. Polym. Sci. Part A: Polym. Chem.* **2010**, *48*, 5053-5062.

166   Levere, M. E.; Ho, H. T.; Pascual, S.; Fontaine, L. *Polym. Chem.* **2011**, *2*, 2878-2887.

167   Barner, L.; Perera, S.; Sandanayake, S.; Davis, T. P. *J. Polym. Sci. Part A: Polym. Chem.* **2006**, *44*, 857-864.

168   Duong, H. T. T.; Huynh, V. T.; Souza, P. D.; Stenzel, M. H. *Biomacromolecules* **2010**, *11*, 2290-2299.

169   Duong, H. T. T.; Nguyen, U. T. L.; Stenzel, M. H. *Polym. Chem.* **2010, *1*, 171-182.

170   Kim, Y.; Pourgholami, M. H.; Morris, D. L.; Stenzel, M. H. *J. Mater. Chem.* **2011**, *21*, 12777-12783.

171   Beck, J. B.; Killops, K. L.; Kang, T.; Sivanandan, K.; Bayles, A.; Mackay, M. E.; Wooley, K. L.; Hawker, C. J. *Macromolecules* **2009**, *42*, 5629-5635.

172   Moraes, J.; Maschmeyer, T.; Perrier, S. *J. Polym. Sci. Part A: Polym. Chem.* **2011**, *49*, 2771-2782.

173   Moraes, J.; Maschmeyer, T.; Perrier, S. *Aust. J. Chem.* **2011**, *64*, 1047-1053.

174   Brouwer, H. D.; Schellekens, M. A. J.; Klumperman, B.; Monteiro, M. J.; German, A. L. *J. Polym. Sci. Part A: Polym. Chem.* **2000**, *38*, 3596-3603.

175   Hao, X.; Stenzel, M. H.; Barner-Kowollik, C.; Davis, T. P.; Evans, E. *Polymer* **2004**, *45*, 7401-7415.

176   Hong, C.-Y.; You, Y.-Z.; Pan, C.-Y. *Polymer* **2006**, *47*, 4300-4309.

177   Boyer, C.; Whittaker, M. R.; Nouvel, C.; Davis, T. P. *Macromolecules* **2010**, *43*, 1792-1799.

178   You, Y.-Z.; Hong, C.-Y.; Pan, C.-Y. *Eur. Polym. J.* **2002**, *38*, 1289-1295.

179   Wu, D.-C.; Hong, C.-Y.; Pan, C.-Y.; He, W.-D. *Polym. Int.* **2003**, *52*, 98-103.

180   Luo, Y.; Gu, H. *Polymer* **2007**, *48*, 3262-3272.

181   Yao, Z.; Zhang, J.-S.; Chen, M.-L.; Li, B.-J.; Lu, Y.-Y.; Cao, K. *J. Appl. Polym. Sci.* **2011**, *121*, 1740-1746.

182   Fleet, R.; Dugen, E. T. A. V. D.; Klumperman, B. *Macromol. Chem. Phys*. **2011**, *212*, 2191-2208.

183   Harrison, S.; Wooley, K. L. *Chem. Commun*. **2005**, 3259-3261.

184   Zhu, M.-Q.; Wei, L.-H.; Li, M.; Jiang, L.; Du, F.-S.; Li, Z.-C.; Li, F.-M. *Chem. Commun*. **2001**, 365-366.

185   Chernikova, E.; Terpugova, P.; Bui, C.; Charleux, B. *Polymer* **2003**, *44*, 4101-4107.

186   Luo, Y.; Wang, A.; Yuan, J.; Gao, Q. *Int. J. Pharm*. **2009**, *374*, 139-144.

187   Davies, M. C.; Dawkins, J. V.; Hourston, D. J. *Polymer* **2005**, *46*, 1739-1753.

188   Zhou, J.; Wang, L.; Yang, Q.; Dong, X.; Yu, H. *Colloid. Polym. Sci.* **2007**, *285*, 1369-1376.

189   Du, F.-S.; Zhu, M.-Q.; Guo, H.-Q.; Li, Z.-C.; Li, F.-M. *Macromolecules* **2002**, *35*, 6739-6741.

190   Relogio, P.; Charreyre, M.-T.; Farinha, J. P. S.; Martinho, J. G. M.; Pichot, C. *Polymer* **2004**, *45*, 8639-8648.

191   Favier, A.; D'Agosto, F.; Charreyre, M.-T.; Pichot, C. *Polymer* **2004**, *45*, 7821-7830.

192   De Lambert, B.; Chaix, C.; Charreyre, M.-T.; Laurent, A.; Aigouit, A.; Perrin-Rubens, A.; Pichot, C. *Bioconjugate Chem.* **2005**, *16*, 265-274.

193   De Lambert, B.; Chaix, C.; Charreyre, M.-T.; Martin, T.; Aigouit, A.; Perrin-Rubens, A.; Pichot, C.; Mandrand, B. *Anal. Biochem.* **2008**, *373*, 229-238.

194   Vosloo, J. J.; Tonge, M. P.; Fellows, C. M.; D'agosto, F.; Sanderson, R. D.; Gilbert, R. G. *Macromolecules* **2004**, *3*, 2371-2382.

195   Yanjarappa, M. J.; Gujraty, K. V.; Joshi, A.; Saraph, A.; Kane, R. S. *Biomacromolecules* **2006**, *7*, 1665-1670.

196   Savariar, E. N.; Thayumanavan, S. *J. Polym. Sci. Part A: Polym. Chem*. **2004**, *42*, 6340-6345.

197   Quan, C.-Y.; Wu, D.-Q.; Chang, C.; Zhang, G.-B.; Cheng, S.-X.; Zhang, X.-Z.; Zhuo, R.-X. *J. Phys. Chem. C*. **2009**, *113*, 11262-11267.

198   Li, Y.; Akiba, I.; Harrisson, S.; Wooley, K. L. *Adv. Funct. Mater*. **2008**, *18*, 551-559.

199   Kakwere, H.; Perrier, S. *J. Am. Chem. Soc*. **2009**, *131*, 1889-1895.

200   Li, Y.; Lokitz, B. S.; McCormick, C. L. *Macromolecules* **2006**, *39*, 81-89.

201   Li, Y.; Lokitz, B. S.; Armers, S. P.; McCormick, C. L. *Macromolecules* **2006**, *39*, 2726-2728.

202   Pascual, S.; Monteiro, M. J. *Eur. Polym. J.* **2009**, *45*, 2513-1519.

203   Quan, Y. C.; Wei, H. ; Shi, Y.; Li, Y. Z.; Cheng, X. S.; Zhang, Z. X.; Zhuo, X. R. *Colloid. Polym. Sci.* **2011**, *289*, 667-675.

204   Zhang, J.; Jiang, X.; Zhang, Y.; Li, Y.; Liu, S. *Macromolecules* **2007**, *40*, 9125-9132.

205   Wan, X.; Liu, T.; Liu, S. *Langmuir* **2011**, *27*, 4082-4090.

206   Li, Y.; Yang, D.; Adronov, A.; Gao, Y.; Luo, X.; Li, H. *Macromolecules* **2012**, *45*, 4698-4706.

207   Liu, R.; Zhao, X.; Wu, T.; Feng, P. *J. Am. Chem. Soc.* **2008**, *130*, 14418-14419.

208   Sun, G.; Lee, N. S.; Neumann, W. L.; Freskos, J. N.; Shieh, J. J.; Dorsho, R. B.; Wooley, K. L. *Soft Matter* **2009**, *5*, 3422-3429.

209   Sun, G.; Berezin, M. Y.; Fan, J.; Lee, H.; Ma, J.; Zhang, K.; Wooley, K. L.; Achilefu, S. *Nanoscale* **2010**, *2*, 548-558.

210   Lee, N. S.; Sun, G.; Lin, L. Y.; Neumann, W. L.; Fresko, J. N.; Karwa, A.; Shieh, J. J.; Dorshow, R. B.; Wooley, K. L. *J. Mater. Chem.* **2011**, *21*, 14193-14202.

211   Sun, G.; Cui, H.; Lin, L. Y.; Lee, N. S.; Yang, C.; Neumann, W. L.; Freskos, J. N.; Shieh, J. J.; Dorsho, R. B.; Wooley, K. L. *J. Am. Chem. Soc.* **2011**, *133*, 8534-8543.

212   Eberhardt, M.; Theato, P. *Macromol. Rapid Commun.* **2005**, *26*, 1488-1493.

213   Gibson, M. I.; Frohlich, E.; Klok, H. A. *J. Polym. Chem. Part A: Polm. Chem.* **2009**, *47*, 4332-4345.

214   Gibson, M. I.; Danial, M.; Klok, H.-A. *ACS Comb. Sci.* **2011**, *13*, 286-297.

215   Günay, K, A.; Schüwer, N.; Klok, H.-A. *Polym. Chem.* DOI: 10.1039/C2PY20162C.

216   Bart, M.; Tarantola, M.; Fischer, K.; Schmidt, M.; Luxenhofer, R.; Janshoff, A.; Theato, P.; Zentel, R. *Biomacromolecules* **2008**, *9*, 3114-3118.

217   Herth, M. M.; Barz, M.; Moderegger, D.; Allmeroth, M.; Jahn, M.; Thews, O.; Zentel, R.; Rösch, F. *Biomacromolecules* **2009**, *10*, 1697-1703.

218   Scheibe, P.; Barz, M.; Hemmelmann, M.; Zentel, R. *Langmuir* **2010**, *26*, 5661-5669.

219   Allmeroth, M.; Moderegger, D.; Biesalski, B.; Koynov, K.; Rösch, F.; Thews, O.; Zentel, R. *Biomacromolecules* **2011**, *12*, 2841-2849.

220   Jochum, F. D.; Roth, P. J.; Kessler, D.; Theato, P. *Biomacromolecules* **2010**, *11*, 2432-2439.

221   Chua, G. B. H.; Roth, P. J.; Duong, H. T. T.; Davis, T. P.; Lowe, A. B. *Macromolecules* **2012**, *45*, 1362-1374.

222   Nuhn, L.; Hirsch, M.; Krieg, B.; Koynov, K.; Fischer, K.; Schmidt, M.; Helm, M.; Zentel, R. *ACS Nano* **2012**, *6*, 2198-2214.

[223]   Boyer, C.; Davis, T. P. *Chem. Commun.* **2009**, 6029-6031.

[224]   Boyer, C.; Whittaker, M.; Davis, T. P. *J. Polym. Sci. Part A: Polym. Chem.* **2011**, *49*, 5245-5256.

[225]   Duong, H. T. T.; Marquis, C. P.; Whittaker, M.; Davis, T. P.; Boyer, C. *Macromolecules* **2011**, *44*, 8008-8019.

[226]   Meuer, S.; Oberle, P.; Theato, P.; Tremel, W.; Zentel, R. *Adv. Mater.* **2007**, *19*, 2073-2078.

[227]   Zorn, M.; Meuer, S.; Tahir, M. N.; Khalavka, Y.; Sönnishsen, C.; Tremel, W.; Zentel, R. *J. Mater. Chem.* **2008**, *18*, 3050-3058.

[228]   Zorn, M.; Zentel, R. *Macromol. Rapid Commun.* **2008**, *29*, 922-927.

[229]   Zorn, M.; Bae, W. K.; Kwak, J.; Lee, H.; Lee, Ch.; Zentel, R.; Char, K. *ACS Nano* **2009**, *3*, 1063-1068.

[230]   Zorn, M.; Weber, S. A. L.; Tahir, M. N.; Tremel, W.; Butt, H.-J.; Berger, R.; Zentel, R. *Nano Lett.* **2010**, *10*, 2812-2816.

[231]   Kessler, D.; Theato, P. *Langmuir* **2009**, *25*, 14200-14206.

[232]   Nilles, K.; Theato, P. *J. Polym. Sci. Part A. Polym. Chem.* **2009**, *47*, 1696-1705.

[233]   Nilles, K.; Theato, P. *J. Polym. Sci. Part A: Polym. Chem.* **2010**, *48*, 3683-3692.

[234]   Hu, Y.-C.; Liu, Y.; Pan, C.-Y. *J. Polym. Sci. Part A: Polym. Chem.* **2004**, *42*, 4862-4872.

[235]   Hu, Y.-C.; Pan, C.-Y. *Macromol. Rapid Commun.* **2005**, *26*, 968-972.

[236]   Hwang, J.; Li, R. C.; Maynard, H. D. *J. Control. Release* **2007**, *122*, 279-286.

[237]   Li, C. R.; Hwang, J.; Maynard, H. D. *Chem. Commun.* **2007**, 3631-3633.

[238]   Coessens, V.; Pyun, J.; Miller, P. J.; Gaynor, S. G.; Matyjaszewki, K. *Macromol. Rapid Commun.* **2000**, *21*, 103-109.

[239]   Jia, Z.; Bell, C. A.; Monteiro, M. J. *Macromolecules* **2011**, *44*, 1747-1751.

[240]   Ho, H. T.; Levere, M.; Soutif, J.-C.; Montembault, V.; Pascual, S.; Fontaine, L. *Polym. Chem.* **2011**, *2*, 1258-1260.

[241]   Yin, Z.; Koulic, C.; Pagnoulle, C.; Jérôme, R. *Macromolecules* **2001**, *34*, 5132-5139.

[242]   Xu, X.; Smith, A. E.; Kirkland, S. E.; McCormick, C. L. *Macromolecules* **2008**, *41*, 8429-8435.

[243]   Cao, Y.; Wang, Y.; Li, B.-T.; Wang, Y.; Tang, L.-M. *Chin. J. Polym. Sci.* **2008**, *26*, 767-774.

[244]   Zheng, H.; Hua, D.; Bai, R.; Hu, K.; An, L.; Pan, C. *J. Polym. Sci. Part A: Polym. Chem.* **2007**, *45*, 2609-2616.

245 Lane, S. M.; Kuang, Z.; Yom, J.; Arifuzzaman, S.; Genzer, J.; Farmer, B.; Naik, R.; Vaia, R. A. *Biomacromolecules* **2011**, *12*, 1822-1830.

246 Keddie, D. J.; Moad, G.; Rizzardo, E.; Thang, S. H. *Macromolecules*, **2012**; DOI: 10.1021/ma300410v.

Chapter II

Synthesis of α-azlactone-functionalized polymers by RAFT polymerization

Chapter II: Synthesis of α-azlactone-functionalized polymers by RAFT polymerization*

1. Introduction

As described in chapter I, well-defined polymers synthesized by CRP and containing reactive functional groups which react easily with amines are of particular interest and have emerged with potential applications such as bioconjugates.[1] Among CRP methods, reversible addition-fragmentation chain transfer (RAFT) polymerization[2] is of particular interest as it can be successfully applied to synthesize a large number of amine-reactive polymers under mild conditions without any metal compounds. Amine-reactive groups can be introduced either by the direct RAFT polymerization of a functional monomer or either on the R or Z groups of the thiocarbonylthio compound (of general formula R-S-C(=S)-Z) used as the RAFT agent.[2] This second method leads to polymer chains characterized by the presence of the R and Z groups at the α- and ω-ends, respectively. As the Z group may easily be removed from the chain *via* hydrolysis or aminolysis, focusing on R group modification seems to be a promising strategy. Several functional groups such as active esters (*N*-hydroxysuccinimidyl ester (NHS-ester)[3-7] and pentafluorophenyl-ester (PFP-ester)[8-15]) and electrophilic rings (epoxide[18] and azlactone[17]) able to react with amines without any catalyst have been incorporated in the R group of RAFT agents. Bathfield *et al.*[3] first reported the synthesis of a NHS-functionalized dithiobenzoate RAFT agent and its selective reactivity towards primary amines with retention of the thiocarbonylthio moiety. Aamer *et al.*[4] showed the

---

synthesis of well-defined NHS-terminated poly(*N*-succinimide *p*-vinylbenzoate)s by RAFT polymerization using a NHS-functionalized dithiobenzoate and subsequent reaction with amine-functionalized terpyridine. Other groups have reported the synthesis of NHS-containing xanthate[6] and trithiocarbonate[7] RAFT agents and their use to prepare polymers for conjugation to lysozyme and selective functionalization of proteins in water, respectively. Theato and coworkers first reported the synthesis of a PFP-functionalized dithiobenzoate RAFT agent[8] and its use to target well-defined reactive polymers towards several amines.[9-14] A PFP-containing trithiocarbonate RAFT agent was also successfully employed to synthesize well-defined poly((2-oxopropyl) acrylate)s. The subsequent reaction of such PFP-functionalized polymers with *N*-propargylamine leads to precursors for "click" chemistry.[15] The main drawback of using activated ester-functionalized polymers to react with amine-compounds is the formation of small molecule side-products such as pentafluorophenol. Ring-opening reactions of electrophilic rings with amines are of particular interest as they do not undergo the formation of molecular side-products and reactions proceed without any catalyst. Therefore, such reactions may be regarded as proceeding with several advantages associated with conventional "click"-type organic reactions as described by Sharpless and coworkers.[16] To date, only two studies have been published on the synthesis of an azlactone-functionalized xanthate[17] and an epoxide-functionalized trithiocarbonate[18] RAFT agents. Typically, azlactone-terminated poly(2-ethylhexyl acrylate)s, poly(isobornyl acrylate)s and polystyrenes were obtained with controlled molecular weights up to 5700 g.mol^{-1} and with high polydispersity indices (PDIs = 1.82-1.88).[17] Several acrylates and styrene were polymerized using the epoxide-functional RAFT agent and for each case, polydispersity

indices were below 1.1.[18] None of these studies shows the reactivity of azlactone-terminated polymers or epoxide-terminated polymers with amines. However, many studies have demonstrated that polymers bearing the azlactone functionality can react rapidly with primary amine-functionalized molecules such as benzylamine and derivatives at room temperature in the absence of catalyst and without generation of by-product.[19-27] CRP of 2-vinyl-4,4-dimethylazlactone, an azlactone-derived vinylic monomer, has been previously used as a convenient strategy to prepare well-defined reactive polymers bearing azlactone rings in the side chain.[24-31] Hence, in this chapter, we report the synthesis and use of a novel azlactone-functionalized trithiocarbonate to prepare polymers having the azlactone functionality at the α-position of the macromolecular chains. Its ability to mediate the RAFT polymerization with a wide range of monomers (such as styrene, acrylate and acrylamide derivatives) and the reactivity of resulting polymers towards amines is discussed. The interest of such an azlactone-functionalized trithiocarbonate in comparison with an azlactone-functionalized xanthate originates from the ability to produce new polymers with controlled molecular weights and narrow molecular weight distributions, having a high reactivity towards amines.

2. Results and discussion

In order to target well-defined α-azlactone-functionalized polymers by RAFT polymerization, the synthesis of a novel azlactone-derived trithiocarbonate RAFT agent was first considered.

2.1. Synthesis of α-azlactone-functionalized trithiocarbonate RAFT agent

The azlactone-derived RAFT agent (**3**) was prepared in three steps as shown in *Scheme 1*.
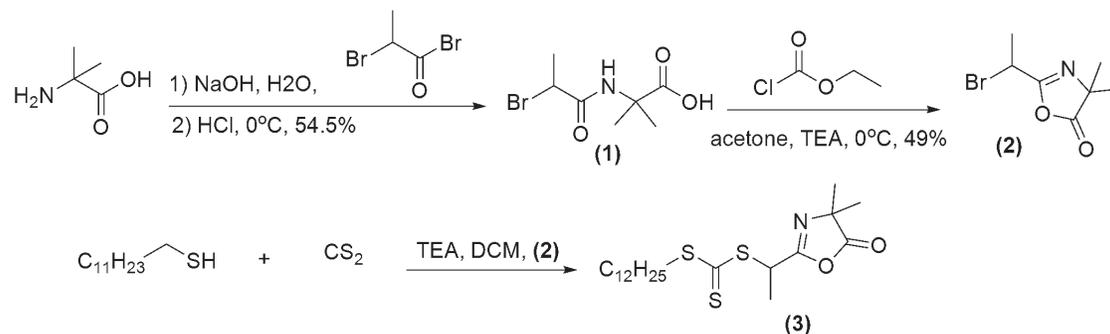
Scheme 1: *Synthesis of the azlactone-functionalized trithiocarbonate RAFT agent (3).*

2-(1-Bromoethyl)-4,4-dimethyl-4H-oxazolin-5-one ((**2**), *Scheme 1*) was synthesized according to the procedure reported by Lewandowski *et al.*[17] in 49% yield. Then, the azlactone-functionalized trithiocarbonate ((**3**), *Scheme 1*) was obtained by nucleophilic substitution of (**2**) in the presence of 1-dodecanethiol, carbon disulfide (CS_2) and triethylamine (TEA). The crude product was eluted through a silica gel column using petroleum ether (100%) following by a solution of ethyl acetate/petroleum ether (20:80% v/v) to yield the pure product as a yellow oil in 30% yield. The structure and purity of the azlactone-functionalized trithiocarbonate (**3**) were confirmed by ^{1}H, ^{13}C nuclear magnetic

resonance (NMR), Fourier transform infra-red (FT-IR) spectroscopies and high resolution mass spectrometry (HRMS). The ^{1}H NMR spectrum of the azlactone-functionalized trithiocarbonate (**3**) is shown in *Figure 1*. The triplet at 3.38 ppm is attributed to the -(CH$_2$)$_{10}$-**CH$_2$**-S- group next to the trithiocarbonate (designated as (c) in the spectrum in *Figure 1*). The quartet at 5.11 ppm due to -**CH**(CH$_3$)-SC(S)S- group is designated as (d) in the spectrum in *Figure 1*. The key peak integral area values for protons (a) (*Figure 1*) due to **CH$_3$**-(CH$_2$)$_{10}$-, (c) (*Figure 1*) due to -(CH$_2$)$_{10}$-**CH$_2$**-S- and (d) (*Figure 1*) due to -**CH**(CH$_3$)-SC(S)S- are 3.0, 2.0 and 1.0 respectively, which correlate well with the theoretical values. The characteristic peaks of the azlactone ring are also identified on the ^{13}C NMR spectrum (*Figure 2*) at 161.15 ppm (-**C**=N-) and 178.62 ppm (-**C**=O) along with one characteristic peak at 219.17 ppm (-**C**=S) of the trithiocarbonate group. The FT-IR spectrum of (**3**) (*Figure 3*) shows the presence of two absorption bands: $\nu_{(C=O)}$ at 1827 cm^{-1} and $\nu_{(C=N)}$ at 1667 cm^{-1} confirming the presence of the azlactone functionality. The purity of the final trithiocarbonate was confirmed by HRMS: the calculated value for C$_{20}$H$_{35}$NO$_2$S$_3$ [M]$^+$ is equal to 417.1830 g.mol^{-1} and the experimental one is 417.1862 g.mol^{-1}.
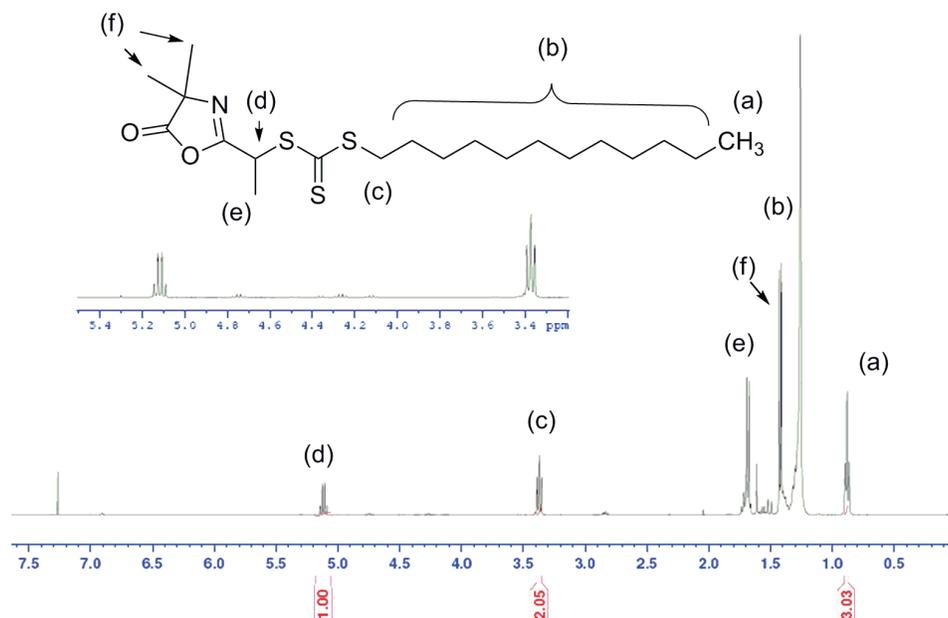
Figure 1: ^1H NMR spectrum of the azlactone-functionalized trithiocarbonate (3) in CDCl$_3$.
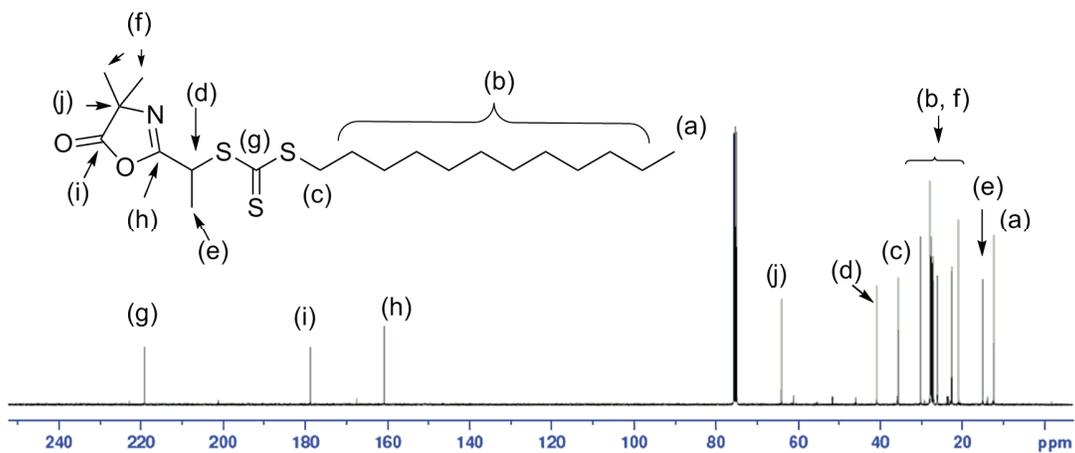
Figure 2: ^{13}C NMR spectrum of the azlactone-functionalized trithiocarbonate (3) in CDCl$_3$.
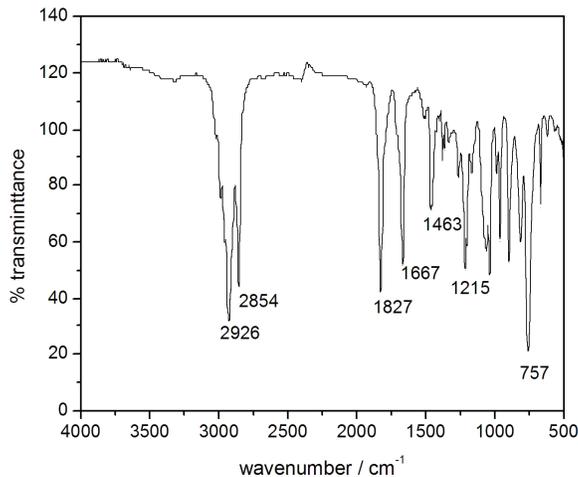
Figure 3: FT-IR spectrum of the azlactone-functionalized trithiocarbonate (3).

The efficiency of the azlactone-functionalized trithiocarbonate to control the RAFT polymerization of styrene (S), ethyl acrylate (EA) and *N*-isopropyl acrylamide (NIPAM) was then studied.

2.2. RAFT polymerization of styrene, ethyl acrylate and *N*-isopropyl acrylamide

The RAFT polymerization of S, EA, and NIPAM were performed using 4,4'-azobis(4-cyanovaleric acid) (ACVA) as the initiator in dioxane at 70°C (*Scheme 2*). Samples were withdrawn periodically to follow monomer conversion with time by ^{1}H NMR spectroscopy for kinetic studies (*Figure 4*) and the evolution of number-average molecular weights and polydispersity indices with monomer conversion (*Figure 5*) by SEC analysis (*Table 1*).

R: -C_6H_5, -CO_2C_2H_5, -CONH(CH_3)_2
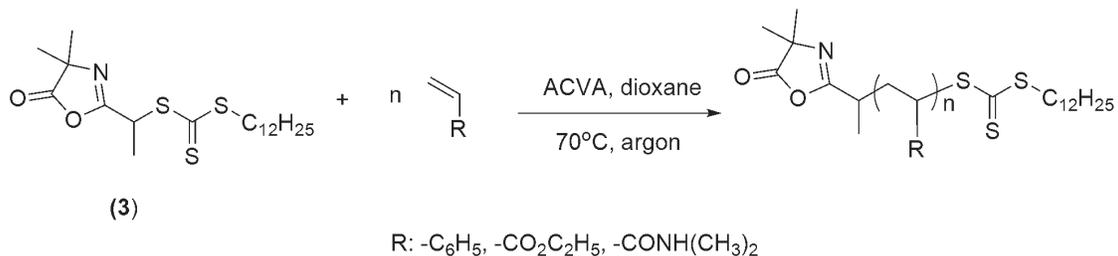
Scheme 2: RAFT polymerizations of S, EA, and NIPAM using the azlactone-functionalized trithiocarbonate (3) as the RAFT agent and ACVA as the initiator in dioxane at 70°C.
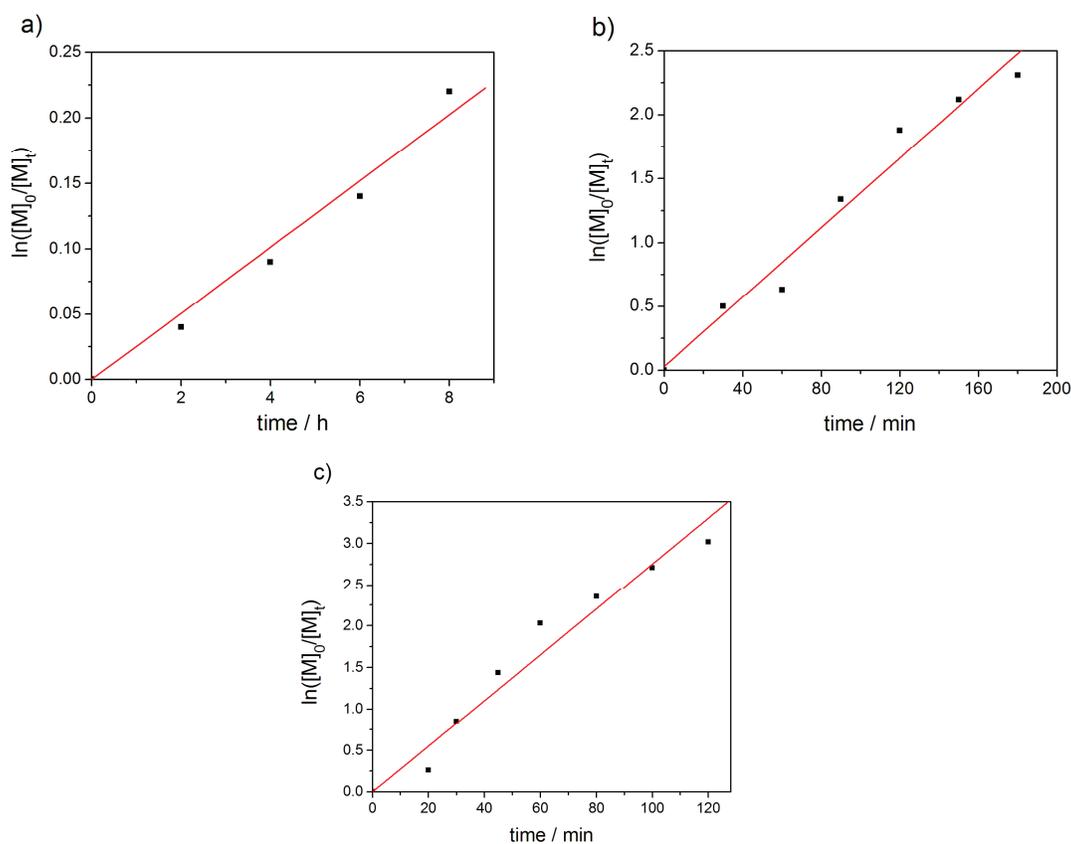
Figure 4: Kinetic plots for the RAFT polymerizations of: a) styrene, $[S]_0$:$[(3)]_0$:$[ACVA]_0$ = 49:1:0.1, b) ethyl acrylate, $[EA]_0$:$[(3)]_0$:$[ACVA]_0$ = 50:1:0.1 and c) N-isopropyl acrylamide, $[NIPAM]_0$:$[(3)]_0$:$[ACVA]_0$ = 55:1:0.1, using ACVA as the initiator and the azlactone-functionalized trithiocarbonate (3) as the RAFT agent in dioxane at 70°C.
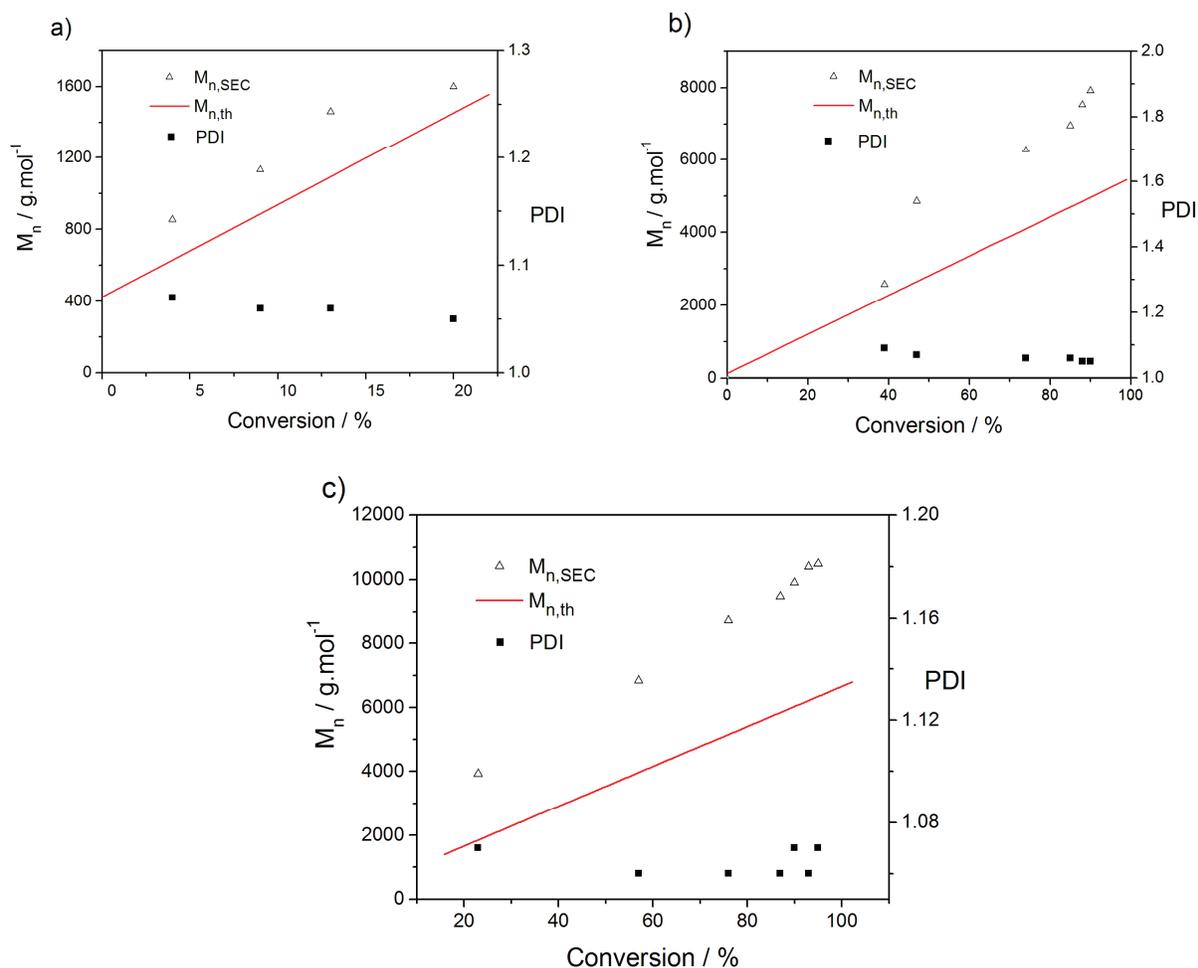
Figure 5: Evolution of number-average molecular weights and polydispersity indices (determined by SEC in N,N-dimethylformamide (DMF) using polystyrene standards) versus monomer conversion for the RAFT polymerization of: a) styrene, $[S]_0:[(3)]_0:[ACVA]_0 = 49:1:0.1$, b) ethyl acrylate, $[EA]_0:[(3)]_0:[ACVA]_0 = 50:1:0.1$ and c) N-isopropyl acrylamide, $[NIPAM]_0:[(3)]_0:[ACVA]_0 = 55:1:0.1$ using ACVA as the initiator and the azlactone-functionalized trithiocarbonate (3) as the RAFT agent in dioxane at 70°C.

Table 1: RAFT polymerizations of S, EA and NIPAM, conducted with the azlactone-functionalized trithiocarbonate (3) as the RAFT agent and using ACVA as the initiator in dioxane at 70°C.

Monomer [monomer]$_0$:[**3**]$_0$:[ACVA]$_0$	Time (min)	Conv.[a] (%)	$M_{n,th}$[b] (g.mol^{-1})	$M_{n,SEC}$[c] (g.mol^{-1})	PDI[c]
Styrene 49:1:0.1	120	4	620	860	1.05
	240	9	875	1130	1.06
	360	13	1079	1460	1.06
	480	20	1436	1600	1.05
Ethyl acrylate 50:1:0.1	30	39	2367	2570	1.09
	60	47	2767	4860	1.07
	90	74	4117	6270	1.06
	120	85	4667	6950	1.06
	150	88	4817	7530	1.05
	180	90	4917	7920	1.05
N-isopropyl acrylamide 55:1:0.1	20	23	1846	3920	1.07
	30	57	3959	6830	1.06
	45	76	5140	8740	1.06
	60	87	5824	9470	1.06
	80	90	6010	9900	1.07
	100	93	6196	10400	1.06
	120	95	6321	10500	1.07

[a] Monomer conversion monitored by ^{1}H NMR spectroscopy. [b] $M_{n,th}$ = ([M]$_0$/[(**3**)]$_0$) × molar mass of the monomer unit × monomer conversion + molar mass of the chain-ends. [c] Determined by SEC in DMF using polystyrene standards.

The kinetic investigations reveal the linearity of the ln([M]$_0$/[M]$_t$) versus time plots for each monomer (*Figure 4*). These first-order kinetic plots are compatible with a constant concentration of propagating radicals throughout the polymerization. The evolutions of number-average molecular weights of polystyrene (PS), poly(ethyl acrylate) (PEA) and poly(*N*-isopropyl acrylamide) (PNIPAM) measured by SEC increased with monomer conversion (*Figure 5*). The SEC traces of PEAs (*Figure 6*) and of PNIPAMs (*Figure 7*) show a shift towards higher molecular weight as the polymerization time increases. Moreover, symmetrical chromatograms were observed throughout the

polymerization. Finally, *Table 1* show that polydispersity indices (PDIs) remained below 1.10.

In order to compare the RAFT polymerization characteristics, some results are highlighted in *Table 2*. It appears that the polymerization rate is lower with S as only 4% of S conversion has been reached after 120 minutes (*Entry 1, Table 2*), while 85% and 95% of EA and NIPAM conversions (*Entries 3 and 5, Table 2*) have been obtained after 120 minutes using a similar molar ratio of $[monomer]_0/[(3)]_0/[ACVA]_0$ of 50/1/0.1, respectively. These results are in good agreement with previous study on the RAFT polymerization of such monomers mediated by trithiocarbonates.[32] Put all together, those results show that the azlactone-functionalized trithiocarbonate (**3**) is an efficient RAFT agent to mediate the CRP of the tested monomers S, EA, and NIPAM.
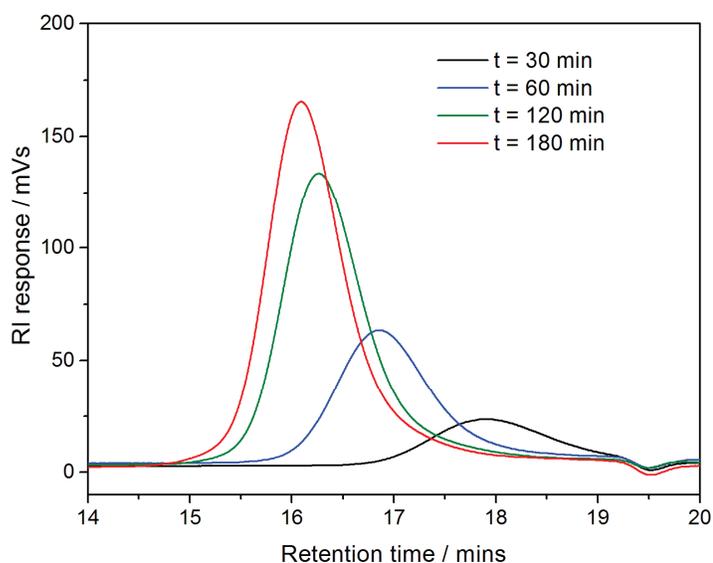
Figure 6: Evolution of the normalized SEC traces of PEAs with time for the RAFT polymerization of EA using ACVA as the initiator and the azlactone-functionalized trithiocarbonate (3) as the RAFT agent in dioxane at 70°C, $[EA]_0:[(3)]_0:[ACVA]_0 = 50:1:0.1$.
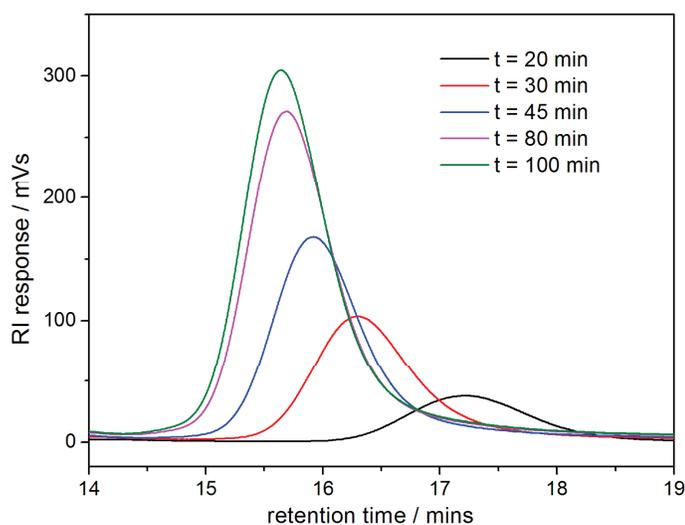
Figure 7: Evolution of the normalized SEC traces of PNIPAMs with time for the RAFT polymerization of NIPAM using ACVA as the initiator and the azlactone-functionalized trithiocarbonate (3) as the RAFT agent in dioxane at 70°C, [NIPAM]$_0$:[(3)]$_0$:[ACVA]$_0$ = 55:1:0.1.

The presence of the trithiocarbonate moiety at the PNIPAM chain-end (*Entry 5, Table 2*) was confirmed by the appearance of a peak at 309 nm in the SEC trace using UV detection, corresponding to the chromophoric C=S bond of the RAFT agent (*Figure 8*).
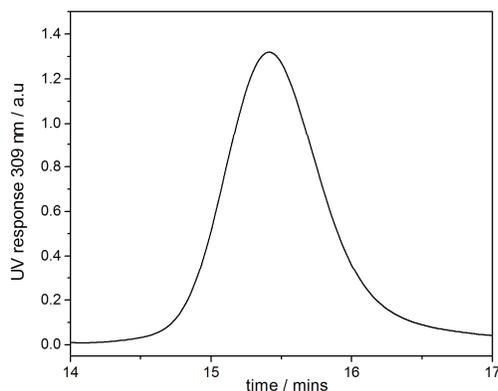
Figure 8: SEC trace of the azlactone-terminated PNIPAM (M $_{n,SEC}$ = 10500 g.mol^{-1}; PDI = 1.07) using UV detection at 309 nm.

Table 2: Comparison of RAFT polymerizations of S, EA, and NIPAM using the azlactone-functionalized trithiocarbonate (3) and ACVA as the initiator in dioxane at 70°C.

Entry	Monomer	$[M]_0/[(3)]_0/$ $[ACVA]_0$	Time (min)	Conv.[a] (%)	$M_{n,th}$[b] (g.mol^{-1})	$M_{n,NMR}$ (g.mol^{-1})	$M_{n,SEC}$[g] (g.mol^{-1})	PDI[g]
1	S	49/1/0.1	120	4	620	nd[c]	860	1.05
2	S	49/1/0.1	480	20	1436	1820[d]	1600	1.05
3	EA	50/1/0.1	120	85	4667	nd[c]	6950	1.06
4	EA	50/1/0.1	180	90	4917	4320[e]	7920	1.05
5	NIPAM	55/1/0.1	120	95	6321	6070[f]	10500	1.07

[a] Monomer conversion monitored by ^{1}H NMR spectroscopy. [b] $M_{n,th}$ = $([M]_0/[(3)]_0)$ × molar mass of the monomer unit × monomer conversion + molar mass of the chain-ends. [c] Not determined. [d] Determined by comparing the integral area values of the peak at 0.75 ppm (CH_3-$(CH_2)_{10}$-) and the multiplet between 6.30 and 7.20 ppm (C_6H_5-) on the ^{1}H NMR spectrum (see *Figure 19 p.138*). [e] Determined by comparing the integral area value of the peak at 0.87 ppm (CH_3-$(CH_2)_{10}$-) and the peak at 4.11 ppm (-C(O)O-CH_2-CH_3) on the ^{1}H NMR spectrum (see *Figure 20 p.139*). [f] Determined by comparing the integral area value of the peak at 0.86 ppm (CH_3-$(CH_2)_{10}$-) and the peak at 4.02 ppm (-NH-$CH(CH_3)_2$) on the ^{1}H NMR spectrum (see *Figure 21 p.141*). [g] Determined by SEC in DMF using polystyrene standards.

In order to precisely determine the polymer chain-ends structures, a matrix-assisted laser desorption and ionization time of flight (MALDI-TOF) mass spectrometry analysis was performed on a PNIPAM (72% monomer conversion; $M_{n,SEC}$ = 3400 g.mol^{-1}; PDI = 1.07), synthesized using the azlactone-functionalized trithiocarbonate (**3**) as the RAFT agent and using ACVA as the initiator ($[NIPAM]_0/[(3)]/[ACVA]_0$ = 17/1/0.1) in dioxane at 70°C. The MALDI-TOF mass spectrum (*Figure 9*) shows a single series of signals separated by 113.08 g.mol^{-1} corresponding to the molecular weight of the NIPAM repeating unit (calculated value = 113.16 g.mol^{-1}). The peak at m/z = 2250.87 g.mol^{-1} in the MALDI-TOF mass spectrum corresponds to a polymer chain consisting of 16 NIPAM units, an azlactone moiety at one chain-end, a trithiocarbonate moiety (with a dodecyl chain) at the other chain-end

and a sodium atom responsible for ionization (calculated value = 2250.51 g.mol^{-1}). Such results confirmed the presence of the azlactone group at the α-position and of the dodecyltrithiocarbonate at the ω-position of the PNIPAM macromolecular chains. The reactivity of the resulting azlactone-functionalized PNIPAM towards model amines was subsequently explored.
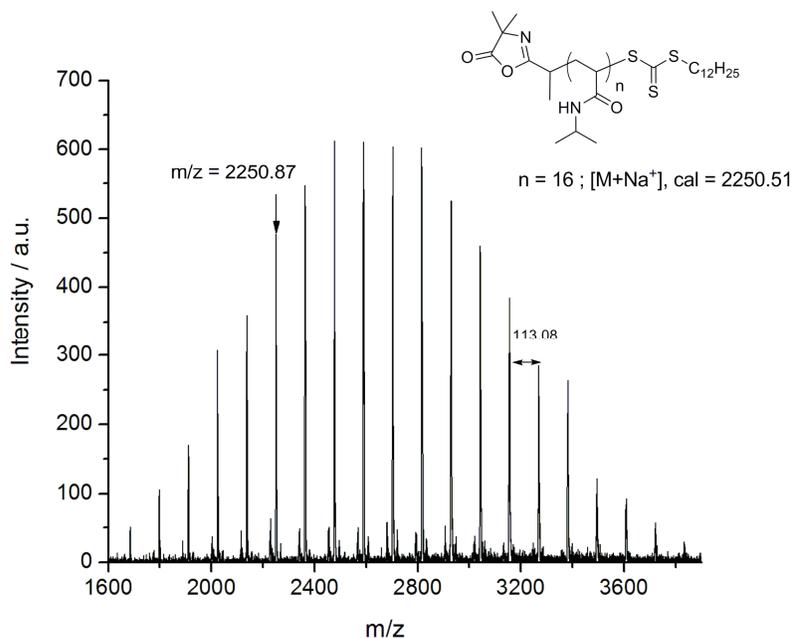
Figure 9: MALDI-TOF mass spectrum of a PNIPAM synthesized by RAFT polymerization using the azlactone-functionalized trithiocarbonate (3) as the RAFT agent and ACVA as the initiator in dioxane at 70°C ([NIPAM]$_0$/[(3)]/[ACVA]$_0$ = 17/1/0.1; 72% monomer conversion; M$_{n,SEC}$ = 3400 g.mol^{-1}; PDI = 1.07). Matrix: trans-2-[3-(4-tert-butylphenyl)-2-methyl-2-propenylidene]malononitrile (DCTB), sodium trifluoroacetate.

123

2.3. Reactivity of azlactone-functionalized PNIPAM towards amines

4-Fluorobenzylamine and allyl amine were chosen as model amines to test the azlactone reactivity in the azlactone-functionalized PNIPAM as they give clear assignable signals on the ^{1}H NMR spectra corresponding to the aromatic and vinylic protons, respectively. An azlactone-terminated PNIPAM ($[NIPAM]_0/[(3)]/[ACVA]_0 = 31/1/0.1$; 80% monomer conversion, $M_{n,SEC} = 6100$ g.mol^{-1}; PDI = 1.05) was reacted with 1 equivalent of 4-fluorobenzylamine in tetrahydrofuran (THF) at room temperature to afford 4-fluorobenzylamine-functionalized PNIPAM (*Scheme 3*).
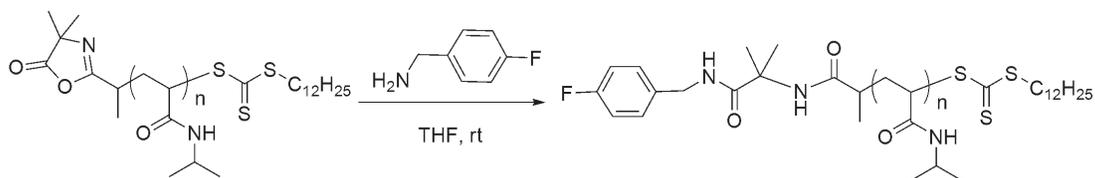
Scheme 3: Coupling reaction between the azlactone-terminated PNIPAM with 4-fluorobenzylamine in THF at room temperature.

Figure 10 shows the disappearance of the band at 1815 cm^{-1} characteristic of the C=O group of the azlactone ring on the FT-IR spectrum. Moreover, SEC trace using UV detection at 309 nm of the resulting polymer confirmed the presence of the C=S of the trithiocarbonate moiety (*Figure 11*).
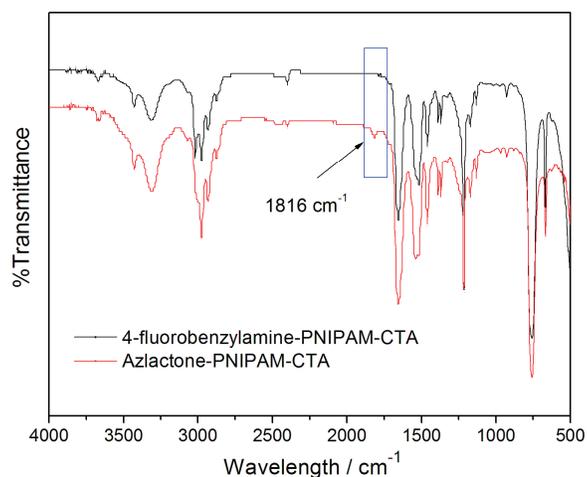
Figure 10: FT-IR spectrum of the α-azlactone-ω-dodecyltrithiocarbonate PNIPAM

before and after reaction with 4-fluorobenzylamine at room temperature in THF for 24h.
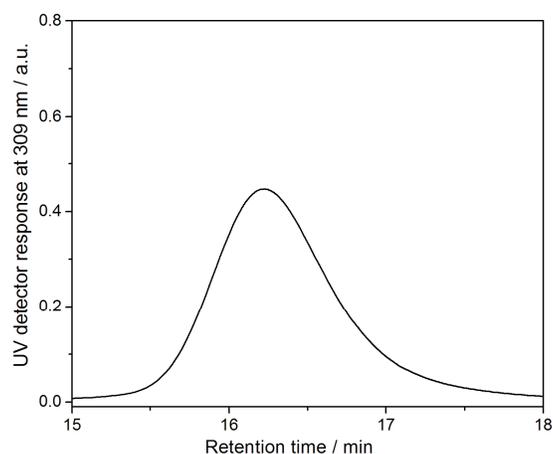
Figure 11: SEC trace of the 4-fluorobenzylamine-terminated PNIPAM ($M_{n,SEC}$ = 6460

g.mol^{-1}; PDI =1.04) using UV detection at 309 nm.

^{1}H NMR spectrum of resulting polymer showed the appearance of signals at 6.92 ppm and 7.27 ppm labeled (f) (*Figure 12*) corresponding to the aromatic protons of 4-fluorobenzylamino moiety. As the signal of aromatic protons of the 4-fluorobenzylamine overlaps with the signal of the NH protons (labeled (d) in *Figure 12*) of the NIPAM units, it was impossible to quantify the 4-fluorobenzylamine

chain-end functionality. Therefore, allyl amine was chosen as it gives clear assignable signals in ^{1}H NMR spectroscopy between 5.0 and 6.0 ppm allowing quantification of the reaction.
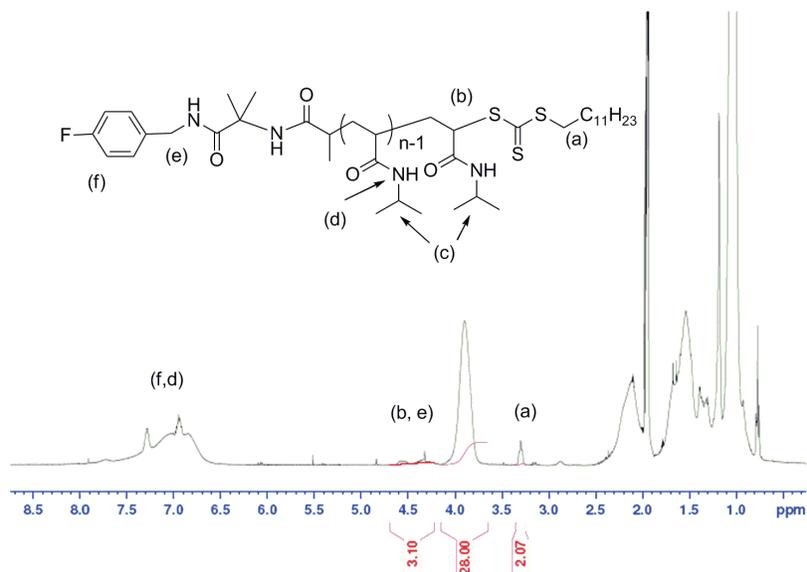
Figure 12: ^{1}H NMR spectrum (solvent: acetone D$_6$) of the polymer obtained after reacting the α-azlactone-ω-dodecyltrithiocarbonate PNIPAM with 4-fluorobenzylamine at room temperature in THF for 24h.

An azlactone-terminated PNIPAM ([NIPAM]$_0$/[(**3**)]/[ACVA]$_0$ = 31/1/0.1; 80% monomer conversion, M$_{n,SEC}$ = 6100 g.mol^{-1}; PDI = 1.05) was reacted with 1 equivalent of allyl amine in THF at room temperature for 24 h (*Scheme 4*).
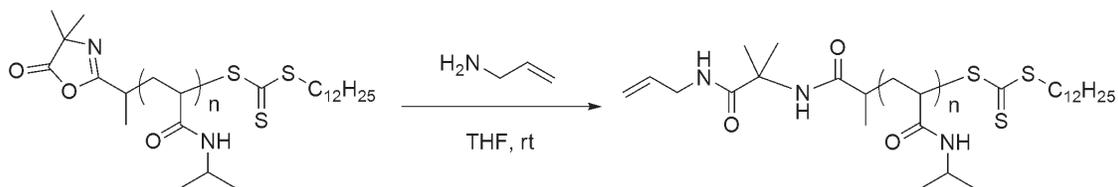
Scheme 4: Coupling reaction between the azlactone-terminated PNIPAM with allyl amine in THF at room temperature.

Figure 13 shows the ^{1}H NMR spectrum of the resulting purified polymer. New peaks corresponding to the vinylic protons of allyl amine are clearly visible on the ^{1}H NMR spectrum between 5.0 ppm and 6.0 ppm. A quantification of the allyl amine chain-end functionality of the PNIPAM was performed by comparing the integral area values of the methylene protons (b) (*Figure 13*) of the dodecyltrithiocarbonate group at 3.40 ppm and of the vinylic protons (e and f) (*Figure 13*) of the allyl group at 5.87, 5.23 and 5.02 ppm, respectively.
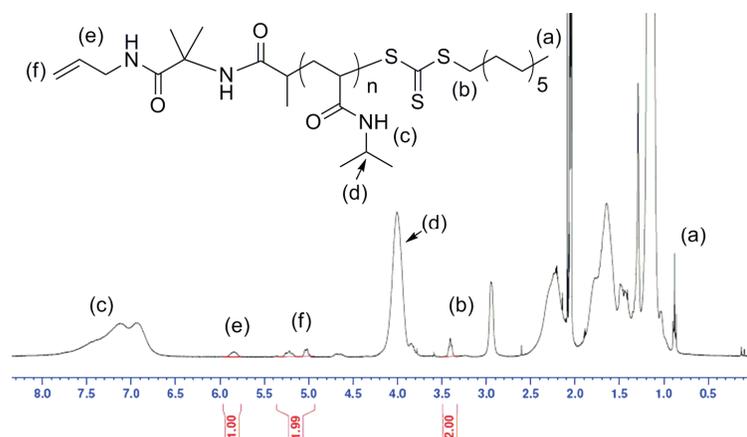
Figure 13: ^{1}H NMR spectrum (solvent: acetone D$_6$) of the polymer obtained after reacting the α-azlactone-ω-dodecyltrithiocarbonate PNIPAM with allyl amine at room temperature in THF for 24h.

The allyl amine chain-end functionality was determined to be quantitative and the dodecyltrithiocarbonate remains intact. Further characterization was performed by MALDI-TOF mass spectrometry (*Figure 14*).
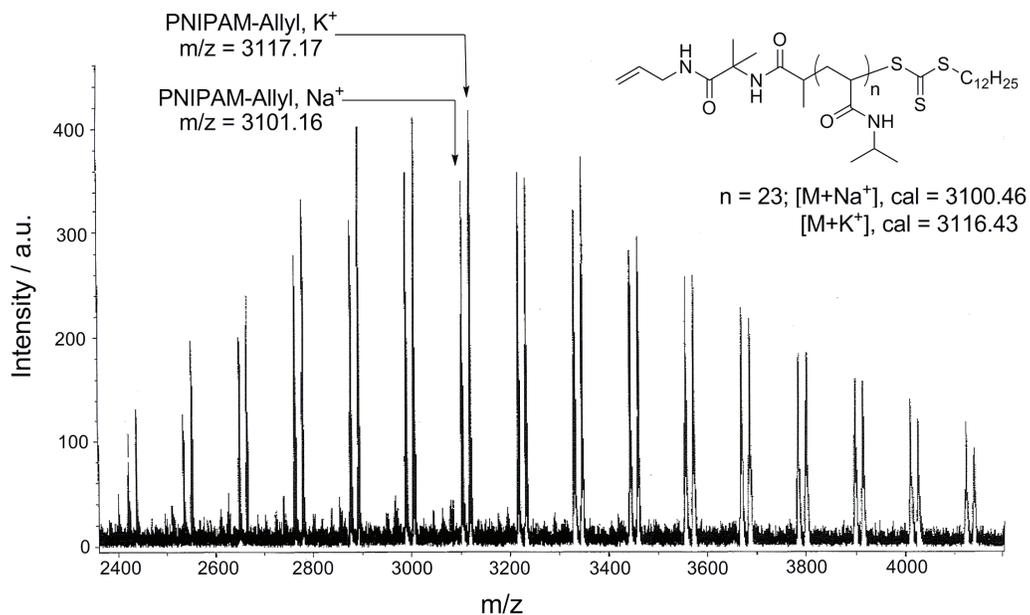
Figure 14: MALDI-TOF spectrum of the allyl amine-functionalized PNIPAM. Matrix: DCTB.

Two series of signals separated by 16 g.mol^{-1} have been detected in which one series is corresponding to the desired macromolecule ionized by a sodium ion (Na$^+$) and the other was generated by the ionization by a potassium ion (K$^+$). The peak at m/z = 3101.16 g.mol^{-1} in the MALDI-TOF mass spectrum corresponds to a polymer chain consisting of 23 NIPAM units, an allyl amine at one chain-end, a dodecyltrithiocarbonate moiety at the other chain-end and a sodium atom responsible for ionization (calculated value = 3100.46 g.mol^{-1}). This result is of particular interest as the azlactone functional trithiocarbonate PNIPAM reacts quantitatively with an amine *without* any modification of the trithiocarbonate.

3. Conclusion

RAFT polymerizations of S, EA, and NIPAM using a new azlactone-functionalized trithiocarbonate provide a facile and mild route to end-functionalized amine-reactive polymers with predictable molecular weights and narrow molecular weight distributions. The azlactone functionality survives intact the RAFT process and the resulting polymers possess an azlactone ring at the α-position of the chain-end, which can react with primary amines under mild conditions without the formation of any by-product and with retention of the thiocarbonylthio moiety. This method should be applicable to a wide variety of monomers and opens the way to the synthesis of various new reactive polymers that can be useful for bioconjugation[33] with various biological entities bearing amine groups, such as proteins.

4. Experimental section

4.1. Materials

1-dodecanethiol (97%, Aldrich), carbon disulfide (CS_2, 99.9%, Aldrich), sodium hydroxide (≥ 98%, Sigma-Aldrich), 2-methylalanine (98%, Aldrich), hydrochloric acid (37%, Sigma-Aldrich), triethylamine (TEA, ≥99%, Sigma-Aldrich), ethyl chloroformate (97%, Aldrich), 4,4'-azobis(4-cyanovaleric acid) (ACVA, ≥ 98, Aldrich), allyl amine (> 99%, Aldrich), 2-bromopropionylbromide (97%, Aldrich), 4-fluorobenzylamine (97%, Aldrich), silica gel for column chromatography (Kieselgel 60, 230-400 mesh Merck) and aluminium oxide, neutral (Aldrich) were used as received. *N*-isopropyl acrylamide (NIPAM) was obtained from Aldrich (97% purity) and was recrystallized from petroleum ether prior to use. Styrene (Acros, 99%) and ethyl acrylate (99.5%, Aldrich) were passed through a column of aluminum oxide prior to polymerization. 1,4-dioxane (> 99%) was purchased from Fisher-Scientific and distilled before use. *N,N*-dimethylformamide (DMF, 99.8%), acetone (99.8%) and dichloromethane (DCM, > 99%), *n*-hexane (97%), ethyl acetate (99.8%), diethyl ether (technical grade), tetrahydrofuran (THF, > 99%) and petroleum ether (Analytic reagent grade, 40-60°C) were obtained from Aldrich and used as received.

4.2. Instrumentation

Nuclear Magnetic Resonance (NMR) Spectroscopy

NMR spectra were recorded on a Bruker AC-400 spectrometer for ^{1}H NMR (400 MHz) and ^{13}C NMR (100 MHz). Chemical shifts are reported in ppm relative to deuterated solvent resonances.

Size Exclusion Chromatography (SEC)

Polymers were characterized on a SEC system operating in DMF eluent at 60^oC fitted with a polymer laboratories guard column (PL Gel 5µm) and two Polymer Laboratories PL Mixed D columns, a Waters 410 differential refractometer (RI) and a Waters 481 UV photodiode array detector. The instrument operated at a flow rate of 1.0 mL.min^{-1} and was calibrated with narrow linear polystyrene (PS) standards ranging in molecular weight from 580 g.mol^{-1} to 460 000 g.mol^{-1}. Molecular weights and polydispersity indices (PDI) were calculated using Waters EMPOWER software.

MALDI-TOF Mass Spectrometry

MALDI-TOF (Matrix-Assisted Laser Desorption and Ionization Time Of Flight) mass spectrometry analysis was performed on a Bruker Biflex III MALDI-TOF instrument equipped with a nitrogen laser operating at 337 nm, a 2GHz sampling rate digitiser, pulsed ion extraction source and reflectron. The laser pulse width is 3ns and maximum power is 200 mJ. Spectra were recorded in the linear mode with an acceleration voltage of 19 kV and delay of 200 ns. 100 single shot aquisitions were summed to give the spectra and the data were analyzed using Bruker XTOF software. Samples of PNIPAM were prepared by dissolving the matrix (*trans*-2-[3-(4-*tert*-butylphenyl)-2-methyl-2-propenylidene]malononitrile, DCTB) in the solvent (DCM, 30 mg.mL^{-1}) and mixing with the polymer (PNIPAM, 2 mg.mL^{-1}) in the ratio 1:50 (v/v). 1 µL was spotted directly onto a thin layer of sodium trifluoroacetate in acetone (concentration 19 mg.mL^{-1}) that had been deposited to act as a cationizing agent.

Fourier Transform Infra-Red (FT-IR) Spectroscopy

FT-IR spectra of copolymers were recorded using a ThermoElectron Corp. spectrometer operating with an attenuated total reflection (ATR solid) gate. Spectra were analyzed with OMNIC software.

High Resolution Mass Spectrometry (HRMS)

HRMS were measured by a Waters Micromass GCT Premier.

4.3. Synthesis of the azlactone functional trithiocarbonate RAFT agent

4.3.1. Synthesis of 2-(2-bromopropionylamino)-2-methyl-propanoic acid (1)
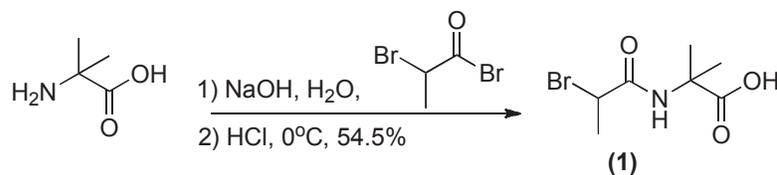
Scheme 5: Synthesis of 2-(2-bromopropionylamino)-2-methyl-propanoic acid (1).

To a stirring homogeneous solution of sodium hydroxide (10.4 g, 0.26 mol) and 2-methylalanine (13.40 g, 0.135 mol) in 20 mL of water, cooled using an ice bath, was added dropwise 2-bromopropionylbromide (13.60 mL, 0.13 mol). After complete addition, the reaction mixture was then allowed to warm to room temperature and stirred for 2h. To this solution was slowly added hydrochloric acid at 0°C. During the addition a white solid is formed. The reaction mixture was stirred for 1h at room temperature. The precipitated solid was filtered and recrystallized from acetone. The white solid was filtered and dried under vacuum. Yield 12.6 g (54.5%). IR (cm^{-1}): 3301, 2995-2922, 1705, 1650, 1540, 1470, 1440. ^{1}H NMR (400 MHz, acetone D$_6$), δ (ppm): 1.36 (s, NHC(C**H**$_3$)$_2$, 6H), 1.55 (d, -CH(C**H**$_3$)Br, 3H)), 4.35 (q, -C**H**(CH$_3$)Br, 1H), 7.50 (s, N**H**,

1H). ^{13}C NMR (100.62 MHz, acetone D$_6$), δ (ppm): 22.3 (CH(**CH$_3$**)Br), 24.5 (NHCH(**CH$_3$**)$_2$), 44.3 (**C**H(CH3)Br), 56.6 (NH**C**(CH$_3$)$_2$), 169.2 (**C**ONH), 175.4 (-**C**OOH). HRMS: theoretical m/z = 238.0079 [M+H]$^+$, experimental m/z = 238.0092 [M+H]$^+$.
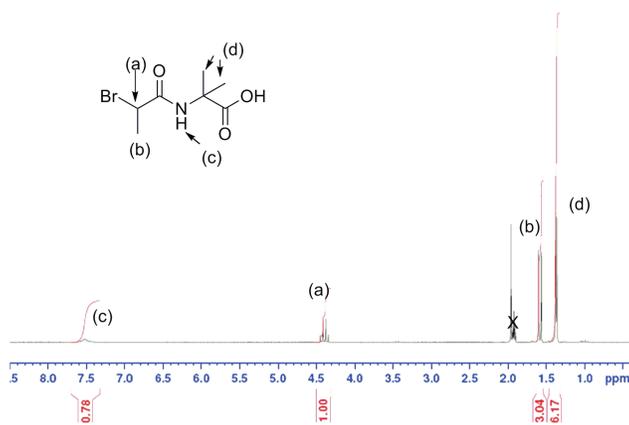
*Figure 15: ^1H NMR spectrum of 2-(2-bromopropionylamino)-2-methyl-propanoic acid (**1**) in acetone D$_6$.*
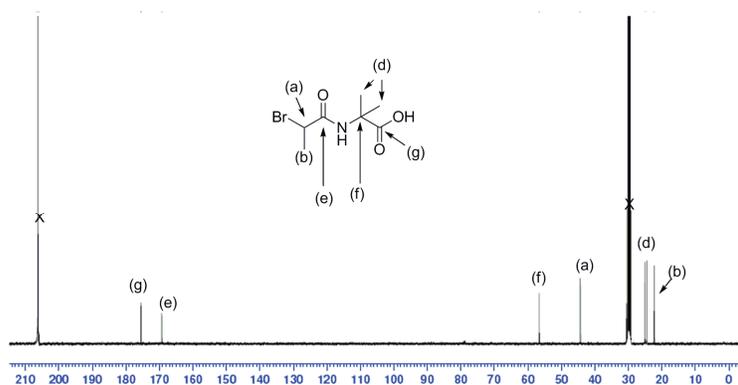
*Figure 16: ^{13}C NMR spectrum of 2-(2-bromopropionylamino)-2-methyl-propanoic acid (**1**) in acetone D$_6$.*

133

4.3.2. Synthesis of 2-(1-bromoethyl)-4,4-dimethyl-4H-oxazolin-5-one (2)
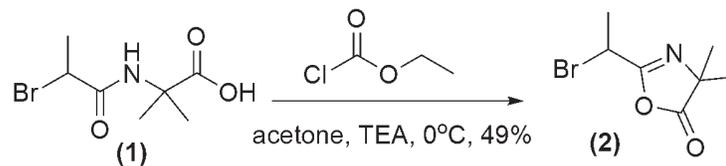
Scheme 6: Synthesis of 2-(1-bromoethyl)-4,4-dimethyl-4H-oxazolin-5-one (2).

To a stirring mixture of 2-(2-bromopropionylamino)-2-methyl propanoic acid ((**1**), 11.90 g, 0.05 mol) and TEA (5.56 g, 0.055 mol) in 36 mL acetone, cooled in an ice bath, was added dropwise ethyl chloroformate (5.41 g, 0.05 mol) *via* a syringe. The reaction mixture was then allowed to proceed at room temperature for 3h. The solution was then filtered and the white solid was washed with diethyl ether. The filtrate was concentrated under vacuum. The filtrate residue was distilled under vacuum (bp = 63-64°C, 1 mmHg) to give a colorless oil. Yield: 5.34 g (49%). IR (cm^{-1}): 2982-2870, 1826, 1667, 1446. ^{1}H NMR (400 MHz, CDCl$_3$), δ (ppm): 1.41 (s, -CH(**CH$_3$**)$_2$, 6H), 1.95 (d, -CH(**CH$_3$**)Br, 3H), 4.90 (q, **CH**Br, 1H). ^{13}C NMR (100.62 MHz, acetone D$_6$), δ (ppm): 22.9 (-**CH**(CH$_3$)Br), 24.6 (-**C**(CH$_3$)$_2$), 37.3 (-**CH**(CH$_3$)Br), 66.4 (-**C**(CH$_3$)$_2$), 180.1 (**C**=O), 163.0 (**C**=N).
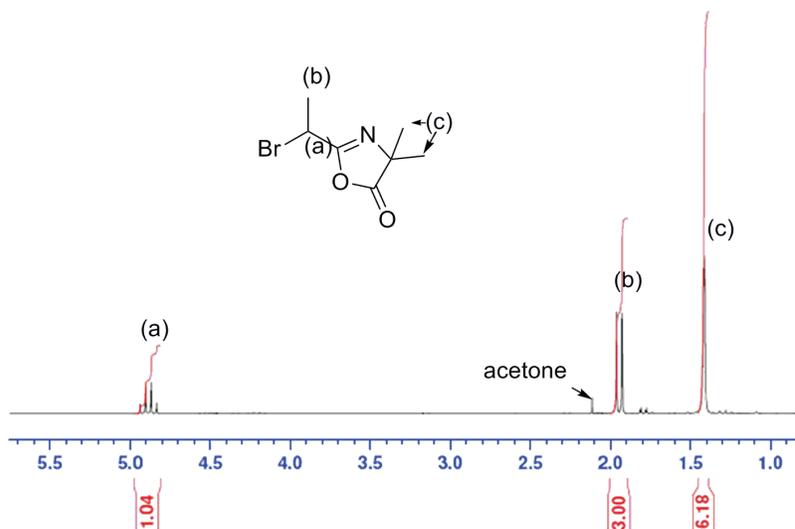
Figure 17: ^{1}H NMR spectrum of 2-(1-bromoethyl)-4,4-dimethyl-4H-oxazolin-5-one (2) in CDCl$_3$.
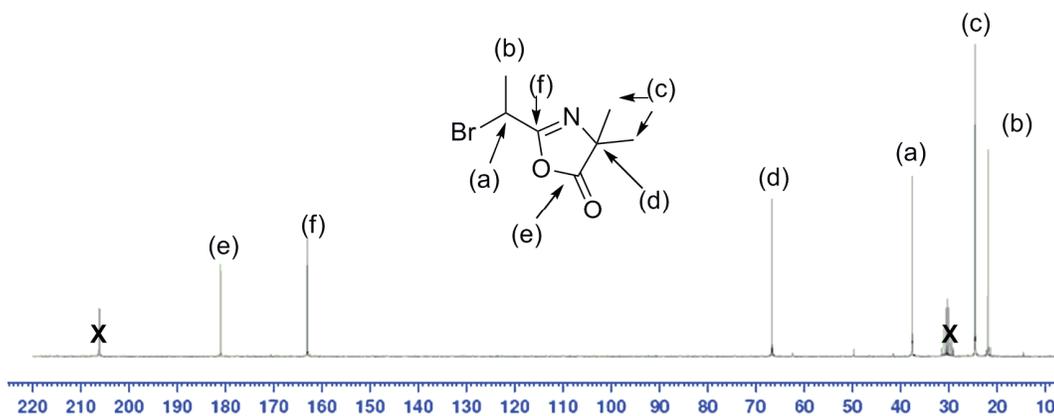
Figure 18: ^{13}C NMR spectrum of 2-(1-bromoethyl)-4,4-dimethyl-4H-oxazolin-5-one (2) in acetone D$_6$.

4.3.3. Synthesis of the azlactone RAFT agent (3)
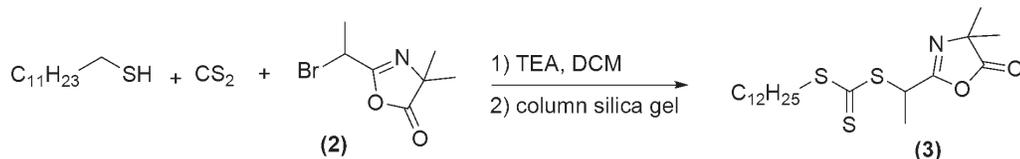
Scheme 7: Synthesis of the azlactone RAFT agent (3).

To a stirred solution of 1-dodecanethiol (3.68 g, 18.20 mmol) and TEA (2.03 g, 20 mmol) in DCM (40 mL), cooled at 0°C using an ice bath, was added carbon disulfide (CS_2, 1.385 g, 18.20 mmol) under N_2 atmosphere. After complete addition, the solution was stirred at room temperature for 2h and cooled down again at 0^oC. Then, 2-(1-bromoethyl)-4,4-dimethyl-4H-oxazolin-5-one ((**2**), 4.00 g, 18.18 mmol) was slowly added at 0^oC. The reaction mixture was stirred at room temperature for 24 h. The solution was then filtered and the white solid was washed with DCM. Solvent of the filtrate was removed under vacuum. The resulting yellow oil was dissolved in *n*-hexane and filtered. The filtrate was concentrated under vacuum and purified by column chromatography on silica gel using petroleum ether (100%) as the eluent and then, using a solution of ethyl acetate/petroleum ether (20:80% v/v) as the eluent. The solvent was removed under vacuum to give a yellow oil. Yield: 2.28 g (30%). IR (cm^{-1}): 2982-2870, 1827, 1667, 1443, 1215, 757. ^{1}H NMR (400 MHz, CDCl$_3$), δ (ppm): 0.88 (t, **CH**$_3$-CH$_2$-, 3H), 1.26-1.35 (m, CH$_3$-(**CH**$_2$)$_{10}$-CH$_2$-, 20 H), 1.40-1.43 (d,-C(**CH**$_3$)$_2$, 6H), 1.67 (d, -CH(**CH**)$_3$-S-C(S)-S, 3H), 3.40 (t, -**CH**$_2$-S-C(S)-S-, 2H), 5.11 (q, -**CH**(CH)$_3$-S-C(S)-S, 1H). ^{13}C NMR (100.62 MHz, CDCl$_3$), δ (ppm): 12.52 (**CH**$_3$-CH$_2$-), 15.12 (-SC(S)-S-CH(**CH**$_3$)-), 21.20 (**CH**$_3$-CH$_2$-), 22.58-27.89 (-C(**CH**$_3$)$_2$ and CH$_3$-CH$_2$-(**CH**$_2$)$_8$-CH$_2$-), 30.24 (-**CH**$_2$-CH$_2$-S-C(S)-S-), 35.55 (-**CH**$_2$-S-C(S)-S-), 40.68 (-SC(S)-S-**CH**(CH$_3$)-), 64.07 (-**C**(CH$_3$)$_2$),

161.15 (**C**=N), 178.62 (**C**=O), 219.17 (-S-**C**(S)-S-). HRMS: theoretical m/z = 417.1830 [M]$^+$, experimental m/z = 417.1862 [M]$^+$.

4.4. RAFT polymerizations

4.4.1. A typical procedure for the RAFT polymerization of styrene
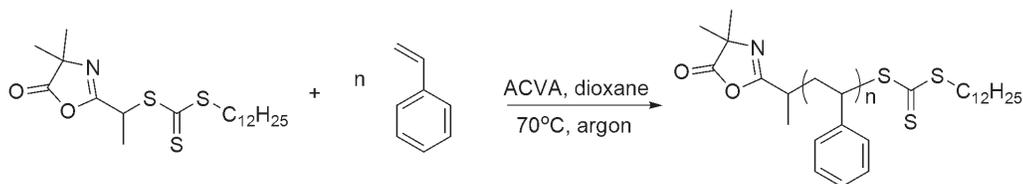
Scheme 8: RAFT polymerization of styrene using $[S]_0:[(3)]_0:[ACVA]_0 = 49:1:0.1$ in dioxane at 70^oC.

Styrene (2.01 g, 0.0193 mol), azlactone functional RAFT agent (**3**) (0.165 g, 3.96×10^{-4} mol), 4,4′-azobis(4-cyanovaleric acid) (ACVA) (11.8 mg, 0.42×10^{-4} mol), dioxane (3.0 mL) were sealed in a 25 mL round-bottomed flask equipped with a magnetic stir bar and purged with argon for 30 min. The reaction mixture was placed in a thermostated oil bath at 70^oC to initiate the polymerization. Samples were removed periodically using a syringe to perform size exclusion chromatography (SEC) analysis and to monitor monomer conversion by ^{1}H NMR spectroscopy. The polymerization was quenched after 8 h by rapid cooling and exposure of the polymerization solution to air (monomer conversion = 20%). The polymer was precipitated twice in methanol and dried under vacuum to obtain a yellow polystyrene with a $M_{n,NMR}$ = 1820 (g.mol^{-1}); $M_{n,SEC}$ = 1600 (g.mol^{-1}); PDI = 1.05. IR (cm^{-1}): 3026, 2995, 1817, 1673, 1217, 757, 699. ^{1}H NMR (400 MHz, acetone D$_6$), δ (ppm): 0.75 (**CH$_3$**-CH$_2$-, 3H), 0.92-1.15 (CH$_3$-(**CH$_2$**)$_{10}$-CH$_2$-S-C(S)-S-), 1.51-2.50

(-**CH₂-CH-**)ₙ, 3.19 (-**CH₂-S-C(S)-S-**), 4.90 (-**CH₂-CH(C₆H₅)-SC(S)-S**), 6.30-7.20

(**C₆H₅-**).
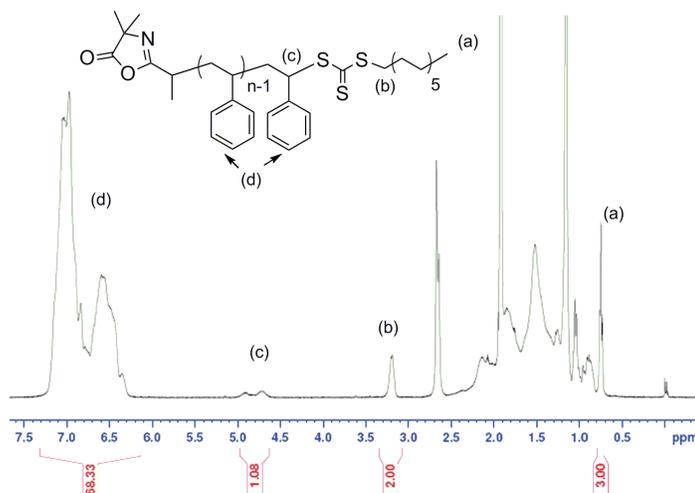
Figure 19: ¹H NMR spectrum of the azlactone-terminated polystyrene in acetone D₆.

4.4.2. A typical procedure for the RAFT polymerization of ethyl acrylate
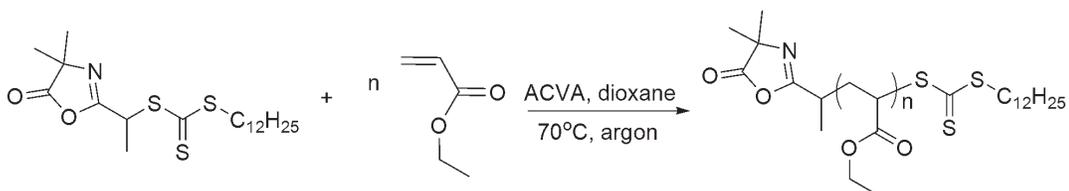
Scheme 9: RAFT polymerization of ethyl acrylate using [EA]₀/[(3)]₀/[ACVA]₀ = 50/1/0.1 in dioxane at 70ºC.

EA (2.00 g, 0.02 mol), azlactone functional RAFT agent (**3**) (0.168 g, 4.03x10⁻⁴ mol), 4,4′-azobis(4-cyanovaleric acid) (ACVA, 2.0 mg, 0.428x10⁻⁴ mol), dioxane (4.0 mL) and DMF (0.1 mL) were sealed in a 25 mL round-bottomed flask equipped with a magnetic stir bar and purged with argon for 30 min. The reaction mixture was placed in a thermostated oil bath at 70ºC to initiate the polymerization. Samples were removed

periodically using a syringe to perform size exclusion chromatography (SEC) analysis and to monitor monomer conversion by ^{1}H NMR spectroscopy. The polymerization was quenched after 3 h by rapid cooling and exposure of the polymerization solution to air (monomer conversion = 90%). The polymer was precipitated twice in *n*-hexane and dried under vacuum to obtain a yellow powder with a $M_{n,NMR}$ = 4320 (g.mol^{-1}); $M_{n,SEC}$ = 7920 (g.mol^{-1}); PDI = 1.05. IR (cm^{-1}): 2983, 1824, 1728, 1217. ^{1}H NMR (400 MHz, CDCl$_3$), δ (ppm): 0.87 (**CH$_3$**-CH$_2$-), 1.10-1.25 (CH$_3$-(**CH$_2$**)$_{10}$-CH$_2$-S-), 1.50-2.10 (-**CH$_2$**-**CH**-)$_n$, 2.30 (-C(O)-O-CH$_2$-**CH$_3$**), 3.33 (-**CH$_2$**-S-C(S)-S-), 4.11 (-C(O)-O-**CH$_2$**-CH$_3$), 4.82 (-CH2-**CH**(COOC$_2$H$_5$)-S-C(S)-S-).
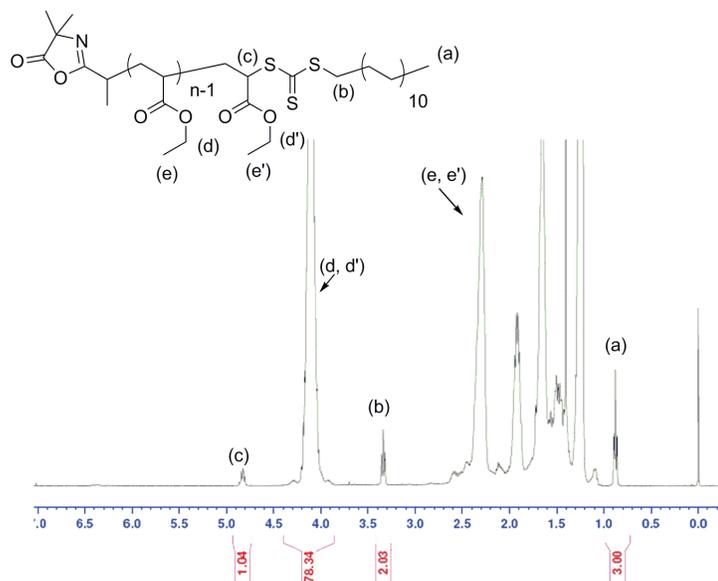
Figure 20: ^{1}H NMR spectrum of the azlactone-terminated poly(ethyl acrylate) in acetone D$_6$.

4.4.3. A typical procedure for the RAFT polymerization of *N*-isopropyl acrylamide
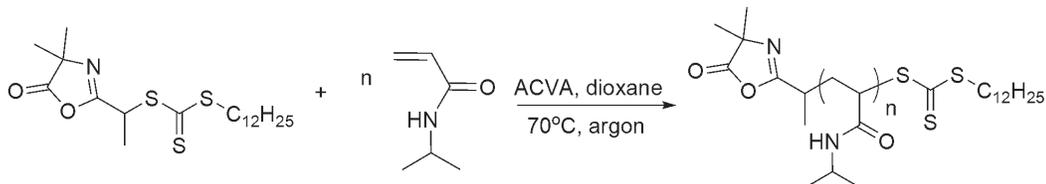
Scheme 10: RAFT polymerization of N-isopropyl acrylamide using
*[NIPAM]$_0$/[(**3**)]$_0$/[ACVA]$_0$ = 55/1/0.1 in dioxane at 70°C.*

NIPAM (3.00 g, 0.0265 mol), azlactone functional RAFT agent (**3**) (0.20 g, 4.80×10^{-4} mol), 4,4′-azobis(4-cyanovaleric acid) (ACVA, 19.3 mg, 0.69×10^{-4} mol), dioxane (8.0 mL) and DMF (0.2 mL) were sealed in a 25 mL round-bottomed flask equipped with a magnetic stir bar and purged with argon for 30 min. The reaction mixture was placed in a thermostated oil bath at 70°C to initiate the polymerization. Samples were removed periodically using a syringe to perform size exclusion chromatography (SEC) analysis and to monitor monomer conversion by ^{1}H NMR spectroscopy. The polymerization was quenched after 2 h by rapid cooling and exposure of the polymerization solution to air (monomer conversion = 95%). The polymer was precipitated twice in *n*-hexane and dried under vacuum oven to obtain a yellow powder with a $M_{n,NMR}$ = 6070 (g.mol^{-1}); $M_{n,SEC}$ = 10500 (g.mol^{-1}); PDI = 1.07. IR (cm^{-1}): 3428-3309, 2983, 1816, 1655, 1217, 756. ^{1}H NMR (400 MHz, CDCl$_3$), δ (ppm): 0.86 (**CH$_3$**-CH$_2$-), 1.10-1.25 (-NHCH(**CH$_3$**)$_2$) and (CH$_3$-(**CH$_2$**)$_{10}$-CH$_2$-S-), 1.40-2.78 (-**CH$_2$-CH**-)$_n$, 3.34 (-**CH$_2$**-S-C(S)-S-), 4.02 (-NHC**H**(CH$_3$)$_2$), 5.77-7.07 (-N**H**-(CH$_3$)$_2$).
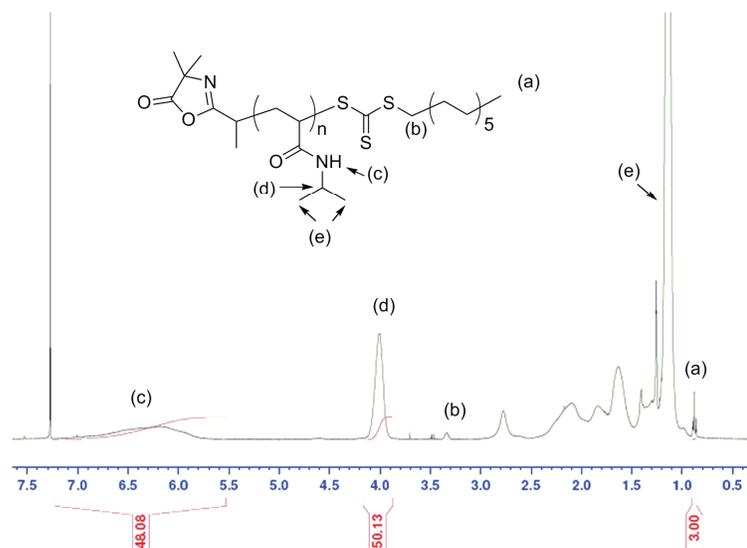
Figure 21: ^{1}H NMR spectrum of the azlactone-terminated PNIPAM in CDCl$_3$.

Using similar polymerization conditions, azlactone-terminated PNIPAMs were synthesized for MALDI-TOF mass spectrometry analysis, SEC analysis using UV detection at 309 nm and for coupling with 4-fluorobenzylamine and allyl amine (*Table 3*).

Table 3: RAFT polymerization conditions of NIPAM and molecular characteristics of resulting azlactone-terminated PNIPAMs used for MALDI-TOF mass spectrometry analysis, SEC analysis using UV detection at 309 nm and for coupling with 4-fluorobenzylamine and allyl amine.

Entry	[NIPAM]$_0$/[(**3**)]$_0$/[ACVA]$_0$	Time (min)	Conv.[a] (%)	$M_{n,th}$[b] (g.mol^{-1})	$M_{n,SEC}$[c] (g.mol^{-1})	PDI[c]
1	17/1/0.1	120	72	1890	3400	1.07
2	31/1/0.1	80	80	3130	6100	1.05

[a] Monomer conversion monitored by ^{1}H NMR spectroscopy. [b] $M_{n,th}$ = ([M]$_0$/[(**3**)]$_0$) × molar mass of the monomer unit × monomer conversion + molar mass of the chain-ends. [c] Determined by SEC in DMF using polystyrene standards

4.5. Reactivity and characterization of azlactone-functionalized PNIPAM towards amines

4.5.1. Coupling reaction of the azlactone-terminated PNIPAM with 4-fluorobenzylamine

To a stirred solution of PNIPAM (0.103 g; 3.29×10^{-5} mol, $M_{n,SEC} = 6100$ g.mol^{-1}, PDI = 1.05) in THF (2.0 mL) was added a solution of 4-fluorobenzylamine (4.00 μL, 3.39×10^{-5} mol) in THF (0.2 mL). The reaction proceeds at room temperature for 24 h. After this time, the solvent was removed under vacuum. The residue was dissolved in DCM and the polymer was precipitated twice in *n*-hexane/diethyl ether (1:1 v/v) under vigorous stirring and dried under vacuum oven to obtain a yellow powder. The final polymer was then characterized by SEC and ^{1}H NMR spectroscopy. $M_{n,SEC} = 6460$ g.mol^{-1}; PDI = 1.04. ^{1}H NMR (400 MHz, acetone D$_6$), δ (ppm): 0.87 (**CH$_3$**-CH$_2$-), 1.10-1.25 (-NHCH(**CH$_3$**)$_2$) and (CH$_3$-(**CH$_2$**)$_{10}$-CH$_2$-S-), 1.40-2.95 (-**CH$_2$-CH**-)$_n$ 3.40 (-**CH$_2$**-S-C(S)-S-), 4.02 (-NHC**H**(CH$_3$)$_2$), 4.21-4.65 (F-**CH$_2$**-C$_6$H$_4$-) and -CH$_2$-**CH**(NHCH(CH$_3$)$_2$)-SC(S)S-), 6.68-7.87 (-N**H**-(CH$_3$)$_2$ and F-CH$_2$-C$_6$**H$_4$**-).
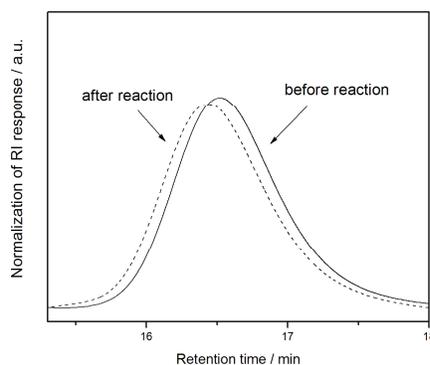
Figure 22: Overlaid of SEC traces of azlactone-terminated PNIPAM before (——) and after(---) reaction with 4-fluorobenzylamine.

4.5.2. Coupling reaction of the azlactone-terminated PNIPAM with allyl amine

To a stirred solution of PNIPAM (0.102 g; 3.29×10^{-5} mol, $M_{n, SEC} = 6100$ g.mol^{-1}, PDI = 1.05) in THF (2.0 mL) was added a solution of allyl amine (2.5 μL, 3.35×10^{-5} mol) in THF (0.2 mL). The reaction proceeds at room temperature for 24 h. After this time, the solvent was removed under vacuum. The residue was dissolved in DCM and the polymer was precipitated twice in *n*-hexane/diethyl ether (1:1 v/v) under vigorous stirring and dried under vacuum oven to obtain a yellow powder. The final polymer was then characterized by SEC, ^{1}H NMR spectroscopy and MALDI-TOF mass spectrometry. $M_{n,SEC} = 6520$ g.mol^{-1}; PDI = 1.04. ^{1}H NMR (400 MHz, acetone D$_6$), δ (ppm): 0.87 (**CH$_3$**-CH$_2$-), 1.10-1.25 (-NHCH(**CH$_3$**)$_2$) and (CH$_3$-(**CH$_2$**)$_{10}$-CH$_2$-S-), 1.40-2.95 (-**CH$_2$**-**CH**-)$_n$ 3.40 (-**CH$_2$**-S-C(S)-S-), 4.02 (-NH**CH**(CH$_3$)$_2$), 5.87 (CH$_2$=**CH**-CH$_2$-), 5.02 and 5.23 (**CH$_2$**=CH-CH$_2$-), 6.68-7.82 (-N**H**-(CH$_3$)$_2$).

References

[1] Boyer, C.; Bulmus, V.; Davis, T. P.; Ladmiral, V.; Liu, J.; Perrier, S. *Chem. Rev.* **2009**, *109*, 5402-5436. Boyer, C.; Huang, X.; Whittaker, R. M.; Bulmus, V.; Davis, T. P. *Soft Matter* **2011**, *7*, 1599-1614. Le Droumaguet, B.; Nicolas, J.; *Polym. Chem.* **2010**, *1*, 563-598. Lutz, J.-F.; Börner, H. G. *Prog. Polym. Sci.* **2008**, *33*, 1-39. Kessler, D.; Metz, N.; Theato, P. *Macromol. Symp.* **2007**, *254*, 34-41.

[2] Chiefari, J.; Chong, Y. K.; Ercole, F.; Krstina, J.; Jeffery, J.; Le, T. P. T.; Mayadunne, R. T. A.; Meijs, G. F.; Moad, C. L.; Moad, G.; Rizzardo, E.; Thang, S. H. *Macromolecules* **1998**, *31*, 5559-5562. Barner-Kowollik, C. *Handbook of RAFT Polymerization*; Wiley-VCH: Weinheim, **2008**.

[3] Bathfield, M.; D'Agosto, F.; Spitz, R.; Charreyre, T. M.; Delair, T. *J. Am. Chem. Soc.* **2006**, *128*, 2546-2547.

[4] Aamer, K. A.; Tew, G. N. *J. Polym. Sci. Part A: Polym. Chem.* **2007**, *45*, 5618-5625.

[5] Han, H. D.; Yang, P. L.; Zhang, F. X.; Pan, Y. C. *Eur. Polym. J.* **2007**, *43*, 3873-3881.

[6] McDowall, L.; Chen, G.; Stenzel, M. H. *Macromol. Rapid Commun.* **2008**, *29*, 1666-1671.

[7] Li, H.; Bapat, A. P.; Li, M.; Sumerlin, B. S. *Polym. Chem.* **2011**, *2*, 323-327.

[8] Roth, P. J.; Wiss, K. T.; Zentel, R.; Theato, P. *Macromolecules* **2008**, *41*, 8513-8519.

[9] Wiss, K. T.; Krishna, O. D.; Roth, P. J.; Kiick, K. L.; Theato, P. *Macromolecules* **2009**, *42*, 3860-3863.

[10] Roth, P. J.; Haase, M.; Baché, T.; Theato, P.; Zentel, R. *Macromolecules* **2010**, *43*, 895-902.

[11] Roth, P. J.; Jochum, F. D.; Zentel, R.; Theato, P. *Biomacromolecules* **2010**, *11*, 234-238.

[12] Roth, P. J.; Jochum, F. D.; Forst, R. F.; Zentel, R.; Theato, P. *Macromolecules* **2010**, *43*, 4638-4645.

[13] Roth, P. J.; Kim, K. S.; Bae, S. H.; Sohn, B. H.; Theato, P.; Zentel, R. *Macromol. Rapid Commun.* **2009**, *30*, 1274-1278.

[14] Wiss, K. T.; Theato, P. *J. Polym. Sci. Part A: Polym. Chem.* **2010**, *48,* 4758-4767.

[15] Godula, K.; Rabuka, D.; Nam, K. T.; Bertozzi, C. R. *Angew. Chem. Int. Ed.* **2009**, *48*, 4973-4976.

[16] Kolb, H. C.; Finn, M. G.; Sharpless, K. B. *Angew. Chem. Int. Ed.* **2001**, *40*, 2004-2021.

[17] Lewandowski, K. M.; Fansler, D. D.; Wendland, M. S.; Heilmann, S. M.; Gaddam, B. N. *US Patent* **2004** Patent No.: US 6762257 B1.

[18]   Vora, A.; Nasrullah, M. J.; Webster, D. C. *Macromolecules* **2007**, *40*, 8586-8592.

[19]   Heilmann, S. M.; Rasmussen, J. K.; Krepski, L.R. *J. Polym. Sci. A: Polym. Chem*. **2001**, *39*, 3655-3677.

[20]   Tripp, J. A.; Stein, J. A.; Svec, F.; Fréchet, J. M. J. *Org. Lett.* **2000**, *2*, 195-198.

[21]   Tripp, J. A.; Svec, F.; Fréchet, J. M. J. *J. Comb. Chem*. **2001**, *3*, 216-223.

[22]   Guyomard, A.; Fournier, D.; Pascual, S.; Fontaine, L.; Bardeau, J. F. *Eur. Polym. J.* **2004**, *40*, 2343-2348.

[23]   Lucchesi, C.; Pascual, S.; Dujardin, G.; Fontaine, L. *React. Funct. Polym*. **2008**, *68*, 97-102.

[24]   Tully, D. C.; Roberts, M. J.; Geierstanger, B. H.; Grubbs, R. B. *Macromolecules* **2003**, *36*, 4302-4308.

[25]   Fournier, D.; Pascual, S.; Montembault, V.; Haddleton, D. M.; Fontaine, L. *J. Comb. Chem*. **2006**, *8*, 522-530.

[26]   Ho, H. T.; Levere, M.; Soutif, J.-C.; Montembault, V.; Pascual, S.; Fontaine, L. *Polym. Chem*. **2011**, *2*, 1258-1260.

[27]   Buck, M. E.; Lynn, D. M. *Polym. Chem*. **2012**, *3*, 66-80.

[28]   Prai-In, Y.; Tankanya, K.; Rutnakornpituk, B.; Wichai, U.; Montembault, V.; Pascual, S.; Fontaine, L.; Rutnakornpituk M. *Polymer* **2012**, *53*, 113-120.

[29]   Fournier, D.; Pascual, S.; Fontaine, L. *Macromolecules* **2004**, *37*, 330-335.

[30]   Lokitz, B. S.; Messman, J. M.; Hinestrosa, J. P.; Alonzo, J.; Verduzco, R.; Brown, R. H.; Osa, M.; Ankner, J. F.; Kilbey II, S. M. *Macromolecules* **2009**, *42*, 9018-9026.

[31]   Pascual, S.; Blin, T.; Saikia, P.J.; Thomas, M.; Gosselin, P.; Fontaine, L. *J. Polym. Sci. A: Polym. Chem.* **2010**, *48*, 5053-5062.

[32]   Mayadunne, R. T. A.; Rizzardo, E.; Chiefari, J.; Krstina, J.; Moad, G.; Postma, A.; Thang, S. H. *Macromolecules* **2000**, *33*, 243-245.

[33]   Sumerlin, B.S. *ACS Macro Lett.* **2012**, *1*, 141-145.

Chapter III

Synthesis of ω-azlactone-functionalized polymers by RAFT polymerization

Chapter III: Synthesis of ω-azlactone-functionalized polymers by RAFT polymerization[*]

1. Introduction

In chapter II, we have studied the synthesis of amine-reactive polymers by introducing the azlactone functionality in the α-position of macromolecular chains by RAFT polymerization. However, this strategy leads to a trithiocarbonate functionality at the ω-position which could be unstable with time and removed by hydrolysis for instance. Therefore, in this chapter, we inverstigate a second strategy to target azlactone-functionalized polymers by introducing the azlactone functionality at the ω-position of macromolecular chains. Such polymers could be obtained by RAFT polymerization using thiocarbonylthio-compound containing an azlactone ring on the Z group. However, the Z group could be easily modified by aminolysis or hydrolysis. That's why the post-modification of RAFT polymers using "click" chemistry is considered in this chapter, in order to target new ω-azlactone-functionalized polymers.

"Click" chemistry is a term given to near-perfect chemical transformations that display high conversions, are highly selective, and produce non-hazardous by-products which can be separated from the reaction medium *via* non-chromatographic methods.[1] Free-radical[2] and thiol-Michael addition[3] reactions between thiols and activated-ene groups have been largely studied as metal-free "click" reactions[4] to synthesize a range of macromolecular structures and to conjugate ene-groups to proteins. Thiol-Michael

---

addition reactions have been used to synthesize biotin-functionalized glycopolymers,[5a] to mediate the reaction between thiol-functionalized polymer and mannose-modified methacrylate,[5b] and to synthesize polymer-protein conjugates between free cysteine residues on proteins and macromonomers,[5c] and other functional methacrylates.[3b,5d] The combination of RAFT polymerization followed by thiol-based "click" chemistry is known as an orthogonal "relay" reaction as one step complements the other.[6] Such orthogonal "relay" reactions are conveniently achieved by using a trithiocarbonate RAFT agent and then reducing the chain-ends to thiols for use in thiol-ene "click" chemistry.[7] Hence, in this chapter, we report such an orthogonal "relay" approach to synthesize polymers with an azlactone ring at the ω-position by "clicking" the 2-vinyl-4,4-dimethylazlactone (VDM) to thiol end-functionalized polymers and assess their reactivity towards a model amine, namely 4-fluorobenzylamine.

2. Results and discussion

The synthesis of azlactone-terminated poly(*N*-isopropyl acrylamide) was considered by using a combination of RAFT polymerization and "thiol-ene" Michael addition. Therefore, the synthesis of trithiocarbonate-terminated poly(*N*-isopropyl acrylamide) (PNIPAM-CTA) by RAFT polymerization is first studied.

2.1. RAFT polymerization of *N*-isopropyl acrylamide

A well-defined poly(*N*-isopropyl acrylamide) (PNIPAM-CTA) was synthesized by RAFT polymerization of *N*-isopropyl acrylamide (NIPAM) in *N,N*-dimethylformamide (DMF) at 70°C using methyl-2-(*n*-butyltrithiocarbonyl) propanoate (MBTTCP)[8] as the RAFT agent and 2,2'-azobisisobutyronitrile (AIBN) as the initiator (*Scheme 1*).
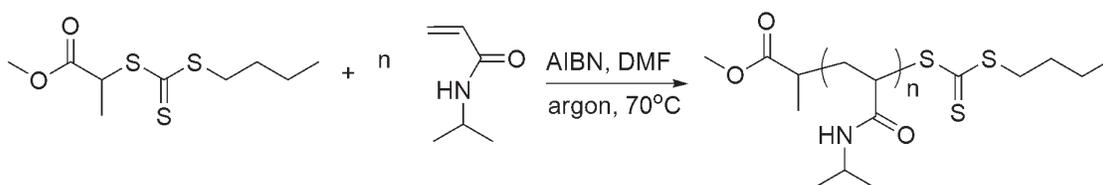
Scheme 1: RAFT polymerization of NIPAM using MBTTCP as the RAFT agent and AIBN as the initiator in DMF at 70ºC, [NIPAM]$_0$:[MBTTCP]$_0$:[AIBN]$_0$ = 24:1:0.2.

After 5h, the polymer was isolated and characterized by steric exclusion chromatography (SEC), ^{1}H NMR spectroscopy and MALDI-TOF mass spectrometry. The number-average molecular weight (M$_{n,SEC}$) and the molecular weight distribution (PDI) were determined relative to polystyrene standards using SEC: M$_{n,SEC}$ = 7840 g.mol^{-1} and PDI = 1.05. The number-average degree of polymerization was also determined to be 26

from ^{1}H NMR spectroscopy by using the ratio of integral area values of the signal at 3.7 ppm (labeled (a) in *Figure 1*) to that of the broad signal at 4.1 ppm (labeled (c) in *Figure 1*), leading to a number-average molecular weight of 3190 g.mol^{-1}. This compared favourably with the data obtained from MALDI-TOF mass spectrometry analysis (*Figure 2*). A single series of signals separated by 113.12 units, corresponding to the molecular weight of the NIPAM repeating unit (calculated value = 113.16 g.mol^{-1}) was detected. The peak at m/z = 3104.02 g.mol^{-1} in the MALDI-TOF spectrum, corresponds to a polymer chain consisting of 25 NIPAM units, an ester at one chain-end, a trithiocarbonate moiety (with butyl chain) at the other chain-end and a sodium atom responsible for ionization (calculated value = 3104.35 g.mol^{-1}). Moreover, the presence of the trithiocarbonate moiety at the chain-end was confirmed by the appearance of a signal at 309 nm in the SEC trace using UV detection, corresponding to the chromophoric C=S bond of the trithiocarbonate (*Figure 3*).
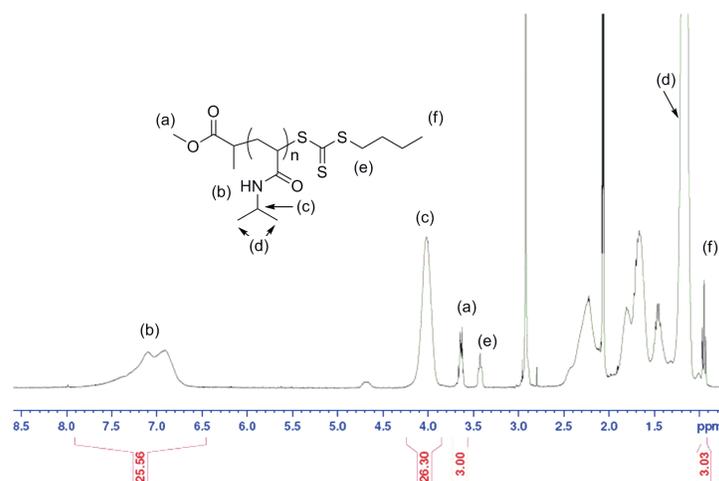
Figure 1: ^{1}H NMR spectrum of PNIPAM-CTA ($M_{n,SEC}$ = 7840 g.mol^{-1}; PDI = 1.05) in acetone D_6.
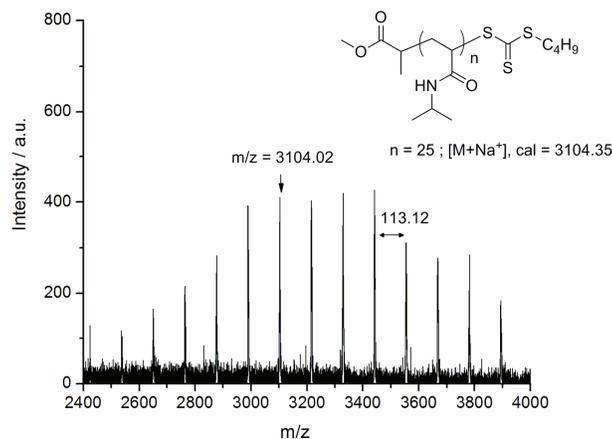
Figure 2: MALDI-TOF mass spectrum of PNIPAM-CTA ($M_{n,SEC}$ = 7840 g.mol^{-1} ; PDI = 1.05) synthesized by RAFT polymerization using MBTTCP as the RAFT agent and AIBN as the initiator in DMF at 70°C ([NIPAM]$_0$:[MBTTCP]$_0$:[AIBN]$_0$ = 24:1:0.2). Matrix: trans-2-[3-(4-tert-butylphenyl)-2-methyl-2-propenylidene]malononitrile (DCTB), sodium trifluoroacetate.
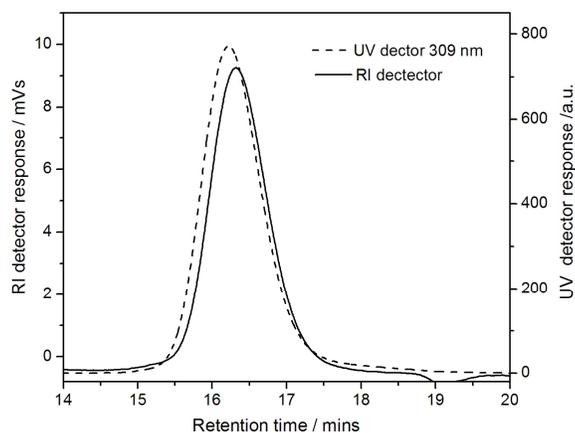
Figure 3: Overlay of SEC traces of PNIPAM-CTA ($M_{n,SEC}$ = 7840 g.mol^{-1}; PDI = 1.05) using differential refractometer (RI) detection and UV detection at 309 nm.

The aminolysis of the trithiocarbonate moiety of the so-obtained well-defined ω-trithiocarbonate-functionalized PNIPAM was then studied.

2.2. Aminolysis of the ω-trithiocarbonate poly(*N*-isopropyl acrylamide) (PNIPAM-CTA)

Recent reviews have reported the chain-end modification of RAFT polymers.[9] ω-Trithiocarbonate polymers are converted to ω-thiol polymers by using amines. However, thiol functionality can be rapidly oxidized to form coupling bisufide products as side-products. Therefore, the addition of a reducing agent (*e.g.* phosphine) was proposed to prevent unwanted coupling bisufide products.[10-16] In order to determinate the optimum conditions to convert the trithiocarbonate chain-end functionality of PNIPAM-CTA into a thiol group, aminolysis (*Scheme 2*) was studied using *n*-hexylamine as the nucleophile and different reducing agents such as sodium hydrosulfide[13,14] (Na$_2$S$_2$O$_4$), triethyl phosphite[15] (P(OEt)$_3$) and dimethylphenyl phosphine[16] (DMPP) (*Table 1*). The formation of bisufide products was monitored by SEC using RI detection (*Figure 4*).
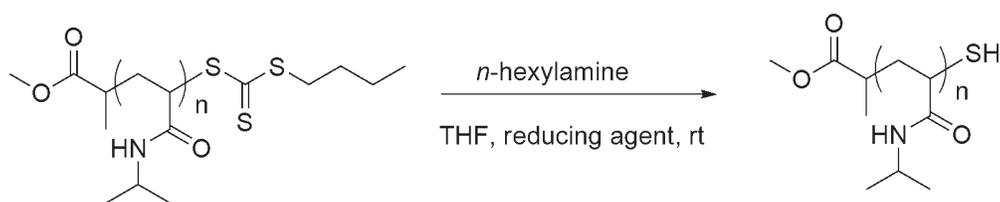
Scheme 2: Aminolysis of PNIPAM-CTA using n-hexylamine.

Table 1: Aminolysis of PNIPAM-CTA using n-hexylamine

Entry	[PNIPAM-CTA]$_0$: [n-hexylamine]$_0$:[reducing agent]$_0$	Reducing agent	Time (h)	Side-product[d]
1	1:60:0[a]	-	3	Bisulfide coupling
2	1:36:10[a]	Na$_2$S$_2$O$_{4aq}$	3	Bisulfide coupling
3	1:12:5[b]	Na$_2$S$_2$O$_{4aq}$	2	Bisufide coupling
4	1:12:5[c]	1) Na$_2$S$_2$O$_{4aq}$ 2) NaBH$_4$	5	No
5	1:12:9.2[b]	P(OEt)$_3$	4	No
6	1: 3.5 :1.4[b]	DMPP	3	No

[a] Aminolysis using PNIPAM-CTA of $M_{n,SEC}$ = 8950 g.mol^{-1} and PDI = 1.05; [b] Aminolysis using PNIPAM-CTA of $M_{n,SEC}$ = 15070 g.mol^{-1} and PDI = 1.06; [c] NaBH$_4$ was added after 2 hours. [d] Determined by SEC in *N,N*-dimethylformamide (DMF) using RI detection and using polystyrene standards.

The results gathered in *Table 1* show that the absence of a reducing agent leads to the formation of bisulfide by-products (*Entry 1, Table 1*). However, the presence of Na$_2$S$_2$O$_4$ does not limit the formation of such bisulfide side-products (*Entries 2 and 3, Table 1*) as shown by the presence of a shoulder towards lower retention time on the SEC trace (*Figure 4a*). These results could be due to the structure of the ω-trithiocarbonate PNIPAM that is different in comparison with CTA-polymer structures reported in previous studies.[13-14] In contrast, the addition of sodium borohydride (NaBH$_4$) as reducing agent can limit the formation of bisulfide compounds (*Entry 4, Table 1, Figure 4a*). Despite the presence of NaBH$_4$ in water cannot prevent the formation of bisulfide compounds.[12] Their reduction could take place by the hydrogenation with the *in-situ* hydrogen formed when NaBH$_4$ reacts with water in the presence of Na$_2$S$_2$O$_4$. Furthermore, the SEC traces of polymers resulting from the aminolysis of PNIPAM-CTA show that coupling bisulfide side-products are limited by using P(OEt)$_3$ and DMPP as

reducing agents (*Figure 4b, Entries 5 and 6, Table 1*). Moreover, DMPP has the advantage to be also a good catalyst for the "thiol-ene" Michael addition.[4b,c] Therefore, DMPP was considered for the aminolysis of the trithiocarbonate moiety and subsequent "thiol-ene" Michael addition of the PNIPAM-CTA synthesized in paragraph 2.1.

a)   b)
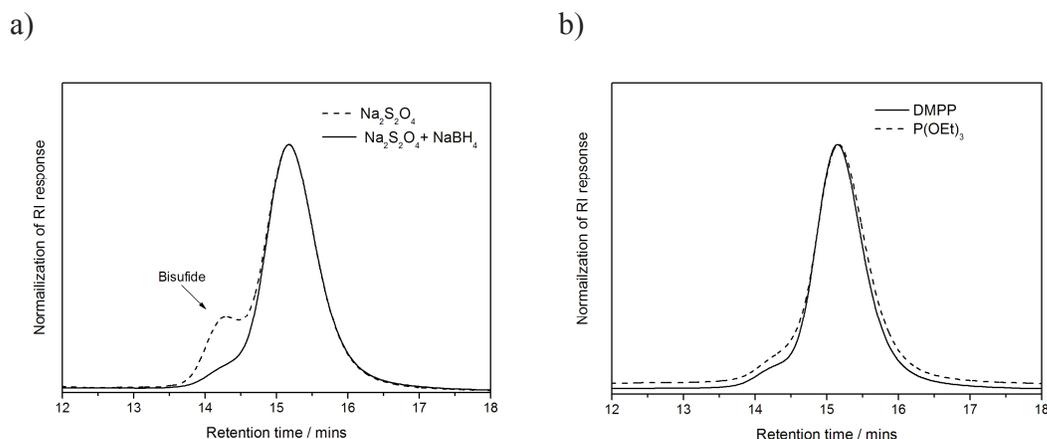
Figure 4: SEC traces of polymers resulting from the aminolysis of PNIPAM-CTA ($M_{n,SEC}$ = 15070 g.mol^{-1}; PDI = 1.06) in tetrahydrofuran (THF) at room temperature: a) using $Na_2S_2O_4$ and the mixture $Na_2S_2O_4/NaBH_4$ as reducing agents, b) using $P(OEt)_3$ and DMPP as reducing agents.

The trithiocarbonate chain-end functionality of the PNIPAM-CTA ($M_{n,SEC}$ = 7840 g.mol^{-1}; PDI = 1.05) was reduced to a thiol in the presence of an excess of DMPP in THF at room temperature. The reduction to a thiol was confirmed by the absence of a peak at 309 nm in the SEC trace using UV detection corresponding to the loss of the C=S bond from the polymer (*Figure 5a*). Coupling between thiol groups to form bisulfide bonds was avoided as revealed by an almost symmetrical monomodal peak shape on SEC trace using RI detection (*Figure 5b*).

a)
b)
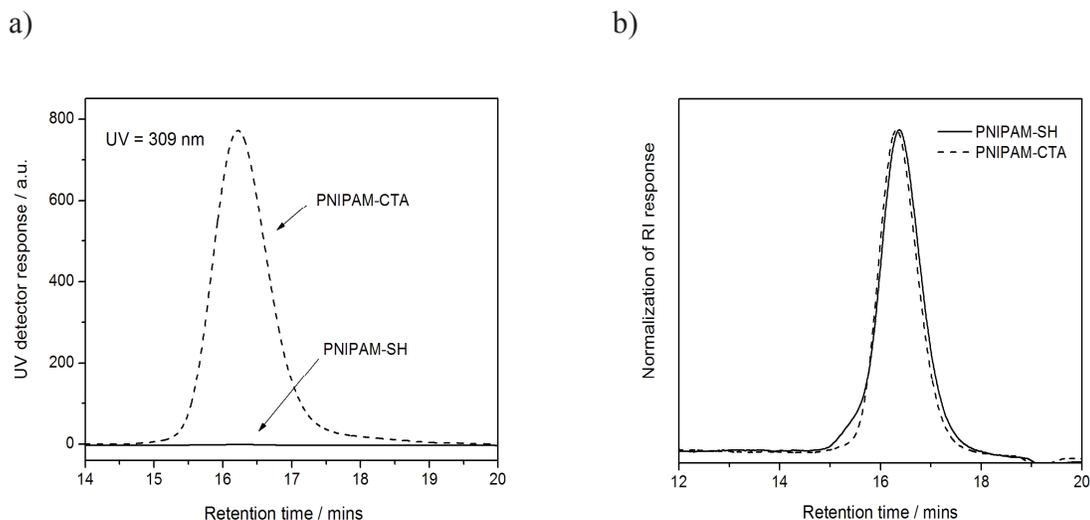
Figure 5: Overlay of SEC traces of PNIPAM ($M_{n,SEC}$ = 7840 g.mol^{-1}; PDI = 1.05) before aminolysis and after aminolysis: a) using UV detection at 309 nm and, b) using RI detection.

A comparison of MALDI-TOF mass spectra of the ω-trithiocarbonate PNIPAM (PNIPAM-CTA) and ω-thiol-terminated PNIPAM (PNIPAM-SH) is presented in *Figure 6*. Main peaks in the MALDI-TOF mass spectrum of PNIPAM-SH decreased by 132.93 relative to main peaks in the MALDI-TOF mass spectrum of PNIPAM-CTA, corresponding to the chemical modification of -S-(C=S)-S-C_4H_9 fragment into -SH fragment at the chain-end of the polymer (calculated value = 132.25 g.mol^{-1}). The MALDI-TOF mass spectrum of PNIPAM-SH shows a single series of peaks separated by *m/z* = 113.11, the molecular weight of the NIPAM repeat unit. Moreover, the peak at *m/z* = 2971.73 (*Figure 6*) corresponds to a polymer of 25 NIPAM units ionized by a sodium atom, with an ester at one chain-end and a thiol group at the other chain-end (calculated value = 2972.10 g.mol^{-1}).

m/z = 3104.66

n = 25 ; [M+Na$^+$], cal = 3104.35

m/z = 2971.73

113.11

n = 25 ; [M+Na$^+$], cal = 2972.10
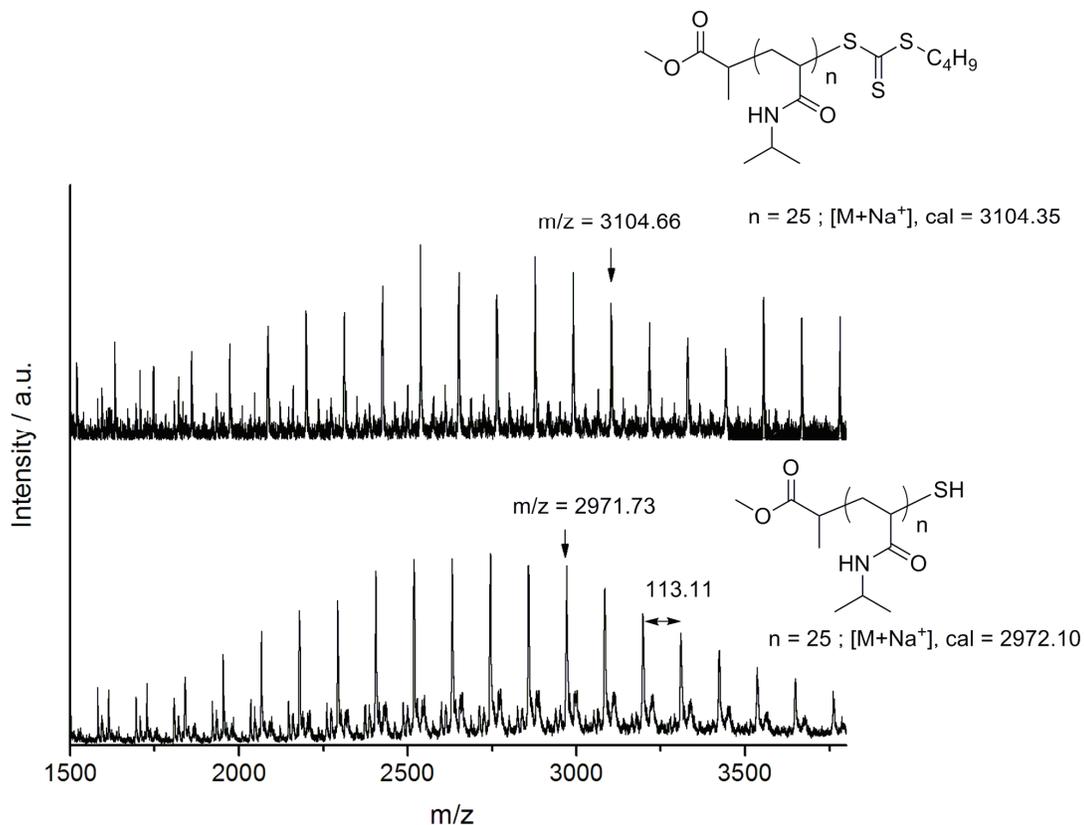
Figure 6: MALDI-TOF mass spectra for PNIPAM-CTA (top) and PNIPAM-SH (bottom).
Matrix: DCTB, sodium iodide.

Comparison between ^{1}H NMR spectra of PNIPAM-SH and PNIPAM-CTA (*Figure 7*) shows that signals at 0.93 ppm and at 3.44 ppm, corresponding to the methyl protons -S-(CH$_2$)$_3$-**CH$_3$** and the methylene protons (-S-**CH$_2$**-(CH$_2$)$_2$-CH$_3$) of the PNIPAM-CTA, respectively, disappeared confirming that PNIPAM-SH is obtained.

A well-defined ω-thiol PNIPAM was obtained and subsequent "thiol-ene" Michael addition with VDM was then studied.
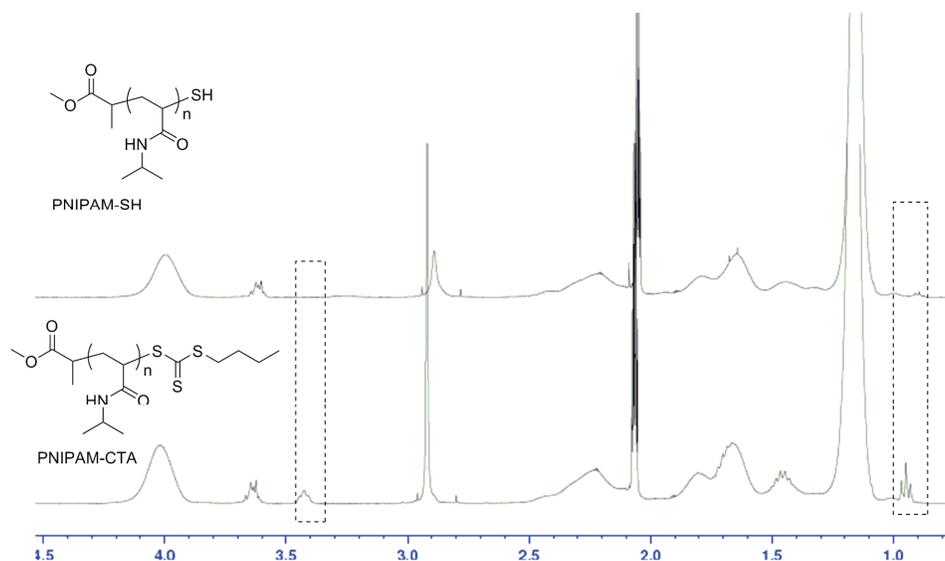
Figure 7: ^1H NMR spectra of PNIPAM-CTA and PNIPAM-SH in acetone D$_6$.

2.3. "Thiol-ene" Michael addition of ω-thiol-functionalized PNIPAM (PNIPAM-SH) with 2-vinyl-4,4-dimethylazlactone (VDM)

The purified PNIPAM-SH (M$_{n,SEC}$ = 7880 g.mol^{-1}, PDI = 1.07) was subjected to react with VDM in the presence of DMPP to afford an ω-azlactone-functionalized PNIPAM (PNIPAM-VDM) (*Scheme 3*). When literature conditions were used for the "thiol-ene" Michael addition, *i.e.* a catalytic amount of DMPP[4c] ([thiol]$_0$:[VDM]$_0$:[DMPP]$_0$ = 5:5:1), a bimodal non-symmetric peak shape was observed on the SEC trace using RI detection, indicating that bisulfide products were formed. This result means that VDM has a different behaviour than (meth)acrylates during the "thiol-ene" Michael addition.[4c]
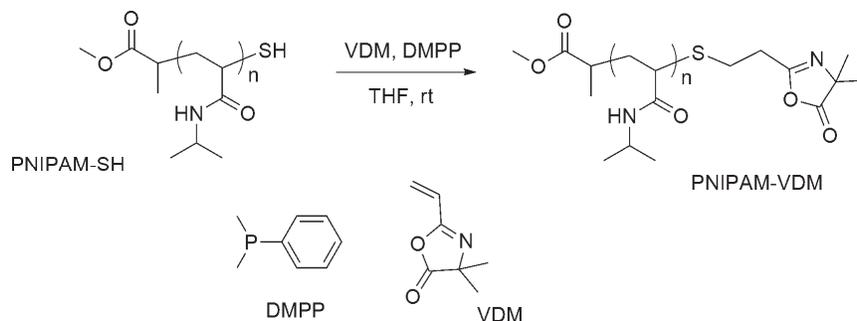
Scheme 3: Synthesis of ω-azlactone-functionalized PNIPAM.

Then, to get a better understanding of our results, a model reaction was performed between VDM and DMPP used in excess ($[VDM]_0:[DMPP]_0 = 1:1.2$) in THF. Analysis of ^{1}H NMR spectra after 15 minutes, 1 hour and 4 hours shows a decrease of the integral area value of the vinyl protons of VDM at 5.9 ppm and at 6.2 ppm, indicating the partial loss of the vinyl group (*Figure 8*). The integral areas of signals at 1.65-1.76 ppm corresponding to protons labeled (g) and (h), and at 2.0-2.1 ppm corresponding to the protons labeled (f) in *Figure 8* inscrease. This result shows that there is addition of DMPP onto the VDM vinyl group leading to the formation of an ylide or a zwitterion Michael adduct. It appears that this ylide or zwitterion is sufficiently basic to react with the thiol of the PNIPAM-SH producing the thiolate which is the nucleophile involved in the Michael addition. Thus, an excess of DMPP is necessary to ensure that all vinyl groups are converted into the ylide or the zwitterion. Therefore, the "thiol-ene" Michael addition was performed using a $[PNIPAM-SH]_0:[VDM]_0:[DMPP]_0$ molar ratio of 1:3.3:8.5 in THF at room temperature (*Scheme 3*).
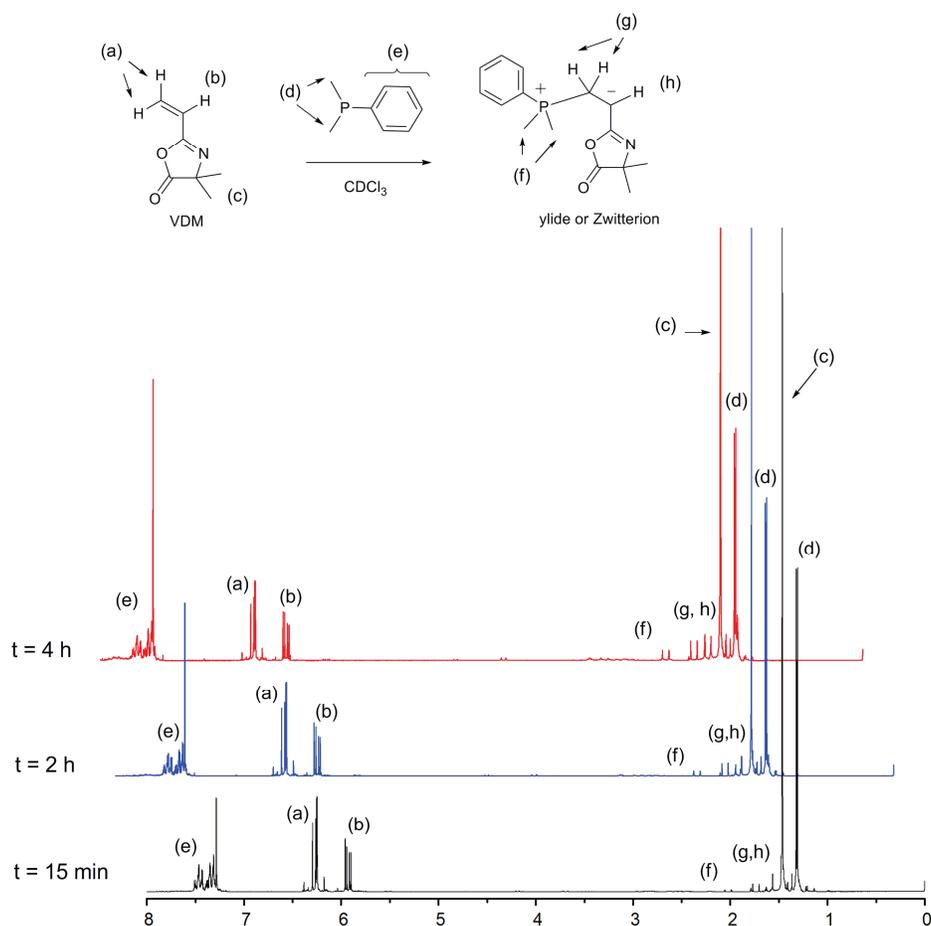
Figure 8: Online ^1H NMR spectra at t = 15 min, t = 1 hour and t = 4 hours for the reaction between DMPP and VDM in CDCl$_3$ ([VDM]$_0$:[DMPP]$_0$ = 1:1.2).

The SEC trace using RI detection of the resulting polymer showed a symmetrical monomodal peak (*Figure 9*). The presence of the azlactone ring at the chain-end of the new polymer was confirmed by FT-IR spectroscopy, with the appearance of a band at 1817 cm^{-1} corresponding to the azlactone C=O group (*Figure 10*).

158
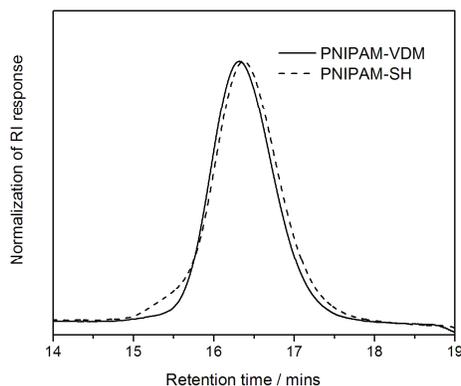
Figure 9: Overlay of SEC traces from the RI detector corresponding to PNIPAM-SH (dotted trace) and the product of the reaction between PNIPAM-SH and VDM (PNIPAM-VDM, solid line) in the presence of DMPP ([PNIPAM-SH]$_0$:[VDM]$_0$:[DMPP]$_0$= 1:3.3:8.5).
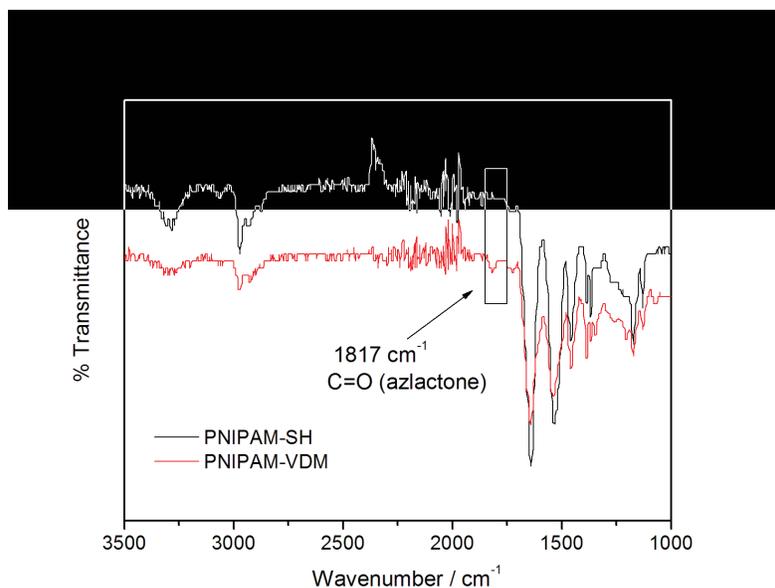
Figure 10: Overlay of FT-IR spectra of PNIPAM-SH before reaction with VDM (dotted trace) and the product of the reaction between PNIPAM-SH and VDM (PNIPAM-VDM, solid line) in the presence of DMPP ([PNIPAM-SH]$_0$:[VDM]$_0$:[DMPP]$_0$= 1:3.3:8.5).

The chain-end functionality was also investigated using MALDI-TOF mass spectrometry. The MALDI-TOF mass spectrum is shown in *Figure 11*.
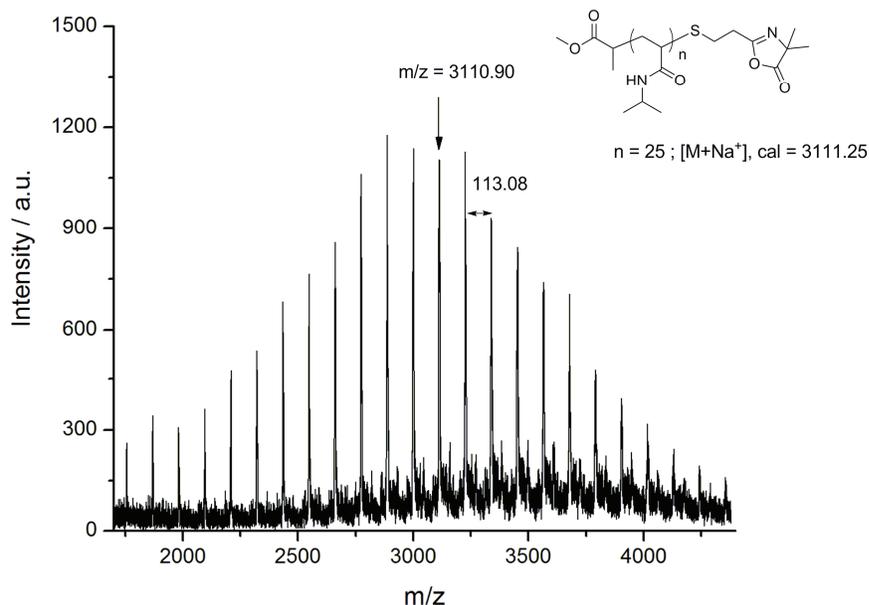
Figure 11: MALDI-TOF mass spectrum for PNIPAM-VDM synthesized by "thiol-ene" Michael addition "click" reaction. Matrix: DCTB, sodium trifluoroacetate.

A single distribution of peaks was observed, separated by 113.08, corresponding to the molecular weight of the NIPAM repeating unit. The peak at *m/z* = 3110.90 was assigned to a polymer consisting of 25 NIPAM units ionized by a sodium atom and featuring an ester at one chain-end and a vinyl azlactone connected *via* a sulphur atom at the other chain-end (calculated value = 3111.25 g.mol^{-1}). In addition, the *m/z* of the peaks increased by 139.52 relative to those in PNIPAM-SH: this value is comparable with the molar mass of the VDM monomer (calculated value = 139.15 g.mol^{-1}).

The azlactone functionality was quantified by ^{1}H NMR spectroscopy by comparing the integral area value of **CH$_3$O-** protons at 3.65 ppm (labeled (a), in

Figure 12) of the ester group at one chain-end and the integral area value of the -CH$_2$S-protons at 2.90 ppm (labeled (e) in *Figure 12*) at the other chain-end. The result showed that the reaction is quantitative.
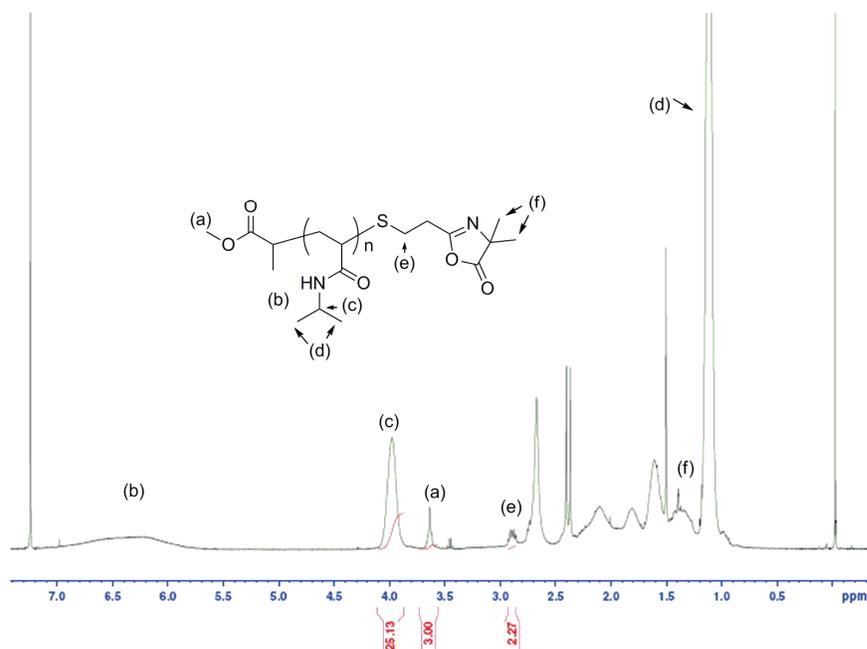
Figure 12: ^{1}H NMR spectrum of PNIPAM-VDM after "thiol-ene" Michael addition "click" reaction in CDCl$_3$.

2.4. Reactivity of ω-azlactone-functionalized PNIPAM towards 4-fluorobenzylamine

The reactivity of the ω-azlactone-functionalized polymer towards a model amine, 4-fluorobenzylamine, was investigated. The PNIPAM-VDM was dissolved in THF and an excess of 4-fluorobenzylamine was added *(Scheme 4)*.
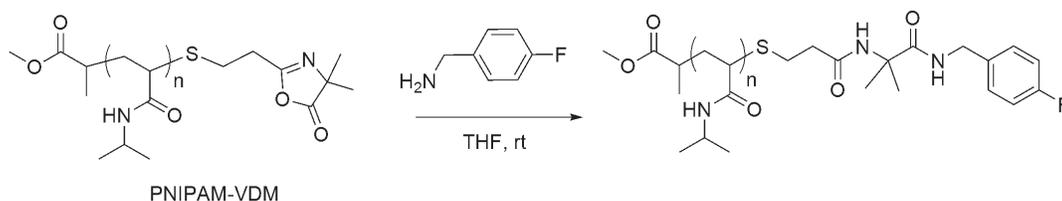
PNIPAM-VDM

Scheme 4: Coupling reaction between ω-azlactone-terminated PNIPAM with 4-fluorobenzylamine in THF at room temperature.

The resulting polymer was analyzed by SEC and ^{1}H NMR spectroscopy. A peak was observed at 263 nm on the SEC trace using UV detection, corresponding to the aromatic group of 4-fluorobenzylamine (*Figure 13*). Two new peaks corresponding to the aromatic protons of 4-fluorobenzylamine were clearly visible in the ^{1}H NMR spectrum at 7.0 ppm and 7.4 ppm (labeled (h) in *Figure 14*). Such results show that the azlactone functionality is able to react with 4-fluorobenzylamine as the model. Moreover, a quantification of the 4-fluorobenzylamine chain-end functionality of the PNIPAM was performed by comparing the integral area value of the signal corresponding to the methylene protons (a) (*Figure 14*) of the ester moiety group at 3.65 ppm and the integral area value of the signal corresponding to the protons (g) (*Figure 14*) of the 4-fluorobenzylamine moiety at 4.32-4.41 ppm, respectively, which was found to be quantitative.

162
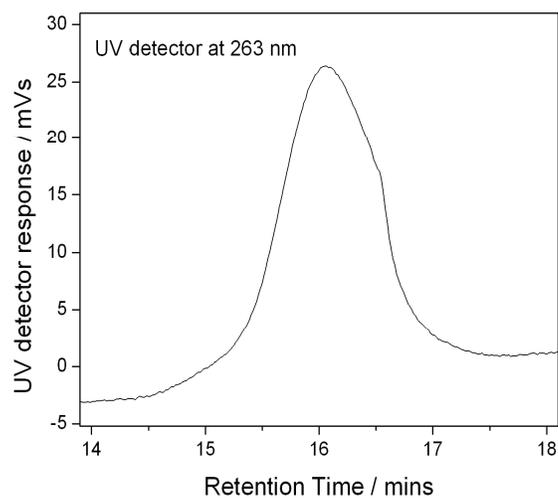
Figure 13: SEC trace using UV detection at 263 nm for the product of the reaction with PNIPAM-VDM and 4-fluorobenzylamine.
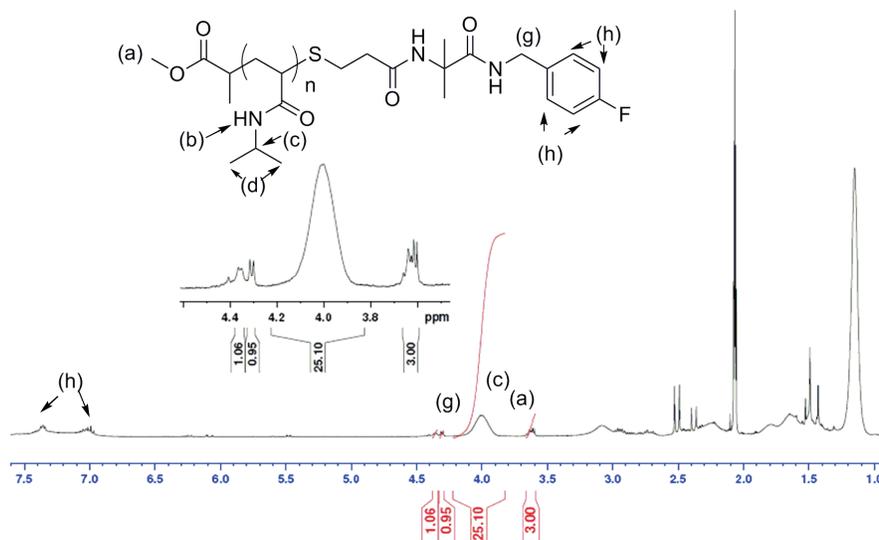
Figure 14: ^{1}H NMR spectrum of 4-fluorobenzylamine-functionalized PNIPAM in acetone D$_6$.

163

3. Conclusion

Well-defined ω-azlactone-functionalized PNIPAMs were synthesized *via* a combination of RAFT polymerization and "thiol-ene" Michael addition approach for the first time.

RAFT polymerizations of NIPAM were mediated with MBTTCP used as the chain transfer agent. Resulting ω-trithiocarbonate PNIPAMs were then converted to ω-thiol PNIPAMs by aminolysis. For such aminolysis, a careful choice of experimental conditions was considered to target the quantitative thiol end-group functionality. The "thiol-ene" Michael addition was then performed though the vinyl group of VDM. Final ω-azlactone-functionalized PNIPAMs were characterized by MALDI-TOF mass spectrometry, ^{1}H NMR and FT-IR spectroscopies. Resulting reaction with 4-fluorobenzylamine as a model amine demonstrates the potential of such a strategy to prepare well-defined bioconjugates.

4. Experimental section

4.1. Materials

Dimethylphenyl phosphine (DMPP, 99%), 4-fluorobenzylamine (97%), *n*-hexylamine (> 99%), sodium thiosulfate ($Na_2S_2O_4$, 85%), triethyl phosphite ($P(OEt)_3$, 98%) were all purchased from Aldrich and were used without further purification. *N*-isopropyl acrylamide (NIPAM, 97%) was purchased from Aldrich and recrystallized from petroleum ether prior to use. 2,2'-Azobisisobutyronitrile (AIBN, 98%) was purchased from Aldrich and recrystallized from methanol before use. Sodium borohydride ($NaBH_4$, 98%) was purchased from Acros. Tetrahydrofuran (THF, > 99.9%), *N,N*-dimethylformamide (DMF, 99.8%), diethyl ether (technical grade), petroleum ether (analytic reagent grade, 40-60°C) and acetone (98%) were obtained from Aldrich and used without additional prior distillation. RAFT agent methyl-2-(*n*-butyltrithiocarbonyl) propanoate[8] (MBTTCP) and 2-vinyl-4,4-dimethylazlactone[17] (VDM) were synthesized following reported procedures.

4.2. Instrumentation

Nuclear Magnetic Resonance (NMR)

NMR spectra were recorded on a Bruker AC-400 Spectrometer for ^{1}H NMR (400 MHz) and [13]C (100 MHz). Chemical shifts are reported in ppm relative to deuterated solvent resonances.

Size Exclusion Chromatography (SEC)

Polymers were characterized on a SEC system operating in DMF eluent at 60°C fitted with a polymer laboratories guard column (PL Gel 5μm) and two Polymer

Laboratories PL Mixed D columns, a Waters 410 differential refractometer (RI) and a Waters 481 UV photodiode array detector. The instrument operated at a flow rate of 1.0 mL.min^{-1} and was calibrated with narrow linear polystyrene (PS) standards ranging in molecular weight from 580 g.mol^{-1} to 460 000 g.mol^{-1}. Molecular weights and polydispersity indices (PDI) were calculated using Waters EMPOWER software.

MALDI-TOF mass spectrometry

MALDI-TOF (Matrix-Assisted Laser Desorption and Ionization Time Of Flight) mass spectrometry analysis was performed on a Bruker Bioflex III MALDI-TOF instrument equipped with nitrogen laser operating at 337 nm, a 2GHz sampling rate digitiser, pulsed ion extraction source and reflectron. The laser pulse width is 3ns and maximum power is 200 mJ. Spectra were recorded in the linear mode with an acceleration voltage of 19 kV and delay of 200 ns. 100 single shot aquisitions were summed to give the spectra and the data were analyzed using Bruker XTOF software. Samples of PNIPAM were prepared by dissolving the matrix (*trans*-2-[3-(4-*tert*-butylphenyl)-2-methyl-2-propenylidene]malononitrile, DCTB) in the solvent (dichloromethane, 30 mg.mL^{-1}) and mixing with the polymer (PNIPAM, 2 mg.mL^{-1}) in the ratio 1:1 (v/v). 1 µL was spotted directly onto a thin layer of sodium trifluoroacetate or sodium iodide in acetone (concentration 19 mg.mL^{-1}) that had been deposited to act as a cationizing agent.

4.3. RAFT polymerization of *N*-isopropyl acrylamide

A magnetic stir bar was charged to a Schlenk tube along with *N*-isopropyl acrylamide (5.03 g, 0.0445 mol), MBTTCP (0.470, 18.65x10^{-4} mol), AIBN (0.0746 g, 4.55x10^{-4} mol) and DMF (5.0 mL). The mixture was deoxygenated by a series of freeze-

pump thaw cycles. When no further bubbles were observed, the reaction mixture was switched to an argon atmosphere and the Schlenk tube immersed in a thermostated oil bath operating at 70°C and left for a period of five hours. After this time had elapsed the polymerization reaction was stopped by opening the reaction to air, and the polymer was purified by precipitation in diethyl ether, separated and drying under vacuum at 30°C overnight. The polymer was analyzed by ^{1}H NMR spectroscopy, SEC, and MALDI-TOF mass spectrometry. $M_{n, NMR}$ = 3190 g.mol^{-1}. $M_{n,SEC}$ = 7840 g.mol^{-1}, PDI = 1.05. ^{1}H NMR (400 MHz, acetone D$_6$), δ (ppm): 0.93 (**CH$_3$**-(CH$_2$)$_2$-CH$_2$-S), 1.10-1.25 (-NHCH(**CH$_3$**)$_2$), 1.46 (CH$_3$-(**CH$_2$**)$_2$-**CH$_2$**-S-), 1.40-2.73 (-**CH$_2$**-**CH**-)$_n$, 3.44 (CH$_3$-(CH$_2$)$_2$-**CH$_2$**-S-C(S)-S-), 3.65 (**CH$_3$**-OC(O)-**CH**(CH$_3$)-), 4.05 (-NH**CH**(CH$_3$)$_2$), 6.58-7.57 (-**NH**-(CH$_3$)$_2$).

4.4. Aminolysis of the ω-trithiocarbonate poly(*N*-isopropyl acrylamide) (PNIPAM-CTA) in the presence of DMPP

A magnetic stir bar was charged to a Schlenk tube along with PNIPAM-CTA (1.0 g, 2.9 x10^{-4} mol), DMPP (60 µL, 4.16 x 10^{-4} mol) and THF (3 mL). The reaction mixture was deoxygenated by a series of freeze-pump thaw cycles. When no further bubbles were observed, the *n*-hexylamine (0.3mL, 0.23 g, 2.2 x 10^{-3} mol) was injected and stirred at ambient temperature for two hours. When this time had elapsed the product was precipitated into diethyl ether, filtered and dried under vacuum at 30°C. A white powder was obtained and analyzed by SEC, ^{1}H NMR spectroscopy and MALDI-TOF spectrometry. $M_{n,SEC}$ = 7880 g.mol^{-1}, PDI = 1.07. ^{1}H NMR (400 MHz, acetone D$_6$), δ (ppm): 1.10-1.25 (-NHCH(**CH$_3$**)$_2$), 1.40-2.73 (-**CH$_2$**-**CH**-)$_n$, 3.65 (**CH$_3$**-OC(O)-), 4.05 (-NH**CH**(CH$_3$)$_2$), 6.58-7.57 (-**NH**-(CH$_3$)$_2$).
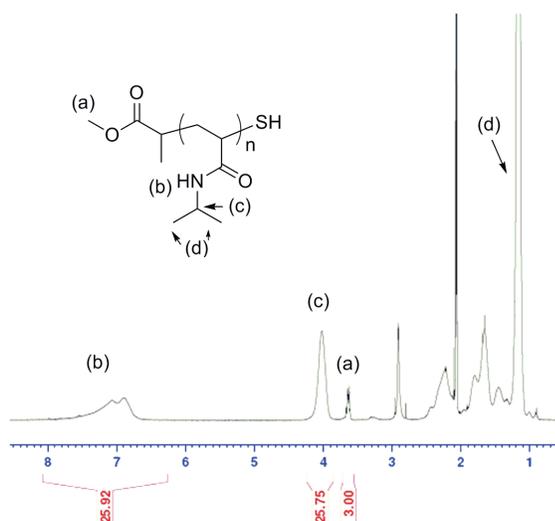
Figure 15: ^{1}H NMR of PNIPAM-SH in acetone D_6.

4.5. "Thiol-ene" Michael addition of the ω-thiol-functionalized PNIPAM (PNIPAM-SH) with 2-vinyl-4,4-dimethylazlactone (VDM)

4.5.1. ^{1}H NMR spectroscopy online study of the DMPP/VDM complex

Online ^{1}H NMR study was used to analyze a mixture of DMPP and VDM. DMPP (20 µL, 0.14 mmol) and VDM (30 µL, 0.22 mmol) were dissolved in CDCl$_3$ and placed in a NMR tube. The sample was analyzed by ^{1}H NMR spectroscopy (200 MHz, 32 scans) at t = 0, t = 1 hour and t = 4 hours.

4.5.2. Synthesis of ω-azlactone-terminated PNIPAM

A magnetic stir bar was charged to a Schlenk tube along with VDM (15 µL, 1.08 x 10^{-4} mol), DMPP (25 µL, 1.73 x 10^{-4} mol), THF (1mL) and stirred at room temperature for 30 minutes. The reaction media increased in viscosity and a yellow color was observed. After this time had elapsed, PNIPAM-SH (0.1 g, 3.1 x 10^{-5} mol) and an additional quantity of DMPP (15 µL, 1.04 x 10^{-4} mol) were added to the reaction mixture

and the solution was left to react for 16 hours. It should be noted that the viscosity decreased upon addition of PNIPAM and the yellow color diminished. When this time had elapsed the polymer was precipitated into diethyl ether, filtered and dried under vacuum at room temperature. A white powder was obtained and analyzed by SEC, ^{1}H NMR spectroscopy and MALDI-TOF mass spectrometry. $M_{n,SEC}$ = 8420 g.mol^{-1}, PDI = 1.05. ^{1}H NMR (400 MHz, CDCl$_3$, δ ppm): 1.10-1.25 (-NHCH(C**H**$_3$)$_2$), 1.40-2.73 ((-C**H**$_2$-C**H**-)$_n$ and (-OCO-C(C**H**$_3$)$_2$-N)$_{azlactone}$), 2.90 (-S-C**H**$_2$-C**H**$_2$-), 3.65 (C**H**$_3$-OC(O)-), 4.05 (-NHC**H**(CH$_3$)$_2$), 6.58-7.57 (-N**H**-(CH$_3$)$_2$).

4.6. Reaction between PNIPAM-VDM and 4-fluorobenzylamine

A magnetic stir bar was charged to a round bottomed flask along with PNIPAM-VDM and anhydrous THF. Once the polymer had dissolved, 4-fluorobenzylamine was added and the mixture left to stir for 4 hours. When this time had elapsed, the polymer was precipitated into diethyl ether, filtered and dried under vacuum at room temperature. A white powder was obtained and analyzed by SEC and ^{1}H NMR spectroscopy. $M_{n,SEC}$ = 9220 g.mol^{-1}, PDI = 1.05. ^{1}H NMR (400 MHz, acetone D$_6$), δ (ppm): 1.10-1.25 (-NH-CH(C**H**$_3$)$_2$), 1.40-2.73 ((-C**H**$_2$-C**H**-)$_n$, 3.65 (C**H**$_3$-OC(O)-), 4.05 (-NH-C**H**(CH$_3$)$_2$), 4.32-4.41 (FC$_6$H$_4$C**H**$_2$-), 6.58-7.57 (-N**H**-(CH$_3$)$_2$), 7.0 and 7.40 (F**C$_6$H$_4$**CH$_2$-).

References

[1]   Kolb, H. C.; Finn, M. G.; Sharpless, K. B. *Angew. Chem. Int. Ed.* **2001**, *40*, 2004-2021.

[2]   (a) Hoyle, C. E.; Lee, T. Y.; Roper, T. *J. Polym. Sci. Part A. Polym. Chem.* **2004**, *42*, 5301-5338. (b) Kade, M. J.; Burke, D. J.; Hawker, C. J. *J. Polym. Sci. Part A. Polym. Chem.* **2010**, *48*, 743-750. (c) Hoyle, C. E.; Bowman, C. N. *Angew. Chem. Int. Ed.* **2010**, *49*, 1540-1573. (d) Killops, K. L.; Campos, L. M.; Hawker, C. J. *J. Am. Chem. Soc.* **2008**, *130*, 5062-5064.

[3]   (a) Cole, B. M.; Foudoulakis H. M.; Bartolozzi, A. *Synthesis* **2008**, *13*, 2023-2032. (b) Chan, J. W.; Hoyle, C. E.; Lowe, A. B. *J. Am. Chem. Soc.* **2009**, *131*, 5751-5753.

[4]   (a) Dondoni, A. *Angew. Chem. Int. Ed.* **2008**, *47*, 8995-8997. (b) Lowe, A. B. *Polym. Chem.* **2010**, *1*, 17-36. (c) Li, G-Z.; Randev, R. K.; Soeriyadi, A. H.; Rees, G.; Boyer, C.; Tong, Z.; Davis, T. P.; Becer, C. R.; Haddleton, D. M. *Polym. Chem.* **2010**, *1*, 1196-1204. (d) Hoyle, C. E.; Lowe, A. B.; Bowman, C. N. *Chem. Soc. Rev.* **2010**, *39*, 1355-1387.

[5]   (a) Boyer, C.; Davis, T. P. *Chem. Commun.* **2009**, *40*, 6029-6031. (b) Boyer, C.; Granville, A.; Davis, T. P.; Bulmus, V. *J. Polym. Sci. Part A. Polym. Chem.* **2009**, *47*, 3773-3794. (c) Jones, M. W.; Mantovani, G.; Ryan, S. M.; Wang, X.; Brayden, D. J.; Haddleton, D. M. *Chem. Commun.* **2009**, *40*, 5272-5274. (d) Yu, B.; Chan, J. W.; Hoyle, C. E.; Lowe, A. B. *J. Polym. Sci. Part A. Polym. Chem.* **2009**, *47*, 3544-3554.

[6]   Kakwere, H.; Perrier, S. *J. Am. Chem. Soc.* **2009**, *131*, 1889-1895.

[7]   Iha, R. K.; Wooley, K. L.; Nystrom, A. M.; Burke, D. J.; Kade, M. J.; Hawker, C. J. *Chem. Rev.* **2009**, *109*, 5620-5686.

[8]   Pascual, S.; Monteiro, M. J. *Eur. Polym. J.* **2009**, *45*, 2513-2519.

[9]   (a) Willcock, H.; O'Reilly, R. K. *Polym. Chem.* **2010**, *1*, 149-157. (b) Moad, G.; Rizzardo, E.; Thang, S. H. *Polym. Int.* **2011**, *60*, 9-25. (c) Roth, P. J.; Boyer, C.; Lowe, A. B.; Davis, T. P. *Macromol. Rapid Commun.* **2011**, *32*, 1123-1143.

[10] Li, M.; De, P.; Gondi, S. R.; Sumerlin, B. S. *J. Polym. Sci. Part A: Polym. Chem.* **2008**, *46*, 5093-5100.

[11] Li, M.; De, P.; Li, H.; Sumerlin, B. S. *Polym. Chem.* **2010**, *1*, 854-859.

[12] Scales, C.W.; Convertine, A. J.; McCormick, C. L. *Biomacromolecules* **2006**, *7*, 1389-1392.

[13] Lima, V.; Jiang, X.; Brokken-Zijp, J.; Shoenmakers, P. J.; Klumperman, B.; Vander Linde, R. *J. Polym. Sci. Part A: Polym. Chem.* **2005**, *43*, 959-973.

14   Patton, D. L.; Mullings, M.; Fulghum, T.; Advincula, R. C. *Macromolecules* **2005**, *38*, 8597-8602.

15   Ho, T. H.; Levere, M. E.; Pascual, S.; Montembault, V.; Soutif, J.-C.; Fontaine, L. *J. Polym. Sci. Part A: Polym. Chem.* **2012**, *50*, 1657-1661.

16   Chan, J. W.; Yu, B.; Hoyle, C. E.; Lowe, A. B. *Polymer* **2009**, *50*, 3158-3168.

17   Levere, M. E.; Ho, H. T.; Pascual, S.; Fontaine, L. *Polym. Chem.* **2011**, *2*, 2878-2887.

Chapter IV

Synthesis of stable azlactone-functionalized nanoparticles prepared from thermoresponsive copolymers synthesized by RAFT polymerization

Chapter IV: Synthesis of stable azlactone-functionalized nanoparticles prepared from thermoresponsive copolymers synthesized by RAFT polymerization[*]

1. Introduction

Two strategies based on RAFT polymerization and "click" chemistry (thiol-Michael addition) have been used to provide well-defined reactive polymers incorporating the azlactone group in the α-position (chapter II) and in the ω-position (chapter III) of macromolecular chains. Moreover, the reactivity of such polymers towards model amines has been demonstrated. In order to increase the loading of azlactone groups within the macromolecular chains, a new strategy providing azlactone rings as pendant groups will be considered in this chapter. Therefore, the RAFT copolymerization of 2-vinyl-4,4-dimethylazlactone (VDM) with acrylamides will be studied. Acrylamides such as *N,N*-dimethyl acrylamide (DMA) and *N*-isopropyl acrylamide (NIPAM) have been chosen as VDM behaviour in copper-mediated controlled/"living" radical polymerization is similar to acrylamides behaviour[1] and polyacrylamides opens the way to polymers with various properties such as thermoresponsive polymers. Only a few studies have been reported on the synthesis by RAFT polymerization of polyacrylamide-based thermoresponsive copolymers reactive towards amines.[2–8] The reactive functionalities towards amines used in these reported studies are activated esters such as *N*-hydroxysuccinimidyl esters[2-7] and

---

[*] Part of this work has been published in Polymer Chemistry (*Polym. Chem.* **2011**, *2*, 2878-2887) and in Australian Journal of Chemistry (*Aust. J. Chem*. DOI: 10.1071/CH12192).

pentafluorophenyl ester.[8] The main drawback of using such functionalities is the formation of small molecule by-products after reaction with amines. The advantages of the azlactone ring are numerous in comparison with *N*-hydroxysuccinimidyl ester[2-7] and pentafluorophenyl ester groups.[8] First, the azlactone ring displays a high reactivity towards amino-functionalized molecules at room temperature by means of a ring-opening addition reaction without the addition of catalysts or the formation of by-products.[9] This has led to the use of solid supported PVDM as a scavenger for amine impurities.[10-15] Furthermore, the azlactone ring has the ability to react with the free amine groups of biomolecules, has opened the way to potential bioapplications.[16-21] Moreover, the azlactone functionality is resistant to hydrolysis at neutral pH: this is a considerable advantage compared to the succinimide group.[20]

In this chapter, we report the synthesis of block copolymers containing a thermoresponsive poly(*N*-isopropyl acrylamide)[22] (PNIPAM), a hydrophilic poly(*N,N*-dimethyl acrylamide) (PDMA) and an amine reactive units from poly(2-vinyl-4,4-dimethylazlactone) (PVDM). Therefore, PDMA-*b*-P(VDM-*co*-NIPAM) block copolymers and PNIPAM-*b*-P(VDM-*co*-DMA) block copolymers will be synthesized, characterized in water and their reactivity towards a diamine to form stable cross-linked core-shell particles in water will be studied. This ''ideal'' and original cross-linking strategy is non-toxic, is facile under mild conditions (*i.e.* ambient temperature and in aqueous solution), does not necessitate the addition of a co-reagent, does not generate small molecule by-products and is hightly efficient. This approach is really a major advantage over previously reported approaches.[23-28] Reactivity of the cross-linked azlactone-functionalized particles will be studied using dansylhydrazine. To the best of

our knowledge, this is the first work concerning the incorporation of the azlactone functionality into thermoresponsive copolymers that can self-assemble into core-shell nanoparticles, which are efficiently stabilized by covalent cross-linking without the presence of a co-reagent and without the formation of a by-product.

2. Results and discussion

In order to synthesize PDMA-*b*-P(VDM-*co*-NIPAM) and PNIPAM-*b*-P(VDM-*co*-DMA) block copolymers, first blocks PDMA and PNIPAM have been previously synthesized using RAFT polymerization. In the second step, the resulting PDMA and PNIPAM have been used as macromolecular chain transfer agents (macroCTAs) to mediate the copolymerization of VDM/NIPAM and of VDM/DMA, respectively. The amount of VDM in the second block was kept low in order to keep the LCST of the P(VDM-*co*-NIPAM) block near 32°C and in order to maintain the hydrophilicity of the P(VDM-*co*-DMA) block.

2.1. Synthesis of poly(*N,N*-dimethyl acrylamide) (PDMA) and poly(*N*-isopropyl acrylamide) (PNIPAM) by RAFT polymerization

A well-defined PDMA was synthesized by RAFT polymerization of *N,N*-dimethyl acrylamide (DMA) using methyl-2-(*n*-butyltrithiocarbonyl) propanoate (MBTTCP) as the RAFT agent and 2,2'-azobisobutyronitrile (AIBN) as the initiator in dioxane at 70°C (*Scheme 1a*). After 90 min, the DMA conversion was calculated to be 85% as determined by ^{1}H NMR spectroscopy by comparing the integral area value of vinylic protons from DMA at 5.55 ppm with the integral area value of C**H**O from *N,N*-dimethylformamide (DMF) used as internal reference at 8.02 ppm. The number-average polymerization degree (DP$_n$) of resulting PDMA was determined to be 23 from ^{1}H NMR spectroscopy using the ratio of integral area values of the signal at 3.35 ppm (-SC(S)S-C**H**$_2$-, labeled (c)) at the chain-end to that of the broad signal at 2.91 ppm (-CO-N(C**H**$_3$)$_2$, labeled (b)) (*Figure 1*).
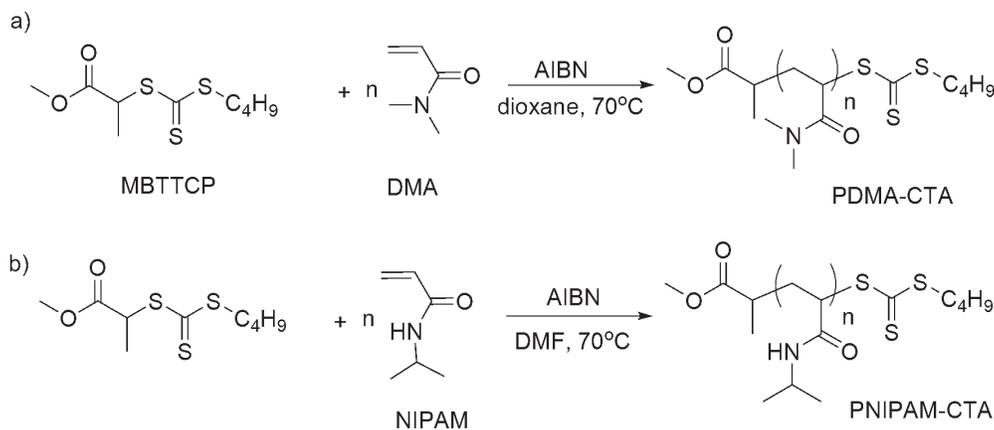
Scheme 1: RAFT polymerizations: a) of DMA and, b) of NIPAM using MBTTCP as the RAFT agent and AIBN as the initiator in solution at 70°C.
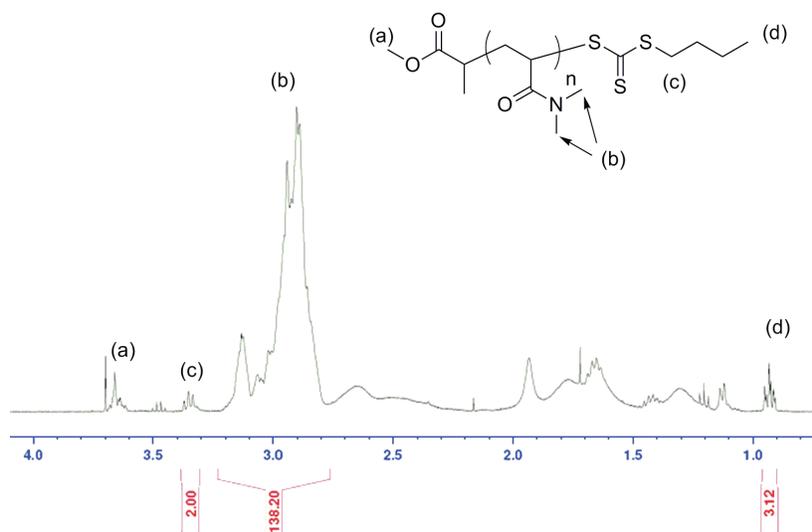
Figure 1: ^1H NMR of PDMA in CDCl$_3$.

The SEC traces obtained by using RI and UV detections showed unimodal traces (*Figure 2*). The presence of the trithiocarbonate moiety at the PDMA chain-end was confirmed by the presence of a signal at 309 nm in the SEC trace using UV detection, corresponding to the C=S bond of the trithiocarbonate, thus indicating that this product

(called PDMA-CTA) could be used as a macroCTA to mediate further RAFT polymerizations.
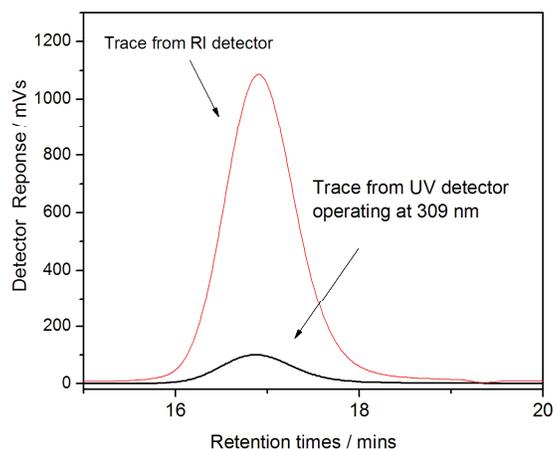
Figure 2: SEC traces of the PDMA-CTA using RI detection and UV detection at 309 nm.

Using similar experimental conditions, a well-defined PNIPAM[*] ($M_{n,SEC}$ = 5600 g.mol^{-1}, PDI = 1.12, DP_n = 46) was synthesized by RAFT polymerization of *N*-isopropyl acrylamide in DMF at 70°C using MBTTCP as the RAFT agent and AIBN as the initiator (*Scheme 1b*).[6,29] As for PDMA-CTA, the presence of the trithiocarbonate moiety at the PNIPAM chain-end was confirmed by the signal at 309 nm corresponding to the chromophoric C=S bond of the trithiocarbonate, in the SEC trace using UV detection (*Figure 3*).

Both trithiocarbonate-terminated PDMA-CTA and PNIPAM (called PNIPAM-CTA) have then been employed as macroCTAs for further RAFT polymerizations.

---

[*] This polymer was synthesized by Dr. Martin E. Levere during his post-doctoral position in 2009.
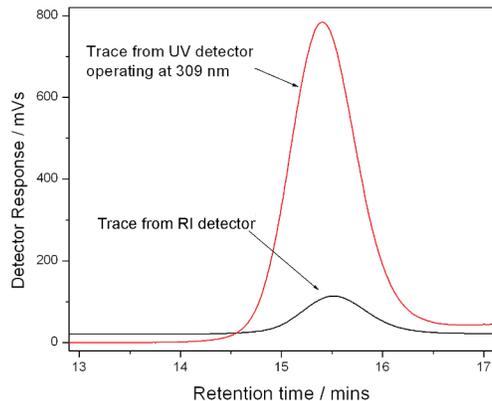
Figure 3: SEC traces of the PNIPAM-CTA using RI detection and UV detection at 309 nm.

2.2. Synthesis of PDMA-*b*-P(VDM-*co*-NIPAM)) copolymers and of PNIPAM-*b*-P(VDM-*co*-DMA) copolymers by RAFT polymerization

In order to target thermoresponsive copolymers with azlactone functionality, we studied the RAFT copolymerizations of VDM with NIPAM and with DMA using PDMA-CTA and PNIPAM-CTA, respectively. Lokitz *et al.*[30] reported the RAFT polymerization of VDM using either 2-cyanoprop-2-yl dithiobenzoate (CPDB) or 2-dodecylsulfanylthiocarbonylsulfanyl-2-methylpropionic acid (DMP) as chain transfer agents (CTAs). Pascual *et al.* have recently described the first detailed investigation of the blocking efficiency of VDM with monomers such as styrene, methyl acrylate, and methyl methacrylate in RAFT polymerization using the cumyl dithiobenzoate (CDB) as the chain transfer agent.[31] To date, only a preliminary study has been reported on the RAFT polymerization of VDM to synthesize thermoresponsive and pH-responsive copolymers.[32]

The previously synthesized PDMA-CTA and PNIPAM-CTA were used as macroCTAs to mediate the RAFT statistical copolymerization of VDM/NIPAM and of VDM/DMA in freshly distilled 1,4-dioxane at 70°C as shown in *Scheme 2*. The results are shown in *Table 1*.
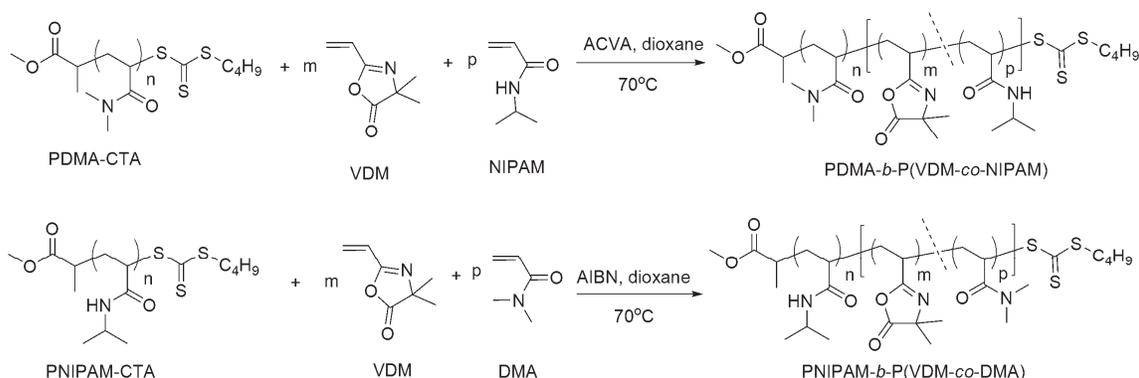
Scheme 2: Synthesis of PDMA-b-P(VDM-co-NIPAM) and of PNIPAM-b-P(VDM-co-DMA) copolymers by RAFT polymerization.

Table 1: PNIPAM, PDMA and PVDM-based block copolymers synthesized by RAFT polymerization.

(Co)polymer structure	$M_{n,SEC}$ (g.mol^{-1})	PDI	DP_n (NIPAM)^c	DP_n (VDM)^c	DP_n (DMA)^c
PDMA$_{23}$	5300^a	1.05^a	0	0	23
PDMA$_{23}$-b-P(VDM$_{10}$-co-NIPAM$_{46}$)	19500^a	1.04^a	46	10	23
PNIPAM$_{46}$*	5600^b	1.12^b	46	0	0
PNIPAM$_{46}$-b-P(VDM$_6$-co-DMA$_{65}$)*	33400^a	1.10^a	46	6	65
PNIPAM$_{46}$-b-P(VDM$_4$-co-DMA$_{94}$)*	59200^a	1.17^a	48	4	94
PNIPAM$_{42}$-b-P(VDM$_{18}$-co-DMA$_{281}$)	64600^a	1.20^a	42	18	281

^{a} Determined from SEC in DMF calibrated with linear polystyrene standards using PL Mixed-D columns. ^{b} Determined from SEC in DMF calibrated with linear polystyrene standards using PolarGel columns. ^{c} Determined from ^{1}H NMR spectroscopy.* These (co)polymers were synthesized by Dr. Martin E. Levere during his post-doctoral position in 2009.

The molar compositions of PDMA-*b*-P(VDM-*co*-NIPAM) and PNIPAM-*b*-P(VDM-*co*-DMA) block copolymers were determined by ^{1}H NMR spectroscopy. For instance, the molar composition of PDMA-*b*-P(VDM-*co*-NIPAM) was determined by comparing integral area values of the signal corresponding to **CH** of PNIPAM ((g), *Figure 4*), of the signal corresponding to **CH**$_3$ of PDMA ((b), *Figure 4*), of the signal corresponding to **CH**$_3$ of PVDM ((e), *Figure 4*) and of -O**CH**$_3$ of the ester at the chain-end ((a), *Figure 4*). In this case, the number-average degrees of polymerization were equal to 46, 23 and 10 for NIPAM, DMA and VDM, respectively.
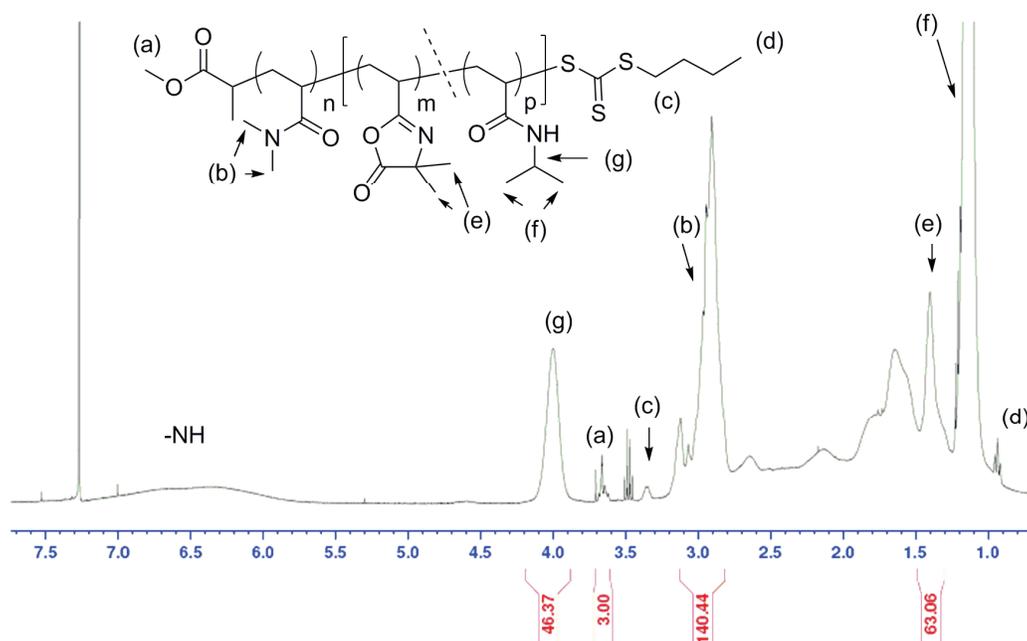
Figure 4: ^{1}H NMR spectrum of the PDMA$_{23}$-b-P(VDM$_{10}$-co-NIPAM$_{46}$) block copolymer in CDCl$_3$.

Chain extensions of PDMA-CTA and PNIPAM-CTA lead to well-defined copolymers as shown by the symmetrical SEC traces of PDMA$_{23}$-*b*-P(VDM$_{10}$-*co*-NIPAM$_{46}$) and of PNIPAM$_{46}$-*b*-P(VDM$_6$-*co*-DMA$_{65}$) (*Figure 5*). Block copolymers SEC

traces shift to earlier retention times as the molecular weight of copolymers increases with respect to the PDMA-CTA and the PNIPAM-CTA. Moreover, polydispersities of the copolymers remain low (PDI $\leq$ 1.20) (*Table 1*). These results show that the copolymerizations are well-controlled and the block copolymers are well-defined.

a)

b)
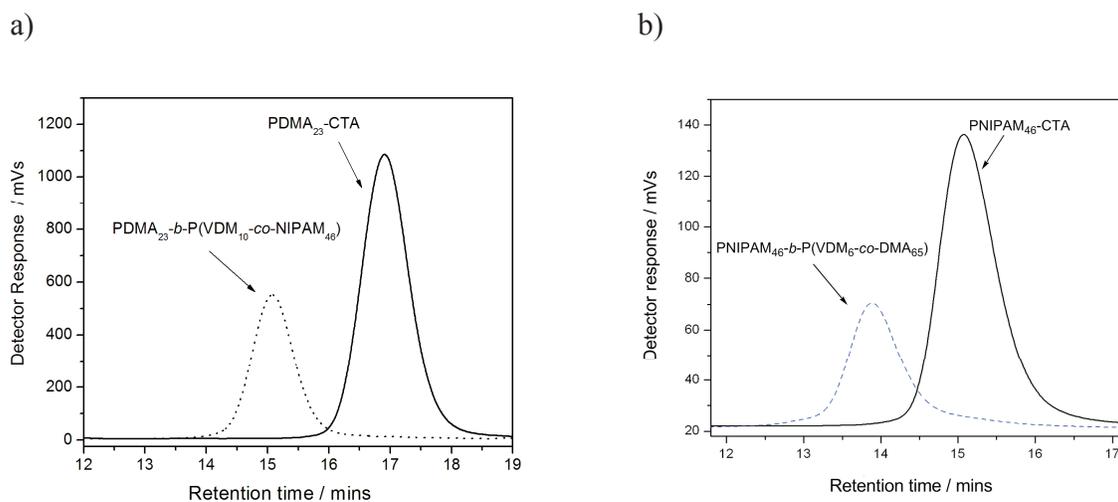
Figure 5: SEC traces of: a) PDMA$_{23}$-CTA and PDMA$_{23}$-b-P(VDM$_{10}$-co-NIPAM$_{46}$) block copolymer and of, b) PNIPAM$_{46}$-CTA and PNIPAM$_{46}$-b-P(VDM$_6$-co-DMA$_{65}$) block copolymer.

The FT-IR spectrum of the precipitated copolymer PDMA$_{23}$-*b*-P(VDM$_{10}$-*co*-NIPAM$_{46}$) (*Figure 6*) reveals the presence of a band at $\nu_{(C=O)} = 1815$ cm^{-1} which is characteristic of the azlactone ring. A similar FT-IR spectrum was obtained for PNIPAM$_{46}$-*b*-P(VDM$_6$-*co*-DMA$_{65}$) block copolymer. Therefore, the azlactone groups remain intact after the copolymerization and are available for further reactions with amines.
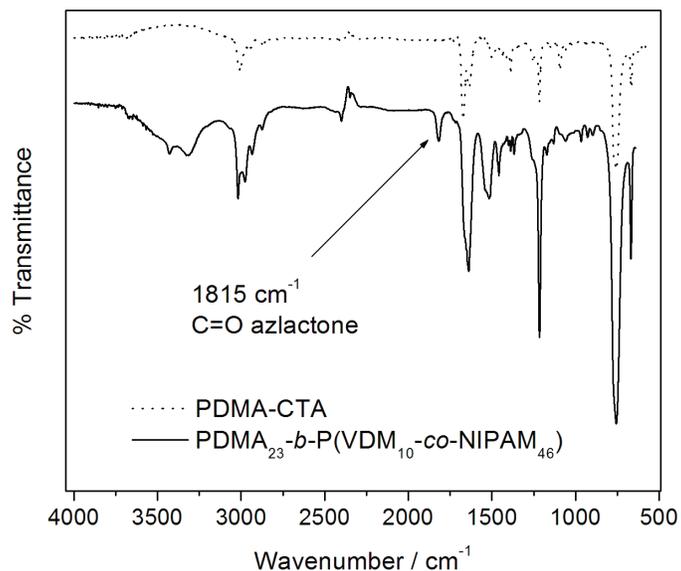
Figure 6: FT-IR spectrum for PDMA₂₃-b-P(VDM₁₀-co-NIPAM₄₆) block copolymer compared with the FT-IR spectrum of PDMA-CTA.

2.3. Thermoresponsive behaviour of the copolymers

The thermoresponsive behaviour of the copolymers was studied in aqueous solution. The lower critical solution temperature (LCST) was determined from cloud point measurements using UV-Vis spectrophotometry by measuring the transmittance through a solution of the copolymer at 500 nm and dynamic light scattering (DLS) at temperatures ranging from 20°C to 60°C (*Figure 7*). As the temperature increases, the copolymers self-assemble into core-shell particles of significantly greater particle size, resulting in a cloudy solution. LCST values for the block copolymers are shown in *Table 2*.

a)

b)
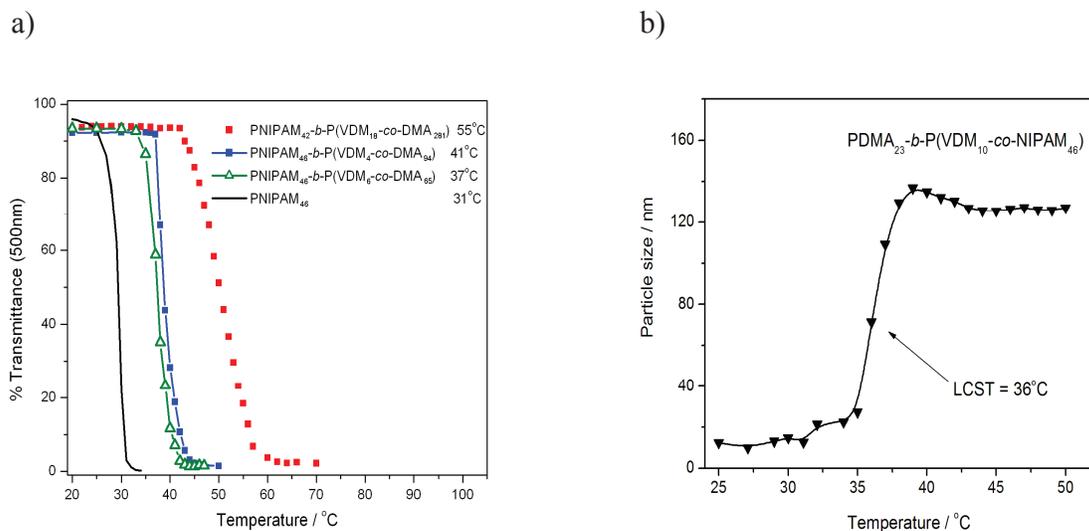
Figure 7: Measured LCST of block copolymers in aqueous solution: a) using UV-Vis spectrophotometry at 500 nm for PNIPAM-b-P(VDM-co-DMA) block copolymers, b) using DLS for PDMA-b-P(VDM-co-NIPAM) block copolymer.

Table 2: LCST values of PNIPAM-b-P(VDM-co-DMA) and PDMA-b-P(VDM-co-NIPAM) block copolymers.

Copolymer structure	$M_{n,SEC}{}^{a}$ (g.mol^{-1})	PDI^{a}	LCST^{c} (^{o}C)
PNIPAM$_{46}$-b-P(VDM$_6$-co-DMA$_{65}$)	33400	1.10	37^{b}
PNIPAM$_{46}$-b-P(VDM$_4$-co-DMA$_{94}$)	59200	1.17	41^{b}
PNIPAM$_{42}$-b-P(VDM$_{18}$-co-DMA$_{281}$)	64600	1.20	55^{b}
PDMA$_{23}$-b-P(VDM$_{10}$-co-NIPAM$_{46}$)	19500	1.04	36^{c}

^{a} Determined from SEC in DMF calibrated with linear polystyrene standards using PL Mixed-D columns, ^{b} Determined by UV-Vis spectrophotometry. ^{c} Determined by DLS.

For PNIPAM-b-P(VDM-co-DMA) block copolymers, the molar composition was found to affect the temperature at which nanoparticles are formed. The increase of the DP$_n$ of DMA with a constant DP$_n$ of NIPAM and a constant DP$_n$ of VDM increased the LCST of the copolymer (*Table 2*). This trend is in agreement with previous literature

data[22] which report that the addition of hydrophilic constituents to a copolymer raises the LCST. Indeed the hydrophilic constituents retain water (or remain hydrated) and limit the formation of hydrogen bonds between the amine groups of PNIPAM, thus preventing the coil-to-globule transition from occurring. Thus, the LCST can be tuned[22] and two block copolymers PNIPAM$_{46}$-*b*-P(VDM$_6$-*co*-DMA$_{65}$) and PDMA$_{23}$-*b*-P(VDM$_{10}$-*co*-NIPAM$_{46}$) have a LCST that occurs at physiological temperatures allowing their use for bioapplications.

2.4. Preparation, characterization and reactivity of azlactone-functionalized cross-linked nanoparticles

Either core-cross-linked or shell-cross-linked nanoparticles were prepared from PDMA$_{23}$-*b*-P(VDM$_{10}$-*co*-NIPAM$_{46}$) and PNIPAM$_{46}$-*b*-P(VDM$_6$-*co*-DMA$_{65}$) copolymers, respectively, using a diamine which reacts with the azlactone rings. Block copolymers were dissolved in deionized water and the temperature of solutions raised to above LCSTs to form nanoparticles. Finally, 2,2'-ethylenedioxybis(ethylamine) was added to react with the azlactone groups and cross-link the copolymer chains, forming covalently stabilized nanoparticles (*Scheme 3*). Analysis of cross-linked nanoparticles issued from PDMA$_{23}$-*b*-P(VDM$_{10}$-*co*-NIPAM$_{46}$) and from PNIPAM$_{46}$-*b*-P(VDM$_6$-*co*-DMA$_{65}$) by SEC shows a significant shift in retention time to high molecular weight and the absence of a peak corresponding to the initial copolymer indicating that an efficient cross-linking of the copolymers into core-shell particles has occurred (*Figure 8*).
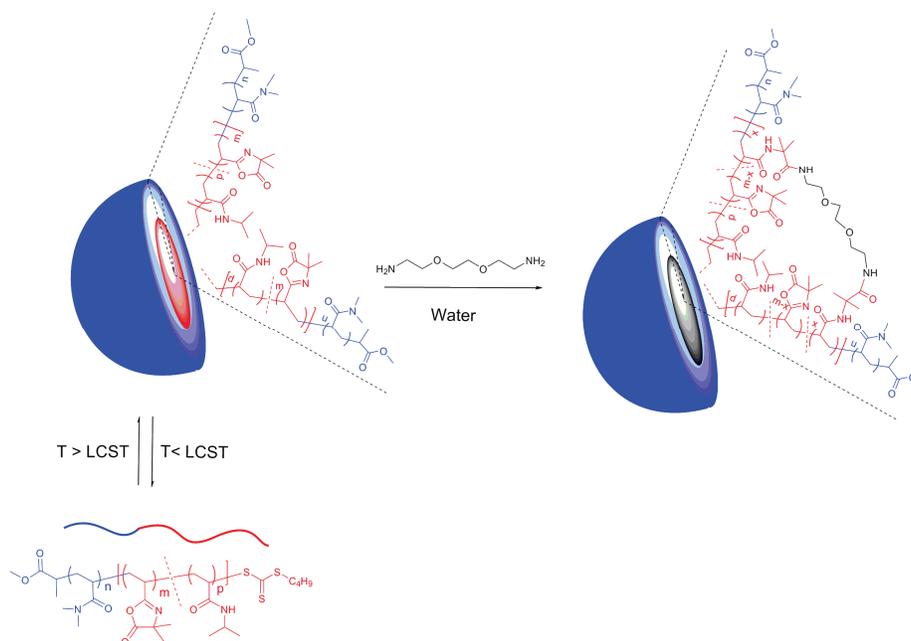
Scheme 3: Formation of core-cross-linked nanoparticles issued from the self-assembly of PDMA$_{23}$-b-P(VDM$_{10}$-co-NIPAM$_{46}$) block copolymers above their LCST and successive reaction of the azlactone groups with 2,2'-ethylenedioxybis(ethylamine).
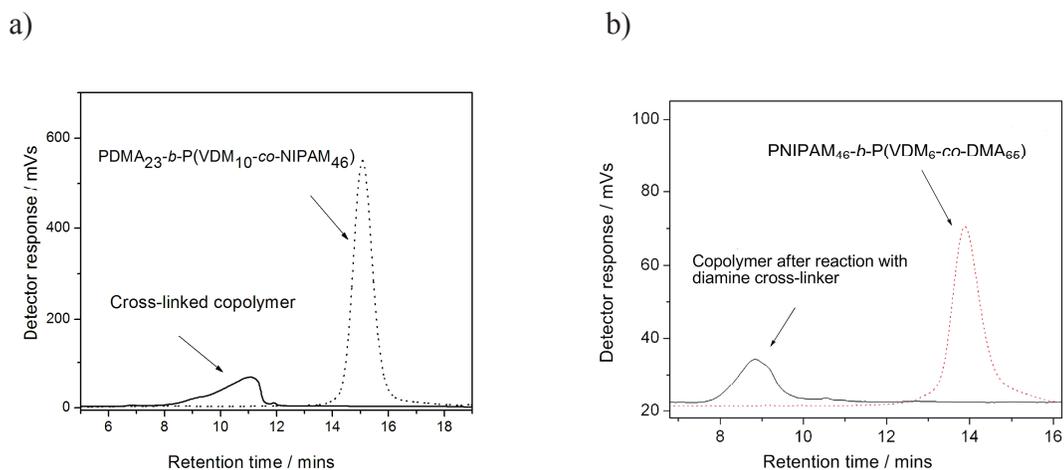
Figure 8: SEC traces of: a) the PDMA$_{23}$-b-P(VDM$_{10}$-co-NIPAM$_{46}$) block copolymer prior to cross-linking and after cross-linking using 2,2'-ethylenedioxybis(ethylamine) and, b) the PNIPAM$_{46}$-b-P(VDM$_6$-co-DMA$_{65}$) block copolymer prior to cross-linking and after cross-linking using 2,2'-ethylenedioxybis(ethylamine).

This strategy to cross-link core-shell nanoparticles is of particular interest in comparison with previous reported ones[23–28] as it is efficient, does not generate small molecules by-products and does not need addition of catalyst or co-reagents. The comparison of FT-IR spectra of the isolated cross-linked nanoparticles obtained from $PNIPAM_{46}$-b-$P(VDM_6$-co-$DMA_{65})$ and $PDMA_{23}$-b-$P(VDM_{10}$-co-$NIPAM_{46})$ block copolymers is shown in *Figure 9*. It appears that when the azlactone rings are located in the shell of nanoparticles obtained from $PNIPAM_{46}$-b-$P(VDM_6$-co-$DMA_{65})$, the disappearance of the band at 1815 cm^{-1} corresponding to the C=O ester of the azlactone ring is observed. In contrast, when azlactone rings are located in the core of nanoparticles issued from $PDMA_{23}$-b-$P(VDM_{10}$-co-$NIPAM_{46})$, this band is still present indicating that azlactone rings have been preserved. In this case, the hydrophobic core, in which azlactone groups are embedded, is therefore efficiently repelling any water penetration.
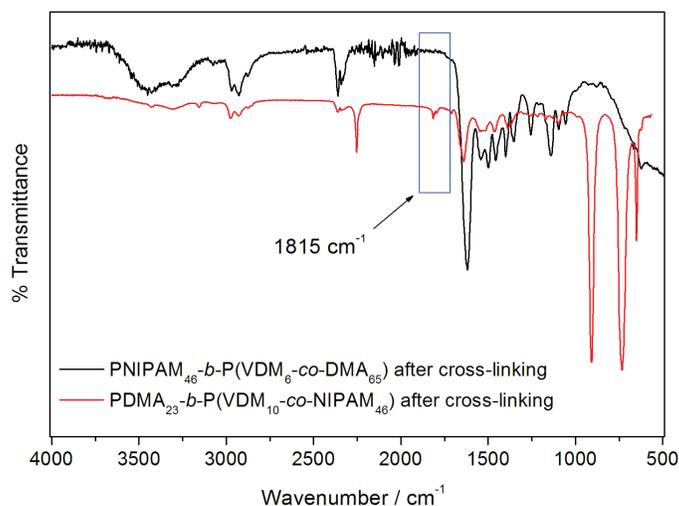
Figure 9: Comparison of FT-IR spectra of the cross-linked nanoparticles issued from PNIPAM₄₆-b-P(VDM₆-co-DMA₆₅) and PDMA₂₃-b-P(VDM₁₀-co-NIPAM₄₆) block copolymers.

This result is important as such original nanoparticles could be employed for further reaction with the amine groups of biomolecules. As the nanoparticles prepared from PDMA$_{23}$-b-P(VDM$_{10}$-co-NIPAM$_{46}$) are of particular interest, further DLS measurements were performed to characterize their size before and after cross-linking. At 25°C, the PDMA$_{23}$-b-P(VDM$_{10}$-co-NIPAM$_{46}$) block copolymer dissolved in water exhibits an average hydrodynamic diameter of 4 nm characteristic of unimers (*Figure 10*). When the LCST is reached, this copolymer shows self-assembly behaviour to form nanoparticles with an average hydrodynamic diameter of 43 nm.

Above the LCST, the resulting nanoparticles have been covalently stabilized using 2,2'-ethylenedioxybis(ethylamine) and the DLS analysis of the resulting core-cross-linked particles at 25°C reveals an average hydrodynamic diameter of 29 nm (*Figure 10*). This result shows that the nanoparticle structure is conserved after lowering the solution temperature below the LCST.
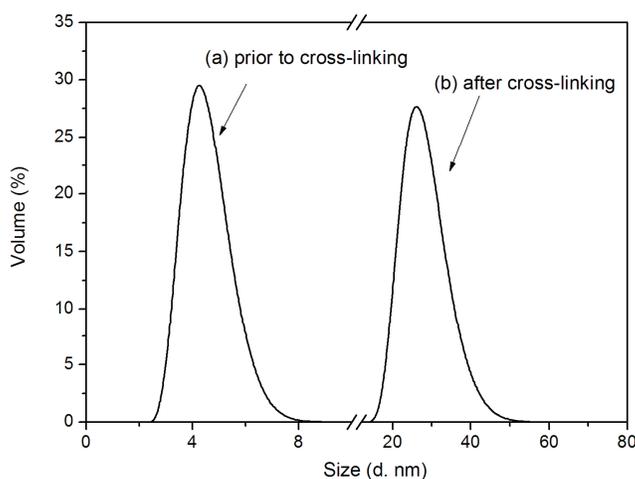
Figure 10: Particle sizes from dynamic light scattering of PDMA$_{23}$-b-P(VDM$_{10}$-co-NIPAM$_{46}$) copolymers in water at 25°C: (a) prior to cross-linking and, (b) after cross-linking of self-assembled structures with 2,2'-ethylenedioxybis(ethylamine).

A preliminary study on the reactivity of azlactone-functionalized stable nanoparticles was performed using dansylhydrazine (*Scheme 4*). This molecule has been selected as it is an easily detectable nucleophile by UV-Vis spectrophotometry. The reaction between the core-cross-linked nanoparticles and the dansylhydrazine was performed in DMF at 40°C for 3 days.
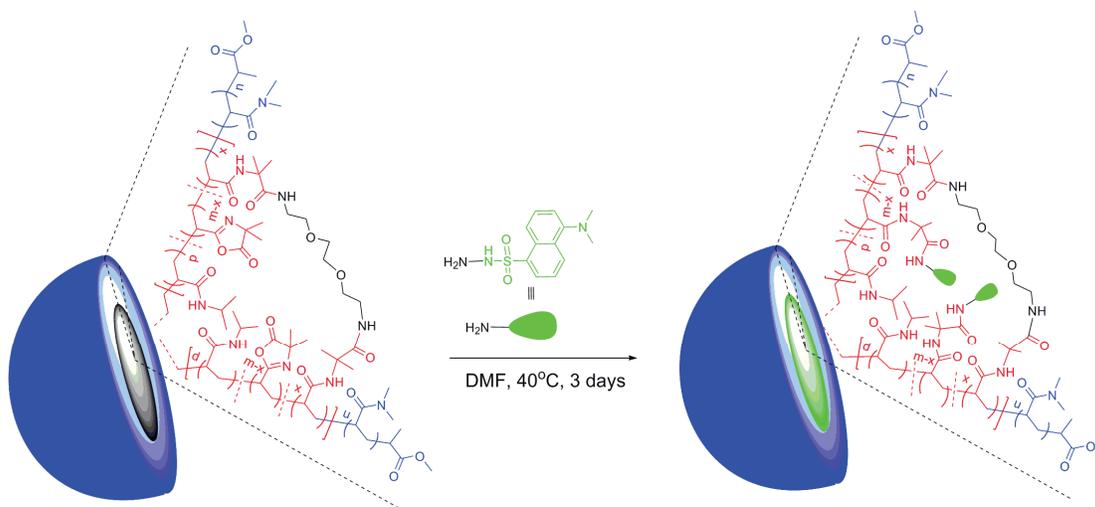
Scheme 4: Reactivity of azlactone-functionalized stable nanoparticles towards dansylhydrazine.

After reaction, nanoparticles were analyzed by SEC using UV detection. By comparing the UV spectra extracted from SEC traces at the maximum elution volume of the core-cross-linked nanoparticles prepared from PDMA$_{23}$-*b*-P(VDM$_{10}$-*co*-NIPAM$_{46}$) before and after reaction with dansylhydrazine, we observed a shift of the maximum wavelengths from 308.9 nm to 319.6 nm. The maximum wavelength at 308.9 nm is characteristic of trithiocarbonyl moieties at the copolymer chain-end and the shift to 319.6 nm indicates that dansylhydrazine has reacted with the core-cross-linked nanoparticles *via* the azlactone groups (*Figure 11*).
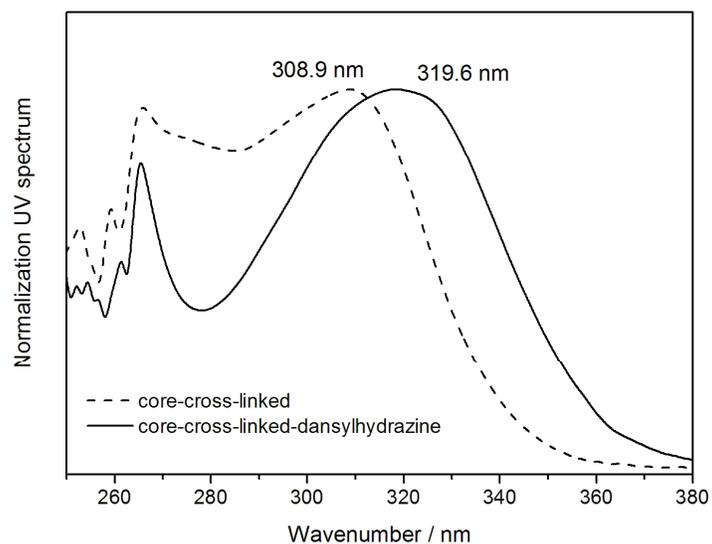
Figure 11: Overlay of UV spectra extracted from SEC traces of the maximum elution volume of core-cross-linked nanoparticles before and after reaction with dansylhydrazine.

3. Conclusion

A series of well-defined copolymers of PDMA-b-P(VDM-co-NIPAM) and PNIPAM-b-P(VDM-co-DMA) have been synthesized using RAFT polymerization. The copolymers are thermoresponsive and the molar composition within the copolymer affects the LCST, above which the structures self-assemble to form nanoparticles. The LCST was tuned to occur at physiological temperatures with the the PDMA$_{23}$-b-P(VDM$_{10}$-co-NIPAM$_{46}$) copolymer and PNIPAM$_{46}$-b-P(VDM$_6$-co-DMA$_{65}$) copolymer. The azlactone was used to form stable core-shell particles by cross-linking either the core or the shell using a diamine in aqueous solution at 40°C. Analysis by SEC suggested that cross-linking was efficient, with all unimers being incorporated into core-shell particles. FT-IR analyses of these stable core-shell particles revealed that some azlactone rings are still present when nanoparticles are formed from PDMA$_{23}$-b-P(VDM$_{10}$-co-NIPAM$_{46}$) copolymer. DLS analysis of the resulting core-cross-linked particles at 25°C reveals an average hydrodynamic diameter of 29 nm. This result shows that the nanoparticle structure is conserved after lowering the solution temperature below the LCST. Moreover, the azlactone functionality is available to anchor dansylhydrazine. The interest of such azlactone-functionalized core-cross-linked particles is that they are stable at different concentrations and temperature, and that they can further react with biomolecules such as proteins.

4. Experimental Section

4.1. Materials

N-Isopropyl acrylamide (NIPAM) was obtained from Aldrich (97%) and was recrystallized from petroleum ether prior to use. Dansylhydrazine (Fluka, 97%), 2,2'-ethylenedioxybis(ethylamine) (98%, Aldrich,), diethyl ether (technical grade, Aldrich), petroleum ether (Analytic reagent grade, bp = 40-60°C, Fischer Scientific) and 4,4'azobis(4-cyanovaleric acid) (ACVA, 98%, Aldrich) were used as received. 2,2'-azobisisobutyronitrile (AIBN, 98%) was obtained from Aldrich and recrystallized from methanol prior to use. *N,N*-Dimethyl acrylamide (DMA, 98%), *N,N*-dimethylformamide (DMF, 99.8%) and 1,4-dioxane (99.8%) were obtained from Aldrich and distilled prior to use. Pure water used for dynamic light scattering measurements was obtained from a Millipore Direct Q system and had a conductivity of 18.2 MΩ.cm at 25°C. The RAFT agent methyl-2-(*n*-butyltrithiocarbonyl) propanoate[6] (MBTTCP) and 2-vinyl-4,4-dimethylazlactone (VDM)[33] were synthesized following reported procedures.

4.2. Instrumentation

Nuclear Magnetic Resonance (NMR)

NMR spectra were recorded on a Bruker AC-400 Spectrometer for ^{1}H NMR (400 MHz) and ^{13}C (100 MHz). Chemical shifts are reported in ppm relative to deuterated solvent resonances.

Size exclusion chromatography (SEC)

PDMA and block copolymers were characterized on a SEC system operating in DMF eluent at 60°C fitted with a Polymer Laboratories guard column (PL Gel 5µm) and two Polymer Laboratories PL Mixed D columns, a Waters 410 differential refractometer (RI) and a Waters 481 UV photodiode array (PDA) detector. The instrument operated at a flow rate of 1.0 mL min^{-1} and was calibrated with narrow linear polystyrene (PS) standards ranging in molecular weight from 580 g.mol^{-1} to 460.000 g.mol^{-1}. Molecular weights and polydispersity indices (PDI) were calculated using Waters EMPOWER software.

PNIPAM homopolymers were characterized on a SEC system operating in DMF eluent at 60°C fitted with a Polymer Laboratories guard column (PL Gel 5 µm) and two Polymer Laboratories PolarGel columns, a Waters 410 differential refractometer (RI) and a Waters 481 UV photodiode array (PDA) detector. The instrument operated at a flow rate of 1.0 mL min^{-1} and was calibrated with narrow linear polystyrene (PS) standards ranging in molecular weight from 580 g.mol^{-1} to 460.000 g.mol^{-1}. Molecular weights and polydispersity indices (PDI) were calculated using Waters EMPOWER software.

Dynamic light scattering (DLS)

DLS measurements were made in order to determine the hydrodynamic diameter (D$_h$) and particle size distribution of copolymers and of resulting core-shell particles over temperatures ranging from 20°C to 60°C. A Malvern Instruments Nanosizer fitted with a 4 mW He-Ne laser operating at 633 nm with dual angle detection (13°, 173°) was used for all measurements and the data were processed using the CONTIN method of analysis. Temperature trend measurements were recorded starting from 20°C and at increasing

temperature increments of 2^oC until 60^oC with an equilibration time of two minutes. Individual measurements were made at 25^oC, 50^oC and 60^oC after an equilibration time of two minutes. In a typical sample preparation for dynamic light scattering, a quantity of copolymer ($1.9x10^{-3}$ g) was measured into a clean glass vial and Millipore deionised water (9 mL) was added. The copolymer was left to dissolve for 2 hours stirring at room temperature, after which the solution was filtered using a glass syringe and a series of syringe filters of decreasing pore size (AT Chromato, 0.45 μm, Whatman Inorganic 0.2 μm and 0.1 μm respectively) into a fresh and clean glass cuvette for analysis.

UV-Vis spectrophotometry characterization

UV-Vis measurements were performed on a Varian Cary 100 Scan spectrophotometer fitted with a dual cell Peltier accessory for heating. Samples of copolymers in deionized water of concentration 10 $g.L^{-1}$ were prepared and left to dissolve over a period of two hours at room temperature. The sample was introduced into a quartz cuvette and placed in the Peltier accessory. The temperature was adjusted manually and the sample allowed to equilibrate for five minutes before two measurements of the transmittance at 500 nm were made.

Fourier Transformed Infra-Red (FT-IR) spectroscopy

Infra-red spectra of copolymers were recorded using a ThermoElectron Corp. spectrometer operating with an attenuated total reflection (ATR solid) gate. Spectra were analyzed with OMNIC software.

4.3. Synthesis of poly(*N,N*-dimethyl acrylamide) (PDMA) and poly(*N-* isopropyl acrylamide) (PNIPAM) by RAFT polymerization

4.3.1. Synthesis of PDMA-CTA

A magnetic stirrer was charged to a Schlenk tube along with DMA (4.02 g, 4.1×10^{-2} mol), MBTTCP (0.402 g, 1.6×10^{-3} mol), AIBN (2.52×10^{-2} g, 1.54×10^{-4} mol), DMF (0.1 mL) used as internal standard and dioxane (8 mL) in the ratio of $[DMA]_0/[MBTTCP]_0/[AIBN]_0 = 26/1/0.1$. The polymerization mixture was deoxygenated by freeze-pump-thawing. When no more bubbles were observed in the reaction mixture, the reaction vessel was switched to a nitrogen atmosphere and placed in a thermostatted oil bath at $70^{\circ}C$ to initiate the polymerization. The immersion in the oil bath defines t = 0 and a sample was removed using a deoxygenated syringe as a reference point. The polymerization was stopped after 90 minutes and the reaction mixture was subjected to ^1H NMR spectroscopy to determine monomer conversion and SEC analysis to determine the molecular weight and the polydispersity index. The monomer conversion was determined to be 85%. Dioxane and DMF were removed using a rotary evaporator and the polymer was purified by a series of precipitations in cold petroleum ether, filtered and dried in a vacuum oven at $25^{\circ}C$. $M_{n,SEC} = 5300$ g.mol^{-1}, PDI = 1.05. $DP_{n,NMR} = 23$. ^1H NMR (400 MHz, CDCl$_3$), δ (ppm): 0.95 (-S-C(S)S-(CH$_2$)$_3$-**CH$_3$**), 1.14 (–S-C(S)S-CH$_2$-(**CH$_2$**)$_2$-CH$_3$), 1.24-2.66 ((**CH$_2$-CH-**)$_n$ and CH$_3$OC(O)-**CH(CH$_3$)**), 2.91 (-N(**CH$_3$**)$_2$), 3.35 (-S-C(S)S-**CH$_2$**-C$_3$H$_7$), 3.66 (**CH$_3$**-OCO).

4.3.2. Synthesis of PNIPAM-CTA

A magnetic stirrer was charged to a Schlenk tube along with NIPAM (11.22 g, 9.93×10^{-2} mole), MBTTCP (0.34 g, 1.35×10^{-3} mole), AIBN (0.0224 g, 1.36×10^{-4} mole) and DMF (22 mL) in the ratio of $[NIPAM]_0/[MBTTCP]_0/[AIBN]_0 = 74/1/0.1$. The polymerization mixture was deoxygenated by freeze-pump-thawing. When no more bubbles were observed in the reaction mixture, the reaction vessel was switched to a nitrogen atmosphere and placed in a thermostatted oil bath at $70^{\circ}C$ to initiate the polymerization. The immersion in the oil bath defines $t = 0$ and a sample was removed using a deoxygenated syringe as a reference point. The reaction was stopped after 140 minutes and monomer conversion was determined to be 62% by ^1H NMR spectroscopy. DMF was removed using a rotary evaporator and the polymer purified by a series of precipitations in cold petroleum ether, filtered and dried in a vacuum oven at $25^{\circ}C$. $M_{n,SEC} = 5600$ g.mol^{-1}, PDI = 1.12. $DP_{n,NMR} = 46$. ^1H NMR (400 MHz, CDCl$_3$), δ (ppm): 0.95 (-S-C(S)S-(CH$_2$)$_3$-CH$_3$), 1.14 (-NH-CH(CH$_3$)$_2$ and –S-C(S)S-CH$_2$-(CH$_2$)$_2$-CH$_3$), 1.40-2.73 (-CH$_2$-CH-)$_n$, 3.35 (-S-C(S)S-CH$_2$–C$_3$H$_7$), 3.66 (CH$_3$-OCO), 4.00 (-NH-CH(CH$_3$)$_2$), 6.24 (-NH-CH(CH$_3$)$_2$).

4.4. Synthesis of PDMA-*b*-P(VDM-*co*-NIPAM) copolymers and of PNIPAM-*b*-P(VDM-*co*-DMA) copolymers by RAFT polymerization

4.4.1. RAFT copolymerization of NIPAM and VDM mediated by PDMA-CTA agent

A magnetic stir bar was charged to a Schlenk tube along with the PDMA-CTA (0.3 g, 1.19×10^{-4} mol), VDM (0.163 g, 1.17×10^{-3} mol), NIPAM (1.07 g, 9.47×10^{-3} mol), ACVA (6.0×10^{-3} g, 2.14×10^{-5} mol), DMF used as internal standard (0.1 mL) and dioxane (3.5 mL). The mixture was deoxygenated by a series of freeze-pump-thaw cycles. When

no further oxygen was produced, the reactor vessel was switched to an inert argon atmosphere and the Schlenk tube placed in a thermostatted oil bath at 70°C. The immersion of the Schlenk tube within the oil bath defines t = 0. The polymerization was stopped after 100 minutes by removing the Schlenk tube from the oil bath and opening the mixture to air. The VDM conversion and the NIPAM conversion were determined to be 100% and 58% respectively. Dioxane and DMF were removed using a rotary evaporator and the synthesized copolymer was dissolved in acetone and precipitated into cold diethyl ether, filtered and dried in a vacuum oven at 25°C. The copolymer was characterized by ^{1}H NMR spectroscopy, FT-IR spectroscopy and SEC analysis. $M_{n,SEC}$ = 19500 g.mol^{-1}, PDI = 1.04. FT-IR: $\nu_{(C=O\,;\,azlactone)}$ = 1815 cm^{-1}, $\nu_{(C=N\,;\,azlactone)}$ = 1628 cm^{-1}, $\nu_{(C=O\,;\,amide)}$ = 1616 cm^{-1}. ^{1}H NMR (400 MHz, CDCl$_3$), δ (ppm): 0.95 (-S-C(S)S-(CH$_2$)$_3$-CH$_3$), 1.14 (-NH-CH(CH$_3$)$_2$ and -S-C(=S)S-CH$_2$-(CH$_2$)$_2$-CH$_3$), 1.40 (-OCO-C(CH$_3$)$_2$-N-)$_{azlactone}$, 1.40-2.73 (-CH$_2$-CH-)$_n$ 2.93 (-N(CH$_3$)$_2$), 3.35 (-S-C(S)S-CH$_2$-C$_3$H$_7$), 3.66 (CH$_3$-OCO), 4.00 (-NH-CH(CH$_3$)$_2$), 6.24 (-NH-CH(CH$_3$)$_2$).

4.4.2. RAFT copolymerization of DMA and VDM mediated by PNIPAM-CTA agent

A magnetic stir bar was charged to a Schlenk tube along with the PNIPAM-CTA (5.03x10^{-1} g, 8.9x10^{-5} mol), DMA (1.173 g, 1.18x10^{-2} mol), VDM (9.28x10^{-2} g, 6.67x10^{-4} mol), AIBN (4.2x10^{-3} g, 2.56x10^{-5} mol) and dioxane (3 mL). The mixture was deoxygenated by a series of freeze–pump–thaw cycles. When no further oxygen was produced, the reactor vessel was switched to an inert argon atmosphere and the Schlenk tube placed in a thermostatted oil bath at 70°C. The immersion of the Schlenk tube within the oil bath defines t = 0. The polymerization was stopped after 50 minutes by removing the Schlenk tube from the oil bath and opening the mixture to air. The synthesized

copolymer was dissolved in acetone and precipitated into cold diethyl ether, filtered and dried in a vacuum oven at 25°C. The copolymer was characterized by SEC, ^{1}H NMR spectroscopy and FT-IR spectroscopy. $M_{n,SEC}$ = 33400 g.mol^{-1}, PDI = 1.10. FTIR: $\nu_{(C=O; zlactone)}$ = 1815 cm^{-1}, $\nu_{(C=O; amide)}$ = 1616 cm^{-1}. ^{1}H NMR (400 MHz, CDCl$_3$), δ (ppm): 0.95 (-S-C(S)S-(CH$_2$)$_3$-**CH$_3$**), 1.14 (-NH-CH(**CH$_3$**)$_2$ and −S-C(S)S-CH$_2$-(**CH$_2$**)$_2$-CH$_3$), 1.40 (-OCO-C(**CH$_3$**)$_2$-N)$_{azlactone}$, 1.40-2.73 (-**CH$_2$-CH**-)$_n$, 2.91 (-N(**CH$_3$**)$_2$), 3.35 (-S-C(S)S-**CH$_2$**-C$_3$H$_7$), 3.66 (**CH$_3$**-OCO), 4.00 (-NH-C**H**(CH$_3$)$_2$), 6.24 (-N**H**-CH(CH$_3$)$_2$).

4.5. A typical preparation of cross-linked core-shell nanoparticles and their reactivity towards dansylhydrazine

A measured quantity of PDMA$_{23}$-*b*-P(VDM$_{10}$-*co*-NIPAM$_{46}$) copolymer (23 mg, 2.52x10^{-6} mol) was placed in a round bottom flask and dissolved in deionized water (20 mL) by magnetically stirring at ambient temperature over a period of two hours. When this time had elapsed the flask containing the solution of copolymer was placed in a thermostatted oil bath preheated to 40°C in order to form the self-assembled structures. When the reaction mixture had reached this temperature, 2,2'-ethylenedioxybis(ethylamine) (2 µL, 1.36x10^{-5} mol) was added and the mixture was stirred for a further 5 h at 40°C. After this time had elapsed, the flask was removed from the oil bath, cooled at room temperature and water removed *via* lyophilisation. The cross-linked core-shell particles were characterized by SEC and DLS. The cross-linked core-shell particles obtained from copolymer PDMA$_{23}$-*b*-P(VDM$_{10}$-*co*-NIPAM$_{46}$) (20 mg) were placed in a round bottom flask in DMF (2 mL). Then, 2 mg of dansylhydrazine were added and the mixture was stirred for 3 days at 40°C. The resulting solution was analyzed by SEC.

References

[1] Fournier, D.; Pascual, S.; Fontaine, L. *Macromolecules* **2004**, *37*, 330-335.

[2] Savariar, E. N.; Thayumanavan, S. *J. Polym. Sci., Part A: Polym. Chem*. **2004**, *42*, 6340-6345.

[3] Li, Y.; Lokitz, B. S.; McCormick, C. L. *Macromolecules* **2006**, *39*, 81-89.

[4] Li, Y.; Lokitz, B. S.; Armes, S. P.; McCormick, C. L. *Macromolecules*, **2006**, 39, 2726-2728.

[5] Zhang, J.; Jiang, X.; Zhang, Y.; Li, Y.; Liu, S. *Macromolecules* **2007**, *40*, 9125-9132.

[6] Pascual, S.; Monteiro, M. J. *Eur. Polym. J.* **2009**, *45*, 2513-2519.

[7] Zhou, D.; Hu, L.; Wang, W.; Zhao, X. *React. Funct. Polym*. **2012**, *72*, 402-406.

[8] Ebnerhardt, M.; Theato, P. *Macromol. Rapid Commun*. **2005**, *26*, 1488-1493.

[9] Heilmann, S. M.; Rasmussen, J. K.; Krepski, L. R. *J. Polym. Sci., Part A: Polym. Chem*. **2001**, *39*, 3655-3677.

[10] Guyomard, A.; Fournier, D.; Pascual, S.; Fontaine, L.; Bardeau, J.-F. *Eur. Polym. J.* **2004**, *40*, 2343-2348.

[11] Fournier, D.; Pascual, S.; Montembault, V.; Haddleton, D. M.; Fontaine, L. *J. Comb. Chem.* **2006**, *8*, 522-530.

[12] Lucchesi, C.; Pascual, S.; Dujardin, G.; Fontaine, L. *React. Funct. Polym.* **2008**, *68*, 97-102.

[13] Drtina, G. J.; Heilmann, S. M.; Moren, D. M.; J. K.; Rasmussen, Krespski, L. R.; Smith, H. K.; Pranis, R. A.; Turek, T. C. *Macromolecules* **1996**, *29*, 4486-4489.

[14] Tripp, J. A.; Stein, J. A.; Svec, F.; Fréchet, J. M. J. *Org. Lett.* **2000**, *2*, 195-198.

[15] Tripp, J. A.; Svec, F.; Fréchet, J. M. J. *J. Comb. Chem.* **2001**, *3*, 216-223.

[16] Fontaine, L.; Lemêle, T.; Brosse, J.-C.; Sennyey, G.; Senet, J.-P.; D. Wattiez, *Macromol. Chem. Phys.* **2002**, *203*, 1377-1384.

[17] Drtina, G. J.; Haddad, L. C.; Rasmussen, J. K.; Gaddam, B. N.; Williams, M. G.; Moeller, S. J.; Fitzsimons, R. T.; Fansler, D. D.; Buhl, T. L.; Yang, Y. N.; Weller, V. A.; Lee, J. M.; Beauchamp, T. J.; Heilmann, S. M. *React. Funct. Polym.* **2005**, *64*, 13-24.

[18] Cullen, S. P.; Mandel, I. C.; Gopalan, P. *Langmuir* **2008**, *24*, 13701-13709.

[19] Barringer, J. E.; Messman, J. M.; Banaszek, A. L.; Meyer III, H. M.; Kilbey II, S. M. *Langmuir* **2009**, *25*, 262-268.

[20] Messman, J. M.; Lokitz, B. S.; Pickel, J. M.; Kilbey II, S. M. *Macromolecules* **2009**, *42*, 3933-3941.

[21] Buck, M. E.; Breitbach, A. S.; Belgrade, S. K.; Blackwell, H. E.; Lynn, D. M. *Biomacromolecules* **2009**, *10*, 1564-1574.

[22] Schild, H. G. *Prog. Polym. Sci*. **1992**, *17*, 163-249.

[23] Rodriguez-Hernandez, J.; Chicot, F.; Gnanou, Y.; Lecommandoux, S. *Prog. Polym. Sci*. **2005**, *30*, 691-724.

[24] O'Reilly, R. K.; Joralemon, M. J.; Wooley, K. L.; Hawker, C. J. *Chem. Mater*. **2005**, *17*, 5976-5988.

[25] O'Reilly, R. K.; Hawker, C. J.; Wooley, K. L. *Chem. Soc. Rev*. **2006**, *35*, 1068-1083.

[26] Read E. S.; Armes, S. P. *Chem. Commun*. **2007**, 3021-3035.

[27] O'Reilly, R. K.; Joralemon, M. J.; Hawker, C. J.; Wooley, K. L. *New J. Chem*. **2007**, *31*, 718–724.

[28] Fu, R.; Fu, G.-D. *Polym. Chem*. **2011**, *2*, 465-475.

[29] Ho, T. H.; Levere, M. E.; Soutif, J.-C.; Montembault, V.; Pascual, S.; Fontaine, L. *Polym. Chem.* **2011**, *2*, 1258-1260.

[30] Lokitz, B. S.; Messman, J. M.; Hinestrosa, J. P.; Alonzo, J.; Verduzco, R.; Brown, R. H.; Osa, M.; Ankner, J. F.; Kilbey II, S. M. *Macromolecules* **2009**, *42*, 9018-9026.

[31] Pascual, S.; Blin, T.; Saikia, P. J.; Thomas, M.; Gosselin, P.; Fontaine, L. *J. Polym. Sci., Part A: Polym.* Chem. **2010**, *48*, 5053-5062.

[32] Schilli, C. M.; Müller, A. H. E.; Rizzardo, E.; Thang, S. H.; Chong, Y. K. Advances in Controlled/Living Radical Polymerization, in ACS Symposium Series 854, American Chemical Society, Washington, DC, **2003**, chapter 41, pp. 603-618.

[33] Levere, M. E.; Ho, H. T.; Pascual, S.; Fontaine, L. *Polym. Chem*. **2011**, *2*, 2878-288.

Chapter V

Synthesis of azlactone-functionalized thermoresponsive copolymers based on poly(ethylene oxide) and poly(*N*-isopropyl acrylamide) by RAFT polymerization

Chapter V: Synthesis of azlactone-functionalized thermoresponsive copolymers based on poly(ethylene oxide) and poly(*N*-isopropyl acrylamide) by RAFT polymerization

1. Introduction

Covalent attachment of biomolecules onto synthetic polymers is widely used to modify properties and to enhance potential utility of native biomolecules such as proteins.[1] The crucial function of the polymer is to reduce immunogenicity and to improve the solubility and stability of proteins by reducing rates of renal excretion and digestion by the proteolytic system. Pioneering works of Langer *et al*.[2] and Abuchowski *et al*.[3] have shown that protein-poly(ethylene oxide) (PEO) conjugates (PEGylation) are able to enhance circulation lifetime and to reduce immunogenicity relative to native proteins. A typical strategy to target protein conjugates is the reaction of reactive functionalized polymers with amine groups of lysine residues due to their relative abundance of this aminoacid in proteins. As shown in chapter I, CRP methods give access to amine reactive polymers with predetermined molecular weights and low molecular weight distributions that are suitable for bioconjugation.[4,5] Therefore, protein reactive functional groups such as *N*-hydroxysuccinimidyl ester (NHS-ester)[6], pentafluorophenyl ester (PFP-ester)[7], aldehyde[8], and thiazolidine-2-thione[9] have been incorporated in polymers synthesized by CRP techniques. Among the amine reactive functional groups available, the azlactone ring can play a prominent role in the area of protein bioconjugates. Our previous work reported in chapters II, III, IV and a recent review[10] on azlactone-functionalized polymers have

highlighted the various advantages of such a functionality. For instance, the reaction between an amine and the azlactone ring do not lead to by-products, which is essential for bioapplications. Moreover, RAFT polymers containing a trithiocarbonate group are potential candidates for bioapplications as their *in vitro* cytotoxicity is low.[11,12] Therefore, in this chapter, we describe new polymer bioconjugates based on PEO and poly(*N*-isopropyl acrylamide) (PNIPAM) with lysozyme exploiting the azlactone functionality. The azlactone functionality is either introduced at the ω-position of macromolecular chain by a combination of RAFT polymerization and "thiol-ene" Michael addition (strategy described in chapter III) or either at the side chains by RAFT copolymerization (strategy presented in chapter IV). PEO is used as a hydrophilic part as it is biocompatible.[13] PNIPAM has a lower critical solution temperature (LCST = 32°C)[14] which can be tuned in order to get a LCST closed to human body temperature. Hence, PNIPAM-protein bioconjugates have been extensively studied and used in biomedical applications.[15,16] Furthermore, to prevent the intermolecular aggregation of PNIPAM segment keeping the associated control of protein's activity, PEO-*b*-PNIPAM block copolymers have been suggested.[17] To the best of our knowledge, only one study has been reported on the PEO-*b*-PNIPAM bioconjugates.[18] Boyer *et al.* have performed the RAFT polymerization of *N*-isopropyl acrylamide (NIPAM) using a trithiocarbonate-functionalized bovine serum albumin-PEO (BSA-PEO) as macromolecular chain transfer agent in the presence of a water soluble thermoinitiator in phosphate buffer (pH = 6) at 25°C to prepare a PEO-*b*-PNIPAM-BSA bioconjugates. In this chapter, we describe the synthesis of new thermoresponsive azlactone-functionalized block copolymers based on PEO and PNIPAM and their direct bioconjugation to lysozyme.

2. Results and discussion

Thermoresponsive copolymers based on poly(ethylene oxide) (PEO) and poly(*N*-isopropyl acrylamide) (PNIPAM) containing azlactone groups within the backbone and in the ω-position of the macromolecular chain were synthesized by statistical RAFT copolymerization and by using a combination of RAFT polymerization and "thiol-ene" Michael addition, respectively (*Scheme 1*). In the first strategy, a PEO macromolecular chain transfer agent (PEO-CTA) was synthesized and used to mediate the copolymerization of NIPAM/VDM to afford PEO-*b*-P(VDM-*co*-NIPAM) copolymers with azlactone groups within the backbone. In the second strategy, the PEO-CTA was used to mediate the RAFT polymerization of NIPAM to afford PEO-*b*-PNIPAM diblock copolymers. The aminolysis of the resulting PEO-*b*-PNIPAM copolymers and subsequent "thiol-ene" Michael addition with VDM lead to azlactone-terminated PEO-*b*-PNIPAM diblock copolymers (PEO-*b*-PNIPAM-Azl).
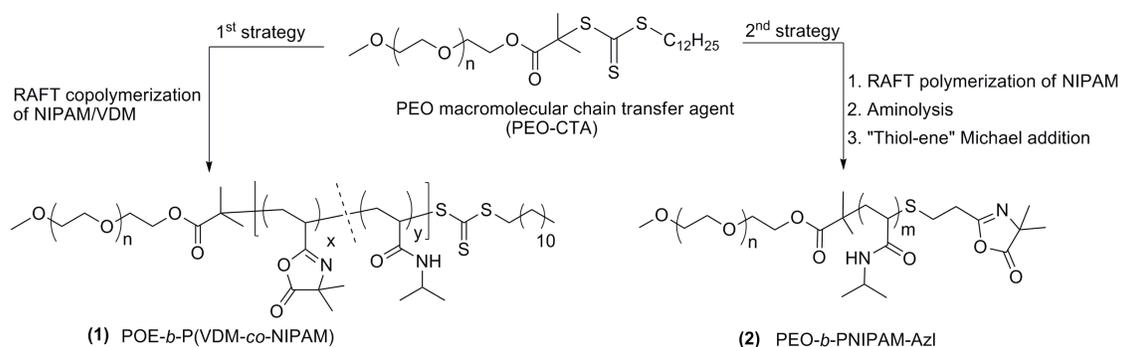
Scheme 1: General strategies for the synthesis of azlactone-functionalized thermoresponsive block copolymers based on PEO, PNIPAM and (P)VDM.

2.1. Synthesis and characterization of the poly(ethylene oxide) macromolecular chain transfer agent (PEO-CTA)

2-dodecylsulfanylthiocarbonylsulfanyl-2-methylpropionic acid (DMP) was first reacted with oxalyl chloride to afford the acid chloride derivative which then reacts with ω-hydroxyl PEO (DP_n = 44) in dichloromethane (DCM) at 25°C (*Scheme 2*).[19] The resulting PEO-CTA was characterized by SEC and ^{1}H NMR spectroscopy. The SEC trace of PEO-CTA using UV detection showed an absorbance at 309 nm corresponding to the presence of the trithiocarbonate group at the PEO chain-end (*Figure 1*). The PEO chain-end functionalization was further confirmed using ^{1}H NMR spectroscopy (*Figure 2*) by the appearance of a signal at 3.26 ppm (labeled b) corresponding to $-S-C(S)-S-CH_2-$ and a signal at 4.23 ppm (labeled c) corresponding to $-CH_2-OC(O)-C(CH_3)_2-S-$. The chain-end functionalization was almost quantitative (more than 95%) as calculated by ^{1}H NMR spectroscopy using the integral area values of signal labeled (c) corresponding to $-CH_2-OC(O)-C(CH_3)_2-S-$ and the signal labeled (a) corresponding to $CH_3-(CH_2)_{10}-CH_2-S-$ (*Figure 2*).
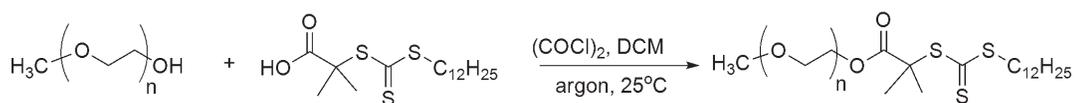
Scheme 2: Synthesis of PEO-CTA.
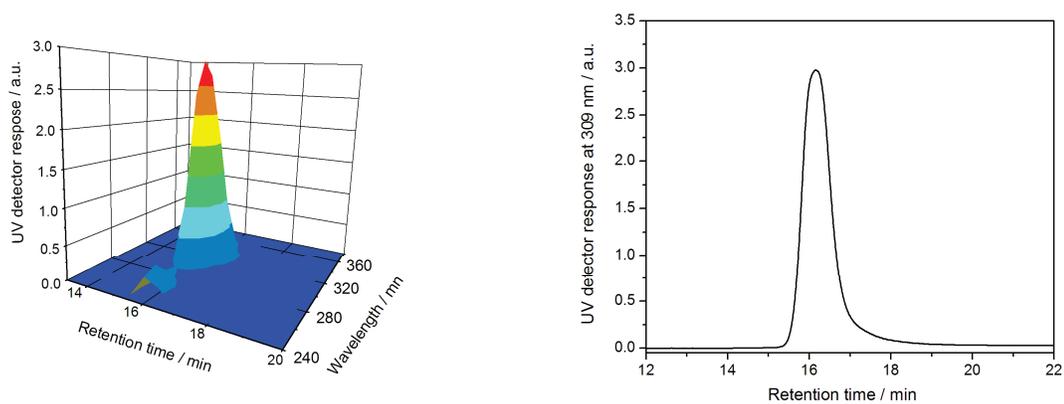
Figure 1: Three dimensional SEC chromatogram of PEO-CTA obtained using a photodiode array detector and the extracted UV trace at 309 nm.
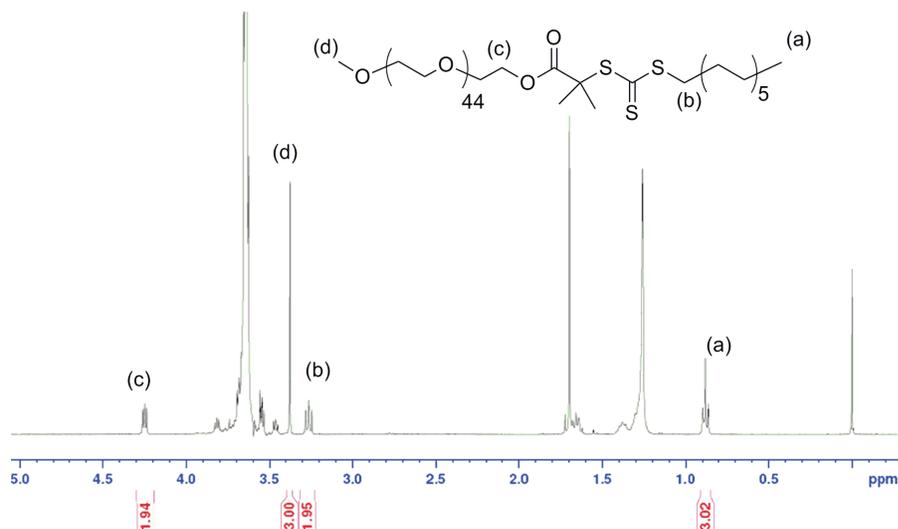
Figure 2: ^1H NMR spectrum of PEO-CTA in CDCl$_3$.

2.2. Poly(ethylene oxide)-*b*-poly(2-vinyl-4,4-dimethylazlactone-*co*-N-isopropyl

acrylamide) (PEO-*b*-P(VDM-*co*-NIPAM)) block copolymers: synthesis and

characterization

In order to introduce azlactone groups within the polymer backbone PEO-*b*-

P(VDM-*co*-NIPAM) block copolymers were synthesized using PEO-CTA as the

macromolecular chain transfer agent to mediate the statistical RAFT copolymerization of

VDM/NIPAM in the presence of 4,4'-azobis(4-cyanovaleric acid) (ACVA) in dioxane at

70°C (*Scheme 3*). The macromolecular characteristics of three different block copolymers

are gathered in *Table 1*. Polydispersity indices of resulting copolymers remain low

(PDI $\leq$ 1.10). *Figure 3* shows that SEC traces of block copolymers shift to earlier

retention times as molecular weights of copolymers increase with respect to the

PEO-CTA. PEO-CTA was efficiently used as macromolecular chain transfer agent

leading to well-defined copolymers as shown by the symmetrical SEC chromatograms of

PEO-*b*-P(VDM-*co*-NIPAM) block copolymers. These results show that the

copolymerizations are well-controlled and that the block copolymers are well-defined.

Furthermore, the ^{1}H NMR spectrum (*Figure 4*) of PEO$_{44}$-*b*-P(VDM$_{18}$-*co*-NIPAM$_{130}$)

diblock copolymer (*Table 1, Entry 1*) shows the presence of signals at 3.38 ppm

(CH$_3$O(CH$_2$-CH$_2$O)$_{44}$-, labeled a) and at 3.65 ppm (CH$_3$O(CH$_2$-CH$_2$O)$_{44}$-CH$_2$CH$_2$-

OC(O)C(CH$_3$)$_2$-, labeled b) characteristics of the PEO block, the presence of signals at

1.14 ppm (-CH(CH$_3$)$_2$, labeled d), at 4.00 ppm (-NH-CH(CH$_3$)$_2$, labeled e) and at 6.24

ppm (-NH-CH(CH$_3$)$_2$) characteristics of PNIPAM and at 1.40 ppm (-OCO-C(CH$_3$)$_2$-N=,

labeled c) characteristics of the PVDM. Moreover, the FT-IR analysis of the precipitated

PEO$_{44}$-*b*-P(VDM$_{18}$-*co*-NIPAM$_{130}$) copolymer shows the characteristic bands of the

azlactone ring and the amide group at 1815 cm^{-1} ($\nu_{(C=O)}$) and 1655 cm^{-1} ($\nu_{(C=O)}$), respectively (*Figure 5*). Therefore, the azlactone group remains intact (as no additional band appears after the copolymerization) and is available for further reactions with amine-based (bio)molecules. Therefore, the potentiality of PEO-*b*-P(VDM-*co*-NIPAM) block copolymers to react with a lysozyme will be described in paragraph 2.5.
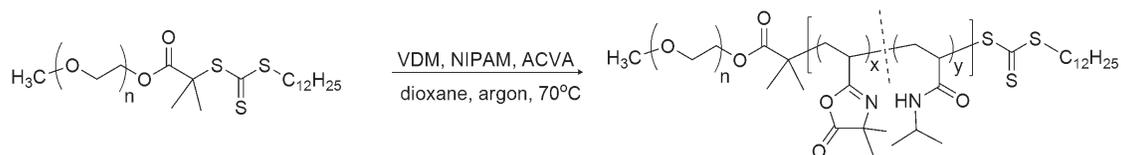
Scheme 3: RAFT copolymerization of VDM and NIPAM using PEO-CTA as the macromolecular chain transfer agent and using ACVA as the initiator in dioxane at 70°C.
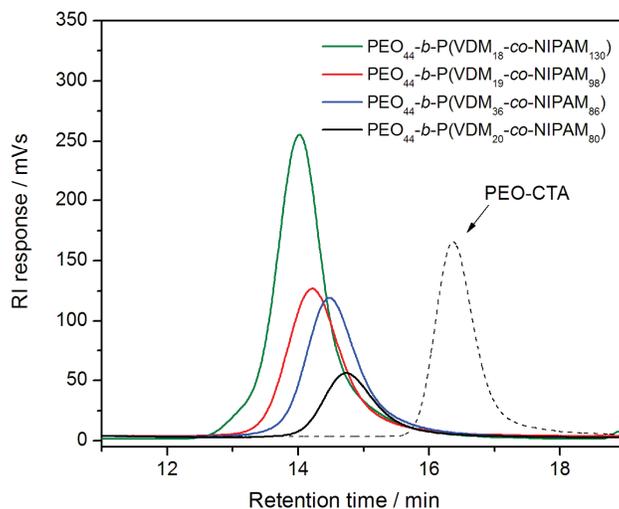
Figure 3: Overlay SEC traces of PEO-CTA and different PEO-b-P(VDM-co-NIPAM) block copolymers.
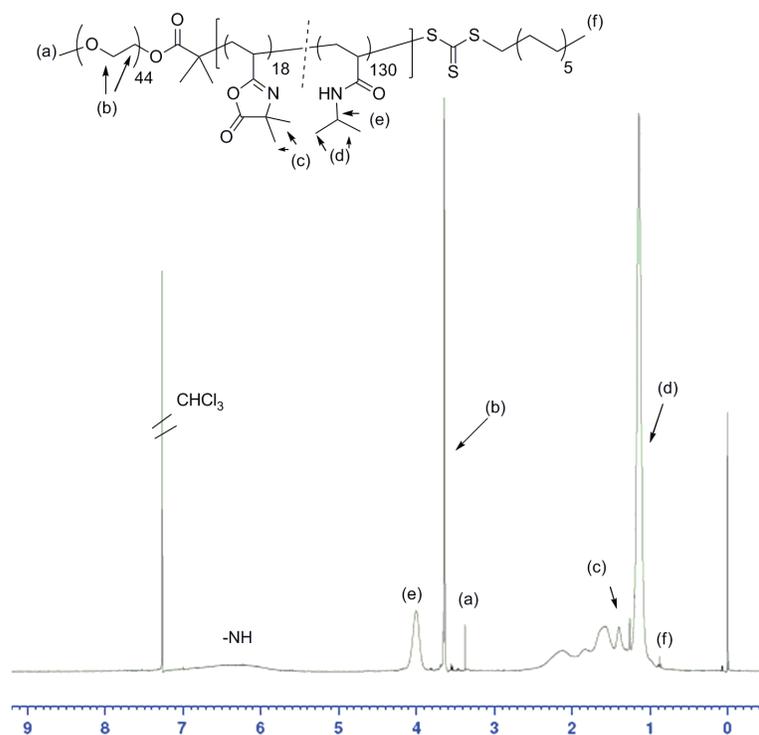
Figure 4: ^{1}H NMR spectrum of PEO$_{44}$-b-P(VDM$_{18}$-co-NIPAM$_{130}$) block copolymer in CDCl$_3$.
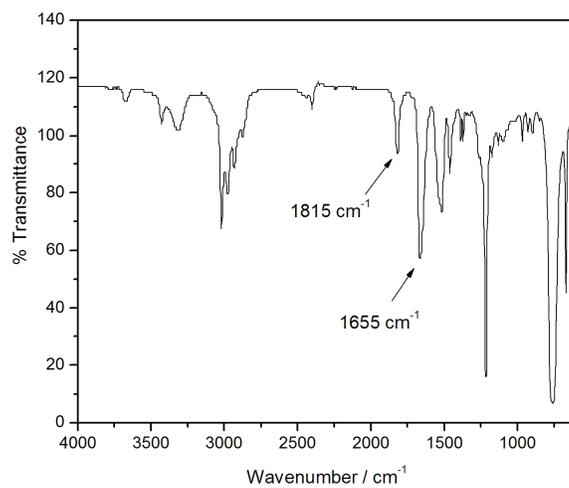
Figure 5: FT-IR spectrum of PEO$_{44}$-b-P(VDM$_{18}$-co-NIPAM$_{130}$) block copolymer.

Table 1: Block copolymers based on PEO, PNIPAM and PVDM synthesized by RAFT polymerization at 70°C in dioxane: experimental conditions and characterizations.

Entry	Copolymer[a]	$[NIPAM]_0:[VDM]_0:$ $[PEO\text{-}CTA]_0:[ACVA]_0$	VDM conv.[b] (%)	NIPAM conv.[b] (%)	$M_{n,th}$[c] (g.mol^{-1})	$M_{n,NMR}$[a] (g.mol^{-1})	$M_{n,SEC}$[d] (g.mol^{-1})	PDI[d]
1	PEO$_{44}$-*b*-P(VDM$_{18}$-*co*-NIPAM$_{130}$)	171:20:1:0.2	100	76	20600	19500	28100	1.10
2	PEO$_{44}$-*b*-P(VDM$_{19}$-*co*-NIPAM$_{98}$)	330:20:1:0.2	100	30	16320	16000	26600	1.09
3	PEO$_{44}$-*b*-P(VDM$_{36}$-*co*-NIPAM$_{86}$)	157:36:1:0.2	100	56	17300	17000	21800	1.08
4	PEO$_{44}$-*b*-P(VDM$_{20}$-*co*-NIPAM$_{80}$)	163:20:1:0.2	100	52	14785	14200	18400	1.08

[a] The number of monomer units and $M_{n,NMR}$ are determined by comparing the integral area values of the signal at 3.38 ppm (C**H**$_3$-O-(CH$_2$-CH$_2$O)$_{44}$) with the signal at 4.00 ppm (-NHC**H**(CH$_3$)$_2$) and the signal at 1.40 ppm (-OCO-C(C**H**$_3$)$_2$-N=) on the ^{1}H NMR spectra. [b] Monomer conversions determined by ^{1}H NMR spectroscopy. [c] $M_{n,th}$= $M_{n,PEO\text{-}CTA}$ + (([NIPAM]$_0$/[PEO-CTA]$_0$) × NIPAM conversion × 113)+ (([VDM]$_0$/[PEO-CTA]$_0$) × VDM conversion × 139). [d] Determined by SEC in DMF using polystyrene standards.

2.3. Azlactone-terminated poly(ethylene oxide)-*b*-poly(*N*-isopropyl acrylamide) (PEO-*b*-PNIPAM-Azl) diblock copolymers: synthesis, characterization and reactivity towards dansylcadaverine

In this part, azlactone-terminated PEO-*b*-PNIPAM block copolymers were synthesized by a combination of RAFT polymerization and "thiol-ene" Michael addition.

2.3.1. Synthesis of PEO-*b*-PNIPAM diblock copolymers by RAFT polymerization

PEO-*b*-PNIPAM diblock copolymers were synthesized by RAFT polymerization of NIPAM using PEO-CTA as the macromolecular chain transfer agent in the presence of ACVA used as the initiator in dioxane at 70°C (*Scheme 4*). Diblock copolymers have been obtained with low polydispersity indices (PDI < 1.10) (*Table 2*). *Figure 6a* shows that the SEC trace of PEO$_{44}$-*b*-PNIPAM$_{101}$ block copolymer shifts to earlier retention times with respect to the SEC trace of PEO-CTA indicating a good block copolymerization efficiency. The presence of the trithiocarbonate moiety at the chain-end was confirmed by the appearance of a SEC trace at 309 nm using UV detection corresponding to the C=S bond (*Figure 6b*). Furthermore, the ^{1}H NMR spectrum (*Figure 7*) of resulting PEO$_{44}$-*b*-PNIPAM$_{101}$ block copolymer (*Entry 1, Table 2*) shows the presence of signals at 3.38 ppm (C**H**$_3$O(CH$_2$-CH$_2$O)$_{44}$-, labeled a) and at 3.65 ppm (CH$_3$O(C**H**$_2$-C**H**$_2$O)$_{44}$-C**H**$_2$C**H**$_2$-OC(O)C(CH$_3$)$_2$-, labeled b) characteristics of the PEO block and the presence of signals at 6.24 ppm (-N**H**-CH(CH$_3$)$_2$, labeled c), at 4.00 ppm (-NH-C**H**(CH$_3$)$_2$, labeled d) and at 1.15 ppm (-NH-CH(C**H**$_3$)$_2$, labeled e) characteristics of the PNIPAM block.

Scheme 4: RAFT polymerization of NIPAM using PEO-CTA as the macromolecular

*chain transfer agent and using ACVA as the initiator in dioxane at 70^oC.*

Table 2: Experimental conditions and characterizations of PEO-b-PNIPAM diblock

copolymers synthesized by RAFT polymerization of NIPAM using PEO-CTA and using ACVA

in dioxane at 70^oC.

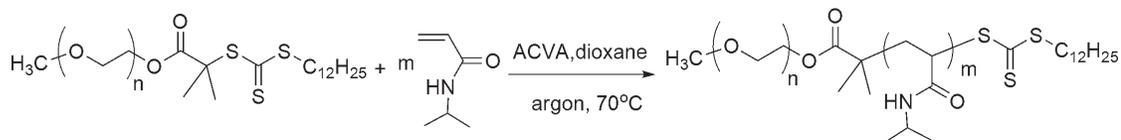| Entry	Copolymer[a]	[NIPAM]$_0$:[PEO-CTA]$_0$:[ACVA]$_0$	NIPAM conv. (%)[b]	$M_{n,th}$[c] (g.mol^{-1})	$M_{n,NMR}$[a] (g.mol^{-1})	$M_{n,SEC}$[d] (g.mol^{-1})	PDI[d]
1	PEO$_{44}$-*b*-PNIPAM$_{101}$	111:1:0.2	95	14220	13800	19300	1.05
2	PEO$_{44}$-*b*-PNIPAM$_{170}$	203:1:0.2	84	21670	21600	30500	1.06

[a] The number of monomer units and $M_{n,NMR}$ are determined by comparing the integral area value of the signal at 3.65 ppm (CH$_3$-O-(CH$_2$-CH$_2$O)$_{44}$-) and the signal at 4.00 ppm (-NHCH(CH$_3$)$_2$) on the ^{1}H NMR spectra. [b] NIPAM conversion determined by ^{1}H NMR spectroscopy. [c] $M_{n,th}$= $M_{n,PEO-CTA}$ + ([NIPAM]$_0$/[PEO-CTA]$_0$) × NIPAM conversion × molar mass of NIPAM unit. [d] Determined by SEC in DMF using polystyrene standards.
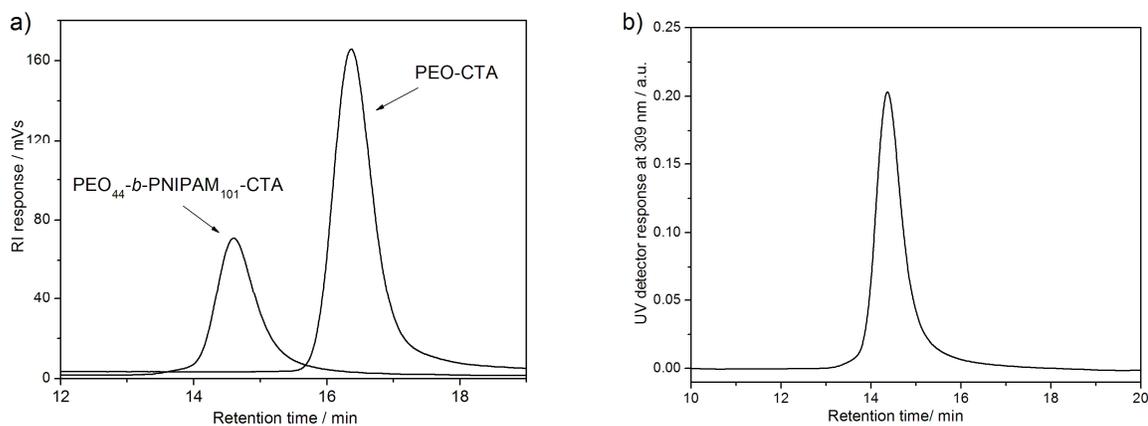
Figure 6: a) Overlay of SEC traces of PEO$_{44}$-b-PNIPAM$_{101}$ and PEO-CTA using RI

detection and, b) extracted UV chromatogram at 309 nm of PEO$_{44}$-b-PNIPAM$_{101}$.
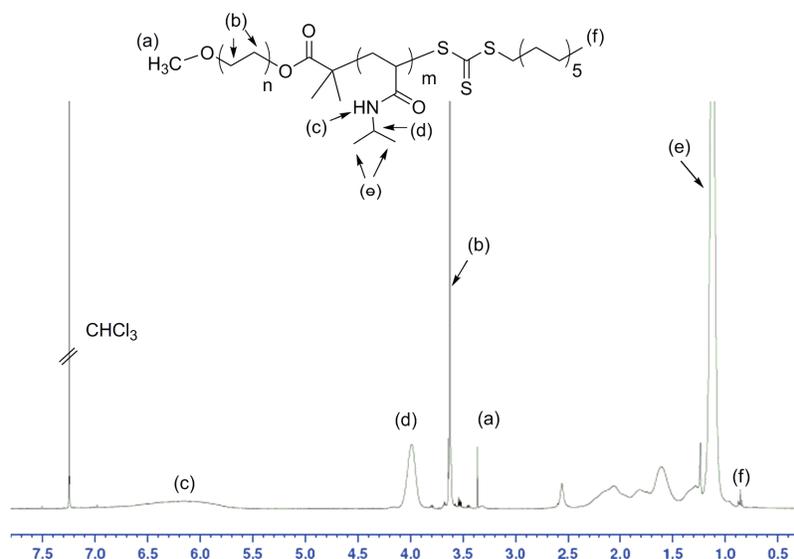
Figure 7: ^1H NMR spectrum of PEO$_{44}$-b-PNIPAM$_{101}$ in CDCl$_3$.

2.3.2. Aminolysis of a PEO-*b*-PNIPAM diblock copolymer and subsequent "thiol-ene" reaction with 2-vinyl-4,4-dimethylazlactone (VDM)

The azlactone functionality at the ω-chain-end of the PEO-*b*-PNIPAM copolymer was introduced *via* a two-step process: step one is the transformation of the trithiocarbonate end-group to a thiol, and step two is the modification of the so-formed thiol group by "thiol-ene" Michael addition. In the first step, the trithiocarbonate chain-end functionality was reduced to a thiol *via* aminolysis using *n*-hexylamine in the presence of an excess of dimethylphenylphosphine (DMPP) at 25°C in tetrahydrofuran (THF) (*Scheme 5*).

Scheme 5: Aminolysis of PEO-b-PNIPAM in the presence of n-hexylamine and DMPP in THF at 25°C.

The aminolysis efficiency was evaluated by SEC and ^{1}H NMR spectroscopy. *Figure 8a* compares the SEC traces using UV detection at 309 nm of PEO$_{44}$-*b*-PNIPAM$_{101}$ before and after aminolysis. The absence of a signal at 309 nm on the SEC trace of PEO-*b*-PNIPAM after aminolysis using UV detection is consistent with the loss of the C=S bond. Coupling between thiol groups to form bisulfide bonds was avoided by using DMPP as reducing agent, as a mostly symmetrical monomodal peak shape was observed on the SEC trace of PEO-*b*-PNIPAM after aminolysis using RI detection (*Figure 8b*). Comparison between ^{1}H NMR spectra of PEO$_{44}$-*b*-PNIPAM$_{101}$ before and after aminolysis (*Figure 9*) shows that signals at 0.86 ppm and at 1.26 ppm, corresponding to protons of the dodecyl group of the trithiocarbonate, has disappeared, confirming that a thiol-terminated PEO$_{44}$-*b*-PNIPAM$_{101}$ was obtained (PEO$_{44}$-*b*-PNIPAM$_{101}$-SH).

a)   b)
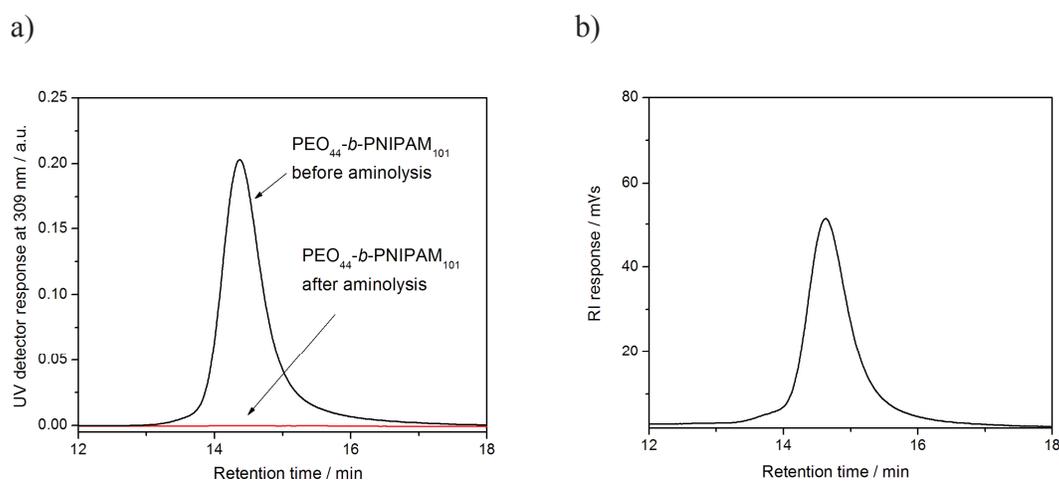
Figure 8: a) Overlay of SEC traces of PEO$_{44}$-b-PNIPAM$_{101}$ before and after aminolysis using UV detection at 309 nm and, b) SEC trace of PEO$_{44}$-b-PNIPAM$_{101}$ after aminolysis using RI detection.
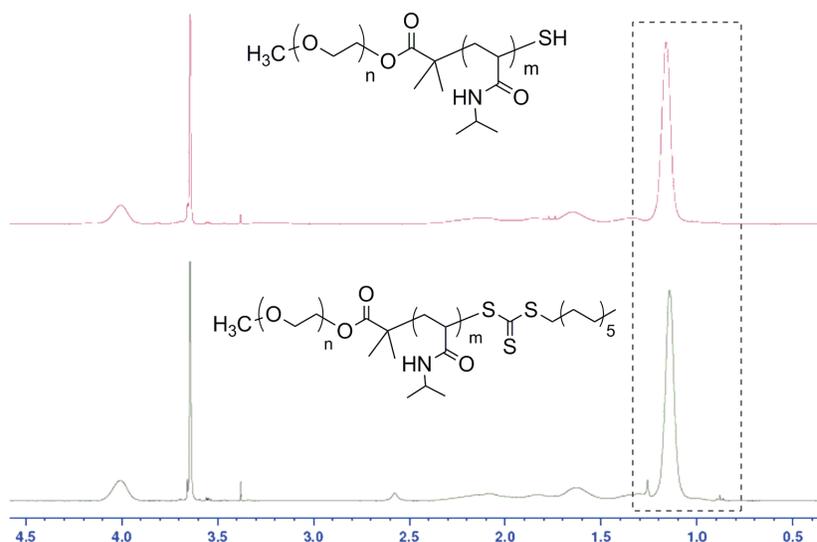
Figure 9: ¹H NMR spectra in CDCl₃ of PEO₄₄-b-PNIPAM₁₀₁ before (bottom) and

after (top) aminolysis.

In the second step, the resulting PEO_{44}-b-$PNIPAM_{101}$–SH block copolymer reacted with VDM in the presence of DMPP in THF at $25^{\circ}C$ to afford an azlactone-terminated PEO_{44}-b-$PNIPAM_{101}$ (PEO-b-PNIPAM-Azl) (*Scheme 6*). The SEC trace of the resulting polymer showed a symmetrical monomodal peak and the PDI of the copolymer remains low and equal to 1.08 (*Figure 10*). Moreover, the presence of the azlactone ring at the chain-end of the block copolymer was confirmed by FT-IR spectroscopy with the appearance of a band at 1817 cm^{-1} corresponding to C=O of the azlactone ring (*Figure 11*). Using the same conditions, a well-defined azlactone-terminated PEO_{44}-b-$PNIPAM_{170}$ diblock copolymer was also synthesized.
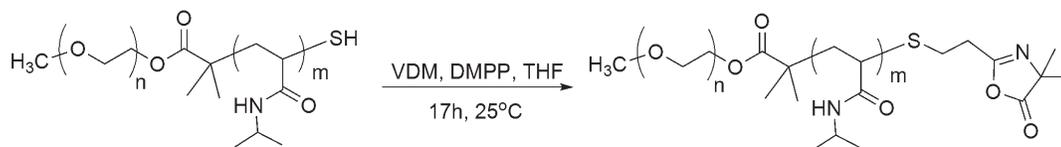
Scheme 6: Synthesis of the azlactone-terminated PEO-b-PNIPAM.
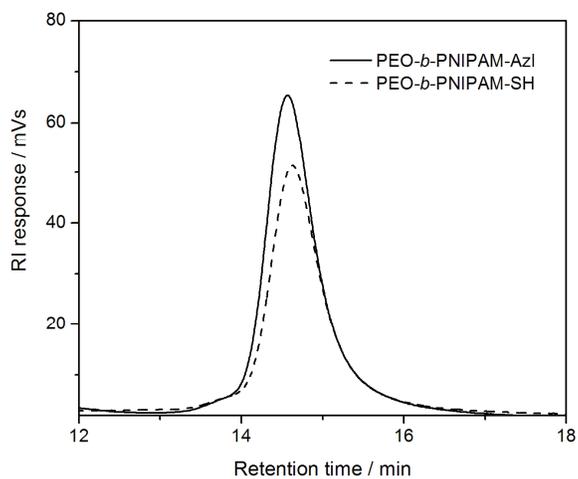
Figure 10: Overlay of SEC traces of PEO_{44}-b-$PNIPAM_{101}$-SH before (---) and after (—) coupling with VDM in the presence of DMPP in THF at $25^{o}C$.
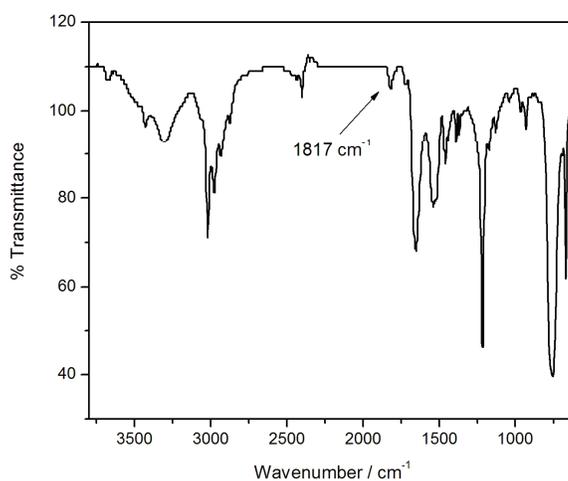
Figure 11: FT-IR spectrum of azlactone-terminated PEO_{44}-b-$PNIPAM_{101}$ diblock copolymer.

2.3.3. Reactivity of azlactone-terminated PEO-*b*-PNIPAM towards the fluorescent dye dansylcadaverine

The reactivity of azlactone-terminated PEO_{44}-*b*-$PNIPAM_{170}$ diblock copolymer (*Entry 2, Table 2*) was studied with dansylcadaverine (a fluorescent dye) in THF at $25^{\circ}C$ (*Scheme* 7). The reaction was monitored by SEC using UV detection. By comparing the UV spectra extracted from SEC traces at the maximum elution volume of the PEO_{44}-*b*-$PNIPAM_{170}$ diblock copolymer before and after reaction with dansylcadaverine, an absorbance at 336 nm was observed corresponding to the presence of the dansylcadaverine group (*Figure 12*). This result indicates that dansylcadaverine has reacted with the PEO-*b*-PNIPAM block copolymer *via* the azlactone group. The potentiality of PEO-*b*-PNIPAM-Azl block copolymers to react with amine-based biomolecules such as lysozyme will be described in paragraph 2.5.
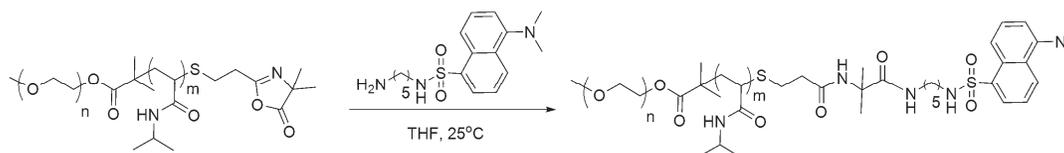
*Scheme 7: Reaction between azlactone-terminated PEO-b-PNIPAM and
dansylcadaverine in THF at $25^{o}C$.*
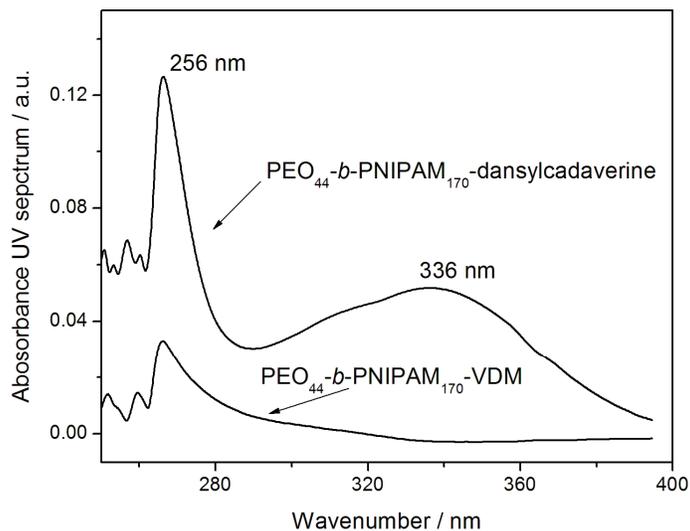
Figure 12: Overlay of UV spectra of azlactone-terminated PEO$_{44}$-b-PNIPAM$_{170}$ before and after reaction with dansylcadaverine.

2.4. Thermoresponsive behaviour

Thermoresponsive behaviour of PEO-*b*-P(VDM-*co*-NIPAM) and PEO-*b*-PNIPAM block copolymers was studied in water. The LCST was determined from cloud point measurements using UV-Vis spectrophotometry at 500 nm and dynamic light scattering (DLS). As the temperature increases the copolymers self-assemble into core-shell particles of significantly greater particle size, resulting in a cloudy solution. LCST values for the block copolymers are shown in *Table 3*.

Table 3: LCST values of PEO-b-PNIPAM and PEO-b-P(VDM-co-NIPAM) block copolymers

Entry	Copolymer	$M_{n,SEC}$[a] (g.mol^{-1})	PDI[a]	LCST[b] (^{o}C)
1	PEO$_{44}$-CTA	7400	1.07	nd[c]
2	PEO$_{44}$-b-PNIPAM$_{101}$	19300	1.05	41
3	PEO$_{44}$-b-PNIPAM$_{170}$	30500	1.06	36
4	PEO$_{44}$-b-P(VDM$_{18}$-co-NIPAM$_{130}$)	28100	1.10	28
5	PEO$_{44}$-b-P(VDM$_{19}$-co-NIPAM$_{98}$)	26600	1.09	37
6	PEO$_{44}$-b-P(VDM$_{36}$-co-NIPAM$_{86}$)	21800	1.08	19
7	PEO$_{44}$-b-P(VDM$_{20}$-co-NIPAM$_{80}$)	18400	1.08	29

[a] Determined by SEC in DMF using polystyrene standards. [b] Determined by UV-Vis spectrophotometry and DLS. [c] Not determined.

It appears that the increase of the PNIPAM chain length decreases the LCST of PEO-b-PNIPAM block copolymer (*Entries 2 and 3, Table 3*). This is due to the fact that when the molar ratio of PNIPAM increases (as the chain length increases), the LCST of the block copolymer gets closer to the LCST of PNIPAM (32°C).[15] Therefore, a LCST approaching the temperature of human body (37°C) could be obtained by controlling the chain length of the PNIPAM block. Moreover, the LCST of PEO-b-PNIPAM was also modified by incorporating VDM units in the PNIPAM block. The incorporation of hydrophobic VDM units within PNIPAM block leads to a decrease of the LCST of block copolymers from 41 to 37°C (*Entries 2 and 5, Table 3*). When the number of VDM units is kept constant within the PEO-b-P(VDM-co-NIPAM), a higher LCST was obtained when the number of NIPAM units decreases (*Entries 4 and 5, Table 3*). In conclusion, the LCST of block copolymers based on PEO block and PNIPAM block or

P(VDM-*co*-NIPAM) block can be tuned by changing the ratio of NIPAM units and VDM units of the second block.

2.5. Bioconjugation of block copolymers based on PEO, PNIPAM, (P)VDM with lysozymes

The conjugation of well-defined azlactone-terminated PEO_{44}-*b*-$PNIPAM_{101}$ copolymer ($M_{n,NMR}$ = 13 700 g.mol^{-1}, PDI = 1.08) and well-defined PEO_{44}-*b*-P(VDM_{20}-*co*-$NIPAM_{80}$) copolymer ($M_{n,NMR}$ = 14 200 g.mol^{-1}, PDI = 1.08) was studied with a lysozyme in dimethylsulfoxide (DMSO) in the presence of triethylamine (TEA). The conjugations were monitored by using sodium dodecyl sulfate polyacrylamide gel electrophoresis (SDS-PAGE).

SDS-PAGE analyses (*Figure 13*) show new bands for conjugation products (*lanes 3 and 4, Figure 13*) at higher molecular weight than the native lysozyme (*lane 2, Figure 13*). These results indicate successful formation of polymer-lysozyme conjugates. The relative narrow bands and apparent molecular weights obtained with azlactone-terminated PEO-*b*-PNIPAM-Azl/lysozyme conjugate (*lane 4, Figure 13*) were consistent with the coupling of one, two, three and four polymer chains attached to one lysozyme. Furthermore, the broad band of PEO_{44}-*b*-P(VDM_{20}-*co*-$NIPAM_{80}$)/lysozyme conjugate (*lane 3, Figure 13*) shows slightly higher apparent molecular weights than the band of azlactone-terminated PEO_{44}-*b*-$PNIPAM_{101}$-Azl/lysozyme conjugate together with the absence of free lysozyme. This result indicates that multiple chains are attached to the lysozyme. It can be explained by the high density of azlactone groups within the second block leading to multi-attachments. Both copolymers structures are thus able to successfully form bioconjugates with lysozyme.
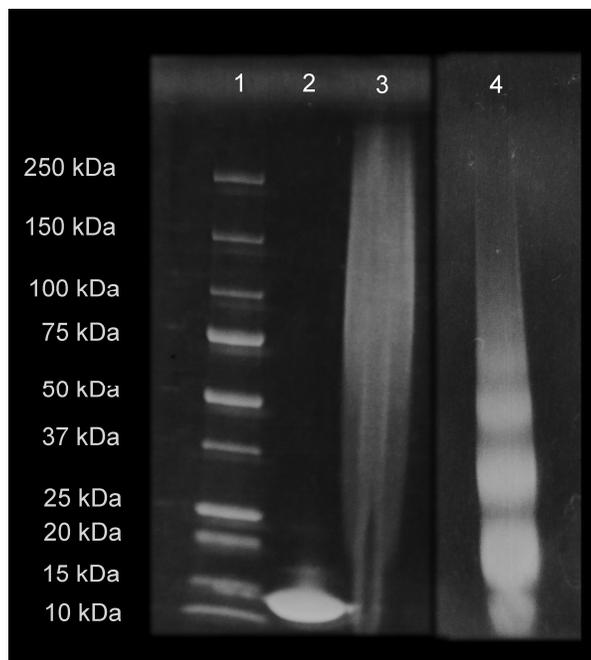
Figure 13: SDS-PAGE results. Protein standards (lane 1); native lysozyme (lane 2); PEO_{44}-b-$P(VDM_{20}$-co-$NIPAM_{80})$/lysozyme with $[PEO_{44}$-b-$P(VDM_{20}$-co-$NIPAM_{80}]_0$:[lysozyme]$_0$ =22.6:1 in TEA/DMSO at 25°C (lane 3); azlactone-terminated PEO_{44}-b-$PNIPAM_{101}$-Azl/lysozyme with $[PEO_{44}$-b-$PNIPAM_{101}$-Azl]$_0$:[lysozyme]$_0$ =20:1 in TEA/DMSO at 25°C (lane 4).

The thermoresponsive behaviour of bioconjugates was also studied by DLS. The PEO_{44}-*b*-$P(VDM_{20}$-*co*-$NIPAM_{80})$/lysozyme conjugate did not show any LCST. This phenomenon is ascribed to the formation of insoluble aggregates in water due to the high density of conjugated lysozymes within the second block copolymer containing a high density of azlactone rings. On the contrary, *Figure 14* shows that the PEO_{44}-*b*-$PNIPAM_{101}$-Azl/lysozyme conjugate presents a LCST of 43°C and therefore, a thermoresponsive behaviour. This result could be explained by the presence of lysozymes that increases the hydrophilicity of the thermoresponsive block copolymer and therefore leads to the formation of more hydrated particles upon aggregation.
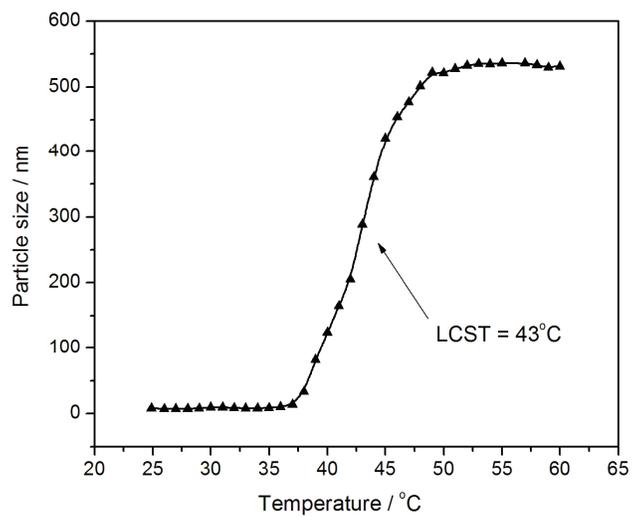
Figure 14: Hydrodynamic diameter versus temperature for (▲) PEO$_{44}$-b-PNIPAM$_{101}$-Azl/lysozyme bioconjugate.

3. Conclusion

In summary, we have described straightforward methodologies to synthesize azlactone end- and mid-functional thermoresponsive copolymers based on PEO and PNIPAM by RAFT polymerization and "thiol-ene" reaction. Subsequent conjugation of the thermoresponsive copolymers to a model protein (lysozyme) showed that azlactone mid-functional copolymers conjugates displayed higher apparent molecular weight compared with conjugates prepared from similar macromolecular characteristics end-functional thermoresponsive copolymers. Moreover, after bioconjugation azlactone-terminated copolymers showed temperature-dependent phase separation and particle formation behaviour.

4. Experimental Section

4.1. Materials

Triethylamine (TEA, ≥ 99%, Sigma-Aldrich), 4,4'-azobis(4-cyanovaleric acid) (ACVA, ≥ 98, Aldrich), neutral aluminium oxide (Aldrich), dimethylphenylphosphine (DMPP, 99%, Aldrich), dansylcadaverine (≥ 97%, Sigma-Aldrich), poly(ethylene oxide) monomethyl ether (PEO, ~2000 g.mol^{-1}, Fluka), oxalyl chloride ((COCl)$_2$, 98%, Aldrich), lysozyme from chicken egg white (dialyzed, lyophilized powder, 100 000 units/mg, Fluka), *n*-hexylamine (99%, Aldrich), dimethylsulfoxide (DMSO, 99.9%, Acros), methanol (99.8%, ProLabo), β-mercaptoethanol (98%, Sigma-Aldrich), *N,N*-dimethylformamide (DMF, 99.8%, Aldrich), acetone (99.8%, Aldrich), dichloromethane (DCM, > 99%, Aldirch), diethyl ether (technical grade, Aldrich), tetrahydrofuran (THF, > 99%, Aldrich) and petroleum ether (Analytic reagent grade, 40-60°C, Fisher Scientific) were obtained and used as received. *N*-isopropyl acrylamide (NIPAM) was obtained from Aldrich (97%) and was recrystallized from petroleum ether prior to use. 1,4-dioxane (> 99%) was purchased from Fisher-Scientific and distilled before use. Dialysis membrane (MWCO = 3500, regenerated cellulose) was purchased from SpectrumLabs. Pure water was obtained form a Millipore Direct Q system and had a conductivity of 18.2 MΩ cm at 25°C. SDS-PAGE gel (mini-Protean TGX, 4-15% gel, Bio-RAD), running buffer (10X tris/glycerine/SDS-buffer), Laemmli sample buffer (Bio-RAD), Coomassive blue and all materials for Sodium dodecyl sulfate polyacrylamide gel electrophoresis (SDS-PAGE) analysis were purchased from Bio-RAD. 2-dodecylsulfanylthiocarbonylsulfanyl-2-methylpropionic acid[20] (DMP) and 2-vinyl-4,4-dimethylazlactone[21] (VDM) were synthesized following reported procedures.

4.2. Instrumentation

Nuclear Magnetic Resonance (NMR) Spectroscopy

NMR spectra were recorded on a Bruker AC-400 Spectrometer for ^{1}H NMR (400 MHz) and ^{13}C NMR (100 MHz). Chemical shifts are reported in ppm relative to deuterated solvent resonances.

Size Exclusion Chromatography (SEC)

Polymers were characterized on a SEC system operating in DMF eluent at 60°C fitted with a Polymer Laboratories guard column (PL Gel 5μm) and two Polymer Laboratories PL Mixed D columns, a Waters 410 differential refractometer (RI) and a Waters 481 UV detector operating at 309 nm. The instrument operated at a flow rate of 1.0 mL.min^{-1} and was calibrated with narrow linear polystyrene (PS) standards ranging in molecular weight from 580 g.mol^{-1} to 460 000 g.mol^{-1}. Molecular weights and polydispersity indices (PDI) were calculated using Waters EMPOWER software.

Fourier Transformation Infra-Red (FT-IR) Spectroscopy

FT-IR spectra of copolymers were recorded using a ThermoElectron Corp. spectrometer operating with an attenuated total reflection (ATR solid) gate. Spectra were analyzed with OMNIC software.

UV-Vis spectrophotometry characterization

UV-Vis measurements were performed on a Varian Cary 100 Scan spectrophotometer fitted with dual cell Peltier accessory for heating. Samples of copolymers in pure water of concentration 10 g.L^{-1} were prepared and left to dissolve over a period of two hours at room temperature. The sample was introduced into a quartz cuvette and placed in the Peltier accessory. The temperature was adjusted manually and

the sample allowed to equilibrate for 4 minutes before two measurements of the transmittance at 500 nm were made.

Dynamic light scattering (DLS) analysis

Dynamic light scattering measurements were made in order to determine the hydrodynamic diameter (D_h) and particle size distribution of copolymers and of resulting core-shell particles over temperatures ranging from 25°C to 60°C. A Malvern Instruments Nanosizer fitted with a 4mW He-Ne laser operating at 633 nm with dual angle detection (13°, 173°) was used for all measurements and the data processed using CONTIN method of analysis. Temperature trend measurements were recorded starting from 20°C and at increasing temperature increments of 1°C until 60°C with an equilibration time of two minutes.

Sample preparation for dynamic light scattering

A quantity of copolymer was measured into a clean glass vial and Millipore deionised water (18.2 MΩ.cm at 25°C) was added in order that a 1 mg/mL solution of (co)polymer was obtained. Typical quantities used were 3 mg of copolymer and 3.00 mL of water. The copolymer was left to dissolve for 2 hours stirring at room temperature, after which the solution was filtered using a glass syringe and a syringe filter with 0.2 μm pore size (Whatman Inorganic) into a clean glass cuvette for analysis.

Sodium dodecyl sulfate polyacrylamide gel electrophoresis (*SDS-PAGE*)

The SDS-PAGE was performed with a Bio-Rad system electrophoresis using 4-15% polyacrylamide gels run at 200 V constant voltage for 40 min and 1X glycerine/SDS-buffer. Samples were dissolved in pure water (10 μL, [lysozyme]$_0$ = 4 mg.mL^{-1}), mixed 10 μL Laemmli sample buffer (containing 5% of β-mercaptoethanol)

and heated at 90°C for 5 min before loading. The gel was stained with Coomassie blue for 60 min.

4.3. Synthesis and characterization of the poly(ethylene oxide) macromolecular chain transfer agent (PEO-CTA)

To a stirring solution of DMP (0.72 g, 1.98×10^{-3} mol) dissolved in dry DCM (5.0 mL) was added dropwise an excess of oxalyl chloride (($(COCl)_2$, 0.9 mL, 10.40×10^{-3} mol) under argon at 25°C. The solution was refluxed and stirred until gaz evolution stopped for 3 h. In the next step, the excess of oxalyl chloride was removed under vacuum. To the remaining mixture were added dry DCM (15.0 mL) and PEO (2.00 g, 10^{-3} mol). The solution was continuously stirred for 24 h under argon at 25°C. The product was then precipitated in diethyl ether. The final product obtained by filtration and dried under vacuum was a yellow solid. Yield : 1.8 g (77 %). ^{1}H NMR (400 MHz, CDCl$_3$), δ (ppm) : 0.86 (t, 3H, -CH$_2$-CH$_3$), 1.25-1.38 (20, CH$_3$-(CH$_2$)$_{10}$-CH$_2$-S), 1.71 (s, 6 H,-C(CH3)2-S-C(S)-S-), 3.26 (t, 2H, -S-C(S)-S-CH$_2$-CH$_2$-), 3.38 (s, 3H, CH$_3$O(CH$_2$-CH$_2$-O)$_{44}$-), 3.65 (CH$_3$O(CH$_2$-CH$_2$O)$_{44}$), 4.23 (t, 2H, -CH$_2$-OC(O)-C(CH$_3$)$_2$-S-C(S)-S-).

4.4. Poly(ethylene oxide)-*b*-poly(2-vinyl-4,4-dimethylazlactone-*co*-N-isopropyl acrylamide) block copolymers: synthesis and characterization

In a typical RAFT copolymerization procedure, a magnetic stir bar was charged to a round bottom flask along with NIPAM (0.87 g, 7.70×10^{-3} mol), VDM (0.123 g, 8.84×10^{-4} mol), PEO-CTA ($M_{n,NMR}$ = 2350 g.mol^{-1}, 0.106 g, 4.51×10^{-5} mol), 4,4'-azobis(4-cyanovaleric acid) (ACVA, 3 mg, 10.7×10^{-6} mol), dioxane (3.0 mL) and *N,N*-dimethylformamide (DMF, 0.10 mL). The mixture was deoxygenated by bubbling

argon for 30 min. The solution was then immersed in an oil bath thermostatted at 70°C to allow the polymerization to occur. The reaction was stopped after 120 min by opening the mixture to oxygen. The VDM conversion and the NIPAM conversion were determined to be 100% and 76% respectively by ^{1}H NMR spectroscopy by comparing the integration areas of the vinylic protons of VDM at 5.96 ppm and NIPAM at 5.55 ppm with the integral area value of the CH proton of DMF at 8.02 ppm. Dioxane and DMF were removed using a rotary evaporator. The resulting product was then dissolved in acetone and precipitated in cold diethyl ether, filtered and dried under vacuum at 25°C. The final product obtained as a yellow powder was characterized by ^{1}H NMR spectroscopy, FT-IR spectroscopy and SEC analysis. $M_{n,SEC}$ = 28100 g.mol^{-1}, PDI = 1.10. FT-IR (ν, cm^{-1}): $\nu_{(C=O\ ;\ azlactone)}$ = 1815, $\nu_{(C=N\ ;\ azlactone)}$ = 1628, $\nu_{(C=O\ ;\ NIPAM)}$ = 1615. ^{1}H NMR (400 MHz, CDCl$_3$), δ (ppm): 0.86 (**CH$_3$**-(CH$_2$)$_{10}$-CH$_2$-S-), 1.14 (-NH-CH(**CH$_3$**)$_2$), 1.40 (-OCO-C(**CH$_3$**)$_2$-N=), 1.42-2.75 (-**CH$_2$**-**CH**-)n, 3.38 (**CH$_3$**O(CH$_2$-CH$_2$O)$_{44}$-), 3.65 (CH$_3$O(**CH$_2$**-**CH$_2$**O)$_{44}$-**CH$_2$CH$_2$**-OC(O)C(CH$_3$)$_2$-), 4.00 (-NH-**CH**(CH$_3$)$_2$), 6.24 (-N**H**-CH(CH$_3$)$_2$).

4.5. Azlactone terminated poly(ethylene oxide)-*b*-poly(*N*-isopropyl acrylamide) (PEO-*b*-PNIPAM-Azl) diblock copolymers: synthesis, characterization and reactivity towards dansylcadaverine

4.5.1. Synthesis of PEO-*b*-PNIPAM diblock copolymers by RAFT polymerization

In a typical RAFT polymerization procedure, a magnetic stir bar was charged to a round bottom flask together with *N*-isopropyl acrylamide (NIPAM, 3.0 g, 0.0265 mol), PEO-CTA (0.56 g, 2.38x10^{-4} mol), 4,4'-azobis(4-cyanovaleric acid) (ACVA, 13.5 mg, 4.82x10^{-5} mol), dioxane (8.0 mL) and *N,N*-dimethylformamide (DMF, 0.3 mL) used as

the internal reference. The mixture was deoxygenated by bubbling argon for 30 min. The solution was then immersed in an oil bath thermostatted at 70°C to allow the polymerization to occur. The reaction was stopped after 120 min by opening the reaction mixture to oxygen. Conversion of NIPAM was determined to be 95% by ^{1}H NMR spectroscopy by comparing the integration areas of the vinylic protons of NIPAM at 6.27 ppm and at 5.55 ppm with the integral area value of the CH proton of DMF at 8.02 ppm. The resulting product was purified by three successive precipitations into diethyl ether, filtration and drying under vacuum at 30°C. The final product obtained as a yellow powder was analyzed by SEC and ^{1}H NMR spectroscopy. $M_{n,SEC} = 19300$ g.mol^{-1}, PDI = 1.05. ^{1}H NMR (400 MHz, CDCl$_3$), δ (ppm): 0.86 (**CH$_3$**-(CH$_2$)$_{10}$-CH$_2$-S-), 1.15 ppm (-NH-CH(**CH$_3$**)$_2$), 1.25 (CH$_3$-(**CH$_2$**)$_{10}$-CH$_2$-S-), 1.42-2.75 (-**CH$_2$-CH-**)$_n$, 3.38 ppm (**CH$_3$**O(CH$_2$-CH$_2$O)$_{44}$-), 3.65 ppm (CH$_3$O(**CH$_2$-CH$_2$O**)$_{44}$-**CH$_2$CH$_2$**-OC(O)C(CH$_3$)$_2$), 4.00 ppm (-NH-C**H**(CH$_3$)$_2$), 6.24 ppm (-N**H**-CH(CH$_3$)$_2$).

4.5.2. Aminolysis of a PEO-*b*-PNIPAM diblock copolymer and subsequent "thiol-ene" reaction with 2-vinyl-4,4-dimethylazlactone

4.5.2.1. Aminolysis of PEO-*b*-PNIPAM diblock copolymer

A magnetic stir bar was charged to a round-bottomed flask along with PEO$_{44}$-*b*-PNIPAM$_{101}$ (0.30 g, 2.12x10^{-5} mol), dimethylphenylphosphine (DMPP, 100 μL, 7.04x10^{-4} mol), and tetrahydrofuran (THF, 5.0 mL). The solution was degassed with argon within 20 min. The *n*-hexylamine (0.10 mL, 7.62x10^{-4} mol) was then added *via* a syringe. The reaction was left to stir for 4 h at 25°C. After this time had elapsed, the polymer was precipitated into diethyl ether, separated by filtration and dried under

vacuum at 30°C. The product obtained as a white powder was analyzed by SEC using RI/UV detections and ^{1}H NMR spectroscopy. $M_{n,SEC}$ = 20300 g.mol^{-1}, PDI = 1.08. ^{1}H NMR (400 MHz, CDCl$_3$), δ (ppm): 1.14 (-NH-CH(**CH$_3$**)$_2$), 1.42-2.75 (-**CH$_2$-CH-**)$_n$, 3.38 (**CH$_3$**O(CH$_2$-CH$_2$O)$_{44}$-), 3.65 (CH$_3$O(**CH$_2$-CH$_2$O**)$_{44}$-CH$_2$CH$_2$-OC(O)C(CH$_3$)$_2$-), 4.00 (-NH-**CH**(CH$_3$)$_2$), 6.24 (-**NH**-CH(CH$_3$)$_2$).
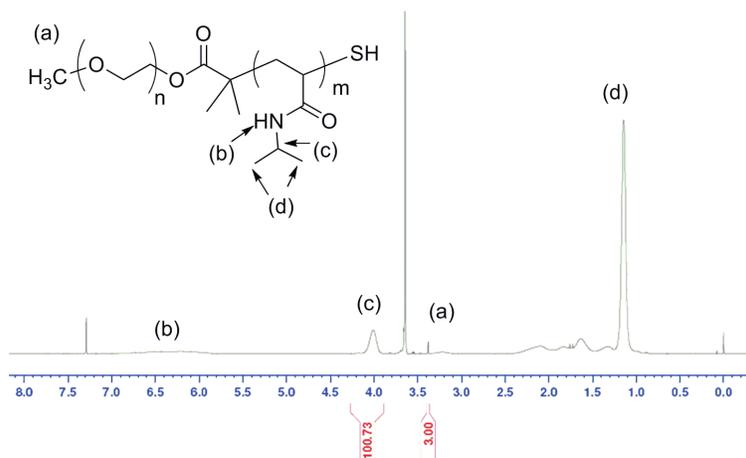
Figure 15: ^{1}H NMR spectrum of a thiol-terminated PEO-b-PNIPAM diblock copolymers in CDCl$_3$.

4.5.2.2. "Thiol-ene" reaction of a thiol-terminated PEO-*b*-PNIPAM with the 2-vinyl -4,4-dimethylazlactone (VDM)

A magnetic stir bar was charged to a Schlenk tube along with VDM (15 mg, 1.08x10^{-4} mol), DMPP (25 μL, 1.73 x 10^{-4} mol) and THF (20 μL, solvent). The resulting solution was stirred at room temperature for 30 minutes. After this time had elapsed, a solution of the thiol-terminated PEO$_{44}$-*b*-PNIPAM$_{101}$ (0.15 g, 1.06x10^{-5} mol) and an additional quantity of DMPP (10 μL, 0.7x10^{-4} mol) in 1.0 mL of THF was added to the reaction mixture and the solution was left to react for 17 hours at 25°C. When this time had elapsed the solution was passed through a column of neutral aluminum oxide. The

filtrate was then precipitated into diethyl ether, filtered and dried under vacuum at room temperature. The product obtained as a white powder was analyzed by SEC using RI detection, FT-IR spectroscopy and ^{1}H NMR spectrsocopy. $M_{n,SEC}$ = 20500 g.mol^{-1}, PDI = 1.08. FT-IR (ν, cm^{-1}): $\nu_{(C=O\ ;\ azlactone)}$ = 1815, $\nu_{(C=O\ ;\ NIPAM)}$ = 1615. ^{1}H NMR (400 MHz, CDCl$_3$), δ (ppm): 1.14 (NH-CH(**CH$_3$**)$_2$), 1.26 (-OCO-C(**CH$_3$**)$_2$-N=) labeled (e), 1.42-2.75 (**-CH$_2$-CH-**)$_{n,}$ 3.38 (**CH$_3$**O(CH$_2$-CH$_2$O)$_{44}$-), 3.65 (CH$_3$O(**CH$_2$-CH$_2$O**)$_{44}$-**CH$_2$CH$_2$**-OC(O)C(CH$_3$)$_2$-), 4.00 (-NH-**CH**(CH$_3$)$_2$), 6.24 (-**NH**-CH(CH$_3$)$_2$).
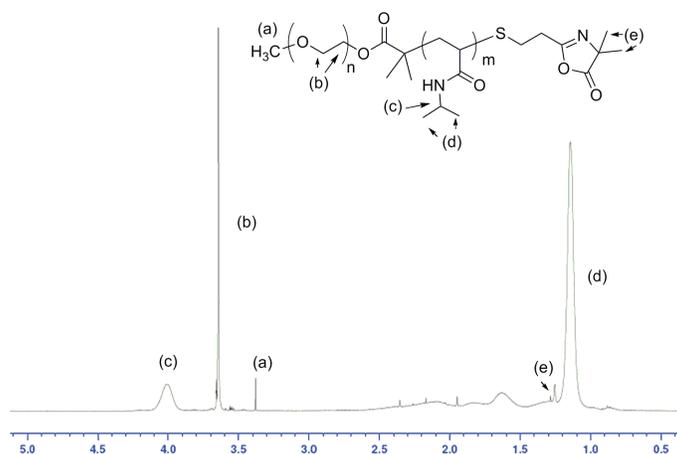
Figure 16: ^{1}H NMR spectrum of an azlactone-terminated PEO-b-PNIPAM diblock copolymer in CDCl$_3$.

4.5.3. Reactivity of the azlactone-terminated PEO-*b*-PNIPAM towards the fluorescent dye dansylcadaverine

A magnetic stir bar was charged to a round bottom flask along with PEO$_{44}$-*b*-PNIPAM$_{170}$ diblock copolymer ($M_{n,SEC}$ = 31200 g.mol^{-1}; PDI = 1.04; 32,8 mg, 1.53x10^{-6} mol), dansylcadaverine (1,5 mg; 4.25x10^{-6} mol) and THF (1.0 mL). The solution was stirred at room temperature for 24 h. The crude reaction was then dialyzed against a mixture of solvent (DMF/acetone = 50:50 v/v) for one day (MWCO =3500 g.mol^{-1}) and

dried under vacuum. The final product was analyzed by SEC using RI/UV detections. $M_{n,SEC}$ = 30700 g.mol^{-1}; PDI =1.08.

4.6. Bioconjugation of the block copolymers based on PEO, PNIPAM and (P)VDM with lysozyme

4.6.1. Conjugation of PEO-*b*-P(VDM-*co*-NIPAM) to lysozyme

Lysozyme (8.3 mg, 5.80x10^{-7}) and the PEO$_{44}$-*b*-P(VDM$_{20}$-*co*-NIPAM$_{80}$) copolymer ($M_{n,SEC}$ = 18400 g.mol^{-1}, $M_{n,NMR}$ = 14 200 g.mol^{-1}, PDI = 1.08) (0.186 mg, 13.10x10^{-6} mol, 22.6 equiv. with respect to lysozyme) were dissolved in dimethylsulfoxide (DMSO, 3.00 mL). The triethylamine (TEA, 0.15 mL) was then added in the solution. The reaction was stirred for 2 days at 25°C. A solution of methanol/water (50:50 v/v, 10.00 mL) was then added to the crude reaction. This solution was subsequently dialyzed against methanol/water (50:50 v/v) for 2 days (MWCO = 3500 g.mol^{-1}). The final product was recovered by lyophilization and analyzed by SDS-PAGE.

4.6.2. Conjugation of azlactone-terminated PEO-*b*-PNIPAM to lysozyme

Lysozyme (4.3 mg, 3.00x10^{-7}) and azlactone-terminated PEO$_{44}$-*b*-PNIPAM$_{101}$ diblock copolymer ($M_{n,SEC}$ = 20500 g.mol^{-1}, $M_{n, NMR}$ = 13700 g.mol^{-1}, PDI = 1.08) (82.0 mg, 6.0x10^{-6} mol, 20 equiv. with respect to lysozyme) were dissolved in dimethylsulfoxide (DMSO, 2.00 mL). The triethylamine (TEA, 0.10 mL) was then added in the solution. The reaction was stirred for 3 days at 25°C. A solution of methanol/water (50:50 v/v, 5.00 mL) was then added to the crude reaction. This solution was subsequently dialyzed against methanol/water (50:50 v/v) for 1 day (MWCO = 3500 g.mol^{-1}). The final product was recovered by lyophilization and analyzed by SDS-PAGE.

References

1   Hermanson, G. T. *Bioconjugates techniques* **2008***,* Elsevier.

2   Langer, R.; Folkman, J. *Nature*, **1976,** *263*, 797-800.

3   Abuchowski, A.; Vanes, T.; Palczuk, N. C.; Davis, F. F. *J. Biol. Chem.* **1977**, *252*, 3578-3581.

4   Le Droumaguet, B.; Nicolas, J. *Polym. Chem.* **2010**, *1*, 563-598.

5   Boyer, C.; Bulmus, V.; Davis, T. P.; Ladmiral, V.; Liu, J.; Perrier, S. *Chem. Rev.* **2009**, *109*, 5402- 5436.

6   (a) Chenal, M.; Boursier, C.; Guillaneuf, Y.; Taverna, M.; Couvreur, P.; Nicolas, J. *Polym. Chem.* **2011**, *2*, 1523-1530. (b) Nicolas, J.; Khoshdel, E.; Haddleton, D. M. *Chem. Commun.* **2007**, 1722-1724.

7   Wiss, K. T.; Krishna, O. D.; Roth, P. J.; Kiick, K. L.; Theato, P. *Macromolecules* **2009**, *42*, 3860-3863.

8   (a) Tao, L.; Mantovani, G.; Lecolley, F.; Haddleton, D. M. *J. Am. Chem. Soc.* **2004**, *126*, 13220-13221. (b) Gauthier, M. A.; Ayer, M.; Kowal, J.; Wurm, F. R.; Klok, H.-A. *Polym. Chem.* **2011**, *2*, 1490-1498.

9   (a) Tao, L.; Liu, J.; Xu, J.; Davis, T. P. *Org. Biomol. Chem.* **2009**, *7*, 3481-3485. (b) Tao, L.; Liu, J.; Xu, J.; Davis, T. P. *Chem. Commun.* **2009**, 6560-6562. (c) Tao, L.; Xu, J.; Gell, D.; Davis, T. P. *Macromolecules* **2010**, *43*, 3721-3727.

10   Buck, M. E.; Lynn, D. M. *Polym. Chem.* **2012**, *3*, 66-80.

11   Chang, C.-W.; Bays, E.; Tao, L.; Alconcel, N. S.; Maynard, H. D. *Chem. Commun.* **2009**, 3580-3582.

12   Pissuwan, D.; Boyer, C.; Gunasekaran, K.; Davis, T. P.; Bulmus, V. *Biomacromolecules* **2010**, *11*, 412-420.

13   Duncan, R. *Nature Rev. Drug. Discov.* **2003**, *2*, 347-360.

14   Schild, H. G. *Prog. Polym. Sci.* **1992**, *17*, 163-249.

15   Hoffman, A. S.; Stayton, P. S. *Prog. Polym. Sci.* **2007**, *32*, 922-932.

16   Li, H.; Bapta, A. P.; Li, M.; Sumerlin, B. S. *Polym. Chem.* **2011**, *2*, 323-327.

17   Kulkarni, S.; Schilli, C.; Grin, B.; Müller, A. H. E.; Hoffman, A. S.; Stayton, P. S. *Biomacromolecules* **2006**, *7*, 2736-2741.

18   Boyer, C.; Bulmus, V.; Liu, J.; Davis, T. P.; Stenzel, M. H.; Barner-Kowollik, C. *J. Am. Chem. Soc.* **2007**, *129*, 7145-7154.

19   He, Y.; Lodge, T. P. *Chem. Commun.*, **2007**, 2732-2734.

20   Lai, J. T.; Filla, D.; Shea, R. *Macromolecules* **2002**, *35*, 5754-6756.

21   Levere, M. E.; Ho, H. T.; Pascual, S.; Fontaine, L. *Polym. Chem.* **2011**, *2*, 2878-2887.

CONCLUSION GENERALE

L'objectif de ce travail était de synthétiser des (co)polymères thermosensibles présentant une fonctionnalité oxazolin-5-one (aussi appelée azlactone) réactive vis-à-vis des amines pour l'ancrage de biomolécules (protéines/ADN). Afin de mener à bien ce projet, la polymérisation radicalaire contrôlée RAFT a été choisie car elle permet, d'une part, d'accéder à des (co)polymères à fonctionnalité spécifique de structure, de composition et de longueur bien définies et, d'autre part, de conduire à des (co)polymères de cytotoxicité limitée.

Trois stratégies de synthèse permettant l'obtention de (co)polymères possédant la fonctionnalité azlactone en position α, en position ω, ou le long des chaînes macromoléculaires (*Schéma 1*) ont plus particulièrement été développées afin d'étudier l'impact de ces structures sur leur réactivité vis-à-vis d'amines variées et d'une protéine modèle (le lysozyme).

fonctionnalité azlactone en position α de la chaîne macromoléculaire

fonctionnalité azlactone en position ω de la chaîne macromoléculaire

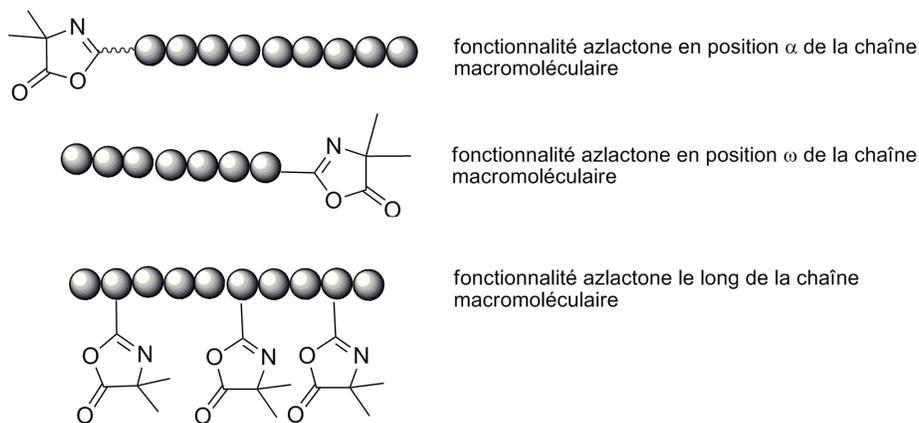fonctionnalité azlactone le long de la chaîne macromoléculaire

Schéma 1 : (Co)polymères à fonctionnalité azlactone.

La **première stratégie** a consisté en la synthèse d'un nouvel agent de transfert trithiocarbonate à fonctionnalité azlactone (azlactone-SC(=S)SC$_{12}$H$_{25}$) et son utilisation en polymérisation RAFT pour atteindre des polymères à fonctionnalité azlactone en

position α. L'agent de transfert azlactone-SC(=S)SC$_{12}$H$_{25}$ a été synthétisé avec succès en trois étapes (rendement global de 30%). Il a ensuite été utilisé comme agent de transfert pour contrôler les polymérisations du styrène (S), de l'acrylate d'éthyle (EA) et de l'acrylamide de *N*-isopropyle (NIPAM). Les études cinétiques, les évolutions des masses molaires moyennes en nombre et des indices de polymolécularité avec la conversion du monomère montrent que l'agent de transfert azlactone-SC(=S)SC$_{12}$H$_{25}$ permet de contrôler la polymérisation RAFT du S, de l'EA et du NIPAM. Les polymères obtenus ont des indices de polymolécularité faibles (I$_p$ < 1,10). L'incorporation de la fonctionnalité azlactone en position α des chaînes macromoléculaires a été mise en évidence par spectroscopies IR, RMN ^{1}H et spectrométrie de masse MALDI-TOF. La réactivité de la fonctionnalité azlactone vis-à-vis de la 4-fluorobenzylamine et de l'allyl amine a été mise en évidence sur l'α-azlactone-PNIPAM de M$_{n,SEC}$ = 6100 g.mol^{-1} (I$_p$ = 1,05). Les caractérisations par spectroscopie RMN ^{1}H et spectrométrie de masse MALDI-TOF des produits obtenus montrent une fonctionnalisation quantitative du PNIPAM considéré. De plus, les résultats ont montré la sélectivité de la réaction vis-à-vis du cycle azlactone par rapport à l'aminolyse du groupement ω-trithiocarbonate (-SC(=S)SC$_{12}$H$_{25}$). Cependant, ce groupement ω-trithiocarbonate (-SC(=S)SC$_{12}$H$_{25}$) peut être hydrolysé avec le temps en milieu aqueux. C'est pourquoi, la **seconde stratégie** qui consiste à introduire la fonctionnalité azlactone en position ω des chaînes macromoléculaires a été étudiée. Pour ce faire, la modification chimique de PNIPAMs obtenus par polymérisation RAFT a plus particulièrement été explorée. Des PNIPAMs de M$_{n,SEC}$ allant jusqu'à 15000 g.mol^{-1} et d'I$_p$ ≤ 1,06 ont été synthétisés par polymérisation RAFT du NIPAM en utilisant le propanoate de méthyl-2-(*n*-butyltrithiocarbonyle)

comme agent de transfert. La fonctionnalité trithiocarbonate mise en évidence par spectroscopie RMN ^{1}H et spectrométrie de masse MALDI-TOF a été réduite en thiol par aminolyse. Différentes conditions opératoires ont été explorées et il s'est avéré que la réaction entre le PNIPAM-SC(=S)SC$_4$H$_9$ (M$_{n,SEC}$ = 7840 g.mol^{-1} et I$_p$ = 1.05) et la *n*-hexylamine en présence de la DMPP conduit à un ω-thiol-PNIPAM (PNIPAM-SH) de structure bien définie. La fonctionnalité azlactone a ensuite été introduite *via* la réaction d'addition de Michaël « thiol-ène » entre le PNIPAM-SH et la VDM en présence de la diméthylphényl phosphine (DMPP) utilisée comme catalyseur. Le polymère obtenu a été caractérisé par spectroscopies IR et RMN ^{1}H et spectrométrie de masse MALDI-TOF. La réactivité de l'ω-azlactone-PNIPAM vis-à-vis de la 4-fluorobenzylamine a été démontrée.

La ***dernière stratégie*** explorée a consisté à incorporer la fonctionnalité azlactone le long des chaînes macromoléculaires afin d'augmenter la capacité en sites réactifs. Pour ce faire, la copolymérisation RAFT d'acrylamides (NIPAM, DMA) et de VDM a été étudiée. Des copolymères à blocs thermosensibles PDMA-*b*-P(VDM-*co*-NIPAM) et PNIPAM-*b*-P(VDM-*co*-DMA) ont été obtenus avec des structures bien définies et des indices de polymolécularité faibles (I$_p$ ≤ 1.20). Ces copolymères présentent une LCST qui peut être modulée en fonction des rapports molaires de NIPAM, DMA et VDM. Les copolymères PDMA$_{23}$-*b*-P(VDM$_{10}$-*co*-NIPAM$_{46}$) et PNIPAM$_{46}$-*b*-P(VDM$_6$-*co*-DMA$_{65}$) présentent une LCST de 36 et 37°C, respectivement. Au-dessus de la LCST, ces copolymères forment des nanoparticules de type « cœur-écorce » en solution aqueuse qui ont été stabilisées par réticulation en présence de 2,2'-éthylènedioxybis(éthylamine). Les nanoparticules obtenues ont été analysées par spectroscopie IR, SEC et par DLS. La spectroscopie IR a montré que des cycles azlactone étaient présents sur les nanoparticules

réticulées obtenues à partir des copolymères PDMA$_{23}$-b-P(VDM$_{10}$-b-NIPAM$_{46}$). L'aptitude de ces nanoparticules fonctionnalisées à capter la dansylhydrazine a été montrée. L'interêt de tels systèmes est qu'ils sont réactifs et stables quelles que soient la concentration et la température utilisées.

Les deux dernières stratégies ont été exploitées pour accéder à des copolymères à blocs thermosensibles à base de PEO et de PNIPAM possédant la fonctionnalité azlactone incorporée le long des chaînes macromoléculaires (PEO-b-P(VDM-co-NIPAM), P1) et en position ω des chaînes macromoléculaires (PEO-b-PNIPAM-azl, P2). La réactivité de ces copolymères vis-à-vis d'une protéine modèle, le lysozyme, a été étudiée. Les résultats obtenus par l'électrophorèse (SDS-PAGE) montrent que les deux types de copolymères forment avec succès des bioconjugués. Les études du comportement en solution aqueuse des bioconjugués avec la température montrent que le bioconjugué P1/lysozyme forme des agrégats et ne présente pas de LCST. Par contre, le bioconjugué P2/lysozyme possède une LCST de 43°C.

En conclusion, différents (co)polymères thermosensibles à fonctionnalité azlactone ont été synthétisés avec succès en utilisant trois stratégies différentes. Leur réactivité vis-à-vis d'amines diverses et du lysozyme a été mise en évidence. Des bioconjugués originaux ont ainsi pu être synthétisés.

Les perspectives de ce travail portent à la fois sur l'étude de la stabilité de la fonctionnalité azlactone en milieu physiologique avec le temps et sur la capacité des copolymères à fonctionnalité azlactone à former des bioconjugés avec l'ADN.